TECHNISCHE UNIVERSITÄT MÜNCHEN

Wissenschaftszentrum Weihenstephan für Ernährung, Landnutzung und Umwelt
Lehrstuhl für Entwicklungsgenetik

The P2X7 receptor and its functional involvement in mood and neurodegenerative disorders

Michael Willi Metzger

Vollständiger Abdruck der von der Fakultät Wissenschaftszentrum Weihenstephan für Ernährung, Landnutzung und Umwelt der Technischen Universität München zur Erlangung des akademischen Grades eines

Doktors der Naturwissenschaften

genehmigten Dissertation.

Vorsitzender: Univ.-Prof. Dr. K. Schneitz

Prüfer der Dissertation:

1. Univ.-Prof. Dr. W. Wurst
2. Univ.-Prof. Dr. A. Kapurniotu

Die Dissertation wurde am 27.04.2016 bei der Technischen Universität München eingereicht und durch die Fakultät Wissenschaftszentrum Weihenstephan für Ernährung, Landnutzung und Umwelt am 20.09.2016 angenommen.

1. Table of contents

2. Table of figures

3. Summary

Due to the demographic development that is currently taking place with constantly increasing life expectancies worldwide, dementia is becoming more and more prominent in our society. The leading cause for dementia is Alzheimer's disease (AD). AD has been shown to be associated with another main contributor to the global disease burden, major depression. Depressive symptoms can develop at any time before or after AD onset. The direct connection between the two pathologies, Alzheimer's disease and major depression, however, has not been investigated extensively so far.

A protein that might represent a potential link between both diseases is the purinergic receptor P2X7R. Several recent linkage and association studies suggest *P2RX7* as susceptibility gene for major depressive disorder. Further, the P2X7R is an important player in the cellular inflammatory response, a process that has repeatedly been shown to facilitate depressive episodes as well as a hallmark feature associated with Aβ deposits in AD brains.

To study the function of the P2X7 receptor and its possible relevance in mood disorders and AD in an appropriate *in vivo* model, we established two novel mouse lines, a constitutive *P2rx7* knockout mouse line and a mouse line in which the murine *P2rx7* is substituted by the human *P2RX7*, using a knock-in approach. This mouse expresses the human P2X7 receptor under the regulatory element of the murine gene. Due to integration of *loxP* sites, this humanized *P2RX7* allele is accessible to Cre recombinase-mediated inactivation. In contrast to previously described *P2rx7* knockout mouse lines these two new knockout lines lack all known *P2rx7* splice variants. We took advantage of these new mouse lines to further investigate the role of the P2X7R in basal emotionality as well as the response to stress as an environmental factor. We found that the lack of the P2X7R does not affect basal emotionality, while upon stress, the loss of the receptor results in lowered susceptibility towards stress induced alterations in behavior.

Moreover, we conducted a detailed expression analysis of *P2rx7* in the mouse brain as well as a comparison of the murine and the human receptor, taking advantage of the humanized *P2RX7* mouse line. We could successfully show the expression of *P2rx7* throughout the mouse brain and for the main cell types including glutamatergic hippocampal neurons.

In combination with a mouse model of AD we additionally investigated the involvement of the P2X7R on cognitive decline characterizing the disease. We found indications that the lack of the P2X7R has a protective effect on cognitive impairment in AD. Furthermore, we studied the receptors functional involvement in the processing of the amyloid precursor protein (APP) and

the deposition of amyloid β (Aβ) in the brain. While we did not observe effects of the receptor knockout on the processing of APP, we found that the amount of Aβ deposits was increased in brains of AD model mice lacking the P2X7R.

Taken together, this work provides important insights into the function of P2X7R as a potential link between two of the most prevalent brain disorders, i.e. major depression and AD.

4. Zusammenfassung

Aufgrund der demografischen Entwicklung die mit einer weltweit zunehmendem Überalterung unserer Gesellschaft einhergeht, rücken auch altersbedingte Erkrankungen wie Demenz mehr und mehr in den Fokus der Öffentlichkeit. Die häufigste Ursache für altersbedingte Demenz ist die Alzheimer Krankheit (AK). Es ist bekannt, dass die AK mit einer weiteren wichtigen Erkrankung unserer Zeit, Depression, in Zusammenhang steht. Symptome einer Depression können sowohl vor als auch zu jedem Zeitpunkt während des Verlaufs der AK auftreten. Wie genau die beiden Erkrankungen in Verbindung stehen ist jedoch weitestgehend unerforscht.

Ein Protein das als Bindeglied beider Erkrankungen gesehen werden kann ist der purinerge Rezeptor P2X7R. Eine Reihe kürzlich veröffentlichter Assoziationsstudien legt nahe, dass das *P2RX7* Gen eine Anfälligkeit zur Enwicklung affektiver Störungen (unipolar + bipolar) fördert. Desweiteren kommt dem P2X7R eine wichtige Rolle bei zellulären Entzündungsreaktionen zu, Prozesse, von denen wiederholt gezeigt wurde, dass sie die Entstehung von depressiven Episoden begünstigen können. Entzündungsreaktionen sind zudem ein häufiger Begleiter von Aβ Ablagerungen in Gehirnen von Alzheimer Patienten.

Um die Funktion des P2X7 Rezeptors und seine Relevanz im Bezug auf Depressionserkrankungen und Alzheimer besser in einer *in vivo* Umgebung untersuchen zu können, haben wir zwei neue Mauslinien etabliert. Zum einen eine neue konstitutive *P2rx7* Knockout Mauslinie, zum anderen eine Mauslinie, bei der das murine *P2rx7* Gen durch das humane *P2RX7* mittels Knock-in ersetzt wurde. Bei dieser Maus wird der humane P2X7 Rezeptor unter Kontrolle der regulatorischen Elemente der Maus exprimiert. Aufgrund der zusätzlichen Integration von *loxP* Sequenzen ist es bei diesem humanisierten Allel zudem möglich, mit Hilfe von Cre Rekombinasen das Allel zu inaktivieren. Anders als zuvor publizierte *P2rx7* Knockout Linien zeichnen sich diese zwei neuen Linien durch die vollständige Abwesenheit aller *P2rx7* Splicevarianten aus. Wir haben die Möglichkeiten dieser Mauslinien genutzt, um weitergehende Untersuchungen hinsichtlich der Rolle des P2X7R in Bezug auf die Emotionalität sowohl unter basalen Bedingungen, als auch in Reaktion auf Stress durchzuführen. Es stellte sich heraus, dass unter normalen Bedingungen der Verlust des P2X7R die Grundemotionalität nicht beeinflusst, während das Fehlen des Rezeptors die Anfälligkeit bezüglich stress-induzierter Verhaltensveränderungen senkt.

Des Weiteren nutzten wir die humanisierte *P2RX7* Mauslinie um sowohl weitreichende *P2rx7* Expressionsanalysen im Maushirn, als auch einen Vergleich von murinem und humanem Rezeptor, durchzuführen. Es gelang uns zu zeigen, dass *P2rx7* in allen Bereichen des Maushirns

und in den Hauptzelltypen, glutamaterge Nervenzellen im Hippokampus eingeschlossen, exprimiert wird.

In Kombination mit einem Alzheimer Mausmodell untersuchten wir zudem einen möglichen Einfluss des P2X7R auf die Abnahme geistiger Fähigkeiten die mit der AK einhergehen. Es ergaben sich Hinweise darauf, dass das Fehlen des P2X7R einen protektiven Effekt auf die Kognition in der AK hat. Darüber hinaus untersuchten wir in dieser Arbeit den Einfluss des P2X7 Rezeptors auf die Prozessierung des Amyloid-Vorläufer-Proteins (APP) und die Ablagerung von Amyloid β (Aβ) im Hirn. Während wir keine Veränderung der APP Prozessierung durch den Knockout des Rezeptors feststellen konnten, so fanden wir eine erhöhte Anzahl von Aβ Ablagerungen in Hirnen von Alzheimer Modellmäusen denen der P2X7R fehlt.

Diese Arbeit stellt einen wichtigen Beitrag zum Verständnis der Funktion des P2X7R als mögliches Bindeglied zwischen zweien der häufigsten Erkrankungen des Gehirns, nämlich von Depression und der Alzheimer Krankheit, dar.

5. Introduction

5.1. Mental disorders – estimation of the World Health Organization

Mental disorders including major depression, bipolar disorder, schizophrenia, developmental disorders (e.g. intellectual disabilities, autism) and dementia are generally characterized by a mixture of abnormal emotions, behavior, perception, thoughts and relationships with other people. With more than 600 million people affected worldwide, mental disorders represent a huge part of the global disease burden. Risk factors can be individual-specific like genetics, nutrition, perinatal infections/complications or the exposure to stress. But also the environment like the exposure to hazards or socioeconomic (e.g. standards of living) and political factors (e.g. national health care) is decisive. These environmental factors also strongly influence the treatment of the respective disorders. In “low” and “middle” income countries the majority of people do not have access to treatments. In “higher” income countries still 35-50% of the affected do not receive adequate treatment or help at all. Even if treatment is implemented, it is per se still a challenge for many mental disorders. Medical treatments of depression for example hardly changed over the last five decades and in general the health care of mental illnesses requires intensive human support and caretaking.

Due to the predicted strong increase of mental diseases, the World Health Organization (WHO) encourages more effective governance for mental health including strategies for promotion, prevention as well as information systems. Nonetheless, both basic and clinical research has to be strengthened in the future in order to develop better and more specific therapies (WHO, 2015a).

5.2. Major depression

Depression, in former times referred to as melancholia has been part of mankind ever since and will probably continue to be in the future. In ancient times melancholia was believed to be one of the four humors each of them represented by different body fluids. Blood (lat. sanguis) favoring a sanguine temperament, phlegm (ancient greek: phlégma) representing phlegmatic temper, yellow bile (ancient greek: kholé) favoring choleric temperament, and black bile (ancient greek: melas kholé) for the melancholic temper. For a very long time the idea of the Greek physician Hippokrátes that melancholia is caused by an excess of the black bile, was the general

assumption. Today we know a little more of the underlying causes of depression but as reflected by the lack of specific and effective treatment we still do not understand the causality and the mechanisms involved in this disorder.

Yet depression gains more and more importance for our today's global health systems. Major depressive disorder (MDD) is the most common form of mental disorders with an estimated number of 350 million affected people worldwide (WHO, 2012; Nature editorial, 2014). Depression is one of the leading causes of disabilities worldwide (Lopez and Murray, 1998; Eaton et al., 2008; Murray and Lopez, 2013) with an estimated economic burden of more than 83 billion US dollar for the year 2000 (Greenberg et al., 2003).

However, the diagnosis is still not always clear or trivial due to inhomogeneous symptoms as well as a high comorbidity of depression with other mental disorders. Characteristic hallmarks of MDD include depressed mood, loss of pleasure, weight changes (gain or loss), loss of energy, disturbed sleep, feelings of low self-esteem and/or guilt, decreased concentration abilities, psychomotor retardation and recurrent suicidal thoughts. A combination of five out of these symptoms described in detail in the Diagnostic Manual of Mental Disorders 5 (DSM-5) are still the main criteria for today's diagnosis of depression (American Psychiatric Association, 2013). Recently strong criticism on this classification of mental illnesses based on the above mentioned symptoms have arisen. The strong comorbidity of mental disorders - e.g. anxiety disorders are comorbid with depression and even stronger with bipolar disorders (Angst et al., 2015) - might render it impossible to separate certain disorders from each other, yet this diagnosis system is still the standard (Adam, 2013).

The causality of depression is very inhomogeneous. Many studies showed that certain environmental factors dramatically increase the risk to develop depressive symptoms. Such environmental influences can be physical abuse (in particular during childhood), drug and alcohol abuse, traumatic events and stress in general. Stressful events have long been correlated with increased susceptibility to develop depression and stress is still assumed to be one of the major contributors (Brown et al., 1987; Nemeroff, 1988; Holsboer, 2001; Sananbenesi and Fischer, 2015).

Whereas it is indisputable that certain environmental risk factors have an important influence as well as the gender - women are affected by depression twice as often as men (Kessler et al., 1994; Kessler and Chiu, 2005) - the genetic impact on depression is still discussed. Studies investigating the likelihood of twins to develop major depression prompt a genetic component of 40-50% (Levinson, 2006). But whereas for other mental disorders, like e.g. bipolar disorder,

several genes have successfully been associated, for MDD this appears to be more challenging up to now. There are several explanations for this phenomenon. Although the genetic contribution of diabetes type II is estimated similarly high as for MDD, several candidates were successfully associated with the disease in genome wide association studies (GWAS). The difference lies in the simplicity of diagnosis of the two pathologies and, therefore, the screening of a high number of patients. Further, a correlation of the effect size and frequency of risk alleles was recently described (Manolio et al., 2009). Namely, pathologies not showing high allelic frequencies (most common diseases) or no strong effect sizes (Mendelian diseases) are way more difficult to associate with a certain risk allele. This could be one possible explanation why a large meta-analysis of GWAS for depression with ~9.500 cases from 2012 did not identify significant results (Major Depressive Disorder Working Group of the Psychiatric GWAS Consortium, 2012). Since the risk of depression is speculated to be highly polygenic, including several hundreds of genes all with rather low effect sizes, recent predictions claimed the necessity of sample sizes of 100.000 MDD patients or more, to successfully assign loci to depression (Hyman, 2014). A very recent study, however, conducted with a very stringent cohort - very severe form of illness, relatively homogeneous cases (women of Han Chinese ethnicity only) – could indeed reproducibly link genetic markers to MDD (Cai et al., 2015). Based on ~5.300 depressed and ~5.300 controls the study revealed association of two loci, one in an intron of the *LHPP* gene and the other close to the *SIRT1* gene with MDD. *LHPP* is coding for an enzyme (phospholysine phosphohistidine inorganic pyrophosphate phosphatase) with so far unknown function, while *SIRT1* (coding for sirtuin 1) has been shown to be crucial for the biogenesis of mitochondria (Gerhart-Hines et al., 2007). This finding shows that careful selection of samples might be of essential importance for future association studies in pathologies with rather low effect sizes.

With several people of public interest recently talking openly about their struggling against depression – Sebastian Deisler (former world-class soccer player), Sven Hannawald (first and so far only winner of all four events of the four hills tournament), Robbie Williams (musician), Angelina Jolie (actress) - just to name some of a long list - a better awareness and acceptance of the disease in society should be possible. Fact, however, is, that still only about half of the affected people actually seek for medical assistance (Epstein et al., 2014). Even more of those who do, only 20% receive adequate and wide-ranging treatment (Wang et al., 2005). Today's most common forms of treatment are psychotherapy, medication with antidepressants and

electroconvulsive therapy. The last is reserved for special or very severe cases e.g. chronic resistant to antidepressant treatment. The most common treatment for moderate to severe depression is a mixture of psychotherapy and medication. Medication, however, did not progress much during the last decades. Since the discovery of antidepressant properties of *iproniazid* – initially developed as tuberculosis treatment – and *imipramine* in the mid 1950's, the pharmacology of antidepressant drugs has hardly changed. All of todays applied antidepressants act on the monoamine neurotransmitter pathways. Even though today's drugs show less side effects and less habituation, the general compounds remained the same since their discovery in the middle of the last century. With this also the main drawbacks remained. Antidepressive drugs show a considerable delay in effectiveness. From treatment onset to first signs of symptomatic improvement it can take up to 6 weeks (Sanacora et al., 2012). Moreover, around 40% of the treated subjects show a resistance towards the medication (Berton and Nestler, 2006a; Maes et al., 2009). Only around one third of all treated patients will achieve full remission of their depressive symptoms (Trivedi et al., 2006; Gaynes et al., 2009; Epstein et al., 2014).

The effective treatment of depression is further complicated by its strong comorbidity with other diseases. Depressive patients for example have a 2 to 4 fold higher risk for cardiovascular diseases (Keck, 2006; Whooley et al., 2008). Increasing evidence for a correlation with MDD has also been shown for metabolic diseases like obesity and diabetes type II (Ciechanowski et al., 2009; McIntyre et al., 2006), osteoporosis (Whooley et al., 1999; Laudisio et al., 2008), cancers (Krishnadas and Cavanagh, 2012) as well as Alzheimer's disease (AD) (Sotiropoulos et al., 2008; Catania et al., 2009; Raison and Miller, 2012). These problems point out the necessity of new entry points for the treatment and medication of major depression. One starting point could be the identification of new candidate genes.

5.3. Dementia

Dementia affects almost 50 million people worldwide with a strong bias towards people with progressed age. Dementia is a pathology that affects cognitive functions like memory, language, learning, thinking and the ability to manage every day's tasks. In general it is referred to as dementia if there is cognitive decline that exceeds the normal decline during aging. The healthcare expenditures, also compared to other mental disorders are tremendous. In 2010 the estimated global costs for dementia are around 600 billion US dollars. Dementia can be

displayed by a variety of disorders or injuries like Parkinson's disease, vascular dementia, Huntington's disease, Creutzfeldt-Jakob disease or stroke. By far the most predominant, however, is Alzheimer's disease contributing to up to 70% of all cases of dementia (WHO, 2015b).

5.4. Alzheimer's disease

Alzheimer's disease (AD) is a neurodegenerative disease that is characterized by a progressive decline in cognitive function most abundant in people above 65 years of age. The pathology was named after the German psychiatrist Alois Alzheimer by his colleague Emil Kraepelin in 1910. Alois Alzheimer described the disease for the first time in 1906 based on his findings with Auguste Deter. Alzheimer met Auguste Deter in 1901 when she was 51 years old. She was disoriented and already showed strong symptoms that, as we know now, were typical for the disease. Within 5 years she passed away and Alzheimer conducted a pathological examination of her brain tissue. He found widespread signs of neurodegeneration and back in that time unfamiliar protein deposits we today refer to as plaques (Alzheimer, 1907). In November 1906 he presented his work entitled "*Über eine eigenartige Erkrankung der Hirnrinde"* to the scientific community in a congress in Tübingen. Even though the work was not paid much attention to in the beginning, it set the basis for today's research on one of the most important diseases of our time.

Worldwide more than 40 million people suffer from Alzheimer's disease. However, it is predicted that only 25% of all affected have been diagnosed. The prevalence to develop AD is 30% higher for women than for men. In both genders one can observe a strong comorbidity of the disease with other pathologies. The most common are diabetes and heart diseases but also major depression shows strong comorbidity with AD (Alzheimer's Association, 2014).

Alzheimer's disease cannot be cured until now. Only symptomatic drugs as well as non-drug based therapies are available today. Both try to ease the symptoms of the disease. The two approved medical therapies are based on cholinesterase inhibitors and NMDA receptor antagonists (Potter, 2010; Berk et al., 2014). Both do not have any beneficial effect on preventing neuronal damage. There is no doubt that new treatment beyond todays two classical ones are of strong need. The main obstacle in the development of new drugs can be found in the insufficient understanding of the underlying mechanisms of the pathology. Today's drug

development mainly focuses on four different approaches to address the disease (Berk et al., 2014). The “metabolic approach” focuses on insulin. Insulin dysregulation has been shown to contribute to the onset of AD and insulin levels as well as its activity is reduced in AD patients (Craft et al., 1998). As the name indicates, “anti-tau approaches” try to inhibit the aggregation of tau protein. By far the most research and development is invested in “amyloid-based approaches” that follow many different ways all more or less with the goal to decrease the amyloid-β protein load (e.g.: Vellas et al., 2011; Coric et al., 2012; Adolfsson et al., 2012). The fourth type of approaches are “mulitarget approaches” that try to combine the first three by targeting several of the pathological hallmarks at the same time (Cole et al., 2007; Faux et al., 2010).

The clinical criteria that underlie the diagnosis of Alzheimer’s disease did not undergo major changes since the 1990’s. The standard diagnosis is still based on physical and neurological examinations checking for cognitive impairment by standardized tests of mental function (Duthey, 2013). There are few very similar guidelines that are used in the field to put together different criteria to the diagnosis of AD. The most common are by the National Institute of Aging (McKhann et al., 2011) and the American Psychiatric Association (American Psychiatric Association, 2013). According to the latest manual of mental diseases the DSM-5, the criteria for a probable AD are met if:

A. The criteria of a major or mild neurocognitive disorder (NCD) are given. The criteria for NCD are basically an impairment in cognitive function and several cognitive aspects like learning, memory and language (for more detailed information see (American Psychiatric Association, 2013).
B. There is insidious onset and gradual progression of impairment in one or more cognitive domains.
C. For major neurocognitive disorder probable AD is diagnosed if either of the following is present;

   1. Evidence of a causative Alzheimer’s disease genetic mutation from family history or genetic testing.

   2. All 3 of the following are present:

   a. Clear evidence of decline in memory and learning and at least one other cognitive domain (based on detail history or serial neuropsychological testing).

   b. Steadily progressive, gradual decline in cognition, without extended plateaus.

c. No evidence of mixed etiology (i.e., absence of other neurodegenerative or cerebrovascular disease or another neurological, mental or systemic disease likely contributing to cognitive decline).

If mild NCD is diagnosed in A., evidence of a genetic AD mutation has to be given by genetic testing in order the criteria for probable AD to be fulfilled.

The already above mentioned strong symptomatic overlap of different mental disorders based on physical and neurological examinations raised the necessity for different diagnostic criteria in the last years. Since its discovery more than 100 years ago it is well known that AD is characterized by the accumulation of insoluble protein aggregates such as amyloid-β plaques and tau-based neurofibrillary tangles. Unfortunately, for a long time this pathological characteristics were only accessible *postmortem* or by biopsy combined with the risk of severe brain damage. Constant progress in modern imaging techniques in the last few years, however, bring up the hope that methods like positron emission tomography (PET)-based measurement of Aβ and tau levels or magnetic resonance imaging (MRI)-based brain atrophy quantification could revolutionize the diagnosis of AD pathology (Nordberg, 2015). A recent study of the US International Institute of Aging and the International Alzheimer's Working Group already proposes to include these new readouts in the diagnostic criteria of AD (Wiste et al., 2014).

Alzheimer's disease can be further classified into two types of the disease - early-onset and late-onset AD. Early onset AD, also referred to as early-onset familial AD (eFAD) occurs in people aged 60 years or younger and accounts for less than 5% of all cases of Alzheimer's disease. Late-onset AD (LOAD) accounts for the vast majority of cases and usually becomes apparent from the age of 60 onwards. Both types have a genetic component. However, whereas in late-onset AD usually a combination of genetic, environmental and lifestyle factors are causal, eFAD can be caused by one mutation of a set of single gene mutations (NIH and National Institute on Aging, 2015). Three different genes have been found to be causative for eFAD: *amyloid precursor protein* (*APP*), *presenilin-1* (*PS1*) and *presenilin-2* (*PS2*). Mutations within these genes affect the processing of the amyloid precursor protein in a dominant way and subsequently lead to excessive production of amyloid β (Aβ). Around 230 of those mutations have been identified in these three genes until now (Wu et al., 2012). Mutations in *APP* (referred to as Alzheimer's disease type1 (AD1)) account for 10-15% of all FAD cases, mutations in *PS1* (referred to as AD3) are responsible for 30-70% and mutations in *PS2* (referred to as AD4) account for less than 5% of

all cases of eFAD (Bird, 1993). For late-onset Alzheimer's disease certain mutations can act as risk factors. Other than for eFAD for LOAD a combination of genetic and environmental risk factors are usually causative. Genes that have been associated with late-onset AD are *CLU*, *CR1*, *SORL1*, *PICALM* and *TREM2* (Meng et al., 2007; Sleegers et al., 2010; Jonsson et al., 2013). The strongest and repetitive association with late-onset AD has been shown for a gene called *apolipoprotein E* (*APOE*) (Corder et al., 1993; Bertram and Tanzi, 2009; Mormino et al., 2014). Certain mutations in this gene can increase the risk to develop AD by up to 12 fold (Verghese et al., 2011). The human APOE has three main isoforms (APOE ε2 - ε4) that differ by single amino acid exchanges at two different positions – 112 and 158. APOE ε2 has Cys at both of this positions; APOE ε3 has Cys at position 112 and Arg at position 158; APOE ε4 contains Arg at both positions (Weisgraber et al., 1981; Tai et al., 2015). The isoform ε4 bears by far the highest risk potential by facilitating Aβ accumulation (Mormino et al., 2014). Carrying this isoform does not necessarily mean one will develop Alzheimer's disease; however, the chances are dramatically increased. It is further speculated that this mutation lowers the onset of AD by several years which in some people will manifest, in others that die before, it does not (Sando et al., 2008). The other two APOE isoforms do not increase the risk to develop AD. APOE ε3, which is the most common isoform, is believed to have a neutral effect, so it is neither increasing nor lowering the risk to develop the disease (NIH and National Institute on Aging, 2015). For APOE ε2, however, a beneficial effect in regard to coming down with AD has repeatedly been shown lately. Unfortunately, it is the least common isoform (Berlau et al., 2009; Conejero-Goldberg et al., 2014).

Alzheimer's disease brains are characterized by basically two main pathologic hallmarks. There are extracellular neuritic plaques consisting of amyloid β and intracellular inclusions of the microtubule-associated tau protein called neurofibrillary tangles. Among these two major ones there are other characteristic effects that can be observed in AD brains. Inflammatory processes and immune response reactions are two of these events (McGeer and McGeer, 2007). Others are neuritic dystrophy, loss of synaptic function and neuronal loss. These characteristics can be regarded as secondary effects (Bignante et al., 2013). Whether AD can be caused by either Aβ formation or tau aggregation or if only a combination is causative is still controversially discussed (Ashe and Zahs, 2010).

5.5. APP processing

The human amyloid precursor protein (APP) gene is located on chromosome 21 and exists in three main isoforms originating by differential splicing (Goate et al., 1991; Goate, 2006). These isoforms differ in size and comprise 695 (APP695), 751 (APP751) and 770 (APP770) amino acids. Whereas APP751 and APP770 are expressed ubiquitously, the 695 amino acids splice variant is most abundant in the CNS and predominantly expressed in neurons (Kang and Müller-Hill, 1990; Rohan de Silva et al., 1997; Bayer et al., 1999). APP is a type-I transmembrane protein with its amino terminus in the extracellular space and the carboxyl terminus within the cytosol. The physiological function of APP is largely unknown (O'Brien and Wong, 2011). Different functions (e.g.: neurite outgrowth, synaptogenesis, protein trafficking, cell adhesion, etc.) have been proposed but all lack ultimate *in vivo* evidence (Zheng and Koo, 2006).

Synthesis of APP takes place in the endoplasmic reticulum (ER) from where it is subsequently transported through the Golgi apparatus to the Golgi/trans Golgi network. There and during that shuffling APP is vulnerable to cleavage by different proteases referred to as secretases (Greenfield et al., 1999; Haass et al., 2012). There are three very well described secretases for the amyloid precursor protein (Haass, 2004; O'Brien and Wong, 2011; Zhang et al., 2011; Haass et al., 2012; Bignante et al., 2013): the α-secretase ADAM10 (a disintegrin and metalloprotease 10) (Sisodia, 1992); the β-secretase BACE1 (β-site APP cleaving enzyme1) (Sinha et al., 1999; Vassar et al., 1999; Yan et al., 1999) and the γ-secretase (Wolfe et al., 1999). γ-secretase is a complex of proteases that consists of four different subunits: A homodimer formed by either presenilin 1 (PS1) or presenilin 2 (PS2), nicastrin (NCT), the stabilization factor APH-1 (anterior pharynx defective) and presenilin enhancer 2 (PEN2) (Wolfe et al., 1999; Yu et al., 2000; Francis et al., 2002; Haass et al., 2012). A fourth secretase, named η–secretase has just recently been described (Willem et al., 2015). Additionally, but less important for the AD pathology, APP can be cleaved by caspases in the intracellular domain (Gervais et al., 1999; Soriano et al., 2001).

In general, two principle APP processing pathways can be discriminated: the non-amyloidogenic and the amyloidogenic pathway that ultimately leads to the production of Aβ (Figure 1). The α-secretase cuts APP between the residues Lys613 and Leu614 (Lys16 and Leu17 of the Aβ subunit). This is within the Aβ domain and, therefore, α-secretase activity is considered non-amyloidogenic (Esch et al., 1990). This cleavage results in the C-terminal product called carboxy-terminal fragment (CTF)-α and a larger amino-terminal domain referred to as soluble APPα (sAPPα). This product can be further cleaved by the η-secretase resulting in the two products

sAPP-η and Aη. Direct cleavage of APP by the η-secretase leads to the products CTF-η and sAPP-η (Willem et al., 2015) .

The amyloidogenic pathway is characterized by a sequential cleavage of full-length APP by β- and γ-secretase. Processing of APP by β-secretase results in the amino terminal product sAPPβ and the membrane bound CTF-β. The later can be cleaved further by the γ-secretase which ultimately brings up the APP intracellular domain (AICD) and the causal fragment of Alzheimer's disease, the neurotoxic amyloid β (Aβ) protein (O'Brien and Wong, 2011; Zhang et al., 2011; Haass et al., 2012; Willem et al., 2015).

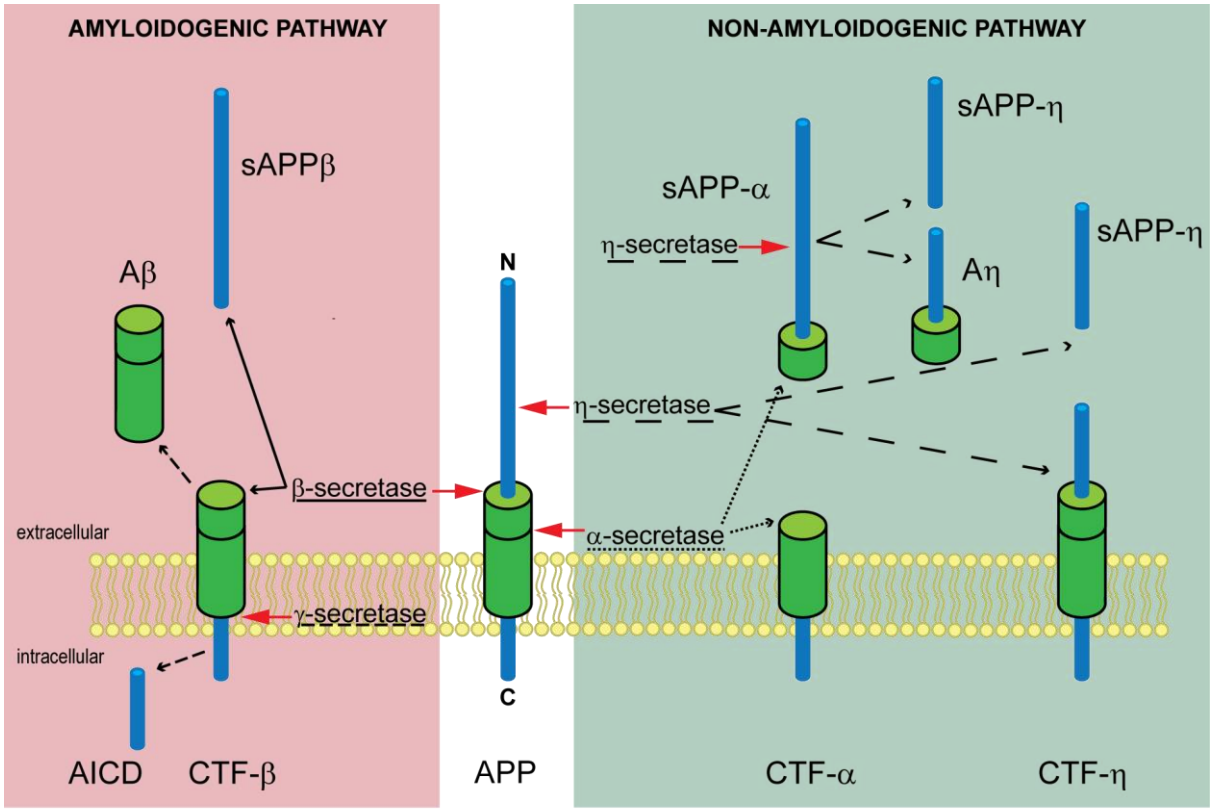

Figure 1: Secretory pathway of the amyloid precursor protein
The processing of APP can be divided in two main pathways: the non-amyloidogenic and the amyloidogenic. Subsequent cleavage of APP by the β- and the γ-secretase leads to the generation of the neurotoxic Aβ fragment. (The figure is based on figures of O'Brien and Wong, 2011; Zhang et al., 2011; Willem et al., 2015)

5.6. Amyloid β

Amyloid β is generated by the sequential cleavage of APP by β- and γ-secretases. Of great importance for the AD pathology is the fact that γ-secretase mediated cleavage is subject to

certain variability in regard to where the cutting occurs. Under physiological conditions γ-secretase cuts somewhere in between the amino acids 37 and 43 of the Aβ subunit (Haass et al., 2012). This degree of unspecificity leads to different Aβ isoforms. Most abundant, however, are two, $A\beta_{40}$ and $A\beta_{42}$ (McGowan et al., 2005). Of those two, $A\beta_{40}$ accounts for almost 90% of all generated Aβ whereas $A\beta_{42}$ only for about 10% (Zhang et al., 2011). $A\beta_{42}$ has been shown to be more prone to aggregation than its two amino acids shorter version due to higher hydrophobicity than $A\beta_{40}$ (Burdick et al., 1992). This facilitates the formation of Aβ fibrils and plaques (Iwatsubo et al., 1996).

Aβ per se tends to form oligomers. These oligomers exist in different sizes and structures. It has been shown that the toxicity of these oligomers differs a lot and, therefore, contributes to the complexity of the AD pathology (Sakono and Zako, 2010). For long time it was believed that the high molecular extracellular fibrillary Aβ deposits (plaques) are the cause for the neurodegenerative symptoms of Alzheimer's disease. Recent studies, however, strongly suggest that profibrillary, low molecular Aβ oligomers are the actual cause. Walsh *et al.* for example showed that soluble Aβ inhibits hippocampal long term potentiation (LTP) *in vivo* (Walsh et al., 2002). Another study directly compared the toxicity of the different oligomers of Aβ and found that soluble dimers are three times and tetramers even up to 13 times more toxic than monomers (Ono et al., 2009). For soluble Aβ it was further shown that it is not restricted to extracellular space, but it also accumulates inside the cell. However, both the formation and the toxicity of extracellular and cytosolic Aβ differ (Sakono and Zako, 2010). For extracellular Aβ, which is released to the extracellular space by subsequent β- and γ-secretase cleavage, there is evidence that its toxicity is mediated by various effects of Aβ oligomers. It has been shown that Aβ oligomers can bind to the nerve growth factor (NGF) receptor which subsequently leads to the induction of apoptosis (Yamamoto et al., 2007). Further, these oligomers can bind to NMDA receptors and cause abnormal calcium homeostasis resulting in oxidative stress (De Felice et al., 2007). Also Wnt signaling can be affected by extracellular Aβ oligomers by binding to the Frizzled receptor causing wide-ranging cellular dysfunction (Magdesian et al., 2008).

Intracellular Aβ can to a smaller extent be produced in a similar manner by subsequent cleavage by β- and γ-secretase in the ER and trans-Golgi network inside the cell (LaFerla et al., 2007). However, intracellular Aβ can as well originate from extracellular Aβ via endocytotic uptake mechanisms (Yang et al., 1998). How toxicity of intracellular Aβ is mediated is largely unknown. It is speculated that it differs from those of extracellular Aβ. It is known however, that molecular chaperones can prevent intracellular Aβ oligomers from forming higher molecular weight

molecules and aggregation and, therefore, stabilize the highly toxic oligomer structure. A discussed way how toxicity is mediated is via inhibiting the proteasomal activity, and thereby inducing cell death (Sakono et al., 2008; Sakono and Zako, 2010).

5.7. Genetic mouse models of Alzheimer's disease

Recent progress in understanding the mechanisms and underlying causes of Alzheimer's disease have strongly facilitated the development of genetically modified mouse models of AD just like those mouse models pushed the research on AD. Search on www.alzforum.org results in way more than 110 different mouse lines that were generated to mimic aspects or hallmarks of AD in mice. Classic approaches to model the disease are to introduce mutations associated with eFAD (e.g. *APP*, *PS1*, *PS2* - see above). Further, genetically introducing human amyloid precursor protein is common to model AD pathology in mice. These mice usually overexpress human APP, often supported by carrying certain mutations that facilitate the onset and progress of AD symptoms based on Aβ formation (LaFerla and Green, 2012). Out of the more than 20 mutations that facilitate Aβ formation (Götz and Ittner, 2008), the most commonly used in transgenic mouse models are the Indiana (V717F), the London (V717I), the Swedish (K670N/M671L) and the Arctic (E693G) mutations. All these mutations result from one or even two amino acid exchanges within the Aβ domain of the amyloid precursor protein. These mutations facilitate the pathology of AD in different ways. Common ways are facilitating β-secretase activity (e.g. Swedish mutation) (Suzuki et al., 1994) or affecting γ-secretase mediated cleavage e.g. by favoring the production of the more toxic $A\beta_{42}$ (e.g. London, Indiana) (Chartier-Harlin et al., 1991). The Artic mutation (E693G) leads to an increased propensity of $A\beta_{40}$ to form protofibrils compared to wild-type $A\beta_{40}$ and thereby facilitating Aβ aggregation (Nilsberth et al., 2001).

A transgenic mouse model that is transgenic for human APP and additionally combines two of the above mentioned APP mutations is the so called arcAβ mouse generated and described by Knobloch *et al.* (2007). This transgenic mouse model expresses the human APP695 under the regulatory elements of the murine prion promoter. Additionally it carries the Swedish and Arctic mutation in the APP sequence (Figure 2A). APP levels in the transgenic mice are about six-fold elevated compared to wild-type mice and are constant over time. Further, the arcAβ mice show an age-dependent increase of Aβ levels (Figure 2B-D) (Knobloch et al., 2007).

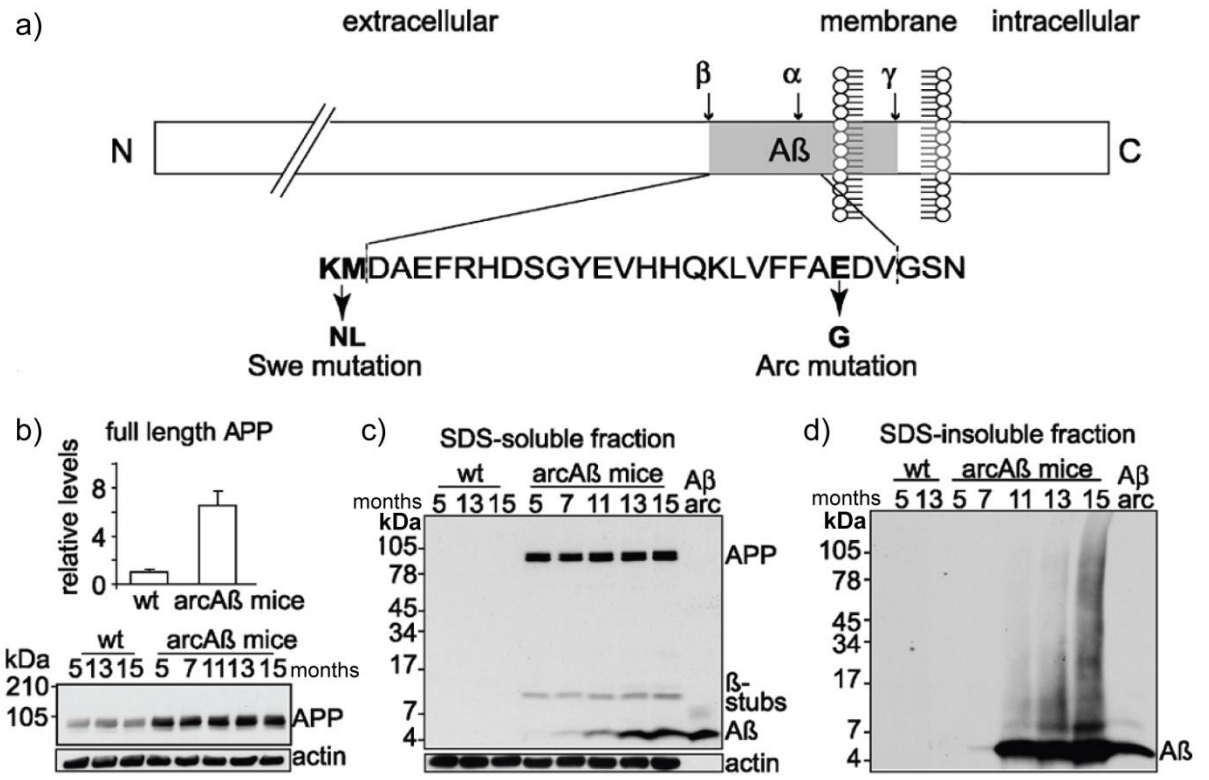

Figure 2: Human APP695 overexpression in arcAβ mice
a) ArcAβ mice express human APP695 with the Swe/Arc mutations; **b-d)** ArcAβ mice overexpress APP and show a time dependent increase in Aβ levels as determined by Western blotting. (Figure modified from Knobloch et al., 2007).

In the original publication Knobloch et al. describe that arcAβ mice show an age dependent increase in β-amyloid plaque deposition starting around 7 months of age. Further, Aβ plaques show a distinct morphology with dense cores and less dense surrounding. ArcAβ mice are additionally characterized by intracellular punctate Aβ deposits around the ER, starting already from month 3 on. Also behavioral alterations were observed by Knobloch and colleagues. ArcAβ mice show hyper-locomotion in early age that decreases over time. Most interestingly these mice show severe cognitive impairments. As determined by several paradigms (Y-maze, Morris water maze, two way active avoidance) arcAβ mice show impaired working memory compared to wild-type littermates starting around 9 months of age (Knobloch et al., 2007).

To sum up, animal models for Alzheimer's disease already contributed in further understanding and unraveling the pathology and will continue to be an important tool in the future (LaFerla and Green, 2012).

5.8. Inflammation

In vertebrates the immune response can in general be sub-divided into two parts: adaptive and innate immune system. The adaptive, also referred to as acquired immune system is based on a specialized group of cells, the so called lymphocytes. A subclass of lymphocytes is capable to discriminate between the body's own cells and foreign organisms by recognizing antigens and subsequently pass the information to a different sort of lymphocytes that is specialized in destruction of invading cells or viruses.

The second, evolutionary older part of the vertebrate immune system, the innate immune system also comprises a set of cells specialized in elimination of intruding cells or organisms. However, these cells cannot adapt or acquire the necessary information which cells are of internal or of foreign origin. Here inflammation as part of the natural immune response of the body takes over an important role. Acute inflammation in a certain affected region is initiated by immune cells already equally distributed throughout the tissue, namely macrophages in the periphery and microglia in the central nervous system. These cells have the ability to recognize special molecules that are commonly shared by pathogens. Following pathogen recognition or activation they can release so-called cytokines. These signaling molecules lead to the recruitment of further immune cells, both of the innate as well as the adaptive immune system.

The general function of inflammation as part of the immune response is therefore to maintain homeostasis as a reaction to harmful stimuli such as pathogens, cell damage or stress. Inflammatory response can be beneficial for the organism to react on such harmful stimuli, however, when it reacts out of proportion it can have an opposing pathologic and damaging effect (Rosenblat et al., 2015). As such it has been proposed to contribute and facilitate a variety of pathologies including mood disorders and Alzheimer's disease. For both pathologies in particular neuroinflammation has long been speculated to be a key element. Already in the late 1980s it was shown that in Alzheimer's disease brains activated immune cells like microglia and astrocytes accumulate within and around amyloid β deposits (Griffin et al., 1989; Perlmutter et al., 1990). It was further shown that cytokine release by microglia is upregulated in AD brains, both in AD mouse models as well as in human patients (Prokop et al., 2013) and thereby facilitating neuroinflammation and subsequent cell death. In this line recent association studies showed that certain variants in genes (*triggering receptor expressed on myeloid cells 2 – TREM2*; *sialic acid binding Ig-like lectin 3 – CD33*; *Complement receptor type 1 – CR1*) encoding for immune receptors expressed on microglia are connected with an increased risk for Alzheimer's

disease (Naj et al., 2011; Guerreiro et al., 2013; Hickman et al., 2013; Bradshaw et al., 2013; Thambisetty et al., 2013).

Very similar, for mood disorders many studies could show an increased incidence of depressive episodes with increased levels of inflammatory markers and cytokines in the cerebral spinal fluid (Lanquillon et al., 2000; Miller et al., 2009; Dowlati et al., 2010; Felger and Lotrich, 2013). It has further been shown that a worsening of depressive symptoms correlates with higher levels of inflammatory markers (Nishino et al., 1989; Howren et al., 2009) and thereby suggests that inflammation is a causative factor also in mood disorders (Rosenblat et al., 2015).

A receptor that has repeatedly been associated with major depression and bipolar disorders (Lucae et al., 2006; Barden et al., 2006a; Hejjas et al., 2009; McQuillin et al., 2009; Soronen et al., 2011) and, moreover, is highly expressed in microglia and is crucially involved in the secretion of cytokines as part of the inflammatory response, is the P2X7 receptor. Due to this commonality and the comorbidity, *P2RX7* might be a link connecting mood disorders and neurodegenerative diseases and is, therefore, of high interest in the attempt to develop new therapeutic strategies for both pathologies.

5.9. The P2X receptor family

Adenosine triphosphate (ATP) is a coenzyme well known as the “cellular currency” of energy transfer (Knowles, 1980). Less famous is the molecule for acting as a signaling molecule (Holton and Holton, 1954). Receptors for ATP can be divided into two classes: metabotropic P2Y receptors, which will not be discussed further (for review see: Burnstock, 2007; Jacobson, 2010) and the ionotropic P2X receptors. The P2X receptor family comprises seven members (P2X1-7R), all ATP-activated ion channels (Alves et al., 2014).

P2X receptors are so called trimeric receptors composed of three subunits which can form homomers or heteromers (North and Jarvis, 2013). Each of these subunits consists of an intracellular C- and N-terminal domain as well as two transmembrane domains, joined by a cysteine rich ectodomain that binds ATP (Lemoine et al., 2012). Sensitivity towards the ligand ATP has been shown to be highly differing between the different members of the P2X receptor family, with P2X1R being the most and P2X7R the least sensitive (see Table 1).

P2X receptors are generally nonselective cation channels with the highest permeability for Ca^{2+} ions. The exception from this is P2X5R which also mediates permeability for negatively charged chloride ions (Lemoine et al., 2012). Three of the seven receptors (P2X2R, P2X4R and P2X7R)

further share another characteristic. Upon prolonged stimulation of the receptor with high levels of the agonist, the receptor forms a pore that is permeable for large molecules up to 900Da (Sorge et al., 2012; Young et al., 2015). This phenomenon has been best described for the P2X7 receptor where pore formation has repetitively been shown to be able to induce cell death (Sorge et al., 2012; Young et al., 2015; Kawano et al., 2012).

EC50 (µM)	P2X1R	P2X2R	P2X3R	P2X4R	P2X5R	P2X6R	P2X7R
ATP	0.07	1.2	0.5	10	10	12	100
BzATP	0.003	0.07	0.08	7	>500	-	20

Table 1: Sensitivity of human P2X receptor family members towards agonists
EC_{50} values for both, the natural ligand ATP (adenosine triphosphate) as well as for the artificial substrate BzATP (3'-O-(4-benzoyl)benzoyl adenosine 5'-triphosphate) are given. (Table modified from Khakh and North, 2012).

5.10. The P2X7 receptor

In the P2X receptor family P2X7R forms the largest subunit with 595 amino acids for both human and mouse (Surprenant et al., 1996; Chessell et al., 1998; Bradley et al., 2011). The gene coding for the human receptor *P2RX7,* is located on chromosome 12 at position 121,132,819-121,188,032 (ensembl.org - *Homo sapiens* -version 83.38). The murine counterpart *P2rx7* can be found on chromosome 5 at position 122,643,911-122,691,432 (ensembl.org – *Mus musculus* - version 83.38). Mouse and human receptor share about 80% sequence homology (see Figure 3). One important difference in functionality between human and mouse receptor is the fact that in addition to ATP, the murine receptor can also endogenously be activated by NAD^+ via ADP-ribosyltransferase, in particular the *P2rx7-k* isoform (see below) (Seman et al., 2003; Adriouch et al., 2008). The general structure of P2X7R is very similar to the other P2X receptors. A striking difference, however, is the long, intracellular C-terminus that comprises 239 aa which is significantly longer than in the rest of the family (Surprenant et al., 1996). This long C-terminal domain comprises several protein and lipid binding motifs as well as a cysteine-rich domain, including a binding domain for lipopolysaccharides (LPS) (Denlinger et al., 2001). The crystal structure of P2X7R has not been described so far. However, the structure of the zebrafish homolog of P2X4R was unraveled recently (Kawate et al., 2009; Hattori and Gouaux, 2012). Due to the substantial homology, the potential structure of P2X7R was recently proposed based on

findings of P2X4R. An individual P2X7 subunit reminds of a “leaping dolphin”, with the extracellular domain representing the body, whereas the tail is formed by the intracellular domains. Assembled as a homotrimer, forming the actual ion channel it reminds of a chalice (Sperlágh and Illes, 2014). Different to the rest of the P2X receptor family, P2X7R tends to form homooligomers. A schematic depiction of a single receptor subunit and a functional homo-trimer can be found in Figure 4. Whether or not a heteromerization with P2X4R can occur is still discussed, but latest results seem not to confirm this assumption (Guo et al., 2007; Antonio et al., 2011; Craigie et al., 2013).

```
Q99572 P2X7R_HUMAN          1    MPACCSCSDVFQYETNKVTRIQSMNYGTIKWFFHVIIFSYVCFALVSDKLYQRKEPVISS      60
Q9Z1M0 P2X7R_MOUSE          1    MPACCSWNDVLQYETNKVTRIQSTNYGTVKWVLHMIVFSYISFALVSDKLYQRKEPVISS      60
                                 ****** .**:************ ****:**.:*:*:***:.****************** 

Q99572 P2X7R_HUMAN         61    VHTKVKGIAEVKEEIVENGVKKLVHSVFDTADYTFPLQGNSFFVMTNFLKTEGQEQRLCP      120
Q9Z1M0 P2X7R_MOUSE         61    VHTKVKGIAEVTENVTEGGVTKLGHSIFDTADYTFPLQGNSFFVMTNYVKSEGQVQTLCP      120
                                 ***********.*::.* **.** **:*********************::*:*** * *** 

Q99572 P2X7R_HUMAN        121    EYPTRRTLCSSDRGCKKGWMDPQSKGIQTGRCVVYEGNQKTCEVSAWCPIEAVEEAPRPA      180
Q9Z1M0 P2X7R_MOUSE        121    EYPRRGAQCSSDRRCKKGWMDPQSKGIQTGRCVPYDKTRKTCEVSAWCPTEEEKEAPRPA      180
                                 *** * : ***** ******************* *: .:********** *  :****** 

Q99572 P2X7R_HUMAN        181    LLNSAENFTVLIKNNIDFPGHNYTTRNILPGLNITCTFHKTQNPQCPIFRLGDIFRETGD      240
Q9Z1M0 P2X7R_MOUSE        181    LLRSAENFTVLIKNNIHFPGHNYTTRNILPTMNGSCTFHKTWDPQCSIFRLGDIFQEAGE      240
                                 **.*************.************* :* :****** :*** ********:*:*: 

Q99572 P2X7R_HUMAN        241    NFSDVAIQGGIMGIEIYWDCNLDRWFHHCRPKYSFRRLDDKTTNVSLYPGYNFRYAKYYK      300
Q9Z1M0 P2X7R_MOUSE        241    NFTEVAVQGGIMGIEIYWDCNLDSWSHHCRPRYSFRRLDDKNTDESFVPGYNFRYAKYYK      300
                                 **::**:***************** * *****:*********.*: *: ************ 

Q99572 P2X7R_HUMAN        301    ENNVEKRTLIKVFGIRFDILVFGTGGKFDIIQLVVYIGSTLSYFGLAAVFIDFLIDTYSS      360
Q9Z1M0 P2X7R_MOUSE        301    ENNVEKRTLIKAFGIRFDILVFGTGGKFDIIQLVVYIGSTLSYFGLATVCIDLLINTYSS      360
                                 ***********.************************************:* **:**:**** 

Q99572 P2X7R_HUMAN        361    NCCRSHIYPWCKCCQPCVVNEYYYRKKCESIVEPKPTLKYVSFVDESHIRMVNQQLLGRS      420
Q9Z1M0 P2X7R_MOUSE        361    AFCRSGVYPYCKCCEPCTVNEYYYRKKCESIMEPKPTLKYVSFVDEPHIRMVDQQLLGKS      420
                                   *** :**:****:**.*************:*************** *****:*****:* 

Q99572 P2X7R_HUMAN        421    LQDVKGQEVPRPAMDFTDLSRLPLALHDTPPIPGQPEEIQLLRKEATPRSRDSPVWCQCG      480
Q9Z1M0 P2X7R_MOUSE        421    LQVVKGQEVPRPQMDFSDLSRLSLSLHDSPLTPGQSEEIQLLHEEVAPKSGDSPSWCQCG      480
                                 ** ********* ***:***** *:***:*  *** ******::*.:*:* *** ***** 

Q99572 P2X7R_HUMAN        481    SCLPSQLPESHRCLEELCCRKKPGACITTSELFRKLVLSRHVLQFLLLYQEPLLALDVDS      540
Q9Z1M0 P2X7R_MOUSE        481    NCLPSRLPEQRRALEELCCRRKPGRCITTSKLFHKLVLSRDTLQLLLLYQDPLLVLGEEA      540
                                 .****:***.:*.*******:*** *****:**:*******..**:*****:***.*  :: 

Q99572 P2X7R_HUMAN        541    TNSRLRHCAYRCYATWRFGSQDMADFAILPSCCRWRIRKEFPKSEGQYSGFKSPY          595
Q9Z1M0 P2X7R_MOUSE        541    TNSRLRHRAYRCYATWRFGSQDMADFAILPSCCRWRIRKEFPKTEGQYSGFKYPY          595
                                 ******* ************************************:******** ** 
```

Figure 3: Protein sequence homology of human and murine P2X7 receptor
Protein sequence comparison showed 481 identical and 73 similar positions. This results in a 80.84% sequence homology rating of http://www.uniprot.org. * (asterisk) indicates positions which have a single, fully conserved residue; : (colon) indicates conservation between groups of strongly similar properties - scoring > 0.5 in the Gonnet PAM 250 matrix; . (period) indicates conservation between groups of weakly similar properties - scoring =< 0.5 in the Gonnet PAM 250 matrix.

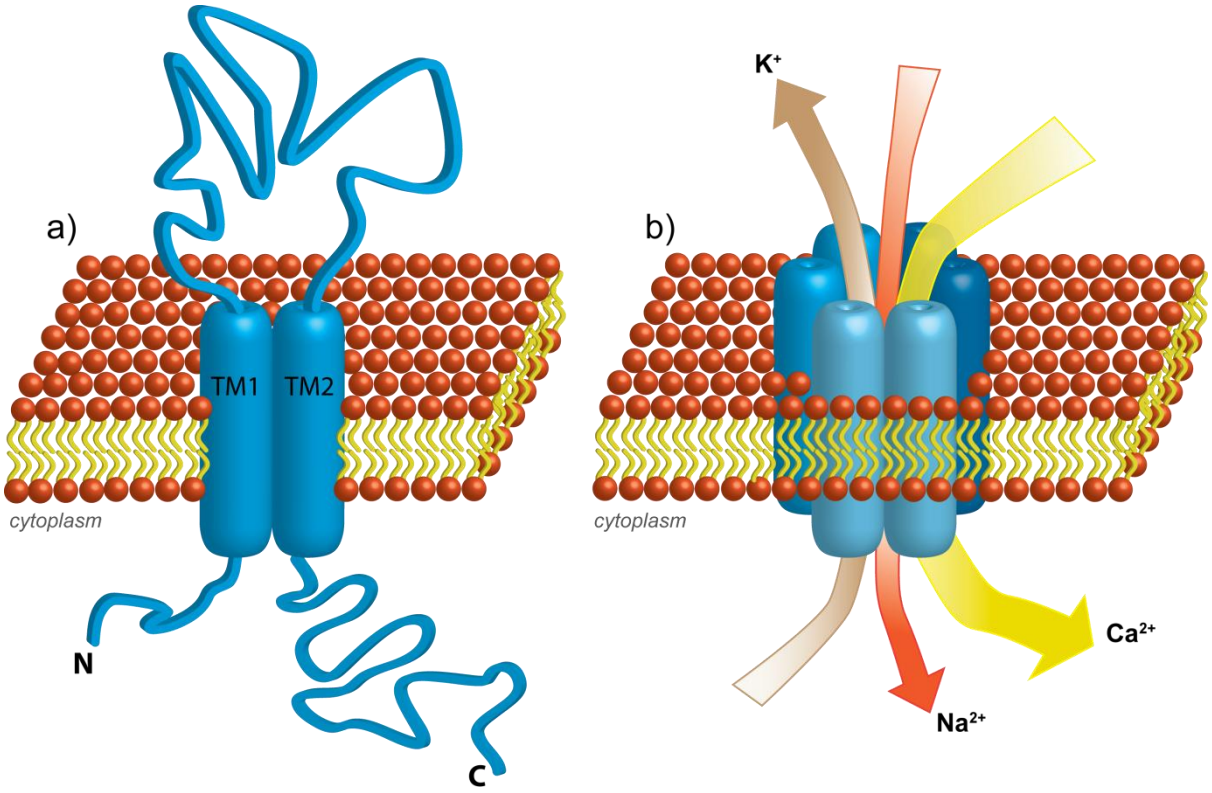

Figure 4: Single P2X7 receptor subunit and functional homo-trimer bound to the membrane
a) A single P2X7R subunit with cytoplasmic N- and C-terminus, two transmembrane (TM) domains and extracellular loop is shown; **b)** The functional ion channel consisting of three receptor subunits. Ion currents are indicated; for simplicity reasons extra- and intracellular domains are not shown. Subunits are depicted in different blue shades.

Another form of heteromerization of the P2X7 receptor occurs with different isoforms of the receptor. It has been shown that this strongly affects the functionality of the receptor (Surprenant et al., 1996; North, 2002; Adinolfi et al., 2005).

Whereas for the human *P2RX7* gene 13 transcripts have been found until now (http://www.ensembl.org - ENSG00000089041), for the mouse there are significantly less described. Only five have been identified so far: *P2rx7*-a, *P2rx7*-b, *P2rx7*-c, *P2rx7*-d and *P2rx7*-k (Figure 5) (Nicke et al., 2009; Masin et al., 2012; Schwarz et al., 2012). *P2rx7*-b to *P2rx7*-d are characterized by a truncated C-terminus. In addition, the first exons in *P2rx7*-c and *P2rx7*-d are altered (Kido et al., 2013). It has repeatedly been shown that in particular the C-terminally truncated isoforms have a negative regulatory effect on the receptor function when co-expressed in a receptor trimer (Surprenant et al., 1996; North, 2002; Adinolfi et al., 2005; Masin et al., 2012). *P2rx7*-k is characterized by an alternative exon 1, whereas exons 2-13 are conserved. This isoform seems not to disturb the common receptor function. However, it shows higher sensitivity towards the endogenous agonist ATP. It has further been shown that different

to the most abundant isoform *P2rx7*-a, it can also be activated by NAD^+ via ADP-ribosylation. Moreover, the expression of these two isoforms in the brain differs. It has been shown that *P2rx7*-a is predominantly expressed in regulatory T cells whereas *P2rx7*-k is mostly expressed in macrophages in the brain (Schwarz et al., 2012).

In general, activation of the P2X7 receptor by ATP leads to the influx of calcium ions into the cell. This event can trigger a variety of cellular responses strongly depending on the type of cell (Sperlágh and Illes, 2014). The P2X7 receptor is a main component of the inflammasome complex and in this context its major function is providing the external stimulus for the subsequent release of proinflammatory cytokines. P2X7R mediated release has been shown for different cytokines like IL-1β (Clark et al., 2010), IL-6 (Shigemoto-Mogami et al., 2001), tumor necrosis factor α (TNFα) (Hide et al., 2000) and cyclooxygenase-2 (COX-2) (Aga et al., 2002) . The most comprehensive and best described connection between P2X7R and cytokine release can be found for IL-1β (Solle et al., 2001; Ferrari et al., 2006). P2X7R has been shown to facilitate the processing of the IL-1β precursor to its biological active form by triggering the formation of the NLRP3 inflammasome and the activation of caspase-1 (Schroder and Tschopp, 2010).

In the central nervous system P2X7R activation leads to the release of neurotransmitters into the extracellular space. The most prominent neurotransmitter in the brain, glutamate has been shown to be released upon stimulation of the P2X7 receptor in the rat brain (Sperlágh et al., 2002). P2X7R-mediated glutamate release accounts for both neurons as well as astrocytes (Duan et al., 2003; Marcoli et al., 2008; Fu et al., 2013). However, it is discussed that neuronal glutamate release upon stimulation of the P2X7 receptor is an indirect event mediated by glutamate release of astrocytes which then subsequently leads to the actual release of glutamate from nerve terminals (Sperlágh and Illes, 2014).

Another described function of P2X7Rs is signaling to downstream components like effector enzymes and protein kinases. Via this P2X7Rs are involved in gene regulation and expression and thereby affect long term events like cell proliferation and growth as well as apoptosis (Duan and Neary, 2006). The best described downstream target in this context is the extracellular signal regulated protein kinase (ERK) (Panenka et al., 2001; Watters et al., 2002; Gendron et al., 2003; Stefano et al., 2007).

Due to the regulative effect of ectonucleotidases on the concentration of the endogenous P2X7R ligand ATP in the extracellular space, it was speculated that P2X7R might only be activated among injury, infection or in tumor environment (Yegutkin, 2008; Lenertz et al., 2011). Alternative speculations consider a possible allosteric modulation of the receptor *in vivo* that

increases the affinity to ATP and thereby also allows for activation upon lower levels of nucleotide concentration (Bartlett et al., 2014).

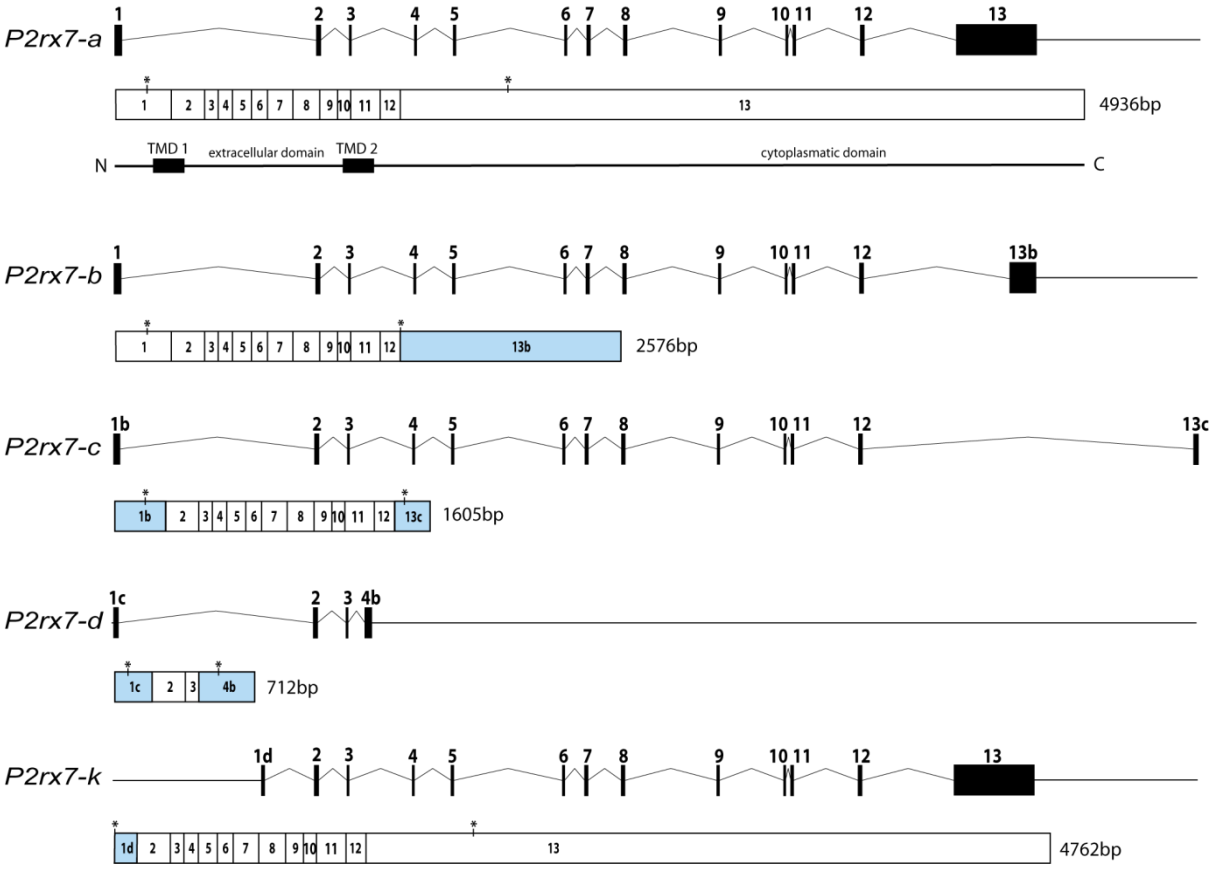

Figure 5: Known splice variants of the murine *P2rx7* gene
Five *P2rx7* splice variants have been described in the mouse. For every variant the genomic locus with exons and introns as well as the resulting mRNA with spliced exons is shown. Relative intron to exon sizes as well as exon sizes of the respective transcripts are true to scale. Exons that differ in the alternative transcripts are highlighted in light blue. Translational start and stop codons are indicate by asterisks. For *P2rx7*-a additionally the protein domain structure is depicted.

5.11. Published *P2rx7* knockout mouse lines

With the P2X7R being involved and associated in various pathologies the necessity for mouse models emerges. There are three mouse lines published so far that were claimed to lack *P2rx7* expression. All three were either directly - or indirectly by funding - established by pharmaceutical companies. A scheme of how disruption of the *P2rx7* expression was intended to be achieved is depicted in Figure 6. However, recent publications indicate that some of the above mentioned *P2rx7* isoforms escape inactivation in some of these “knockout” lines. The first published knockout line that was created by Pfizer has a neomycin-cassette insertion in exon 13

that replaces 80bp of the gene and by that supposedly disrupts protein function (Solle et al., 2001). The splice variants *P2rx7*-b, -c, and -d, however, escape this approach (compare Figure 5). The knockout lines created by Glaxo Smith Kline (GSK) and Lexicon Genetics follow a similar approach by inserting a selection and LacZ reporter cassette. In the GSK line this cassette replaces parts of exon 1 (Chessell et al., 2005). However, due to the alternative exons the isoforms *P2rx7*-c, -d, -e are not inactivated by this insertion approach (compare Figure 5). In the third published knockout line exon 2 and 3 are replaced by a LacZ reporter-selection cassette (Basso et al., 2009). This should indeed lead to the successful disruption of all five splice variants. However, this mouse line has not been used except in the original publication by Basso *et al.* from 2009.

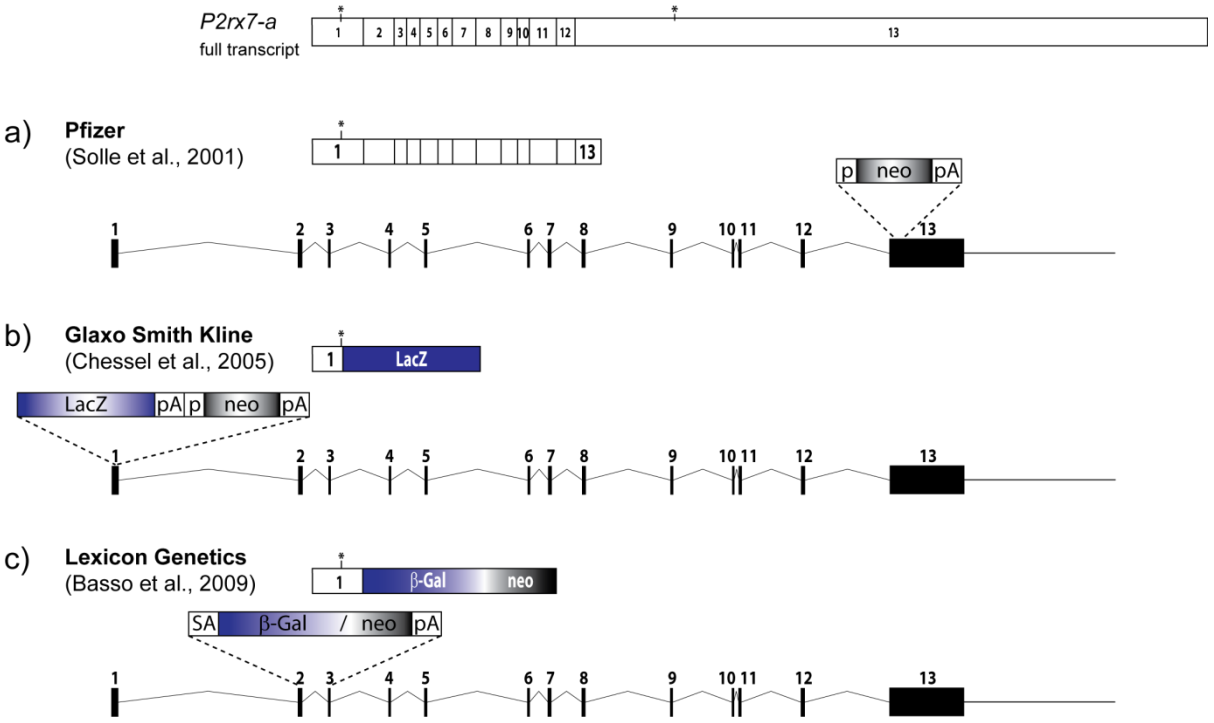

Figure 6: Published *P2rx7* knockout mouse lines
Depicted are the applied targeting strategies to disrupt the *P2rx7* gene in respective mouse lines. **a)** The knockout developed by Pfizer is mediated by replacing 28 aa of exon 13 with a PGK-neomycin selection cassette (for detailed information see US-patent number: US 6677501 B2) leading to a C-terminally truncated transcript. **b)** In the GSK mice the knockout is achieved by the integration of a LacZ/neo expression construct (compare Le Mouellic et al. (1990)) 2bp after the initial ATG. This results in a fusion transcript of the beginning of exon 1 and LacZ. **c)** The strategy of Lexicon Genetics was to replace big parts of the gene (exon 2 – 3) by a gene trap vector comprising a splice acceptor followed by the β-Gal/neo reporter selection cassette and a polyA sequence. This should lead to the truncation of the transcript after exon 1, followed by the LacZ reporter. For comparison the full transcript of *P2rx7*-a is shown. Translation start and stop sites are indicated by asterisks; p: promotor; pA: polyadenylation signal.

5.12. Constitutive knockout mice

To study the function of the P2X7 receptor in an *in vivo* model and to overcome the above described drawbacks of the published knockout lines, a new *P2rx7* knockout mouse line was previously established in our lab. This new mouse line is characterized by deletion of a 2.3kb segment of the *P2rx7* gene including exon 2 and the introduction of a LacZ reporter-selection cassette. This approach leads to a frameshift due to the deletion of exon 2 combined with truncation of the transcript caused by the additional integration of a triple transcriptional termination sequence in the cassette (compare Figure 7) (Walser, 2012). Homozygous *P2rx7* knockout mice are fully vital and reproduce normally. No pathological alterations were observed in these mice. The absence of *P2rx7* transcript was successfully demonstrated by *in situ* hybridization. Furthermore, the functional disruption of the receptor was confirmed by the inability of immune cells obtained from those mice, to release IL-1β upon stimulation with LPS and BzATP. Moreover, cells isolated from this new *P2rx7* knockout mice were characterized by a significantly reduced calcium influx into the cell upon stimulation with agonist BzATP compared to wild-type controls (Walser, 2012).

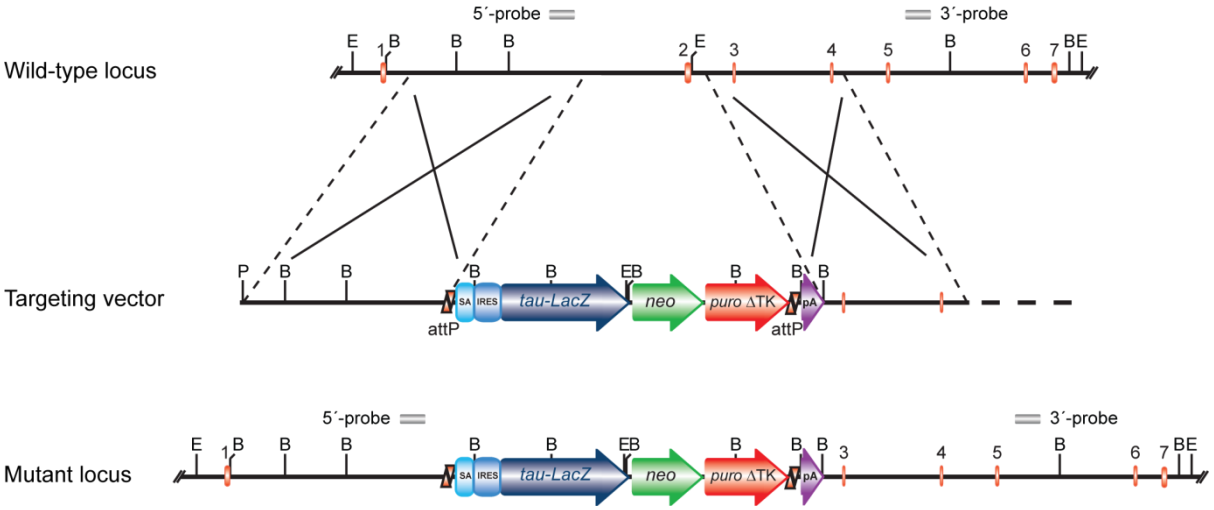

Figure 7: Targeting scheme for the generation of *P2rx7* knockout mice
Strategy to inactivate the *P2rx7* gene. The wild-type locus, the targeting vector and the final recombined locus are depicted (B: BamHI; E: EcoRI; P: PacI; SA: splice acceptor; IRES: internal ribosome entry site; neo: neomycin; pA: polyadenylation signal)
(Figure modified from Walser, 2012)

A basal behavioral characterization of this new knockout line was previously conducted. Both males and females were analyzed in regard to locomotion, anxiety-related and stress coping-

behavior. Indeed female *P2rx7* knockout mice showed reduced floating in the forced swim test paradigm (FST), indicating a less active stress coping behavior compared to wild-type mice. Also anxiety was slightly elevated in female knockouts as indicated by the open field test (OF). However, other paradigms investigating anxiety could not further confirm these findings. Moreover, in males deficient for the P2X7 receptor no behavioral alterations were observed using a comprehensive behavioral test battery. A comparison with previous publications characterizing the already published *P2rx7* knockout lines shows substantial discrepancies in the results (Figure 8). The only somewhat similar outcome was found in the forced swim test paradigm, namely a more active stress coping phenotype as manifested in reduced floating and increased struggling. However, the way these experiments were conducted (gender, duration, time of repetitions, breeding and housing of the mice) shows strong inconsistencies which disputes the conclusions (Basso et al., 2009; Boucher et al., 2011; Csölle et al., 2012). We could not observe this effect in our own newly generated knockout line. A final statement whether or not the knockout of the P2X7 receptor leads to phenotypic behavioral alteration seems therefore difficult and cannot finally and conclusively be given.

mouse line (created by)	publication	type of knockout	gender	active stress-coping	anxiety	locomotion
Glaxo Smith Kline (Chessel et al., 2005)	Sim et al., 2004	conventional	-	-	-	-
Pfizer (Solle et al.,2001)	Boucher et al., 2011	conventional	♀	↑ (FST, day 2 and 3)	↑(EPM); no difference (DaLi)	↓ (DaLi)
	Csölle et al., 2012	conventional	♂	"↑" (FST); ↑(TST)	no difference (OF, EPM)	-
Lexicon Genetics (Basso et al., 2009)	Basso et al., 2009	conventional	♂	↑ (TST, FST)	no difference (EPM, NSF)	no difference (OF)
MPI of Psychiatry (RG Dr. Jan Deussing)		conventional	♀	↓ (FST)	"↑" (OF, DaLi)	no difference (OF, DaLi)
			♂	no difference (FST)	no difference (OF, DaLi)	no difference (OF, DaLi)

Figure 8: Comparison of basal behavioral phenotypic screenings of different *P2rx7* knockout mouse lines
EPM: elevated plus maze; FST: forced swim test; DaLi: dark-light box; NSF: novelty suppressed feeding; OF: open field; TST: tail suspension test; ↑: elevated; ↓: decreased

5.13. Conditional knockout mice

A second *P2rx7* mouse line was previously established in our lab. This mouse line expresses the human *P2RX7* transcript under the murine *P2rx7* regulatory elements. The initial motivation to establish this mouse was to investigate a single point mutation (single nucleotide polymorphism

- SNP) of *P2RX7* that has repeatedly been associated with increased risk for major depression (Lucae et al., 2006; Barden et al., 2006a; Hejjas et al., 2009; McQuillin et al., 2009; Soronen et al., 2011). Therefore, mouse lines were established in our lab in which parts of the murine *P2rx7* gene were replaced by a construct which allows expression of human wild-type *P2RX7* or human *P2RX7* containing the SNP, respectively. These mouse models would allow to investigate the molecular effects of the SNP on receptor function in an *in vivo* model (for further information see (Walser, 2012)). The construction of these "humanized" *P2RX7* mice, however, further allows for Cre-mediated inactivation of the *P2rx7* gene. The murine *P2rx7* gene is, similar to the above mentioned conventional knockout, partially (exon 2) replaced and, therefore, disrupted by the construct. Furthermore, the cassette for expression of human *P2RX7* can be excised which is achieved by Cre-mediated recombination between the *loxP* sites flanking the human *P2RX7* sequence. This ultimately results in an inactivated *P2rx7* locus lacking exon 2 but comprising the remaining polyA signal leading to a truncated murine transcript (Figure 9).

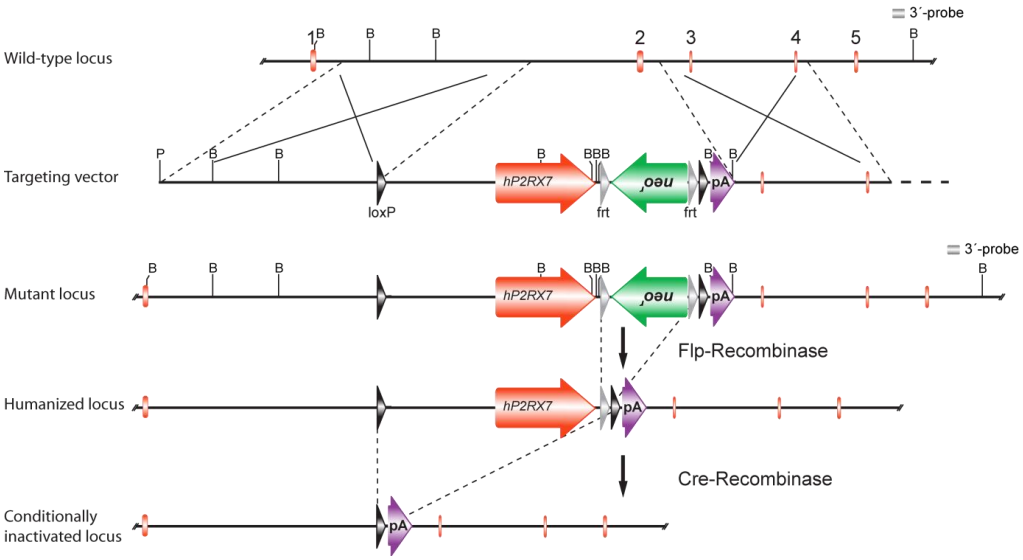

Figure 9: Targeting scheme for the generation of humanized *P2RX7* and conditional *P2rx7* knockout mice
Strategy to humanize the *P2rx7* locus and the resulting liability towards Cre recombinase-mediated inactivation of the gene are depicted. (B: BamHI; P: PacI; *loxP*: locus of crossover in P1 site; *hP2RX7*: human *P2RX7* cDNA; *frt*: flippase recognition target site; neo: neomycin; pA: polyadenylation signal) (Figure modified from Walser, 2012)

6. Aims of the thesis

The aim of this thesis was to more deeply investigate the function and possible involvement of the P2X7 receptor in mental disorders, mainly major depression and the neurodegenerative AD pathology. The bases for this work were two previously established *P2rx7* knockout mouse lines (Walser, 2012) - a conventional knockout mouse line (compare 5.12 and Figure 7) and a conditional knockout mouse line that is based on floxed "humanized" *P2RX7* mice, allowing for temporal and spatial control of the receptor (compare 5.13 and Figure 9).

The following questions were the main subjects of this thesis:

1) **Are the newly established knockout mouse lines full knockouts for all splice variants and is the receptor function indeed disrupted?**

   To address these questions we conducted RT-PCRs specific for all known splice variants of the murine *P2rx7* gene. The functional disruption of the receptor was studied by different readouts like the capacity to trigger calcium influx, cytokine secretion and Yo-Pro-1-iodide uptake upon stimulation of the P2X7 receptor.

2) **Does the loss of the P2X7 receptor have behavioral phenotypic consequences?**

   We tested our different knockout mouse lines in a variety of different behavioral paradigms, mainly for locomotion, anxiety- and depression-related, as well as stress-coping behavior. Depending on the knockout line we tested the mice under basal conditions (conditional knockout) or after chronic social defeat stress (conventional knockout).

3) **Are there functional differences between the human and murine P2X7 receptor?**

   Differences between human and murine P2X7 receptor e.g. with regard to ligand affinity have been described before, however, only in constitutively expressing *in vitro* models. Here we tested both the murine as well as the human receptor, endogenously expressed in primary cells of established mouse models regarding their sensitivity towards the ligand BzATP and pharmacological modulators of receptor activity. For that we compared the pore formation capacities of these cells.

   We further conducted a basal behavioral comparison of mice expressing the murine P2X7 receptor versus mice expressing the human counterpart.

4) **In which cells and to which extent is the P2X7 receptor expressed in the murine brain?**

To unravel this question we conducted both *in situ* hybridization analyses as well as quantitative real-time PCRs. All these analyses are based on breedings of the conditional knockout mice with tissue- / cell type-specific Cre recombinase driver lines.

5) **Does the P2X7 receptor have an influence on Alzheimer's disease pathology and if yes what kind of effect does it have and how is it mediated?**

To enlighten this question we combined *P2rx7* knockout mice with a well-established AD mouse model. The offspring underwent different behavioral screenings with the focus on memory and cognition. Further, we compared the APP processing and the Aβ plaque formation in these mice.

This study comprises one of the most complete expressional analyses of the P2X7 receptor in the murine brain today. It further validates the effectiveness and importance of two new *P2rx7* knockout mouse models as well as a mouse model expressing the human P2X7 receptor under the control of endogenous murine regulatory elements of the gene. Thereby, this work will strongly contribute to better understand the function and functional involvement of the P2X7 receptor in various pathologies.

7. Materials and methods

7.1. Materials

7.1.1 Mouse lines

All animal experiments were conducted in accordance with the guidelines of the government of Bavaria (Germany) for the care and use of laboratory mice. All mice were housed under standard laboratory conditions (temperature: 21 ± 1°C; relative humidity: 50 ± 10 %) and were kept on a 12h dark-light cycle (7:00am-7:00pm) with food *ad libitum*.

External mouse lines used for the experiments:

Name (referred to in the thesis)	Features	Original publication
Alpha6	Expresses Cre recombinase under the Alpha6 promotor	(Aller et al., 2003)
Cnp	Expresses Cre recombinase under the Cnp-promotor	(Lappe-Siefke et al., 2003)
Cx3cr1	Expresses Cre recombinase under the Cx3cr1-promotor	(Yona et al., 2013)
Deleter	Expresses Cre recombinase under the Rosa26-promotor	(Otto et al., 2009)
Dlx	Expresses Cre recombinase under the Dlx5/6-promotor	(Monory et al., 2006)
En1	Expresses Cre recombinase under the En1-promotor	(Kimmel et al., 2000)
Glast	Expresses Cre recombinase under the Glast-promotor	(Mori et al., 2006)
Nes	Expresses Cre recombinase under the Nestin promotor	(Tronche et al., 1999)
Nex	Expresses Cre recombinase under the Nexin promotor	(Goebbels et al., 2006)
ArcAβ	Carries transgene for human APP with swe/arc mutation	(Knobloch et al., 2007)

7.1.2 Antibodies

Primary antibodies:

Antibody		Company, product #	Application	dilution
Anti-*P2rx7* / C-term (rabbit)		Alomone, APR-004	WB	1:1000
Anti-*P2rx7* / N-term (rabbit)		Alomone, APR-008	WB	1:200
Anti-GFAP (rabbit)		DakoCytomation, Z 0334	IHC	1:1000
Anti-Iba1 (rabbit)		Wako Chemicals (019-19741)	IHC	1:1000
Anti-1-16 β-amyloid/6E10 (mouse)		Signet, SIG-39320	IHC, WB	1:500/1:1000
Anti-β-actin (rabbit)		Cell Signalling, #4967S	WB	1:2000
Anti-tubulin (rat)		Abcam, ab6160	WB	1:10.000
Anti-calnexin (rabbit)		kind gift of Michael Willem	WB	1:5000
APP	22C11 (mouse)	kind gift of Michael Willem	WB	1:5000
	2D8 (rat)	kind gift of Michael Willem	WB	1:100
	3F5 (rat)	kind gift of Michael Willem	WB	5µg/ml
	IBL18957 (rabbit)	kind gift of Michael Willem	WB	1:2000
	M3.2 (mouse)	kind gift of Michael Willem	WB	1:2000
	SIG-39151 (rabbit)	Sigmet kind gift of Michael Willem	WB	1:2000
	Y188 (rabbit)	kind gift of Michael Willem	WB	1:4000

Secondary antibodies:

Antibody	Company, product #	Application	dilution
Anti-rabbit (Alexa 488/594)	Invitrogen	IHC	1:1000
Anti-mouse (Alexa 488/594)	Invitrogen	IHC	1:1000
Anti-chicken (Alexa 488/594)	Invitrogen	IHC	1:1000
Anti-rabbit (HRP-linked)	Cell Signalling	WB	1:1000
Anti-mouse (HRP-linked)	Cell Signalling	WB	1:1000
Anti-chicken (HRP-linked)	Cell Signalling	WB	1:1000

7.1.3 Oligonucleotides

All DNA oligos were purchased from Metabion AG (Planegg).

Oligos used for genotyping:

Name	Sequence 5'-3'	Comment
ArcAb-Prp-sens	CAG AAC TGA ACC ATT TCA ACC GAG C	180bp product
ArcAb-hAPPdn	TCA GTG GGT ACC TCC AGC GCC CGA G	
Cnp-Cre E3s	GCC TTC AAA CTG TCC ATC TC	Cnp-Cre E3s+E3as (wild-type) resulted in 1,180bp fragment; Cnp-CreE3s+puro3 (mutant) in 894bp
Cnp-Cre E3as	CCC AGC CCT TTT ATT ACC AC	
Cnp-Cre puro3	CAT AGC CTG AAG AAC GAG A	
CTSQ-up	ACA AGG TCT GTG AAT CAT GC	1098 bp product
CTSQ-dn	TTA CAA TGT GGA TTT TGT GGG	
Cx3cr1-Cre 14278	CTC CCC CTG AAC CTG AAA C	mutant = ~500 bp wild-type = 410 bp
Cx3cr1-Cre 14277	CCC AGA CAC TCG TTG TCC TT	
Cx3cr1-Cre 14276	GTC TTC ACG TTC GGT CTG GT	
CRE-F	GAT CGC TGC CAG GAT ATA CG	372bp product
CRE-R	AAT CGC CAT CTT CCA GCA G	
Dlx-Cre for	CAC GTT GTC ATT GGT GTT AG	313bp product
Dlx-Cre rev	CCG GTC ATG ATG TTT TAT CT	
Glast-Cre F8	GAG GCA CTT GGC TAG GCT CTG AGG A	GlastF8+GlastR3 (wild-type) results in 700bp band; GlastF8+GlastCER1 (mutant) in 400bp
Glast-Cre R3	GAG GAG ATC CTG ACC GAT CAG TTG G	
Glast-Cre CER1	GGT GTA CGG TCA GTA AAT TGG ACA T	
h*P2RX7*_mIntron1_for	AGA CTG TCA CCA GCA GCA GCT C	mIntron1_for+mIntron2_rev (wild-type) 933bp product; mIntron1-for+hEx6-7_rev (mutant) 613bp
h*P2RX7*_hEx6-7_rev	CAG GAT GTT TCT CGT GGT GTA G	
h*P2RX7*_mIntron2_rev	CAT ACA CTT CTC CGT GGT CTA C	
h*P2RX7*_KO_for	GCA GTC TCT CTT TGC CTC GT	186bp product
h*P2RX7*_KO_rev	CGT CGA CTG TCT TCT GGT CA	
NexCre 4	GAG TCC TGG AAT CAG TCT TTT TC	Cre4+Cre5 (wild-type) results in 770bp product; Cre4+Cre6 (mutant) in 525bp
NexCre 5	AGA ATG TGG AGT AGG GTG AC	
NexCre 6	CCG CAT AAC CAG TGA AAC AG	

Nes-Cre rev	CGG GAA ACC ATT TCC GGT TA	595bp product
191f	ACT TTG GTT CTT CTC TTC TGC ACC CGG ATG	
***P2rx7*-108**	GCA GTC TCT CTT TGC CTC GT	108+134 (wild-type) results in 536bp product; 108+137 (mutant) in 369bp
***P2rx7*-134**	CAC TTG CTG ACA AGA TTG AC	
***P2rx7*-137**	CGG ATC CAC TAG TTC TAG AG	

Oligos used for qRT-/RT- PCRs:

Name	Sequence 5'-3'	Comment
LC_hP2RX1-for	GGC CCT TGA GTT TCA CAG AG	All qRT-oligos were designed to amplify ~100bp products
LC_hP2RX1-rev	GTC CTG GTC TAC GTC ATC GG	
LC_hP2RX2-for	CCC TTG ACC TTG GTG ATG AT	
LC_hP2RX2-rev	ACT ACG AGA CGC CCA AGG T	
LC_hP2RX3-for	CAC TGC CAT TTT CCA TTT TG	
LC_hP2RX3-rev	AAT ACT CCT TCA CCC GGC TC	
LC_hP2RX4-for	CCC TGT GTC TGG TTC ATG GT	
LC_hP2RX4-rev	GTG CAA CTG CTC ATC CTG G	
LC_hP2RX5-for	CAG GTC GCA GAA GAA AGC A	
LC_hP2RX5-rev	GAT ATT ACC GAG ACG CAG CC	
LC_hP2RX6-for	ACT TCG TGA AGC CAC CTC AG	
LC_hP2RX6-rev	CCC TAG GAG GCA AGT CTC AA	
LC_h*P2RX7*-for3	ATG TCA AGG GCC AAG AAG TC	
LC_h*P2RX7*-rev3	AGG AAT CGG GGG TGT GTC	
LC_mP2RX1-for	GCT TGT CAC TCA CCA GAG CA	
LC_mP2RX1-rev	TCT TAG GCA GGA TGT GGA GC	
LC_mP2RX2-for	CGT GTG GTA CGT CTT CAT CG	
LC_mP2RX2-rev	TGG CAG GTA GAG CTG TGA AC	
LC_mP2RX3-for	ACA AGA TGG AGA ATG GCA GC	
LC_mP2RX3-rev	GCA GGA TGA TGT CAC AGA GAAC	
LC_mP2RX4-for	GAC CAA CAC TTC TCA GCT TGG	
LC_mP2RX4-rev	GTG ACG ATC ATG TTG GTC ATG	
LC_mP2RX5-for	GCC TAT ACC AAC ACC ACG ATG	

LC_mP2RX5-rev	CTT CAC GCT CAG CAC AGA TG
LC_mP2RX6-for	GTT AAG GAG CTG GAG AAC CG
LC_mP2RX6-rev	AGG ATG CTC TGG ACA TCT GC
LC_m*P2RX7*-for3	CTG GTT TTC GGC ACT GGA
LC_m*P2RX7*-rev3	CCA AAG TAG GAC AGG GTG GA
hRPL19 for	GGA TTC TCA TGG AAC ACA
mRPL19 for	GCA TCC TCA TGG AGC ACA T
m/hRPL19 rev	CTG GTC AGC CAG GAG CTT
LC_Aif1(iba1)-for (mouse)	CCA AAC CAG GGA TTT ACA GG
LC_Aif1(iba1)-rev (mouse)	CGT CTA GGA ATT GCT TGT TGA TCT
LC_GFAP-for (mouse)	ACC AGC TTA CGG CCA ACA G
LC_GFAP-rev (mouse)	CCA GCG ATT CAA CCT TTC TCT
LC_Synaptophysin-for (mouse)	AGT GCC CTC AAC ATC GAA GTC
LC_Synaptophysin-rev (mouse)	CGA GGA GGA GTA GTC ACC AAC
LC_CatepsinS-for (mouse)	CCA TTG GGA TCT CTG GAA GAA AA
LC_CatepsinS-rev (mouse)	TCA TGC CCA CTT GGT AGG TAT
LC_Synapsin-for (mouse)	GAG CAG ATT GCC ATG TCT GA
LC_Synapsin-rev (mouse)	CAC TGC GCA GAT GTC AAG TC
P2X7	
LC_mouse Exon1 for	CAC ATG ATC GTC TTT TCC TAC
LC_mouse Ex2rev2	CCC TCT GTG ACA TTC TCC G
LC_human Ex2rev2	TTC TCC ACG ATC TCC TCT T
LC_Ex2rev3_m/h	GCA AAG GGA AGG TGT AGT C
HPRT-fwd	GTC AAG GGC ATA TCC AAC AAC AAA C
HPRT-rev	CCT GCT GGA TTA CAT TAA AGC ACT G

Oligos used for splice variants analysis:

1st round

Primername	Exon	code for scheme	sequence 5'-3'
Ex1-for	1	A	cgcccccgctgcagtcactg
Ex13-rev	13	B	cgtggagagatagggacagcc
Ex12-for	12	E	cgttgaagtatgtgtcctttgtcg
Ex13b-rev	13b	F	ttcttaaataaatgaattgaaatcaag
Masin mX7-j-for	4	I	tgctcttctgaccggcgttg
Masin X713c-rev	13c	J	tcaggtgcgcatacatacatg
Nicke Primer 1-for	1c	M	cacatgatcgtcttttcctac
Ex4b-rev	4b	N	tgaccattctcctggctgac
Nicke Primer 1'-for	1d	Q	gcccgtgagccacttatgc
Nicke Ex5-rev	5	R	ccttgtcttgtcatatggaac

2nd round

Primername	Exon	code for scheme	sequence 5'-3'
Ex1-for2	1	C	ccgctgcagtcactggag
Ex13rev2	13	D	gtcggagaagtccatctggggtc
Ex12-for2	12	G	gcatggtggaccagcagctgc
Ex13/13b-rev2	13/13b	H	cagtcgtccaggaagtcagccg
Masin Exon9-for	9	K	gagaacaatgtggaaaagcgg
Ex13c-rev2	13c	L	catgcaggcaaagcacccgtac
Ex2-for	2	O	tggtgagcgataagctgtac
Ex4b-rev2	4b	P	caagtatctgcctccctttgagc
Ex1d-fwd2	1d	S	gcatatggatcgggacgctgaag
Nicke Exon4-rev	4	T	ggtcagaagagcactgtgc

Table 2: RT-PCR primers used to specifically detect different *P2rx7* isoforms
The different primer sequences form 5' to 3' are given. Nested PCRs were conducted. Primers of first round of PCR are depicted in the left table, those of the second round are given in the right table. For a scheme of the binding sites of the primers see Figure 10)

7.1.4 Buffers and solutions

All chemical and solutions were purchased from Carl Roth (Karlsruhe) or Sigma-Aldrich (Munich) if not stated differently.

7.1.4.1. Standard buffers for agarose gel electrophoresis

6 x DNA loading buffer (orange)

1g	orange G
10ml	2 M TRIS/HCL, pH 7.5
150ml	glycerol
adjust volume to 1 l	H_2O_{bidest}

1 x Tris acetate EDTA (TAE) buffer

4.84g	tris(hydroxylmethyl)-amino methane (TRIS)
1.142ml	acetic acid
20ml	0.05 M ethylendiaminetetraacetate (EDTA), pH 8.0
800ml	H_2O_{bidest}

⇨ adjust pH to 8.3 with acetic acid

adjust volume to 1l	H_2O

7.1.4.2. *in situ* hybridization buffers and solutions

10 x Phosphate buffered saline (PBS)

1.37M	NaCl
27mM	KCl
200mM	Na_2HPO_4 x 12 H_2O (Merck, Darmstadt)
20mM	KH_2PO_4 (Merck)
adjust volume to 1l	H_2O_{bidest}

⇨ adjust pH to 7.4

DEPC- H_2O

1l	H_2O_{bidest}
add 1ml	diethylpyrocarbonate (DEPC)

⇨ incubate overnight and autoclave 2x

20% Paraformaldehyde (PFA)

1000g	paraformaldehyde
in 5l	1x PBS-DEPC

⇨ adjust pH to 7.4

10 x Triethanolamine (TEA)

1.0M	TEA
adjust volume to 1l	H_2O_{bidest}

⇨ adjust pH to 8.0

1ml	DEPC

⇨ incubate overnight and autoclave 2x

20 x Standard saline citrate (SSC)

3M	NaCl
300mM	sodium citrate
adjust volume to 1l	H_2O_{bidest}

⇨ adjust pH to 7.4

1ml	DEPC

⇨ incubate overnight and autoclave 2x

5 x NTE

146.1g	NaCl
50ml	1M TRIS/HCl, pH 8.0
50ml	0.5M EDTA, pH 8.0
adjust volume to 1l	H_2O_{bidest}

⇨ adjust pH to 7.4

1ml	DEPC

⇨ incubate overnight and autoclave 2x

Hybridization mix

50ml	formamide
1ml	2M TRIS/HCl, pH 8.0
1.775g	NaCl
1ml	0.5M EDTA, pH 8.0
10g	dextran sulphate
0.02g	ficoll 400
0.02g	polyvinylpyrrolidone 40
0.02g	bovine serum albumin (BSA)
5ml	tRNA (10mg/ml) (Roche Diagnostics GmbH, Mannheim)
1ml	carrier DNA (salmon sperm, 10mg/ml)
4ml	5 M dithiothreitol (DTT) (Roche Diagnostics GmbH, Mannheim)

⇨ stored as 5 ml aliquots at -80°C

Hybridization chamber fluid

250ml	Formamide
50ml	20 x SSC
200ml	H_2O_{bidest}
5M	DTT/DEPC
7.715g	DTT
4ml	H_2O-DEPC

⇨ shake falcon tube until the powder is nearly solved

adjust volume to 10l	H_2O-DEPC

3 M NH_4OAc

3.0M	ammonium acetate (NH_4OAc)
in	H_2O_{bidest}

7.1.4.3. Protein isolation

RIPA buffer

20mM	TRIS/HCl
150mM	NaCl
1mM	Na_2EDTA
1mM	EGTA
1%	NP-40
1%	Sodium deoxycholate
2.5mM	Sodium pyrophosphate

⇨ add protease inhibitor mix

DEA buffer

50mM	NaCl
0.2%	Diethylamine

⇨ add protease inhibitor mix and adjust pH to 10

7.1.4.4. Western blot buffers

10 x TBS

200mM	TRIS/HCl
1.35M	NaCl
adjust volume to 1l	H_2O_{bidest}

⇨ adjust pH to 7.6

TBS-T

1ml	Tween20
100ml	10x TBS
adjust volume to 1l	H_2O_{bidest}

Blocking solution and solution for antibodies

0.2%	I-Block (Applied Biosystems) **or**
5%	milk
0.1%	Tween-20
adjust volume	1 x PBS

Lämmli 4x

40%	Glycerol (v/v)
0.25M	TRIS/HCl
8%	SDS
0.008%	Bromphenol blue
in	H_2O_{bidest}
add 7.5%	ß-mercapto-EtOH prior to use.

Running buffer

25mM	TRIS/HCl
190mM	Glycine
0.1%	Sodium dodecyl sulfate (SDS)
in	H_2O_{bidest}

7.1.4.5. Solutions for immunohistochemistry

Blocking solution

4%	NGS
3 %	BSA
0.1 %	tritonX 100
in	1xPBS

Solution for antibodies

4%	NGS
3%	BSA
0.1%	tritonX 100
in	1xPBS

Cryoprotection solution

125ml	ethylene glycol
125ml	glycerol
250ml	1xPBS

7.1.4.6. Cell culture media

Growth medium cell lines

500ml	Dulbecco's modified eagle medium (DMEM)
50ml	fetal bovine serum (FBS)
5ml	penicillin (100units/ml) + streptomycin (100units/ml) (PS)

Freezing medium

10%	dimethylsulfoxide (DMSO)
90%	fetal bovine serum (FBS)

Calcium imaging buffer

125mM	NaCl
5mM	KCl
0.4mM	$CaCl_2$
1mM	$MgSO_4$
5mM	$NaHCO_3$
1mM	Na_2HPO_4
10mM	Glucose
20mM	Hepes
in	H_2O_{bidest}

Yo-Pro-1 assay buffer

5mM	KCl
0.5mM	CaCl2
280mM	Sucrose
10mM	Glucose
10mM	HEPES
in	H_2O_{bidest}

⇨ adjust pH to 7.4

7.2. Methods

7.2.1 Animal housing and breeding

Mice were housed 2-4 per cage and acclimated to standard laboratory conditions (light-dark cycle: 12:12 h, lights on at 7 a.m.; temperature: 21 ± 1°C; relative humidity: 50 ± 10 %) with food and water available *ad libitum*. All mouse breedings and experiments were conducted in accordance with the Guide for the Care and Use of Laboratory Mice of the Government of Bavaria.

All mice were genotyped according to the indicated protocol. The tail biopsies were taken at weaning, when mice were 3 to 4 weeks old.

7.2.2 Behavioral testing

For all conducted experiments mice were single housed as well as accustomed to standard laboratory conditions (light-dark cycle: 12:12 h, lights on at 7 a.m.; temperature: 21 ± 1°C; relative humidity: 50 ± 10 %) for at least 7 days prior to the experiment, with food and water *ad libitum*. Following habituation mice were conducted to a general health check including fur and general physical examination as well as bodyweight measurements, also to ensure that possible behavioral findings are not confounded by the health status of the mice.
The behavioral paradigms open field (OF), elevated plus maze (EPM), dark-light box (DaLi), forced swim test (FST), social avoidance (SA), Y-maze, object recognition in the Y-maze and social object recognition (SOR) were recorded and analyzed using the *ANY-maze* software (Stoelting Co.). FST, SA, object recognition in the Y-maze and SOR had in addition to be evaluated manually. Fear conditioning (FC) and the water cross maze (WCM) were evaluated fully manually. All used apparatuses were properly cleaned before the experiment and each individual trial.

7.2.2.1. Open field test (OF)

The open field paradigm was used as a general readout for locomotor activity as well as general anxiety related behavior in a novel environment. The apparatus is a custom made gray PVC box (WLH 48 x 48 x 40cm) with open top. Light intensity inside the OF was 15-20 lux. To start an individual trial the mouse was placed in a corner of the OF, facing the wall. The animal's movements were recorded on video and automatically analyzed by the ANY-maze software. For this the apparatus was virtually subdivided in two compartments, the inner zone (20 x20 cm) and the outer zone along the walls. Evaluated parameters were total distance, number, distance, time and latency of inner zone exploration. The arena was cleaned before testing the next animal.

7.2.2.2. Elevated plus maze test (EPM)

This test was assessed to investigate anxiety related behavior. The apparatus is a custom made gray PVC plus-shaped elevated (37cm above the floor) platform with four intersecting arms. The two opposing open (30 x 5cm, 15-20 lux) and closed arms (30 x 5 x 15cm, 8-10 lux) are connected by the central zone (5 x 5cm). To start and individual trial the mouse was placed in a closed arm facing the wall. The mouse was allowed to freely explore the maze for 10 minutes.

Investigated parameters included open and closed arm times as well as numbers and latency to open arm entries.

7.2.2.3. Dark-light box test (DaLi)

The dark-light box test was assessed to investigate anxiety related behavior. The custom made PVC apparatus exist of two compartments, a black (15 x 20 x 25cm; < 10lux) and a white one (30 x 20 x 25cm; brightly illuminated: ~650-700lux). The two compartments are connected by a tunnel (4 x 7 x 10 cm) that allows the mice to freely move from one compartment to the other. To start and individual trial the mouse was placed in the dark compartment of the apparatus, facing the tunnel. The mouse was allowed to freely explore the test setting. Investigated parameters included latency, number of entries and time spent in the lit compartment.

7.2.2.4. Forced swim test (FST)

The forced swim test was conducted to investigate stress-coping behavior. Mice were gently placed in a glass beaker (height 24cm, diameter 12cm) filled with water (23 ± 1°C). The mice behavior was videotaped for 6 minutes and afterwards manually scored regarding the times of struggling, swimming and floating (immobility except small movements to keep balance). Scoring was conducted by a trained observer, blind to the genotypes of the animals.

7.2.2.5. Object recognition test (OR)

The object recognition paradigm was conducted in the OF arena with low illumination (10 lux). The test consists of two trials, one 10 min acquisition trial were two identical objects were presented to the mice and a 30 min trial were one of the familiar objects was exchanged for a novel object. The percentage of time exploring the novel object compared to the familiar was afterwards calculated. A higher preference of the mice towards the novel object indicates a normal object recognition memory

7.2.2.6. Y-maze test

The Y-maze test was conducted to investigate short term special memory. The custom made PVC apparatus consists of three Y-shaped, evenly illuminated (15 lux) arms each of them marked with

distinct intra-maze cues. The actual test consisted of two trials, an acquisition and a retrieval stage, separated by a 30 minutes break. During acquisition one of the arms was blocked and mice were allowed to freely explore the other two arms for 10 min. During the retrieval, the mice were allowed to freely explore the entire maze for another 10 min. The percentage of time the mouse spent in the different arms was afterwards calculated. Learning was successful if the mouse spent significantly more time exploring the novel arm over the familiar ones than just chance level (33%).

7.2.2.7. Spatial object recognition test (SOR)

The spatial object recognition test (SOR) was conducted in the OF arena with low level of illumination (10 lux). Spatial cues were provided outside of the arena, fully visible for the mice. The test consisted of two trials. During the 10 min acquisition trial two identical objects were placed in the OF arena and the mice were allowed to freely explore the objects. After a 30 min break mice were again free to explore the arena for 10 min. However, one of the objects was relocated inside the apparatus. The percentage the animal spent with the displaced object was afterwards calculated. A higher percentage spent with this displaced object reflects intact spatial memory.

7.2.2.8. Social avoidance test (SA)

The social avoidance test was conducted as a modified version from (Berton et al., 2006b; Golden et al., 2011). The test consists of two trials and was conducted in the OF arena. In the first trial the mice were placed in the apparatus for 2.5 min. The arena was equipped with an empty wire mash cage on one side of the arena. The time the mice spent exploring the wire mash cage was determined. In the second trial an unfamiliar BL6 mouse was placed in the wire cage. The test animal was again free to explore the arena for 2.5 min and interaction time was measured. Afterwards the ratio of the interaction times was calculated.

7.2.2.9. Fear conditioning (FC)

Fear conditioning was conducted in conditional chambers (ENV-307A, MED Associates) as previously described (Kamprath and Wotjak, 2004). Conditioning of the mice as well as context-dependent freezing measurements, were conducted in a chamber with metal grid flooring. This

chamber was sprayed with 70%EtOH before inserting the mice. The tone dependent freezing was determined in a neutral contextual environment namely a plexiglass cylinder with bedding material sprayed with 1& acetic acid. To apply the foot shock of day 1 a test animal was placed in the conditioning chamber for 3 minutes. After 180 seconds a sine wave tone (80dB, 9kHz) was applied for 20 sec, which was terminated by a 2sec electric foot shock of 0.7mA. Afterwards the mice remained in the chamber for another 60 sec. In order to measure freezing response on day 2 towards the tone, mice were placed into the neutral environment. After 3 min the tone was applied for another 3 min. After another 60 seconds mice were returned to their cages. Contextual fear (day 3) was investigated by re-exposing the mice to the conditional chamber for 3 min.

All experiments were videotaped and freezing behavior as measure of fear was manually determined by a trained observer blind to the genotypes of the mice.

7.2.2.10. Water cross maze (WCM)

The water cross maze paradigm was implemented to investigate spatial memory performance of our mice. It was conducted as previously described (Kleinknecht et al., 2012). As in the classic Morris water maze the WCM makes use of water to motivate the mice to find a platform. Other than in the classical paradigm, however, it allows for the assessment of different learning strategies by determining parameters like accuracy and start bias scores.

The water cross maze consists of four arms forming a cross made of plexiglas which enables the mouse to orientate by visual cues of the test room. One arm contains a platform 1cm underneath the surface, invisible for the mouse.

The test protocol exceeds 6-7 days on which every animal performs six consecutive trials. During this first week the platform was always located in the same arm, however, the start arm of the mice was alternated from one side (North) to the other (South) in a pseudorandom manner. Learning performance of the mice was assessed by determining the accuracy, the number of wrong platform visits, the latency to reach the platform and the start bias.

Accuracy: A trial was considered accurate (i.e., value 1), if the animal directly entered the arm containing the platform and climbed onto it. Aberrant behavior was considered as non-accurate (i.e., value 0). Thus, accuracy reflects the percentage of accurate trials on each day per animal. An animal reached the criterion of an accurate learner, if it accomplished more than 83% accurate trials per day.

Start bias: Start bias was described as the absolute value of the sum of accurate trials from the South arm minus the sum of accurate trials from the North arm $|\sum(\text{accurate North trials}) - \sum(\text{accurate South trials})|$. An animal with a daily score ≥2 was considered to be biased, suggesting a response-, rather than spatial-based learning strategy.

7.2.2.11. Chronic social defeat stress (CSDS) paradigm

The CSDS paradigm is a well-established paradigm to induce anxiety and depression related endophenotypes in mice and it was conducted as previously described (Wagner et al., 2012; Wang et al., 2013; Hartmann et al., 2015). Experimental mice were submitted to chronic defeat stress for 21 consecutive days by introduction of a dominant male CD1 resident into the home cage (45 x 25 cm). Smaller experimental mice (BL6) were subsequently defeated for not longer than 5 min. Until the next day both mice remained in the same cage, physically separated only by a perforated steel partition enabling sensory contact. This procedure was repeated every day with a new unfamiliar resident for a 21 day period. By varying the starting time of the defeats over the days it was tried to decrease the predictability to the stressor and thereby minimize habituation effects.

Not stressed control mice were housed in their regular home cages throughout the experiment. Additionally to weight and fur status assessment every 3-4 days, all mice were handled every day. Actual behavioral testing was conducted in the last week of the CSDS paradigm. To assess the efficiency of the stress protocol, mice were subjected to an acute stress challenge on day 19 of the chronic stress procedure. Acute stress was applied by a 5 min FST. Blood samples were subsequently collected by tail cut, 30 min and 90 min following the start of the FST. Plasma corticosterone levels were measured with a radioimmune assay according to the manufacturers protocol (MP Biomedicals Inc). The mice were finally sacrificed on day 21 of the experiment by decapitation. Hereby trunk blood was collected for subsequent measurement of basal corticosterone levels. Additionally thymus and adrenal glands were removed for weight measurement.

7.2.3 Nucleic acids methods

7.2.3.1. DNA preparation from mouse tail tissue

Genomic DNA for genotyping PCRs was isolated from tail tissue. Tissue sample was digested in 100µl NaOH (50mM) for 30 min at 99°C followed by a neutralization step with 30µl Tris-HCl (1M; pH 7.0) and subsequent storage at 4°C. 1µl of the lysate was used for genotyping PCR reaction.

7.2.3.2. Plasmid DNA preparation

Plasmid DNA was isolated from E.coli bacteria with a Plasmid Mini-, Midi- or Maxi-Kit (Qiagen) depending on the amount of LB medium cells were grown in. Typical scales for these different size overnight cultures were 5ml, 25ml and 100ml of LB medium with a selective antibiotic (100µg/ml ampicillin or 50µg/ml kanamycin) respectively. In all cases the procedures were carried out following the manufacturer's protocols.

7.2.3.3. RNA isolation and RNA integrity control

RNA from both cells and tissue was isolated using a modified TRIzol protocol established by Invitrogen. Therefore, cells were harvested in 1ml of TRIzol per 10cm dish; for tissue samples 1ml was used per 50mg of fresh tissue. Cells/tissue was subsequently homogenized – by pipetting (cells) or using a TURRAX (IKA Labortechnik) (tissue samples). Solutions were incubated for 5 min at room temperature. 200µl of chloroform was subsequently added to the samples and samples were mixed vigorously before incubation for 3 min at RT. Phenol and water phases were separated by centrifugation for 15 min at 4°C and 12.000g. The aqueous supernatant containing the RNA was transferred to a fresh 2,0ml cup and precipitated with 500µl isopropanol per 1ml of TRIzol for 10 min at RT. The mixture containing the precipitated RNA was afterwards centrifuged (12.000g) for 10 min at 4°C. The RNA pellet was subsequently washed with 1ml of 70% EtOH by mixing and centrifuged (7.500g) at 4°C for 5 min. The RNA pellet was dried and re-dissolved in an appropriate amount of RNase-free water.

RNA integrity was determined by agarose gel electrophoresis. For more precise analysis RNA was measured on the Agilent 2100 Bioanalyzer (Agilent Technologies) using the Agilent RNA 6000 Nano Kit (Agilent Technologies). This analysis based on electrophoresis through microchannel was conducted following the manufacturer's protocol.

7.2.3.4. cDNA synthesis

First strand cDNA synthesis from RNA was performed using the SuperScript II Reverse Transcriptase Kit (Invitrogen) following the manufacturers protocol. For each sample one control reaction was included lacking the reverse transcriptase to test for genomic DNA contamination. 1µg of total RNA was incubated with 1µl dNTPs (10nM) and 1µl of oligo (dT) primers (Invitrogen) in a total volume of 12µl for 5 min at 65°C. After quick chill on ice 4µl of 5x buffer (Invitrogen), 2µl of DTT (0,1M) and 1µl of RNaseOUT (40units/µl (Roche)) were added and samples were incubated at 42°C for 2min. After the addition of 1µl of SuperScript II samples were again incubated at 42°C for another 50 min. The reaction was terminated by inactivation of the enzyme at 70°C for 15 min. To destroy the RNA template a 20 min incubation with RNaseH (Invitrogen) at 37°C was conducted. This was again followed by an inactivation step at 70°C for 15 min. cDNA was afterwards stored at -20°C.

7.2.3.5. Agarose gel electrophoresis

Agarose gel electrophoresis was applied to size separate nucleic acids. Therefore, agarose was boiled in 1x TAE buffer. The agarose concentration was dependent on the nucleic acid fragment size. For fragments from ~100bp to ~1000bp 2% agarose gels were prepared. Fragments bigger than 1000bp were separated in 0,8-1% agarose gels. Before adding 0,1µg/ml ethidiumbromide to the liquid agarose the agarose was cooled down for some minutes while shaking. The liquid agarose/ethidiumbromide mixture was then applied to a gel electrophoresis chamber (PeqLab) and combs were inserted. After cooling down of the agarose nucleic acid samples containing the appropriate amount of 6x loading buffer could be loaded on the solid agarose gels. As a marker for size and quantity smart ladder (Eurogentec) was used. Electrophoresis was carried out with 100-170V for 1-2h. For visualization of the fragment the gel imaging system QUANTUM ST5 (Analis) was used.

7.2.3.6. Determination of nucleic acids concentrations

To determine the concentration of DNA/RNA samples the optical density (OD) at 260/280nm was measured using the Nanophotometer P330 (Implen). 1µl of the sample was applied to the photometer and the concentration was automatically calculated based on the following equation:

$$\text{Concentration DNA/RNA [µg/ml]} = OD_{260} \times f \times n$$

OD260=Optical density of a strongly diluted DNA/RNA solution determined with a spectrophotometer at a wavelength of260nm

f = Dilution factor

n = Set by default 50µg/ml for DNA and 40µg/ml for RNA

The purity of DNA/RNA preparation was estimated by determining the ratio of absorbance at 260nm and 280nm. Theoretically expected values for pure DNA/RNA are 1,8 and 2,0, respectively.

7.2.3.7. Sequencing

DNA sequencing and editing of the raw data was done by Sequiserve GmbH in Vaterstetten. For analysis of the sequences, Vector NTI (Invtrogen) or the open source software Serial Cloner (Serial Basics) were used.

7.2.3.8. Polymerase chain reaction (PCR)

For amplification of DNA fragments up to 2kb, standard polymerase chain reaction (PCR) using Thermoprime Plus DNA polymerase (Thermo Scientific)was performed. Therefore, the following composition was used:

1-2µl	template DNA
5µl	10x reaction buffer IV (Thermo Scientific)
3µl	25mM MgCl2
1µl	dNTPs (dATP, dTTP, dGTP and dCTP, 10nM each) (Roche)
1µl	10pmol forward primer
1µl	10pmol reverse primer
0,5µl	ThermoprimePlus DNA polymerase

⇨ fill up to 50µl with H_2O - bisdest

PCR was carried out in PCR machines by Biorad and PeqLab with modifications of the following program:

step		cycles	temperature [°C]	time
preincubation		1	95	2min
amplification	denaturation	30-35	95	30sec
	annealing		X	30sec
	elongation		72	Y
elongation		1	72	12min
cooling		1	8	hold

The annealing temperature (X) and the elongation time (Y) were adjusted according to the melting temperature of the primers and the amplicon size, respectively.

7.2.3.9. Quantitative real-time PCR (qRT-PCR)

cDNA was prepared as described above. Quantitative RT-PCR was carried out in a LightCycler96 (Roche) using the *SYBR Green I Master* – kit (Roche). For each PCR reaction the following volumes were used: 5µl of PCR-mix (*SYBR Green I Master*) (including SYBR-green and polymerase), 1µl of forward primer (10µM), 1µl of reverse primer (10µM), 1µl of H_20 and 2µl of template cDNA. All together was applied to one well of a white 96 well plate (ThermoFisher). After all samples were applied to the plate the plate was sealed with a clear film (ThermoFisher) and quickly spinned before placing it into the machine. A regular 3-step PCR protocol followed by a melting curve analysis was applied for all runs conducted. Crossing points for each sample were determined by the LightCycler96 software (V1.1). The relative expression levels were subsequently determined using the ΔΔCT method (Livak and Schmittgen, 2001; Pfaffl, 2004) normalized to the housekeeping gene (RPL19). All calculations were based on an assumed PCR efficiency of 2.

7.2.4 Cell culture

All cell culture experiments were conducted under sterile conditions using a sterile bench or hood (Heraeus Istruments). All reagents were purchased from Invitrogen (ThermoScientific) if not stated otherwise. The same accounts for the consumable which were purchased from Nunc (ThermoScientific).

7.2.4.1. Maintenance of cells

Cell lines like human embryonic kidney cells (HEK), Neuro2A and 1321N1 were maintained in Dulbecco's modified eagle medium (DMEM) supplemented with 10% fetal bovine serum (FBS) and 1% penicillin (100units/ml) + streptomycin (100units/ml) (Pen/Strep) at 37°C in an atmosphere with 5% CO_2. Cells were passaged when reaching confluency.

7.2.4.2. Splitting / passaging of cells

For passaging of cells, medium was aspirated and cells were washed with phosphate buffered saline (PBS). For a 10cm culture dish 1ml of trypsin/EDTA (ethylenediaminetetraacetic acid) was added to the cells and incubated for 5 min at 37°C. As soon as cells started to de-attach the reaction was aborted by adding 10ml of maintenance medium and cells were re-suspended by pipetting. The desired amount (cell-number was determined with a Neubauer chamber (Roth)) of cells was transferred to a new culture dish and fresh growth medium was added.

7.2.4.3. Freezing and thawing of cells

For long term storage of cells in liquid nitrogen confluent cells were trypsinized and subsequently harvested by centrifugation. Cells of one 10cm culture dish were re-suspended in 1ml of freezing medium and transferred into cryo tubes (Nalgene). Vials were slowly cooled down to -80°C in Mr. Frosty freezing containers (Nalgene). The next day cells were transferred to liquid nitrogen.

To thaw cells a frozen vial was quickly put into a water bath at 37°C. Thawed cells were transferred to a falcon containing growth medium and subsequently centrifuged at 1200rpm for 5 min. The cell pellet was re-suspended in 10ml of growth medium and plated on a culture dish.

7.2.4.4. Preparation of primary cultures

Neuronal cultures

Primary neuronal cultures were prepared from pups of time pregnant mice on embryonic day 18 as previously described (Møller et al., 2013; Dotti et al., 1988).
For the cultures the brains of the embryos were dissected free of meninges and cortices/hippocampi were isolated. The tissues were subsequently dissociated and prepared as cited above. Neurons were cultivated in Neurobasal A medium supplemented with 2% B27 and 0,24% GlutaMAX.

Astrocytic / microglial / mixed cultures

Preparation of astrocytic, microglial and mixed cultures was based on newborn pups (postnatal day2). Again brains were dissected and cortices/hippocampi free of meninges were isolated. Subsequently tissues were dissociated and re-suspended in growth medium. Astrocytes were grown in DMEM supplemented with 10% FBS + 1% Pen/Strep, microglia and mixed cultures in DMEM/F12 also supplemented with 10% FBS + 1% Pen/Strep. To dissect astrocytes and microglia in mixed cultures, cultures were trypsinized when confluency was reached until the astrocyte containing cell layer detached. To enrich astrocytes, the floating cell layer was dissociated and transferred to a new plate – for microglia enriched cultures it was aspirated and replaced by fresh media. For more detailed information of microglia preparation see (Saura et al., 2003).

7.2.4.5. ELISA

Enzyme linked immunosorbent assays (ELISA) were conducted on supernatants of primary macrophages. Cells were, therefore, primed with 3µg of lipopolysaccharide (LPS) for 2 hours and subsequently stimulated with 1mM BzATP for 30 minutes. Following this, the supernatants were analyzed regarding Il-1β levels with an ELISA kit following the manufacturer's (Thermo Scientific) protocol.

7.2.4.6. Calcium imaging

Calcium imaging experiments were conducted on a Olympus IX81 inverted confocal microscope and the Fluoview 1000 software. Individual images over time were captured with the 10x UPlanSApo (0.4 numerical aperture) objective. Cells were plated on 8-well culture slides (Nunc Lab-Tek II Chamber Slide / Thermo Scientific) and prior to the experiment incubated in 4µM Fluo-4 AM (Invitrogen) and 0.01% Pluronic F-127 (Invitrogen) in calcium buffer for 45 min. After 20 min of washout in calcium buffer fresh buffer was added and the experiment was started by application of the respective amount of BzATP.

7.2.4.7. Yo-Pro-1-uptake assay

The Yo-Pro-1-uptake assay was conducted on the plate reader Tecan Genios Pro (Tecan). Cells were plated in black 96 well plates. Prior to the experiment culture medium was carefully aspirated and Yo-Pro-1-assay buffer with 1µM Yo-Pro-1 was applied. Measurement was immediately started and after acquisition of a basal value BzATP in the respective concentration was applied.

7.2.5 Protein biochemistry

7.2.5.1. Protein isolation

Proteins of tissue or cells were isolated by adding of an appropriate amount (~10 times the volume) of RIPA lysis buffer and homogenized by using a Turax (VWR international) for tissue samples or simply by pipetting for cells. For better lysis cells were subsequently rotated for 20-40 min. This was followed by a centrifugation step at 13.000g for 30 min and supernatant containing the proteins was transferred into a new vial. All steps were conducted on ice or at 4°C, respectively. Until further processing, samples were stored at -80°C.

For APP processing analyses half brains were homogenized in DEA buffer and centrifuged twice at 4°C. After the initial centrifugation step at 5.000g for 10 min the supernatant was centrifuged at 130.000g for 30 min. Supernatant was afterwards collected and pH adjusted to 6.8 with 0.5M Tris. Pellets of both centrifugation steps were collected and resuspended in RIPA buffer, followed by a centrifugation step at 130.000g for 60 min. Supernatant was used for further analyses.

7.2.5.2. Western blot

Prior to immunoblotting the protein samples were separated by SDS-PAGE and subsequently transferred on a 0.45µm Immobilon-P PVDF membrane (Millipore). To minimize unspecificity the membranes were blocked in 5% fat-free milk or I-block in TBS-T for 1h at RT. Primary antibodies were incubated overnight at 4°C. Secondary horseradish peroxidase conjugated igG antibodies were incubated for 2h at RT. Antibody incubation was always followed by washing steps (3x10 min with TBS-T). Signals were visualized by enhanced chemiluminescence reagent (Millipore) and the ChemiDoc imaging system (BioRad)

7.2.6 Histology

7.2.6.1. Preparation of brain sections

For subsequent preparation of cryo sections, mice were sacrificed by an overdose of isoflurane (Forene, Abbott), followed by decapitation. Brains were immediately removed. For in situ hybridization brains were immediately shock-frozen on dry ice and stored at -80°C until cutting on cryostat.

For subsequent preparation of vibratome sections, mice were sacrificed by an overdose of isoflurane and immediately stably attached to a perfusion table. The chest cavity was carefully opened allowing access to the heart. The left ventricle was opened by a small cut and perfusion needle was inserted all the way up to the main aorta. The mouse was then perfused for 1 min with 1xPBS, 5 min with 4%PFA and another minute with 1xPBS. All solutions were ice cold.

After perfusion of the animal the brain was carefully extracted and stored in 4%PFA overnight in the fridge for post-fixation. The next day brains were transferred into a 20% sucrose solution until sectioning on a vibratome.

7.2.6.2. Immunohistochemistry

Free-floating brain sections (50µm prepared on a vibratome) were washed for 3x5 min in PBS to remove cryo-protection solution. Afterwards sections were incubated in 3%BSA/2%NGS in PBS-T for 1h at RT to block unspecific binding. This is followed by the overnight incubation with the primary antibodies (diluted in the blocking solution) at 4°C. The next day the secondary antibodies were applied for 2h at RT. Antibody incubation was always followed by washing steps

(3x15 min with PBS-T). Sections were mounted on super frost plus slides (Menzel) with anti-fading fluorescence VectaShield medium containing DAPI.

7.2.6.3. Thioflavin staining

Vibratome brain sections were stained with 0.5% aqueous Thioflavin S (Biomol GmbH) for 8 minutes at room temperature. Residual staining solution was subsequently removed by 3 x 3 minutes in 1xPBS. During the entire procedure exposure to light was kept to a minimum.

7.2.7 *In situ* hybridization

In situ hybridization (ISH) was conducted as previously described (Refojo et al., 2011). Mice were sacrificed by an overdose of isoflurane (Abbott) and dissected brains were shock-frozen on dry ice. For ISH 25µm thick coronal brain sections were used. Therefore, a cryo-microtome (HM560M, Thermo Scientific) was used. Brain sections were mounted on SuperFrost slides (Menzel).

7.2.7.1. Preparation of ribo-probes

Radiolabeled riboprobes specific for the mRNA of a gene of interest were generated by in vitro transcription of a specific PCR product with ^{35}S-UTP. Prior to this a standard PCR with SP6 and T7 primer was conducted using plasmids (PCRIITopo backbone) as a template that contained the respective cDNA fragments.

For the in vitro transcription the composition was as follows:

2µl	PCR product (1.5µg)
13µl	RNase-free H20
3µl	10x transcription buffer (Roche)
3µl	NTP-mix (rATP/rCTP/rGTP – 10mM, Roche)
1µl	0,5M DTT
1µl	Rnasin (Rnase-inhibitor, Roche)
6µl	^{35}S-UTP (12,5mCi/mM, 1250 Ci/mM, Amersham)
2µl	SP6 or T7 RNA polymerase (Roche)

After mixing of the reactions, samples were incubated at 37°C for a total of 3h; after 1h an additional 0,5µl of RNA polymerase was applied. To terminate the reaction the DNA template was destroyed by application of 2µl of RNase-free DNaseI (Roche) and subsequent incubation for 15 min at 37°C.

The riboprobes were purified using a RNeasy Mini Kit (Quiagen) following the manufacturer's protocol. The RNA was solved in 100µl RNase-free water. To determine the yield of the in-vitro transcription 1µl of the RNA was measured with 2ml scintillation fluid (Zinsser Analytic) in a beta-counter (LS6000 IC, Beckmann Coulter).

7.2.7.2. Pretreatment and hybridization

Frozen tissue samples were warmed up at RT for at least 1 hour before pretreatment.

To prepare the sections for hybridization with riboprobes the protocol was conducted as follows:

1)	10 min	4% PFA in PBS (ice-cold)
2)	3x5 min	PBS/DEPC
3)	10 min	0,1M triethanolamine-HCl (TEA)(pH 8,0) + 600µl acetic anhydride (Sigma-Aldrich) => while rapidly stirred
4)	2x5 min	2xSSC/DEPC
5)	1 min	60% EtOH/DEPC
6)	1 min	75% EtOH/DEPC
7)	1 min	95% EtOH/DEPC
8)	1 min	100% EtOH/DEPC
9)	1 min	CHCl3
10)	1 min	100% EtOH/DEPC
11)	drying (dustfree)	

For the hybridization of the riboprobe with the mRNA of interest a total of 90-100µl of hybmix and 3.5 to 7 million counts per slide were required. The mixture of hybridization solution and probe was heated up to 90°C for 2 min and quickly cooled down on ice again. After cooling down the mix was kept on RT. 90-100µl of the solution were applied to each slide and carefully

mounted with a coverslip trying to avoid air pockets. For hybridization the samples were incubated overnight at 55-68°C in an incubation oven (Memmert). Prior to this, slides were placed in a hybridization fluid humidified chamber to prevent them of desiccation.

7.2.7.3. Washing

The next day the coverslips were carefully removed and the reaction was stopped by the following washing procedure. All steps were conducted at room temperature except stated otherwise.

1)	14x5 min	4x SSC
2)	20 min	NTE + 20µg/ml RNaseA (@37°C)
3)	2x5 min	2x SSC / 1mM DTT
4)	10 min	1x SSC / 1mM DTT
5)	10 min	0,5x SSC / 1mM DTT
6)	2x30 min	0,1x SSC / 1mM DTT (@64°C)
7)	10 min	0,1x SSC
8)	1 min	30% EtOH in 300mM NH_4OAc
9)	1 min	50% EtOH in 300mM NH_4OAc
10)	1 min	70% EtOH in 300mM NH_4OAc
11)	1 min	95% EtOH
12)	2x1 min	100% EtOH
13)	drying (dustfree)	

7.2.7.4. Autoradiography and development

In situ sections were put in a light proof photo cassette and a high performance x-ray film (Kodak BioMax MR) was exposed to the slides for an appropriate time of days. For long term preservation and analysis with the microscope slides were dipped in a pre-warmed photo-emulsion (Kodak NTB2 emulsion). Afterwards slides were dry-stored at 4°C, protected of light for an appropriate amount of time (~ time of exposure to x-ray film). For development these slides were equilibrated to room temperature for 2h and subsequently developed in Kodak D19 developer for 3 min at RT. Before fixation of the slides in Kodak fixer solution for 5 min, sections

were quickly rinsed with water for 30 sec. This was followed by a longer washing step (~30 min) with tap water. Before air drying slides were freed of residual emulsion solution at the back of the slides by scratching it off with a razor blade.

After overnight drying the sections were dehydrated by stringency washing steps in 30% EtOH, 50% EtOH, 70% EtOH and 96% EtOH , 30 seconds each. After 2x5 min in xylol the slides were covered with DPX (VWR international) and coverslips.

Dark-field photography of the sections was taken with a Zeiss AxioCam MRm digital camera attached to a Zeiss axioplan2 microscope. The imaging software used was Axio Vison 4.5 (Zeiss). Post processing (brightness, contrast) was done using Adobe Photoshop and figure design was done with Adobe Illustrator or Adobe InDesign.

7.2.8 Statistical analysis

All results are presented as mean ± standard error of the mean (SEM). Behavioral phenotypic alterations were evaluated with appropriate statistical testing as indicated in the figure legends. Statistical significance in post-hoc tests was defined as $p < 0.05$.

8. Results

8.1. Constitutive *P2rx7* knockout mice

8.1.1 Transcript analysis

Total *P2rx7* knockout (KO) mice were previously established in our lab as described before by Walser (2012). A complete analysis investigating all known *P2rx7* splice variants has, however, not yet been performed. Therefore, we conducted a reverse transcriptase (RT) PCR analysis based on specific primer combinations detecting the different known splice variants (Figure 10). The PCR strategy and primer design (nested PCRs were performed) are depicted in Figure 10. This design allowed the specific amplification of all five so far described murine splice variants. The primer sequences can be found in Table 2 (7.1.3).

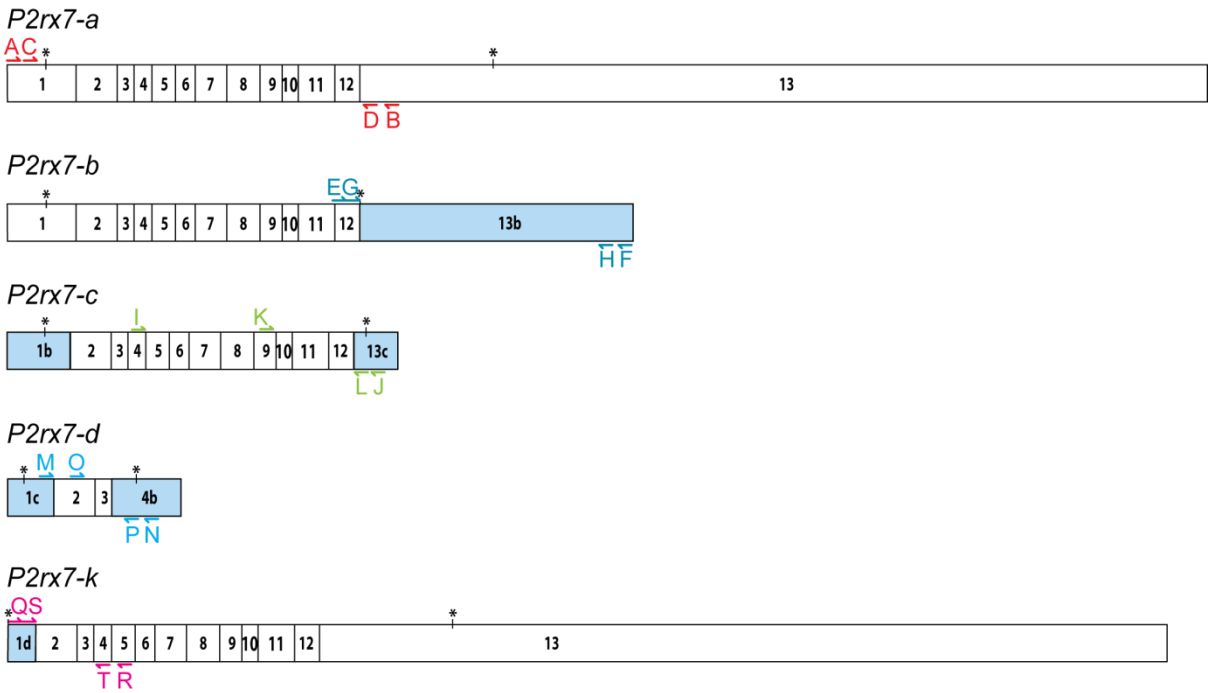

Figure 10: Mouse *P2rx7* splice variants
The five described splice variants are depicted. Exon sizes are true to scale. Exons that differ to the most abundant variant *P2rx7*-a are highlighted in blue. The primer binding sites are schematically depicted above or below the transcripts and indicated by capital letters. Translation start and stop sites are indicated by asterisks.

As shown in Figure 11 there is a complete absence of transcripts in our KO mouse line in all investigated tissues. Both CNS and periphery were studied (brain, salivary gland and spleen are shown). Further, we investigated liver, lung and kidney (data not shown). Every organ showed complete absence of all known splice variants. In contrast to previously described *P2rx7* knockout mouse lines (Nicke et al., 2009; Masin et al., 2012) we could not detect any transcript escaping disruption of the *P2rx7* gene.

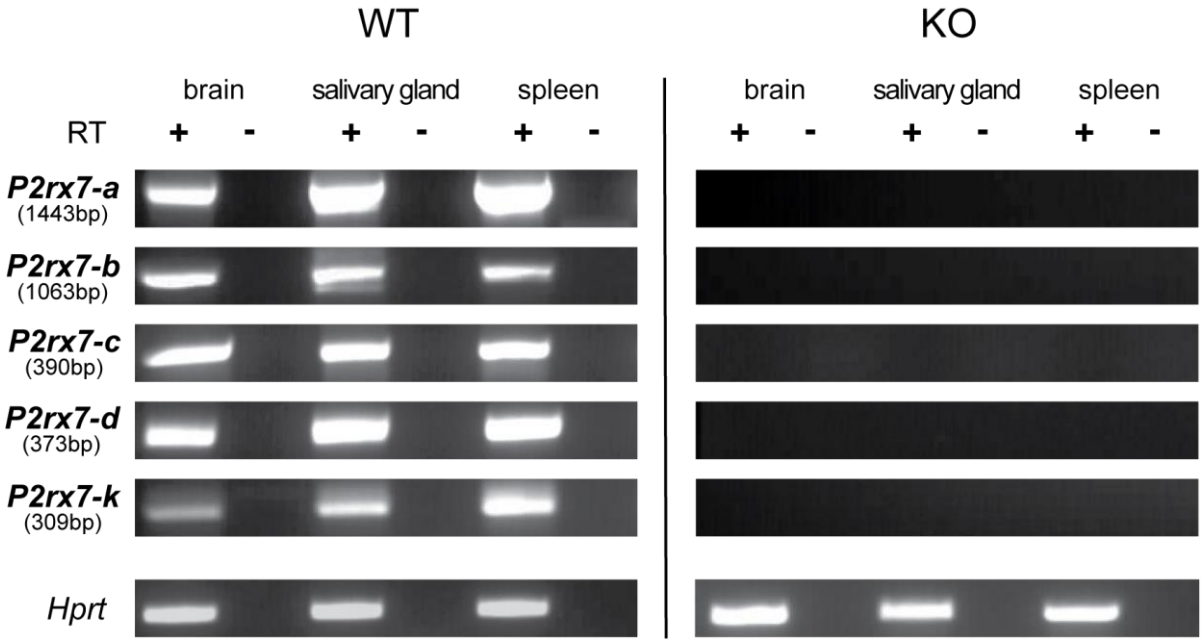

Figure 11: All known *P2rx7* splice variants are absent in *P2rx7* KO mice
The different splice variants of *P2rx7* were detected by nested RT-PCR. Specific primers for the different splice variants were used (compare Figure 10). Analyses of brain, salivary gland and spleen tissue comparing wild-type (WT) and knockout (KO) are shown. In samples of KO mice no expression of any *P2rx7* transcripts was detectable. The integrity of the RNA/cDNA was controlled by the expression of the ubiquitously expressed *Hprt* (hypoxanthine-phosphoribosyl-transferase) gene.

8.1.2 Effects of chronic social defeat stress on *P2rx7* knockout mice

Basal characterization of *P2rx7* KO mice did not reveal strong behavioral differences compared to wild-type (WT) littermates as described above. The development of mood disorders might not exclusively depend on the genetic background but also on environmental factors. Genetic predisposition in combination with an environmental trigger can result in the development of mood disorders. One of the best described environmental factors is stress (de Kloet et al., 2005). Therefore, we exposed *P2rx7* KO mice to three weeks of chronic social defeat stress (CSDS), a

well-established paradigm to trigger endophenotypes of depression in rodents (Nestler and Hyman, 2010; Berton et al., 2012). The chronic social defeat paradigm was conducted as previously described (Hartmann et al., 2012b; Wang et al., 2013).

Both genotypes (KO and WT) showed the typical physiological changes evoked by the CSDS paradigm (Figure 12). Typical changes include decreased fur quality (Figure 12a), atrophy of the thymus (2-Way ANOVA, genotype $F_{(1,44)} = 20.16$, $p < 0.0001$; stress $F_{(1,44)} = 11.71$, $p < 0.005$; Bonferroni post-test, $p < 0.05$) (Figure 12b), enlargement of the adrenal glands (2-Way ANOVA, stress $F_{(1,44)} = 28.34$, $p < 0.0001$; Bonferroni post-test, $p < 0.05$) (Figure 12c), elevated early morning corticosterone levels (2-Way ANOVA, stress $F_{(1,44)} = 30.86$, $p < 0.0001$; Bonferroni post-test, $p < 0.05$) (Figure 12d) and increased vulnerability to a novel stressor as modelled in a forced swim test (FST) (2-Way ANOVA, stress $F_{(1,44)} = 9.34$, $p < 0.005$; Bonferroni post-test, $p < 0.05$) (Figure 12e). These readouts were shown before to be reliable indicators for the effectiveness of the stress paradigm (Wagner et al., 2012; Wang et al., 2013; Balsevich et al., 2015; Hartmann et al., 2015).

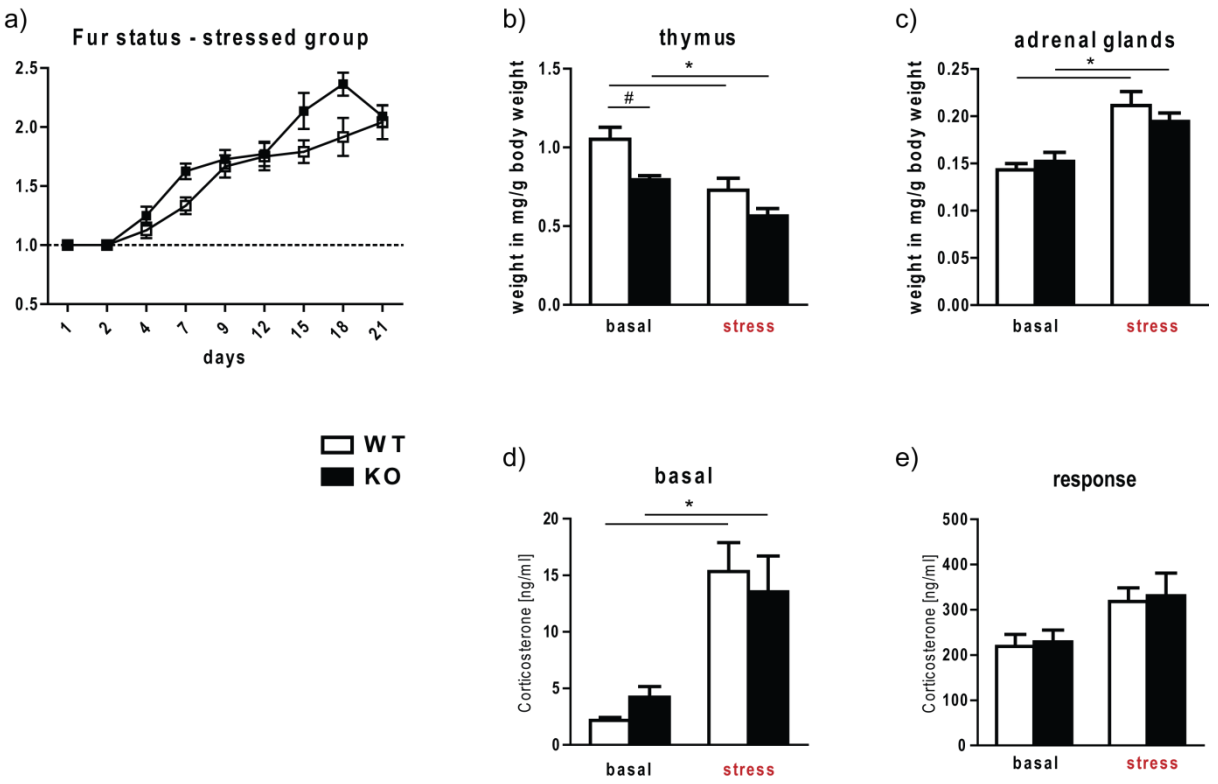

Figure 12: Figure legend see next page

Figure 12: Chronic social defeat stress induced physiological and endocrinological changes
a) Four days after onset of CSDS the stressed mice showed an increase in fur status indicating decreased fur quality; **b)** stressed mice showed a significant atrophy of the thymus compared to unstressed controls; **c)** in the opposite direction adrenal glands of stressed mice were significantly enlarged; **d)** in line with the relative enlargement of the adrenal glands CSDS led to increased basal corticosterone level. Also the corticosterone response following a FST challenge was increased in the stressed compared to the non-stressed group, yet not significantly **e)**. # significant from control of same condition, * significant from chronically stressed group of the same genotype; 2-way ANOVA, $P < 0.05$; Bonferroni post-test, $p < 0.005$; n=11-13.

A general effect of stress on locomotion was not observed in any of the conducted tests (Figure 13) with the exception of a significant decrease in locomotion in the open field (OF) test observed for the KO mice (2-Way ANOVA, genotype x stress $F_{(1,44)} = 7.28$, $p < 0.05$; stress $F_{(1,44)} = 23.57$, $p < 0.0001$; Bonferroni post-test, $p < 0.05$)(Figure 13a). The fact that WT mice did not show this stress response might be explained by the relatively low basal locomotion levels of the WT mice. One can speculate about a floor effect (Weiss et al., 2010), i.e. the basal levels are already that low that there is no more range for a stress induced decrease in locomotion. A similar picture was observed in the analysis of the time mice spent in the inner zone of the apparatus and the number of entries to the inner zone. In both cases the WT mice showed under basal conditions a significant genotype effect (2-Way ANOVA, genotype x stress $F_{(1,44)} = 7.96$, $p < 0.05$; stress $F_{(1,44)} = 9.75$, $p < 0,005$; Bonferroni post-test, $p < 0.05$). Due to the low basal inner zone time of the WT mice we observed a significant stress effect only for the KO mice (2-Way ANOVA, genotype x stress $F_{(1,44)} = 7.96$, $p < 0.05$; stress $F_{(1,44)} = 9.75$, $p < 0,005$; Bonferroni post-test, $p < 0.05$) (Figure 13a). A very similar picture was observed when evaluating the amount of inner zone entries. Again KO mice showed significantly increased entries compared to WT mice. Following CSDS only KO mice showed a significant stress induced increase in anxiety in the OF (2-Way ANOVA, genotype x stress $F_{(1,44)} = 9.79$, $p < 0.005$; genotype $F_{(1,44)} = 4.43$, $p < 0,05$; stress $F_{(1,44)} = 20.78$, $p < 0,005$; Bonferroni post-test, $p < 0.0001$) (Figure 13a). In another anxiety-related paradigm - the dark-light box (DaLi) – this basal genotype effect was not observed. Evaluating the entries to the lit zone, we neither detected a basal difference between WT and KO mice nor a stress induced increase in anxiety-related behavior (Figure 13b). However, comparing the time spent in the lit compartment we observed a genotype effect among the group of chronically stressed mice, namely KO mice spent less time in the lit zone (2-Way ANOVA, genotype x stress $F_{(1,44)} = 4.31$, $p < 0.05$; genotype $F_{(1,44)} = 6.93$, $p < 0,05$; Bonferroni post-test, $p < 0.05$) (Figure 13b). Stress coping behavior, as investigated by the FST paradigm, did not reveal significant

differences or effects of genotype or stress (Figure 13c). This test is a well-established antidepressant screening paradigm since the 1970_{ies}, with high predictive validity for antidepressants acting via biogenic monoamines (Porsolt et al., 1977; Petit-Demouliere et al., 2005).

The paradigm that seems to work best in regard to effects of chronic social defeat stress is the social avoidance test. This paradigm was described by Berton et al. (2006) and is one of the best established readouts of stress susceptibility. Both WT and KO mice spent more time interacting with an unfamiliar mouse than with an empty target zone under basal conditions. For mice that underwent chronic social defeat stress on the other hand we observed a genotype dependent difference in social interaction. Whereas WT mice showed the expected social avoidance, meaning less interaction time with the experimental mouse, the KO mice showed no such decreased interaction (2-Way ANOVA, genotype $F_{(1,44)} = 4.85$, $p < 0,05$; genotype $F_{(1,44)} = 12.17$, $p < 0,005$; Bonferroni post-test, $p < 0.05$) (Figure 13d).

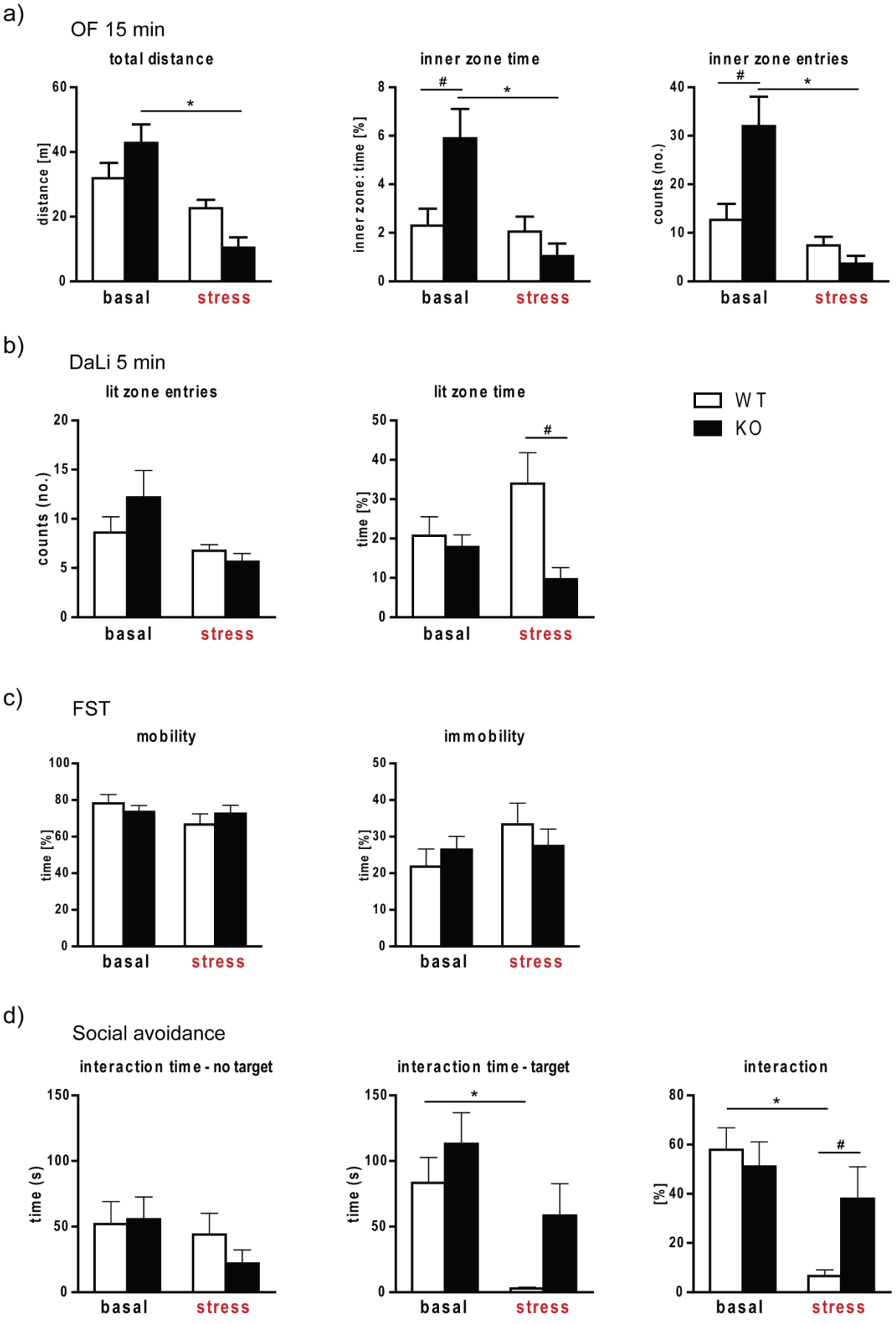

Figure 13: Figure legend see next page

Figure 13: *P2rx7* knockout mice are less susceptible towards chronic social defeat stress
a) The open field test showed that already under basal housing conditions inner zone time and inner zone entries differ between knockout and wild-type mice. Following CSDS a significant reduction of distance travelled, inner zone time and entries was observed exclusively for the knockout mice. **b)** The dark-light box test did not reveal any stress effect on neither of the two genotypes. KO mice of the stressed group, however, spent less time in the lit compartment than controls. **c)** A forced swim test revealed no differences in stress coping behavior. **d)** The social avoidance paradigm showed a significant stress effect in wild-type mice. Both, in regard to the time spent with the social target as well as in regard to the interaction time. This decreased interaction upon stress was not observed for *P2rx7* knockout mice, which suggests resilience to the CSDS.
significant from control of same condition, * significant from chronically stressed group of the same genotype; 2-way ANOVA, $P < 0.05$; Bonferroni post-test, $p < 0.005$; n=11-13. (OF = open field; DaLi = dark-light box; FST = forced swim test)

8.2. Conditional *P2rx7* knockout mice

8.2.1 Expression-based validation of conditional *P2rx7* knockout mice

Based on the results of the CSDS showing a decreased stress susceptibility of *P2rx7* KO mice in social avoidance compared to WT mice as well as previous results, we decided to conduct more detailed analyses using a conditional *P2rx7* knockout mouse line. Based on the above and in Walser (2012) described humanized *P2RX7* mice (hWT) we established constitutive knockout mice (hKO). As depicted in Figure 9 (5.13) the human *P2RX7* cDNA is flanked by *loxP* sites (floxed) that render it vulnerable to Cre recombinase-mediated gene inactivation. The excision of the human *P2RX7* cDNA results in the loss of parts of the endogenous locus including the entire exon 2. This was achieved by breeding the floxed humanized mice to Cre-deleter mice expressing Cre recombinase under the ubiquitously active regulatory elements of the ROSA26 locus.

As a first step to validate this new knockout line based on the humanized *P2RX7* mice, we conducted an *in situ* hybridization analysis with a probe specifically designed to exclusively detect the human mRNA. It has previously been shown that the expression pattern of the human *P2RX7* in these humanized mice fully resembles the endogenous expression pattern in the mouse (Walser, 2012). As shown in Figure 14a, we could not observe the typical *P2rx7*-specific expression pattern in the CA3 of the hippocampus following Cre-deleter-mediated recombination. In addition, the weak homogenous signal observed throughout the brain was abolished suggesting that this represents low expression of *P2rx7* throughout the brain.

To elucidate the expression of *P2rx7* in the entire body we conducted RT-PCRs for the different *P2rx7* splice variants in the brain and additional peripheral tissues. As mentioned above this is a

crucial analysis because there are several *P2rx7* splice variants described of which some escape inactivation in previously published *P2rx7* knockout mouse lines (Nicke et al., 2009; Masin et al., 2012). Similar to the new conventional *P2rx7* knockout mouse line (KO) we could not detect any viable splice variant in the conditional knockout mouse line (hKO) (Figure 14b). The remaining PCR products for splice variants *P2rx7*-a (brain, salivary gland and spleen) and *P2rx7*-b (only brain) were truncated transcripts lacking exon 2 (169 bp). This was confirmed by sequencing of the RT-PCR products. Therefore, these hKO mice lack viable transcripts for all known *P2rx7* splice variants.

In addition, we could show that hKO mice lack the protein as shown for some peripheral tissues like salivary gland (SG) and spleen (Figure 14c). For brain tissue we could not show this due to the unspecificity of the available antibodies. All commercially available antibodies detect an unspecific protein in the brain, which masks endogenous P2X7R. This has been reported by several studies (Sim et al., 2004; Sánchez-Nogueiro et al., 2005). In Western blots investigating brain tissue of both new P2X7R knockout lines we saw a very similar picture (data not shown). This unspecific signal makes it very difficult to discriminate between P2X7R knockout and WT. Further, it indicates that immunohistochemical analysis of brain tissue is not a suitable method for the detection of the P2X7 receptor due to strong unspecific binding of the antibodies in the brain.

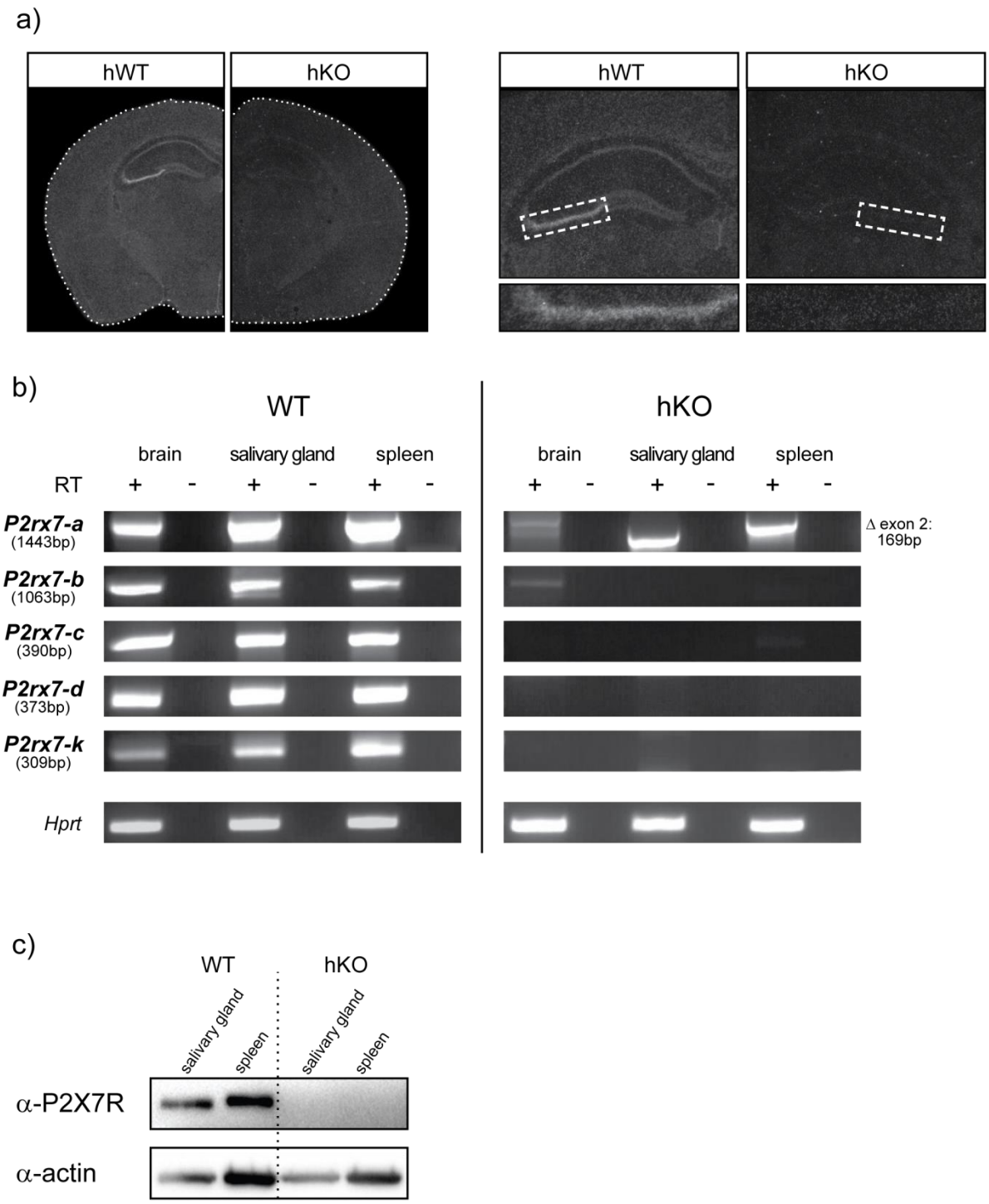

Figure 14: Validation of humanized conditional loss-of-function allele
a) *In situ* hybridization showing the absence of *P2rx7* transcripts in hKO mice. **b)** RT-PCR proving the absence of all splice variants. In case of *P2rx7*-a and *P2rx7*-b some truncated transcripts lacking exon 2 could still be detected. **c)** Western blot analysis showing the absence of P2X7R protein in peripheral tissues.

8.2.2 Functional validation of conditional *P2rx7* knockout mice

Furthermore, we assessed the absence of the P2X7 receptor in our mice also on a functional level. Therefore, we used several well established readouts to test the functionality of the receptor. At first we investigated the ability of primary cells obtained from brains of hWT versus hKO mice in regard to calcium influx into the cells upon stimulation with the P2X7 receptor agonist 3'-O-(4-benzoyl)benzoyl adenosine 5'-triphosphate (BzATP). This readout has been intensively used to investigate the functionality of the receptor for many years (Marcoli et al., 2008; Bhattacharya et al., 2013; Ursu et al., 2014; Sperlágh and Illes, 2014). In our experiments with different setups we were able to show that P2X7R-dependent calcium influx is ablated in hKO mice. We saw this effect both on a single cell level (Figure 15a) as well as in a readout carried out on a plate reader, measuring an entire population of primary cells. Here we observed that the fluorescence levels of the KO were on the same level as cells treated with the P2X receptor antagonist pyridoxalphosphate-6-azophenyl-2',4'-disulfonic acid (PPADS) (Figure 15b). This further confirms the specificity of the readout for the P2X7 receptor.

Moreover, we used ELISA measurements to prove that immune cells of this novel hKO mouse line were no longer capable to release interleukin-1β (IL-1β). Therefore, we isolated peritoneal macrophages from hWT and our constitutive hKO mice based on the conditional allele and measured IL-1β release upon priming with lipopolysaccharide, and subsequently stimulated with BzATP (Figure 15c). The stimulation with the bacterial membrane polysaccharide alone did not trigger the release of cytokines, whereas the combined stimulation with the receptor agonist triggered the release of IL-1β to the supernatant of cultivated macrophages. This response was totally ablated in cells isolated from hKO mice, providing additional proof for the loss of receptor function.

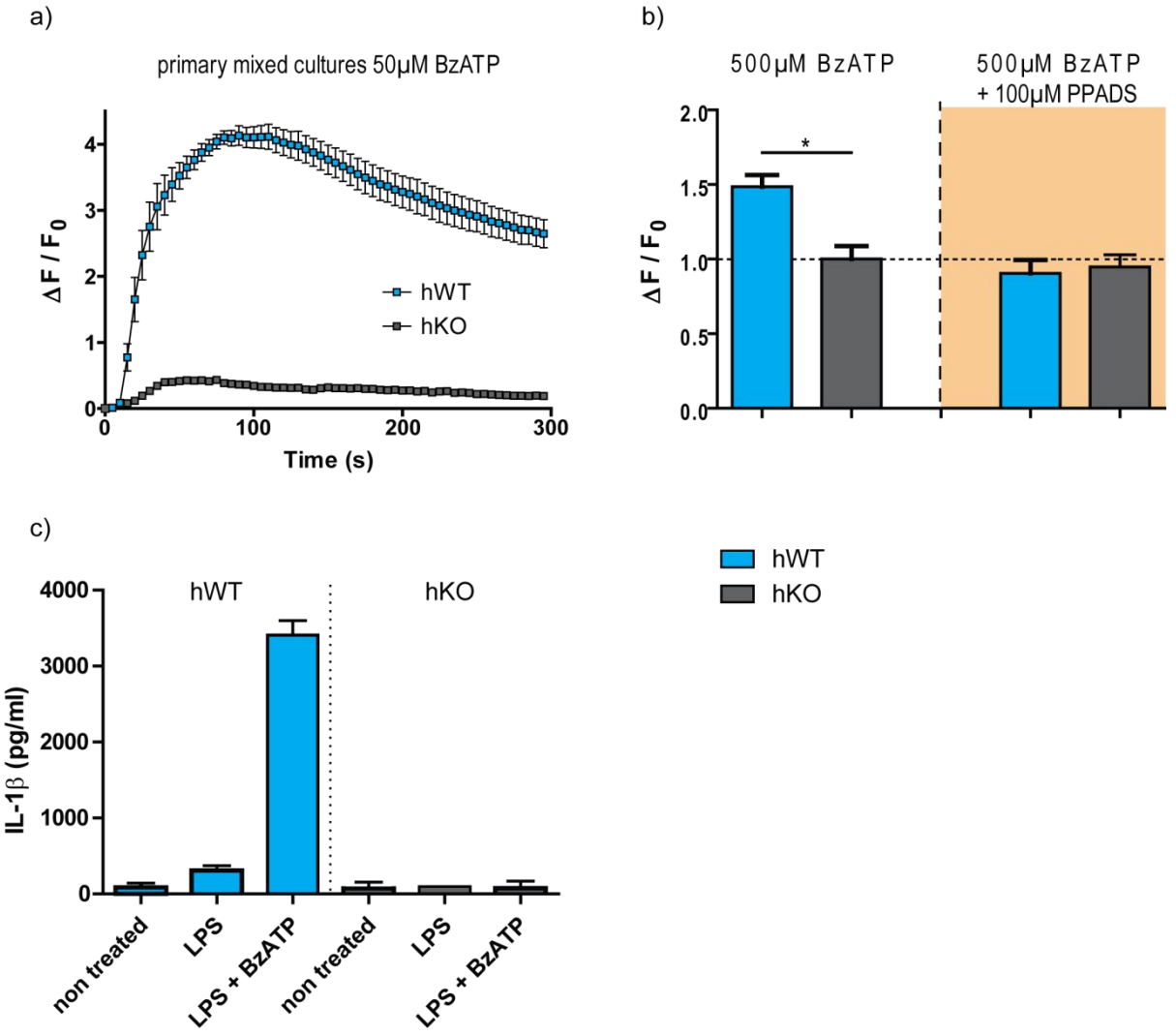

Figure 15: Functional validation of humanized conditional *P2rx7* knockout mice
a) Calcium imaging with single cell resolution shows that P2X7R-mediated calcium influx is ablated in primary brain cells of hKO mice compared to humanized P2X7R mice; **b)** Application of the P2X receptor antagonist PPADS diminishes calcium influx of hWT cells to the level of hKO cells as determined by plate-reader-based measurement; **c)** Peritoneal macrophages obtained from hKO mice no longer show the release of IL-1β upon priming with LPS and stimulation with BzATP.

Another well-established readout for the P2X7R is the pore formation capacity of this receptor. Upon prolonged stimulation the receptor can form pores that are permeable to molecules of high molecular weight up to ~900Da (Volonté et al., 2012; Sperlágh and Illes, 2014). This unique character can be measured by the uptake of high molecular weight dyes such as Yo-Pro-1 iodide (Yo-Pro-1)(Virginio et al., 1997; Nörenberg et al., 2012). Comparing peritoneal macrophages obtained from hWT and hKO mice we observed that macrophages obtained from hKO mice no longer show the dye uptake capacity over time following stimulation with P2X7R agonist BzATP (Figure 16). In this measurement we also included macrophages obtained from those mice that

express the human P2X7R. Not fully surprising, we observed a much stronger dye uptake of those cells expressing the human receptor compared to those expressing the endogenous murine receptor. Differences of the P2X7 receptor, e.g. regarding affinity to the natural ligand ATP or sensitivity towards it between different species like mouse and rat (Young et al., 2007; Donnelly-Roberts et al., 2009) but also mouse and human (Chessell et al., 1998; Donnelly-Roberts et al., 2009) have been demonstrated before.

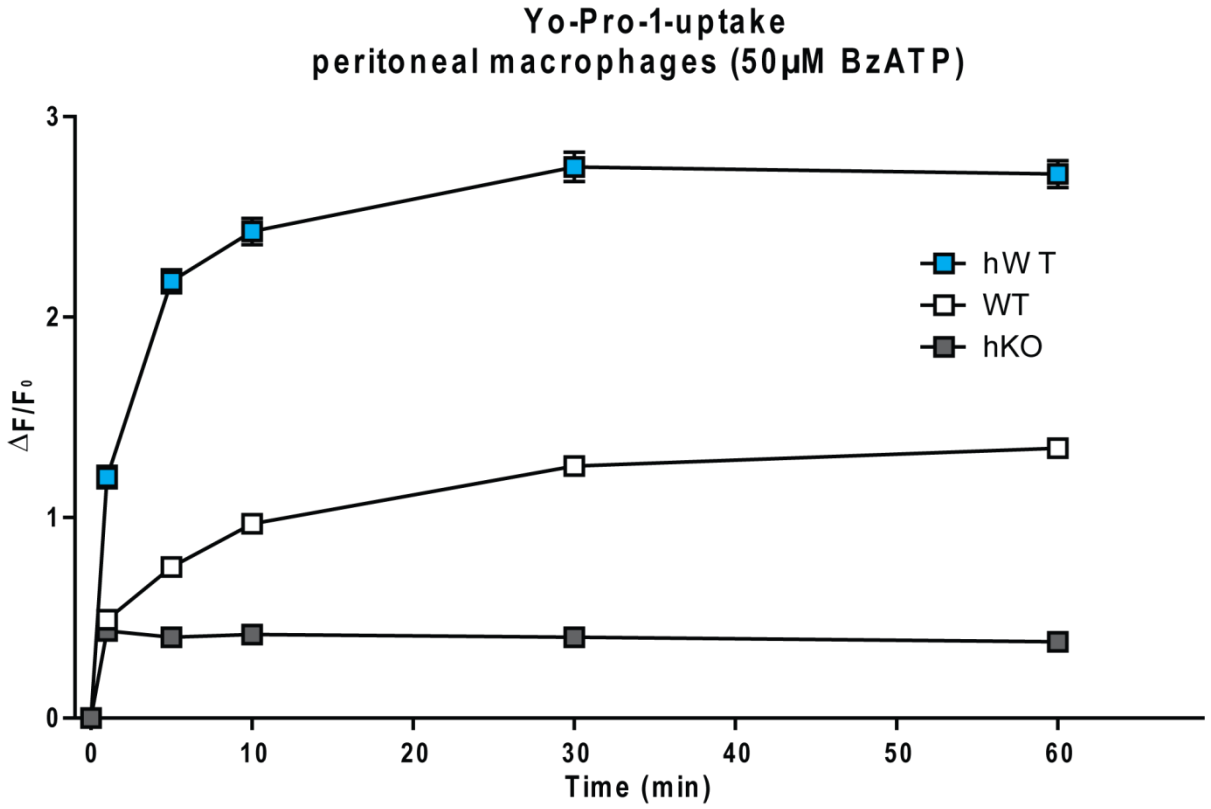

Figure 16: Pore formation capacity of the P2X7 receptor
Upon prolonged stimulation, the P2X7 receptor forms a large pore that is permeable to molecules up to 900Da. This pore formation was studied by examining Yo-Pro-1 uptake capacity of peritoneal macrophages. While the human receptor is more potent upon stimulation with 50µM BzATP than the murine receptor, macrophages lacking the human receptor showed a blunted Yo-Pro-1 uptake. (n = 3)

8.2.3 Functional differences between human and murine receptors

Investigating the large pore formation mediated uptake of Yo-Pro-1, we observed a functional difference between human and mouse receptor. The sensitivity towards the agonist BzATP has been shown to be 10-100 times higher for the human compared to the mouse receptor in transfected cells (Donnelly-Roberts et al., 2009). Therefore, we compared primary peritoneal macrophages obtained either from mouse WT or humanized *P2RX7* mice, in more detail. For the

murine receptor we could not detect a pore formation with BzATP concentrations below 50µM (Figure 17a). The amount of Yo-Pro-1 uptake increased with higher concentrations. For the human receptor we already observed pore formation with an agonist concentration of 5µM (Figure 17b). This shows that the human receptor is roughly 10 times more sensitive towards activation with BzATP compared to the murine homolog. Also the kinetics were different: While the activation levels of the human receptor are more or less stable between concentrations of 10µM and 100µM, this plateau in activation was not observed for the murine receptor. Only with concentrations of 1mM, a further increase in Yo-Pro-1 uptake was observed for the human receptor.

The slight activation at low concentrations also visible upon pure buffer application, has been described before (Sperlágh and Illes, 2014). P2X7 receptors are quite sensitive towards all kinds of stimuli (e.g. saline injection is sufficient) and, therefore, can respond with low levels of activation.

It has further been described that human and murine P2X7 receptors differ with regard to their susceptibility towards different pharmacological modulators (potentiation and inhibition). Therefore, we tested the well described substance trifluoperazine (TFP) (Hempel et al., 2013). Trifluoperazine is a common antipsychotic drug of the phenothiazine class. We tested the modulator on macrophages obtained from WT and hWT mice in the established Yo-Pro-1 uptake assay. Based on our dose response experiments (Figure 17a/b) we chose a BzATP concentration of 50µM for this experiment. Again we could observe a difference between the murine and the human P2X7 receptor in Yo-Pro-1 uptake. From 5 minutes after application of the agonist on, this difference was statistically significant (RM-2way ANOVA, time x genotype $F_{(3,6)} = 55, 95$, $p < 0.0001$; time x treatment $F_{(3,6)} = 12.8$, $p < 0.005$; genotype $F_{(1,8)} = 15.0$, $p < 0,005$; Bonferroni post-test, $p < 0.05$). Moreover, we observed a different response of human compared to murine receptors towards TFP. TFP has a potentiation effect with regards to Yo-Pro-1 iodide uptake exclusively on the murine P2X7 receptor. This potentiating effect was observed for all time points reaching statistical significance 10 min after BzATP application. This readout, therefore, nicely confirms that human and murine receptors differ in aspects of activation levels upon different concentration of the agonist as well as the susceptibility towards modulation by certain compounds.

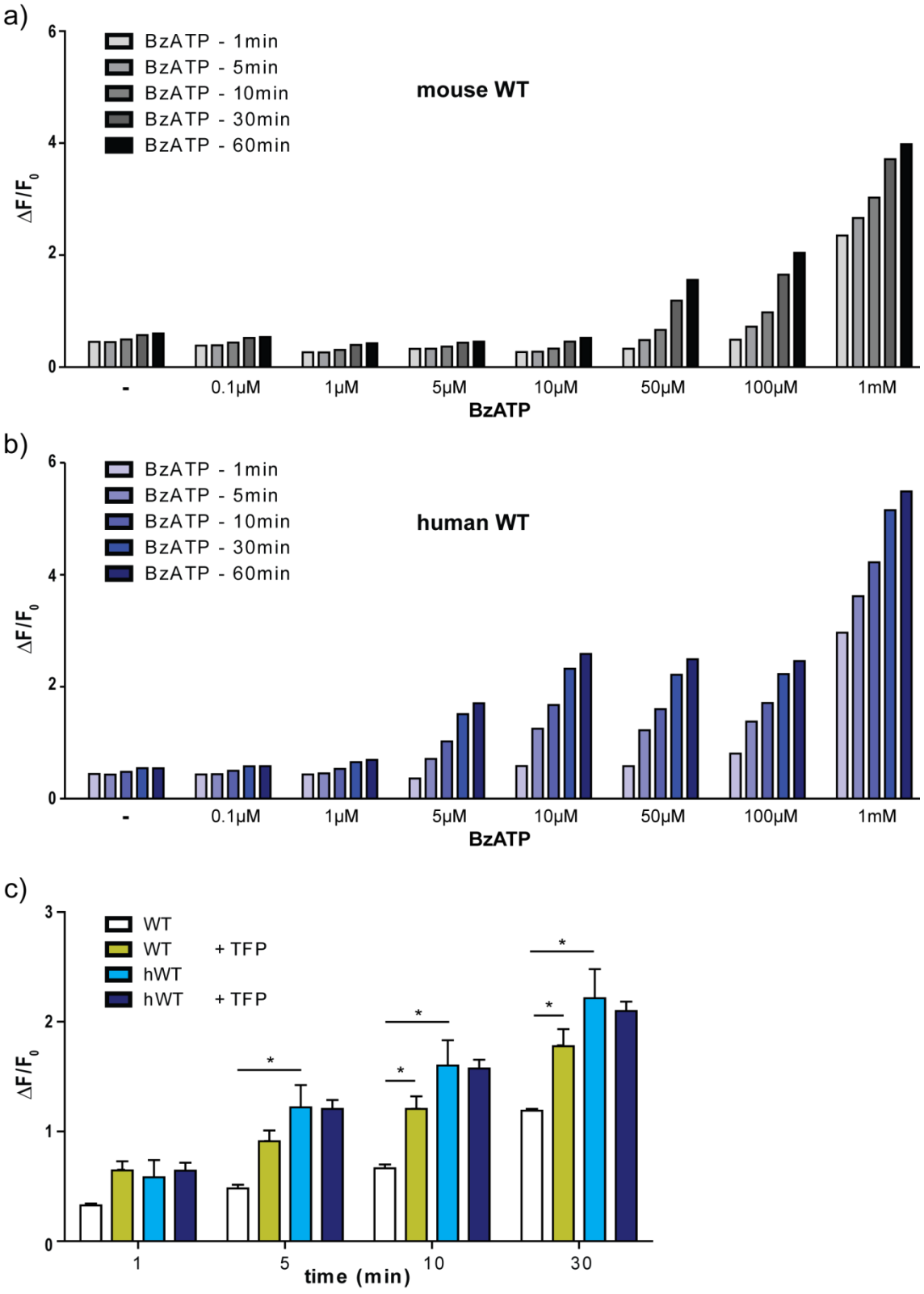

Figure 17: Comparing pore formation capacity of human and mouse P2X7 receptors
Pore formation capacity of the **a)** murine and **b)** human P2X7R in response to increasing concentration of BzATP. **c)** Peritoneal macrophages expressing the murine or the human P2X7 receptor react differently to TFP (3µM) upon concurrent stimulation with BzATP (50µM).
* significant; RM-2way ANOVA, time x genotype $F_{(3,6)} = 55, 95$, $p < 0.0001$; time x treatment $F_{(3,6)} = 12.8$, $p < 0.005$; genotype $F_{(1,8)} = 15.0$, $p < 0,005$; Bonferroni post-test, $p < 0.05$; n=2

8.2.4 Behavioral comparison of wild-type, humanized *P2RX7* and *P2rx7* knockout mice based on the humanized allele

All studies showing an association of the P2X7 receptor with mood disorders were conducted on human patients. Therefore, and also due to the findings of our Yo-Pro-1 uptake experiments as well as previous publications showing differences between human and mouse receptor (Chessell et al., 1998; Donnelly-Roberts et al., 2009), we saw the necessity to not just compare WT mice with the knockout mice based on the novel conditional *P2rx7* allele but also include the humanized *P2RX7* wild-type mice in behavioral experiments.

We tested the mice in a 15 min open field test (OF), 10 min elevated plus maze (EPM), 5 min dark-light box (DaLi) and a 6 min forced swim test (FST). Different to a previous experiment comparing wild-type mouse and these humanized *P2rx7* mice (Walser, 2012) we could not observe any significant difference comparing the three groups. We did not observe differences in general locomotion as depicted in the total distance travelled in the OF and EPM test (Figure 18a,b). Further, no alterations in anxiety-related readouts in the OF, EPM and DaLi were observed (Figure 18a,b,c). Also stress coping behavior modelled in the FST was not changed between the different genotypes (Figure 18d).

The inconclusive results of the behavioral screenings of the published knockout lines together with our data from two new knockout lines strongly suggests that the knockout of the P2X7R in the mouse does not lead to any alteration in behavioral readouts or phenotypes under basal conditions. Several possibilities that could interfere with a reasonable conclusion will be discussed later on. The most likely are probably compensatory mechanisms (Rossi et al., 2015) that could compensate in all so far characterized knockout mouse lines. Due to the loss of the *P2rx7* gene from the first day of development on it seems likely that the function of the P2X7 receptor is compensated by different receptors/ion channels e.g. different P2X receptor family members.

To prevent this type of compensation that can take place during early development it seems reasonable to make use of the conditional capacity of the humanized allele and to induce the *P2rx7* knockout in adulthood. In the humanized allele the entire sequence between the two *loxP* sites flanking the human transcript can be excised by the Cre recombinase. By breeding these mice to mice that express Cre recombinase that is fused to a mutant version of the human estrogen receptor ER^{T2} the Cre recombinase can be specifically activated by the application of the estrogen analogue tamoxifen (Feil et al., 1997; Erdmann et al., 2007). By placing such Cre

recombinases under the control of specific promoter elements one can further induce tissue- or cell type-specific knockouts (Kühn and Torres, 2002). This new conditional *P2rx7* allele, therefore, provides the opportunity to investigate the effect of *P2rx7* inactivation without developmental compensation and restricted to certain tissue or cell types. Unfortunately, it is still highly discussed where exactly and to which extent and even if the P2X7R is expressed in the brain at all (Deuchars et al., 2001; Atkinson et al., 2004; Sim et al., 2004; Masin et al., 2012; Sperlágh and Illes, 2014).

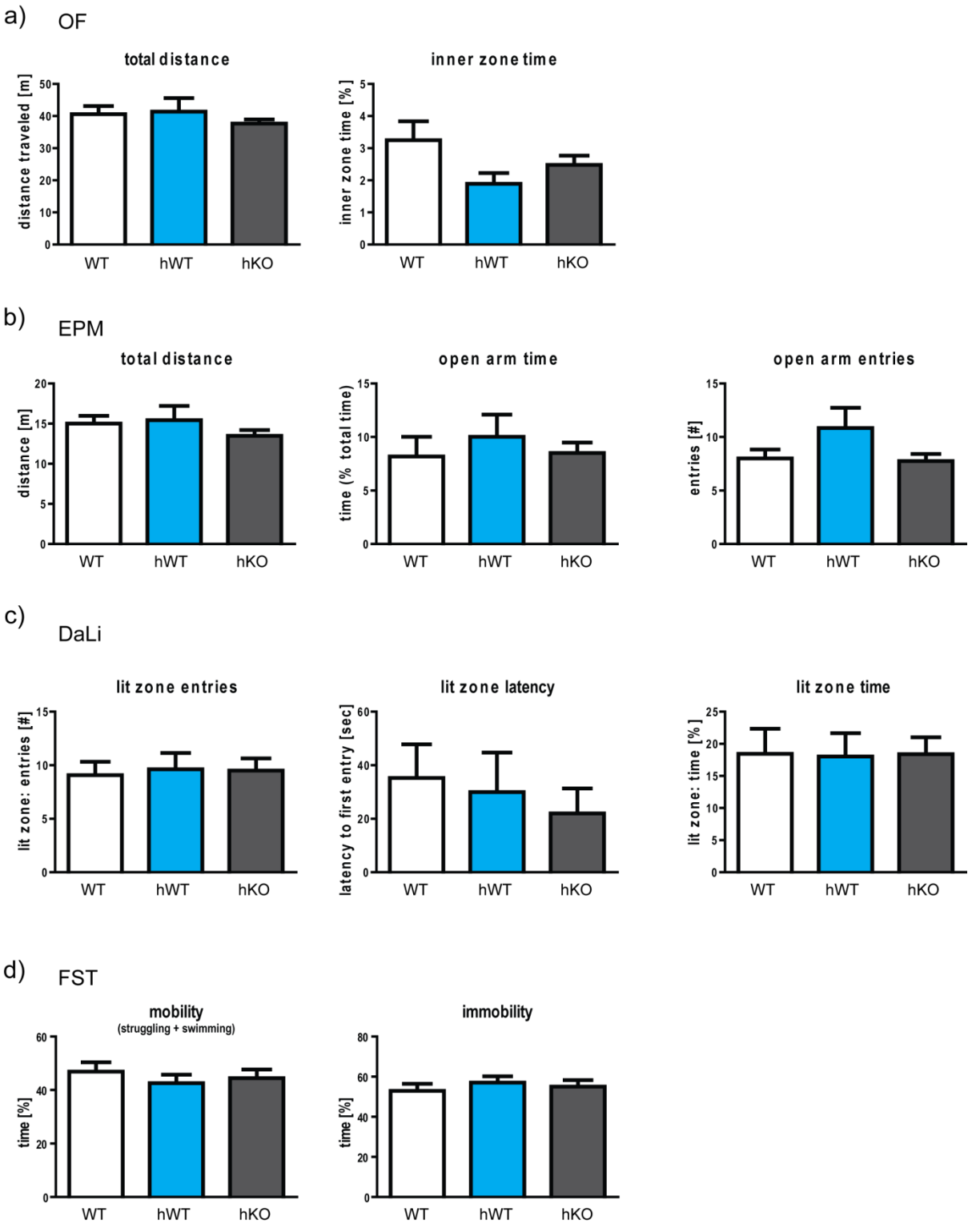

Figure 18: Basal behavioral screening of hKO, hWT and WT mice
Basal behavioral screening included **a)** open field test (OF), **b)** elevated plus maze (EPM), **c)** dark-light box test (DaLi) for locomotion and anxiety, as well as the **d)** forced swim test (FST) investigating stress coping behavior. Under basal conditions we could neither detect significant phenotypic alterations in humanized *P2RX7* (hWT) nor in knockout mice based on the humanized *P2RX7* allele (hKO) compared to wild-type (WT) littermates. This accounts for locomotion as well as anxiety related or stress coping behavior. (n=13-20)

8.2.5 *P2rx7* expression analysis

Many studies showed the presence of functional P2X7 receptors on different cell types of the brain recently: e.g. hippocampal neurons (Cho et al., 2010), cortical astrocytes (Nörenberg et al., 2010; Oliveira et al., 2011), microglia (Arnoux et al., 2013). Nonetheless, good expression analyses including quantitative comparison have not been done so far. A reason for this can be found in the lack of specific antibodies to detect P2X7R in the brain (Sim et al., 2004; Sánchez-Nogueiro et al., 2005).

Therefore, we conducted a detailed expression analysis for *P2rx7* in the brain based on mRNA expression. In a first attempt we isolated RNA from cortices and hippocampi of our humanized mice and compared relative expression levels of all P2X receptor family members via quantitative real-time PCR (qRT-PCR) (Figure 19). We observed that the relative expression levels of *hP2RX7* are not differing much between cortex and hippocampus. As expected, the mouse *P2rx7* transcript was not detected anymore in homozygous humanized mice. Relative expression of *hP2RX7* in the cortex was second highest followed by *P2rx3* and *P2rx6*. In both tissues expression levels of *P2rx4* were by far the highest, exceeding those of *hP2RX7* by 2.5 - 4.5 folds. In the hippocampus we further observed higher expression levels of other members of the P2X receptor family compared to cortical levels. *P2rx6* expression was similar to *hP2RX7* whereas *P2rx3* and *P2rx5* were even slightly higher.

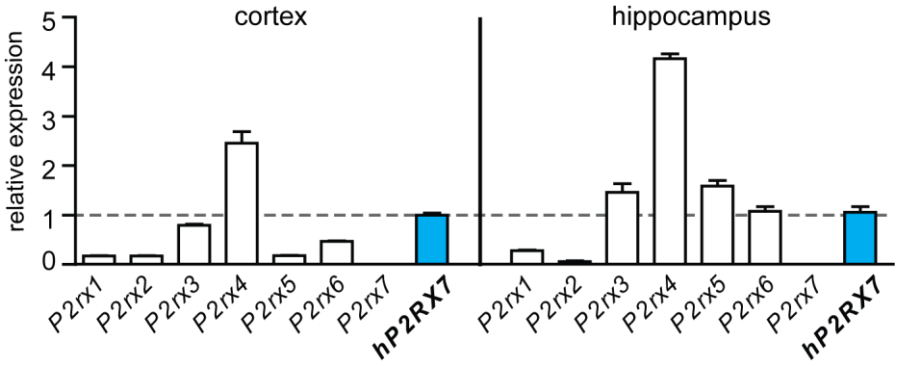

Figure 19: P2X receptor family mRNA expression levels in murine cortex and hippocampus
Relative expression levels of P2X receptor family members for both cortical and hippocampal tissue are shown. Humanized *P2RX7* mice were used for the analysis. Relative expression levels were normalized to the expression of *hP2RX7* of the cortex, which is set to 1.

In a next step we analyzed expression of *P2rx7* compared to its family members in different primary cultures obtained from humanized *P2RX7* mice. We investigated mixed (used for calcium experiments – compare Figure 15a/b) (Figure 20a), neuronal (Figure 20b), astrocytic (Figure 20c) and microglial (Figure 20d) primary cultures. For technical reasons microglia cultures were prepared from regular WT mice and not from humanized *P2RX7* mice. Purity or relative composition of these cultures was confirmed by expression analysis of specific markers. For neurons we used *synaptophysin* (*Syp*), for astrocytes *glial fibrillary acidic protein* (*Gfap*) and for microglia *cathepsin S* (*Ctss*), respectively. We could observe *hP2RX7/P2rx7* expression in all cultures and, therefore, in neurons, astrocytes and microglia. Like in the tissue samples, we observed highest expression for *P2rx4*, throughout all cultures. Except for *P2rx1* which was expressed at lowest level in all investigated cultures the expression levels and the pattern of the rest of the family members varied between the different cell types we isolated. It should, however, be noted that the short period of *in vitro* cultivation could induce ectopic expression of *P2rx7*, just as of any other of the family members.

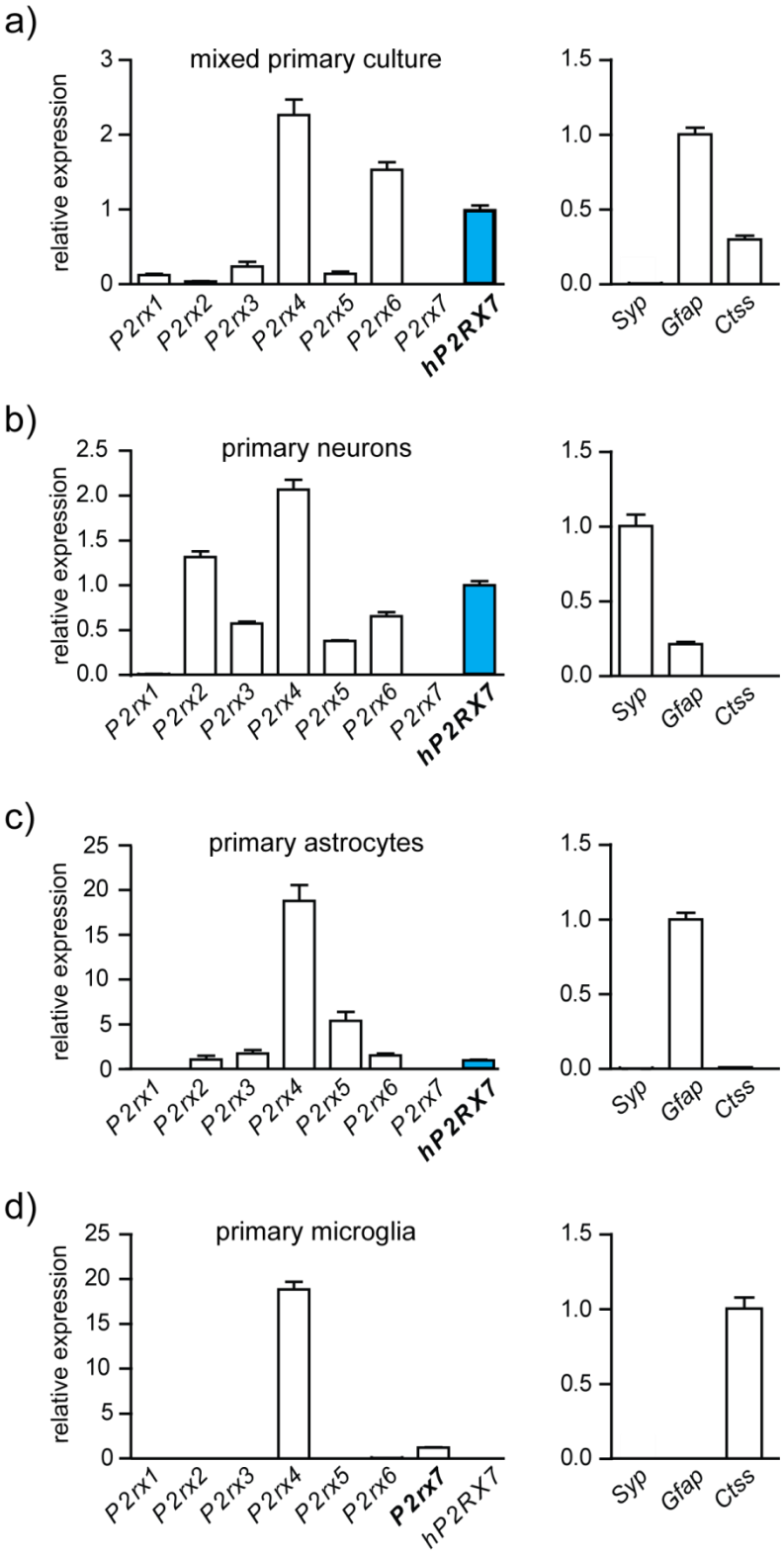

Figure 20: P2X receptor family expression levels in different primary cell cultures
Relative mRNA expression levels of P2X receptor family members assessed in **a)** mixed, **b)** neuronal, **c)** astrocytic and **d)** microglia primary cultures. The composition and purity of each culture was determined by the expression levels of cell type-specific markers (right). Humanized *P2RX7* mice were used for preparation of cultures except for **d)**, were regular wild-type mice were used. For each culture *hP2RX7* acts as reference and is set to 1. For the graphs of the markers of the respective cell type we chose the highest expression as reference.

In order to rule out ectopic expression, we decided to investigate expression levels in more detail *in vivo.* We took advantage of our conditional humanized *P2RX7* line and bred these mice to different tissue- and cell type-specific Cre driver lines. In a first attempt we used *in situ* hybridization analysis to study *P2RX7* expression in more detail (Figure 21). We observed that the neuron and macroglia specific *nestin* (*Nes*)-*Cre* addressed much of the *P2rx7* signal in the forebrain including the prominent signal in the CA3 (cornu ammonis area 3) of the hippocampus. Analyzing the sections of *NeuroD6* (*Nex*)-*Cre* positive mice, we found that this signal in the CA3 is of neuronal origin, more specifically it originates from glutamatergic neurons (Figure 21). The analysis of mice carrying the astrocyte-specific *Glast-CreERT2* (*Glast-Cre*) did not reveal a striking difference in the expression pattern compared to control mice but more a slight overall reduction of expression intensity, indicating a broad and homogeneous expression of *P2rx7* throughout the brain. However, compared to *Nes-Cre* mice more of the ubiquitous signal remained.

To get more insights into the expression of the P2X7 receptor in the hindbrain we analyzed mice which lack *hP2RX7* expression in *engrailed 1* positive cells (by breeding to *En1-Cre*). As expected, *P2rx7* expression was not affected in forebrain regions like the hippocampus. However, we could observe strong differences in the hindbrain. Whereas the expression in the medulla was untouched, the signal for *P2rx7* was heavily diminished in all regions of the cerebellum.

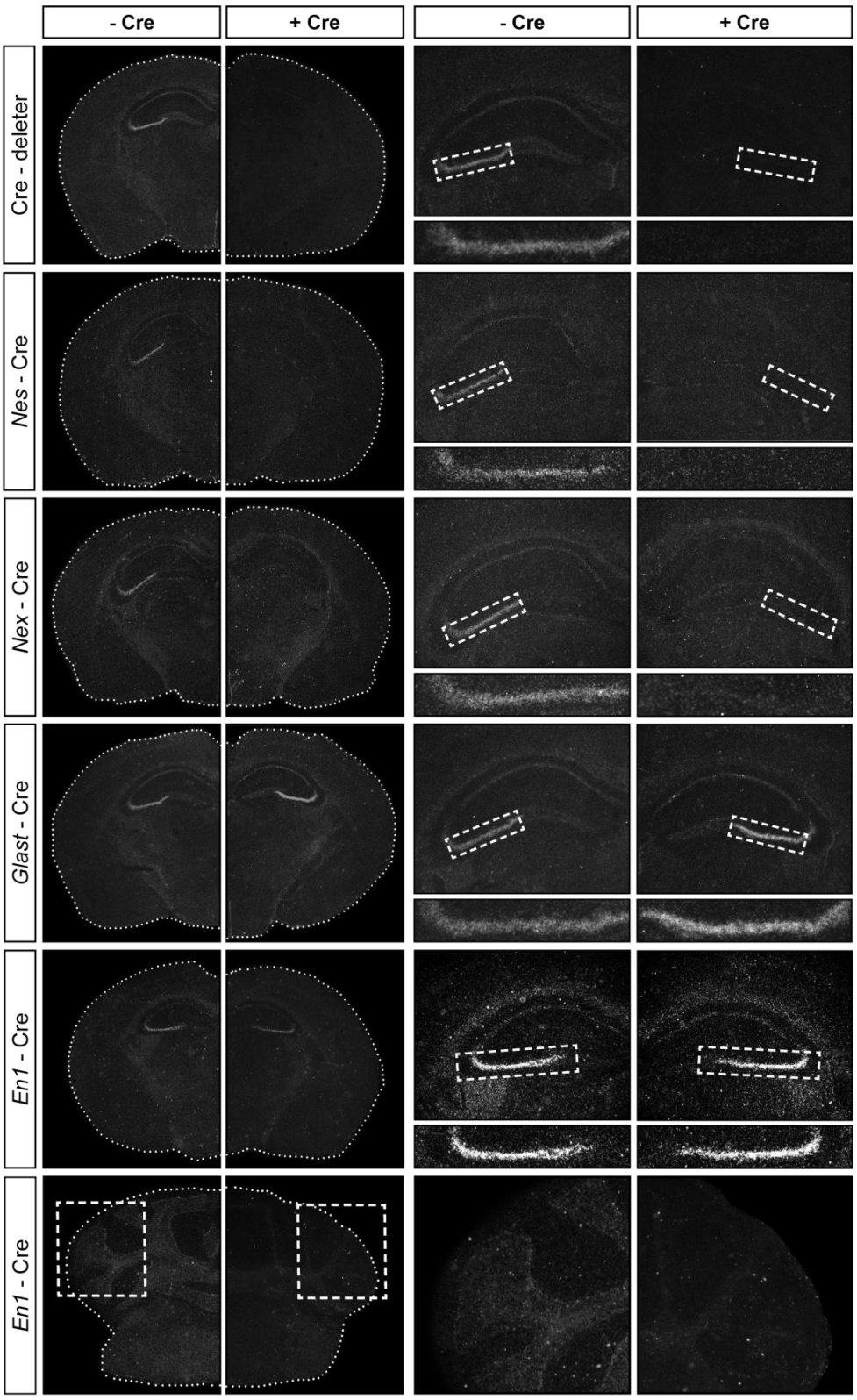

Figure 21: *In situ* hybridization-based *P2RX7* expression analysis
In situ hybridization using a human *P2RX7*-specific riboprobe. The different rows show control versus tissue-specific knockout via *Nes-Cre*, *Nex-Cre*, *Glast-Cre* and *En1-Cre* driver. For comparison the top panel shows a comparison of wild-type vs Cre-deleter mediated ubiquitous knockout. The left row shows coronal sections of the forebrain; the right panel shows a higher magnification of the hippocampus; for *En1-Cre* a coronal section of the cerebellum is included, additionally.

To gain deeper understanding where and in particular also to which extent *P2rx7* is expressed, we conducted qRT-PCR analysis. For this analysis we chose heterozygous mice carrying one wild-type and one humanized conditional allele bred to different cell type-specific Cre drivers (Figure 22). We chose heterozygous mice in order to enable a normalization of the expression of the human *P2RX7* expression to the mouse wild-type *P2rx7* allele which is insensitive to Cre recombinase mediated inactivation.

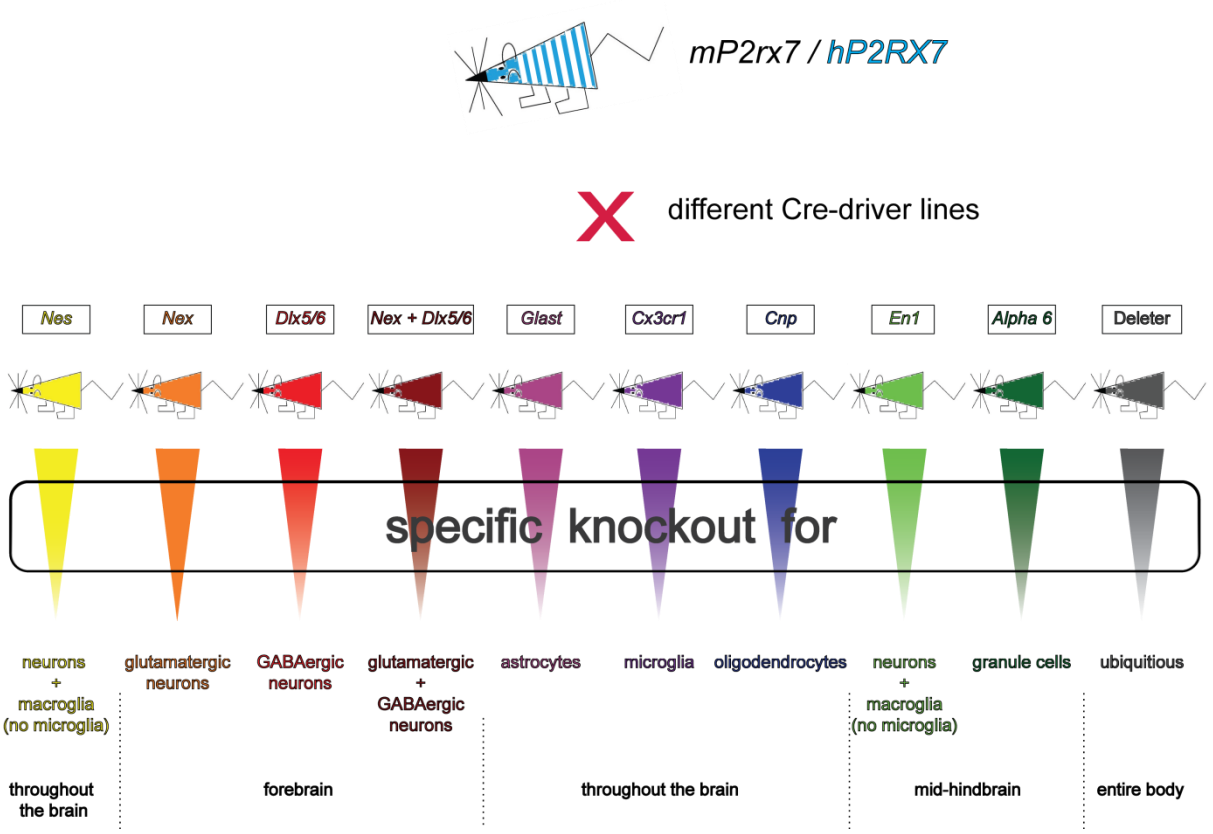

Figure 22: *P2RX7* expression analysis using Cre driver lines
Breeding scheme and Cre driver lines used for detailed expression analysis via *in situ* hybridization and quantitative real-time PCR.

We, therefore, measured the level of human *P2RX7* expression in relation to the endogenous mouse *P2rx7* expression level. As depicted in Figure 23 the expression of *P2RX7* for each of the three investigated tissues (cortex, hippocampus and cerebellum) in heterozygous (+/hWT) mice without Cre recombinase is set to 100%. As shown before (Figure 14) the expression in Cre-deleter positive mice (+/-) is completely abolished or below detection level, respectively.

Taking a detailed look at the expression analysis data one can see that in Nes-*Cre* positive mice the *P2RX7* expression levels are heavily decreased in all investigated brain regions down to roughly 10-20%. *Nes-Cre* is expressed in both neuronal and macroglial lineages (Tronche et al., 1999). These expression levels perfectly fit to the levels observed in those mice expressing the microglia-specific Cre recombinase driven by the *Cx3cr1* promoter (Yona et al., 2013). Both Cre lines together should basically cover almost all cell types (except of some blood cells and cells forming blood vessels) found in the brain and consequently they sum up to ~ 100%. This suggests 15-20% of the relative *P2RX7* expression in the brain, originate from microglia. To study the neuronal expression in more detail we used Cre recombinase drivers specific for glutamatergic (*Nex-Cre*) (Goebbels et al., 2006) and GABAergic (*Dlx5/6-Cre*) (Monory et al., 2006) neurons. We saw that P2RX7-signal reduction and, therefore, relative expression for both *Nex-Cre* and *Dlx5/6-Cre* was highest in the hippocampus. In the cortex we could not observe any significant *P2RX7* expression, neither in glutamatergic nor in GABAergic neurons. One should consider the relatively higher number of neurons in the hippocampus compared to the cortex, though. The slight reduction with the *Nex-Cre* also in the cerebellum can be explained with a partial recombination of this Cre-recombinase also in the hindbrain as it has been reported before in the original publication of the Cre-line (Goebbels et al., 2006). Regarding glial expression, we could detect a reasonable expression of P2X7R mRNA in astroglial cells as determined by using the *Glast-CreERT2* driver (Mori et al., 2006). Higher expression of glial cells was only observed in oligodendrocytes (*Cnp-Cre*) (Lappe-Siefke et al., 2003). These two Cre lines showed a ~50% and ~60% reduction in all analyzed brain regions compared to wild-type mice, respectively. Further, we could prove the expression of P2X7R in the cerebellum by using the *En1-Cre* mice as driver line (Kimmel et al., 2000). In this case the Cre recombinase under the control of the *En1* promoter covers most of the cells of the cerebellum due to its expression in early stage of mid hindbrain development (Orvis et al., 2012). This explains the dramatic drop of mRNA levels in the cerebellum of analyzed mice.

To sum up, by these analyses we unequivocally show that *P2rx7* is expressed throughout the brain and in every cell type analyzed with the exception of alpha6 subunit of $GABA_A$ receptor-positive granule cells of the cerebellum. There we could not detect a significant decrease of human transcript. By that, this analysis finally resolves the still controversial discussion with regards to neuronal *P2rx7* expression and its expression in the CNS in general. It has to be stated that these results do not display absolute expression levels in percent. It is of importance to take the relative number of cells of a given cell type into account when directly comparing the

expression levels. Unfortunately, there is limited knowledge regarding which cells contribute to what extent to the total number of cells in the brain.

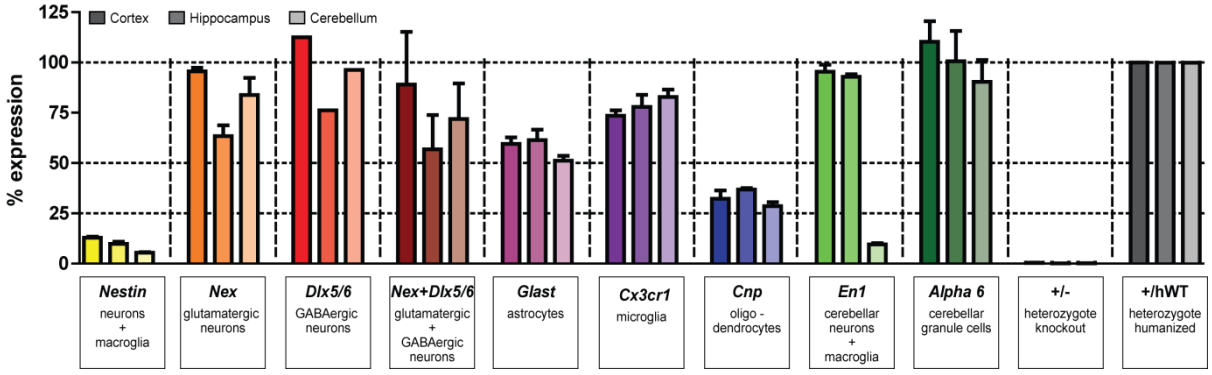

Figure 23: Cell type-specific analysis of *P2RX7* expression in the mouse brain
Relative reduction of *P2RX7* expression, as determined by qRT-PCR; cortex, hippocampus and cerebellum were investigated. Expression of the floxed human transcript was normalized to the expression of the murine transcript and relative expression to the respective region of heterozygous (+/hWT) mice is depicted. n=3.

8.3. Towards the involvement of the P2X7 receptor in neurodegeneration

As mentioned earlier a possible involvement of the P2X7 receptor in neurodegenerative pathologies like Alzheimer's Disease (AD) has been postulated before (Parvathenani et al., 2003; McLarnon et al., 2006; Delarasse et al., 2011; Diaz-Hernandez et al., 2012; Darmellah et al., 2012; Ni et al., 2013; Chen et al., 2014b; Miras-Portugal et al., 2015). However, all of these papers either investigate the downregulation or pharmacological inhibition of P2X7R in transgenic AD mouse models (Diaz-Hernandez et al., 2012; Chen et al., 2014a; Miras-Portugal et al., 2015) or they use *P2rx7* knockout mice investigating the endogenous APP processing (Delarasse et al., 2011). The combination of a transgenic mouse model for Alzheimer's disease and P2X7 receptor deficient mice has not been studied so far.

In order to directly study the potential involvement of P2X7R in Alzheimer's disease in an *in vivo* model, we crossed our *P2rx7* knockout mice (see introduction and 8.1) to a previously described AD mouse model (Knobloch et al., 2007; Lerche, 2012). These transgenic mice overexpress the human amyloid precursor protein (APP) carrying the two well described Swedish and Arctic

mutations. The Swedish mutation (K670N + M671L) has been shown to increase total Aβ levels *in vivo* (Mullan et al., 1992; Citron et al., 1992; Nilsberth et al., 2001) whereas the Arctic mutation (E693G) displays an increased propensity of Aβ40 to form protofibrils, compared to wild-type Aβ40 (Nilsberth et al., 2001).

8.3.1 Behavioral findings in ArcAβ mice lacking the P2X7R

We were interested in comparing four different genotypes obtained by breeding mice of the ArcAβ transgenic AD model overexpressing amyloid precursor protein (APP-OE) to our conventional *P2rx7* constitutive knockout animals (KO). The four genotypes we wanted to compare in behavioral experiments were therefore: pure wild-type mice (WT), *P2rx7* knockout mice (KO), transgenic AD mice (WT+APP-OE) and transgenic AD mice with the *P2rx7* knockout (KO+APP-OE). We choose mice between 11 and 16 months of age for our experiments.

As described by Knobloch et al. (2007) we observed a slight increase in locomotion of the APP-OE compared to WT (Figure 24a). We did not observe a significant effect of *P2rx7* on anxiety-related behavior in the OF test (Figure 24a). However, we saw an increased time spent in the inner zone, indicating reduced anxiety-related behavior in the APP transgenic mice. However, this result has to be taken with caution considering the increased locomotion of these mice. Aside of this known phenotype we could not detect any behavioral alteration in a first set of behavioral experiments.

Furthermore, we conducted three cognitive tests in our first screening. Neither the Y-maze (Figure 24b) nor the object recognition in the Y-maze test (Figure 24c) nor the spatial object recognition paradigm (Figure 24d) indicated significant alterations in cognitive performance between the different genotypes. The test per se seemed reliable due to the increased interest of the WT mice in the novel arm / novel objects. APP transgenic mice, however, showed similar interest indicating no impairment on hippocampus dependent short term memory.

To assess memory formation capacity over a slightly longer period of time we conducted the fear conditioning paradigm (Davis et al., 1999; Marsch et al., 2007). This paradigm also discriminates between more amygdala dependent learning (day 2-tone) and more hippocampus dependent memory (day 3-context) (Maren, 2005). Whereas we did not observe significant differences between the genotypes on day 2 while confronting the mice with the acoustic stimulus from day one, we did see differences on day 3 (Figure 25). On day 3 the mice are exposed to the same environment (context) they received the foot shock on day 1. This contextual memory is mainly

hippocampus dependent. WT+APP-OE mice showed less freezing than WT and KO mice. This indicates impaired memory formation in the transgenic AD mice. This impairment was reversed in those transgenic AD mice that in addition carry the *P2rx7* knockout (KO+APP-OE).

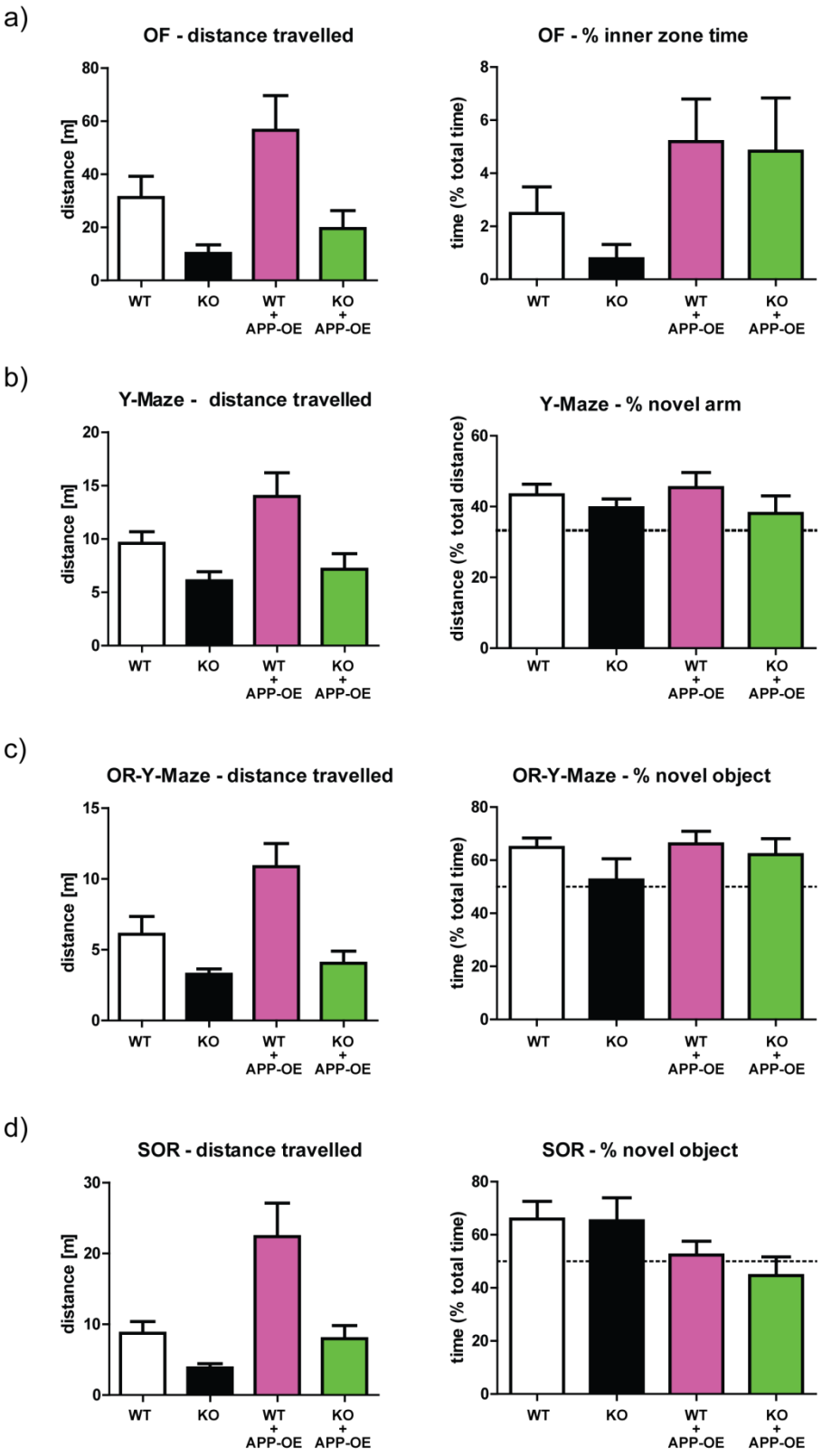

Figure 24: Basic behavioral screening of *P2rx7* knockout mice bred to the ArcAβ AD mouse model
A basic behavioral screening for locomotion and cognition did not show significant differences between the genotypes. The test paradigms **a)** open field (OF) for locomotion (left panel) and anxiety (right panel), **b)** Y-maze, **c)** object recognition (OR) in Y-maze and **d)** spatial object recognition (SOR) for locomotion (left panel) and cognition (right panel) were conducted. First 5 minutes of the experiments are shown. (n=11-12)

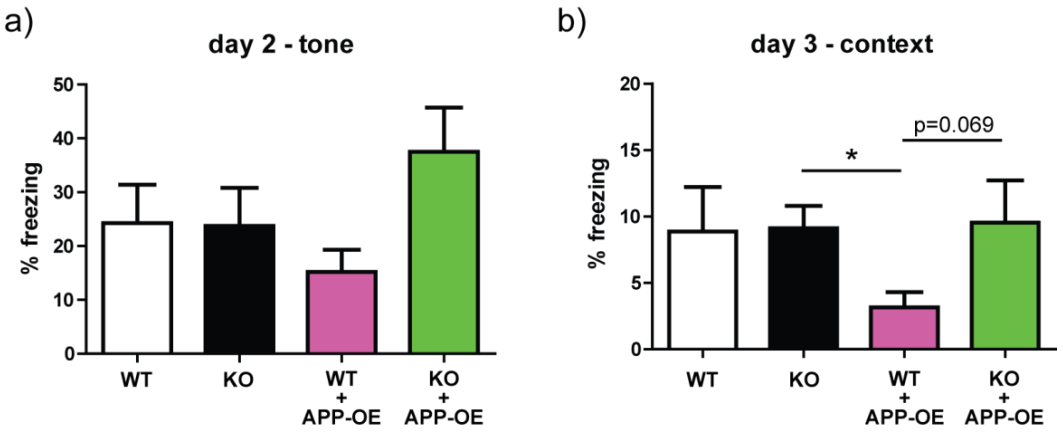

Figure 25: *P2rx7* knockout effect on fear memory formation of ArcAβ AD model
Fear conditioning paradigm. **a)** No genotype-dependent differences in amygdala-dependent learning as investigated on day 2 were observed; **b)** hippocampus dependent contextual learning was disturbed in APP-overexpressing mice and partially rescued in APP-OE mice lacking P2X7R. (ANOVA, ***** $p < 0.05$; n=11-12)

To more deeply enlighten these findings of the fear conditioning paradigm we decided to conduct the well-established water cross maze (WCM) paradigm (Kleinknecht et al., 2012; Giusti et al., 2014; Reichel et al., 2015; Vogl et al., 2015). This two-week paradigm is separated in the learning (first week) and the re-learning phase (second week) where the target platform is moved to the opposing site of the apparatus (Figure 26). After the first week we observed a significant effect of the transgene on the accuracy in finding the platform (RM-2way ANOVA, time: $F_{(37, 6)} = 34.45$, $p < 0.000$). APP-OE transgenic mice did not reach the 80% accuracy level after 6 days of learning (Figure 26a). Additionally, all APP non-transgenic mice fulfilled the criterion of an "accurate learner" on day 6 of the first week, whereas for both APP-OE genotypes less than 40% of the mice fulfilled this criterion (Figure 26b). The second week with the "re-learning" did again show the deficiency of the APP-OE transgenic mice to reach accuracy levels of 80% (Figure 26c). In fact, they even remained at chance levels (RM-2way ANOVA, Time: $F_{(38, 5)} = 56.07$, $p < 0.000$; Time x Genotype: $F_{(38, 5)} = 7.76$, $p < 0.000$). However, APP-OE transgenic mice lacking P2X7R performed considerably better and were as good as WT mice on day 6 of the re-learning protocol in regard to accuracy. A similar picture was seen for the number of accurate learners. Whereas the number of KO+APP-OE mice reaching the criterion for an accurate learner was comparable to WT and KO mice, WT+APP-OE mice stayed far below, with only about 10% of accurate learners (Figure 26d).

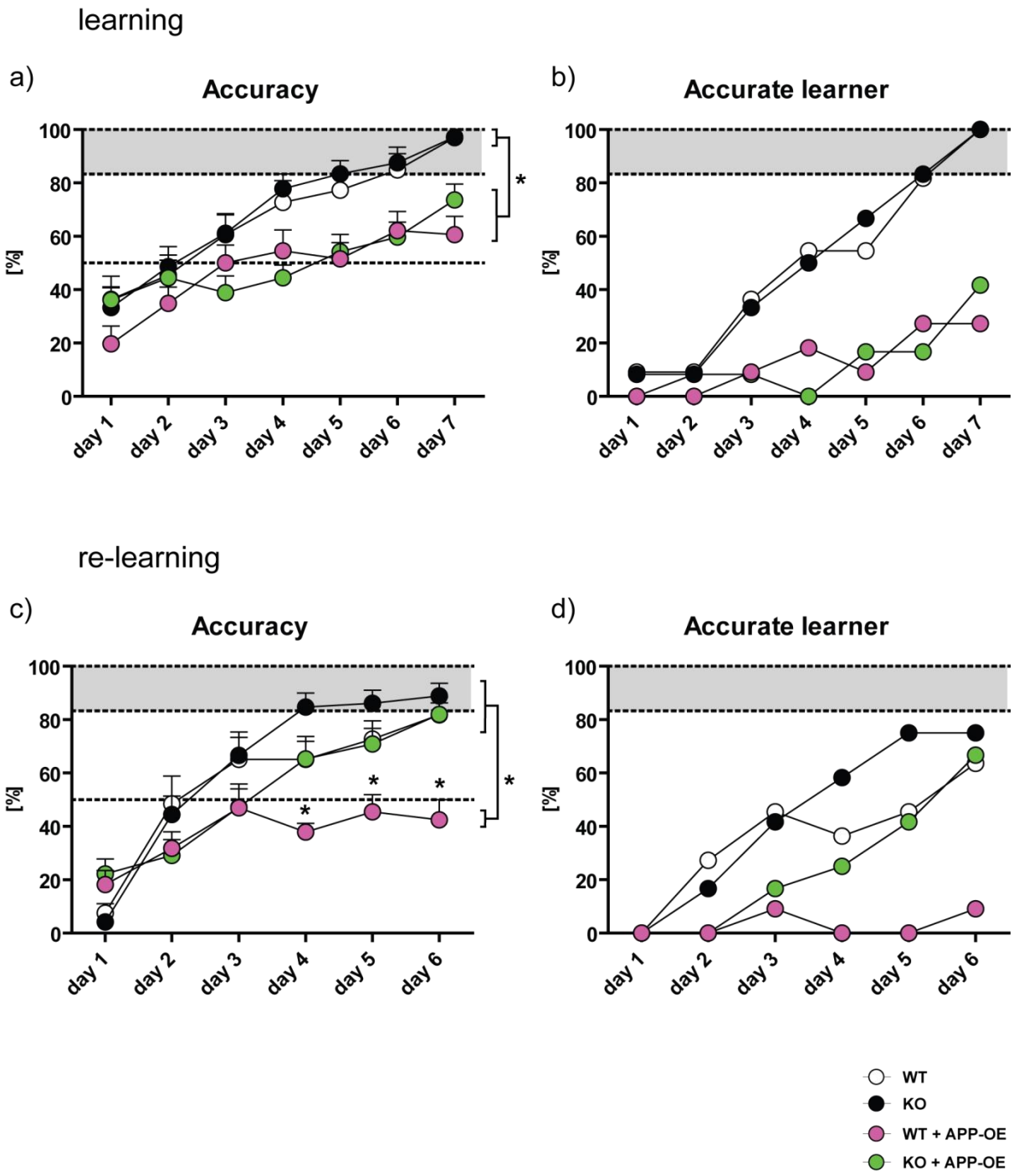

Figure 26: *P2rx7* knockout effect on long-term memory formation in the ArcAβ AD model as determined by water cross maze paradigm

The water cross maze paradigm reveals genotype-dependent differences. First week of learning (upper panels) and second week of re-learning (lower panels) of the WCM paradigm are depicted. The left panels show the accuracy in percent (**a)** + **c)**); the right panels the number of mice that fulfill the criterion of an accurate learner (**b)** + **d)**). In the second week of re-learning it becomes obvious that APP-OE mice deficient in P2X7R show improved memory performance. (RM-2way ANOVA; ***** $p < 0.05$; n=11-12)

8.3.2 Investigating molecular and cellular mechanisms potentially underlying the beneficial effects of P2X7R deficiency on cognitive function

8.3.2.1. Investigation of potential effects of the P2X7 receptor on APP processing

Amyloid β (Aβ) the detrimental molecule that is one of the hallmarks in Alzheimer's disease is derived from the amyloid precursor protein (APP). Many different secretase pathways have been described for the processing of this protein. However, the critical one for the AD pathology is the combined cutting of the precursor protein with β– and γ–secretase. Only this combination of secretases results in the Aβ molecule. Therefore, we took special interest in the activity of the different known secretases and their respective products derived from APP. We conducted Western blot analysis of those female mice that underwent the behavioral screening. Two different fractions (membrane bound and soluble proteins) were obtained from brains of these mice. In order to visualize all possible processing products of APP we used a variety of different antibodies. An overview of the epitopes detected by these antibodies is depicted in Figure 27b.

As expected we observed a strong enrichment of full-length APP (APP-FL) in the APP-OE transgenic mice compared to WT mice in both fractions (Figure 27a). Independent of the *P2rx7* genotype, the amount of APP in the APP-OE mice was not altered. Further, we only detected soluble APPα and APPβ in transgenic mice expressing the human APP since we used human specific antibodies for these processing products. No differences in the amount of sAPPα and sAPPβ between the two groups of APP-transgenic mice were observed. This indicates that the P2X7R has no direct effect on α- and β-secretase activity in these animals. Also γ-secretase activity seemed not to be affected by the inactivation of P2X7R. Aβ levels were identical for all transgenic mice. Along this line we could neither see *P2rx7* genotype dependent differences in the amount of carboxy-terminal fragment-α (CTF-α) nor of CTF-β. This supports the assumption that the P2X7R has no direct effect on α- or β-secretase activity. Also the recently discovered η-secretase (Willem et al., 2015) activity seemed to be untouched by the loss of P2X7R as indicated by the unaltered levels of amyloid-η (Aη) and CTF-η.

Based on these Western blot analyses it seems likely that the P2X7R has no direct effect on the processing of APP. In particular, we did not see an increase of α–secretase products or a decrease of β- and γ-secretase products, respectively in the KO mice. Therefore, alterations in the APP processing seem not to be the underlying mechanisms that could explain the beneficial

effect of the P2X7 receptor knockout on cognitive function in our ArcAβ mouse model of Alzheimer's disease.

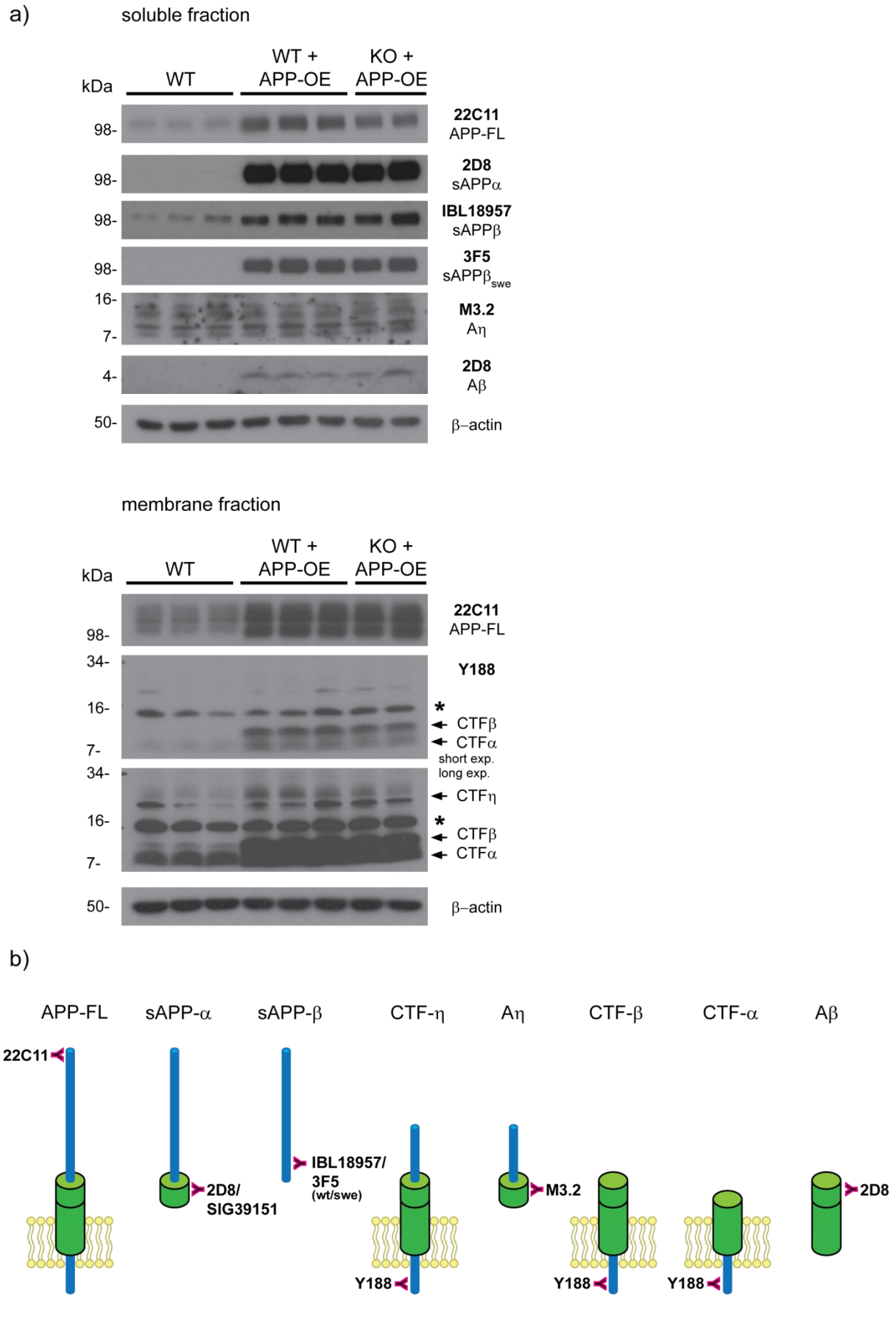

Figure 27: Figure legend see next page

Figure 27: P2X7R does not interfere with APP processing
a) Soluble (DEA) and membrane/nuclear (RIPA buffer) - fraction of WT, WT+APP-OE and KO+APP-OE mice are shown. **b)** Antibodies used for this experiment and a scheme of which epitope they bind to within the different APP processing products, is depicted. (APP-FL: 8 full-length amyloid precursor protein isoforms; sAPP-α: solubleAPPα ; sAPP-β: solubleAPPβ; sAPP-β_{swe}: solubleAPPβ with Swedish mutation (human); CTF-η: carboxy-terminal fragment-η; Aη: amyloid-η; CTF-α: carboxy-terminal fragment-α ; CTF-β: carboxy-terminal fragment-β; Aβ: amyloid β; *****(asterisk) indicates unspecific signal)

We further investigated whether the P2X7 receptor has any impact on the processing of endogenous APP. Moreover, we wanted to test if the human P2X7 receptor has any influence on the activities of the different APP secretases. Therefore, we isolated protein of mouse brains and conducted Western blot analyses similar to the experiment described above (Figure 28). For this experiment we included regular WT mice, conventional *P2rx7* KO mice as well as our humanized *P2RX7* mice and the *P2rx7* hKO mice derived of the humanized *P2RX7* mice.
As in the previous experiment with the APP-transgenic mice, we could in general not observe an effect of the P2X7R knockout on the processing of APP. Nonetheless, we observed slight differences for those samples originating from mice expressing the human P2X7 receptor. Total full-length APP levels seemed to be - if at all - only moderately lower in mice expressing the human receptor. But, levels of sAPPα were markedly decreased. Even more obvious is the effect of the human P2X7 receptor on the levels of the newly described Aη (Willem et al., 2015). Whereas these levels for WT and both *P2rx7* knockout lines seemed to be very comparable, in humanized mice they were evidently lower. Whether or not sAPPβ levels were also altered in humanized mice remains unclear. The signal appears slightly decreased for humanized mice compared to the other genotypes, as well.
In the membrane fraction we could not observe any alterations. Also FL-APP levels did not differ which might favor the assumption that total APP levels are not altered between the different genotypes.

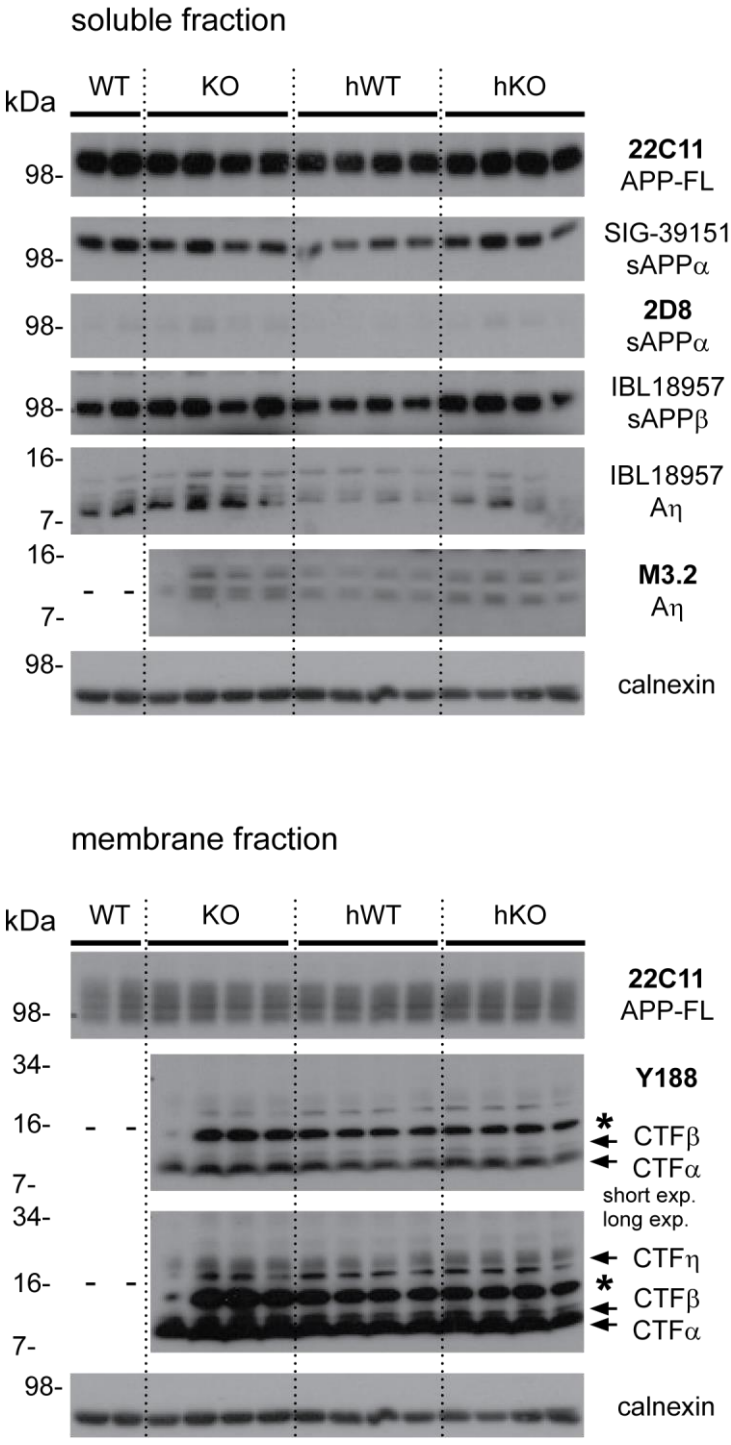

Figure 28: APP processing in different P2X7R mouse lines
Soluble (DEA) and membrane/nuclear (RIPA buffer) - fraction of WT, conventional *P2rx7* knockout (KO), humanized *P2RX7* (hWT) and conditional *P2RX7* knockout mice (hKO) are shown; for orientation of the different used antibodies compare scheme of Figure 27b. (APP-FL: 8 full-length amyloid precursor protein isoforms; sAPP-α: solubleAPPα ; sAPP-β: solubleAPPβ; sAPP-β_{swe}: solubleAPPβ with Swedish mutation (human); CTF-η: carboxy-terminal fragment-η; Aη: amyloid-η; CTF-α: carboxy-terminal fragment-α ; CTF-β: carboxy-terminal fragment-β; Aβ: amyloid β; *****(asterisk) indicates unspecific signal)

8.3.2.2. Quantification of amyloid β plaque load

As a further, rather basic investigation to unravel the underlying causes of the protective effect of *P2rx7* knockout we conducted a quantification of amyloid β deposition. Aβ plaque formation is one of the hallmarks in progression of Alzheimer's disease (Seeman and Seeman, 2011). Also the original publication of the transgenic arcAβ AD model mice showed a progressive increase in Aβ plaque formation over time starting around an age of 6 months. Therefore, we chose aged mice between 14 and 20 months of age for this analysis. To visualize Aβ plaques in brain sections, a staining with Thioflavin S was conducted. The staining with Thioflavin S is a standard method to visualize Aβ deposits (Sun et al., 2002; Bussière et al., 2004). For the analysis three similar coronal brain sections, including dorsal hippocampus of 9 mice of each genotype (n=9), were chosen. The analyzed area including hippocampus and cortex is depicted in (Figure 29c).
We found that both the number of Aβ plaques ($t_{52}=4.253$, $p<0.0001$) as well as the size of these plaques ($t_{52}=5.024$, $p<0.0001$) was significantly increased in transgenic mice deficient for P2X7R compared to APP-transgenic mice with normal P2X7R expression. The number of plaques in the knockouts was increased by about 60% (Figure 29a) and the actual size of the plaques was more than doubled (Figure 29b).

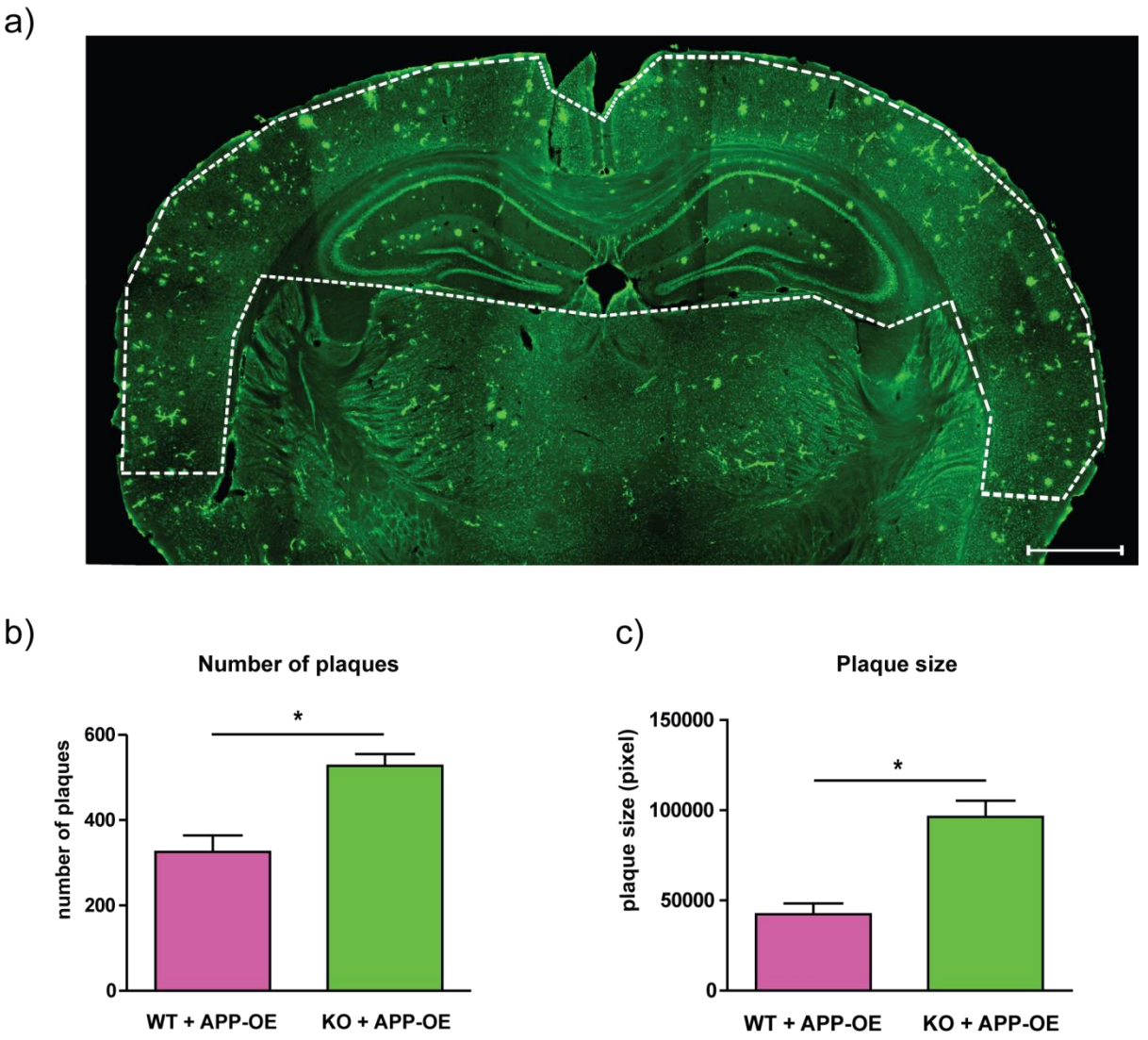

Figure 29: Quantification of amyloid β plaque burden in ArcAβ mice
Quantitative analysis of Aβ deposition in APP-OE mice with or without P2X7 receptor expression. Thioflavin S staining was performed on coronal brain section (Bregma: ~-1.2 to -2.2mm) ; the analyzed area is surrounded by dashed line; scale bar: 100µm.
Both the number **b)** and the size **c)** of Aβ plaque deposits in the cortex and dorsal hippocampus was analyzed. (Student's t-test, ***** $p < 0.05$; n=9) (data by Sebastian Teschner)

9. Discussion

9.1. New *P2rx7* knockout mouse lines

The P2X7 receptor is a long studied ligand gated ion channel. Alterations in the function of the receptor, in particular caused by a variety of single nucleotide polymorphisms (SNPs) in the human *P2RX7* gene have repetitively been associated with a diversity of different diseases, both affecting the CNS and / or other organs (Di Virgilio et al., 2009; Volonté et al., 2012; Swartz et al., 2015). The human *P2RX7* gene is highly polymorphic with more than 3400 reported SNPs (National Center for Biotechnology Information SNP database, accessed 11.01.2016). Many of these polymorphisms have been associated with increased risk for musculoskeletal, cardiovascular, infectious, inflammatory and psychiatric disorders (Gartland et al., 2012; Gidlöf et al., 2012; Fernando et al., 2007; Barden et al., 2006b; Lucae et al., 2006). But also independent of these risk polymorphisms, the P2X7 receptor has been suggested to play an important role in the pathology of many diseases like e.g. amyotrophic lateral sclerosis and multiple sclerosis (Yiangou et al., 2006), neuropathic and inflammatory pain (Chessell et al., 2005), rheumatoid arthritis (Bhattacharya et al., 2011), cancer (Ghiringhelli et al., 2009; Adinolfi et al., 2012) as well as Alzheimer's disease (Parvathenani et al., 2003; McLarnon et al., 2006; Delarasse et al., 2011; Diaz-Hernandez et al., 2012; Darmellah et al., 2012; Ni et al., 2013; Chen et al., 2014b; Miras-Portugal et al., 2015). A very recent study, moreover, showed that the well described non-synonymous SNP Q460R changes receptor function if co-expressed with the wild-type P2X7R (Aprile-Garcia et al., 2016), a state that was shown to be overrepresented in cohorts of depressed patients (Lucae et al., 2006).

This possible involvement and the therefore potential importance of the P2X7 receptor in health and disease made it an important target for the development of selective antagonists. Some of the oldest and still used antagonists are Brilliant Blue G (BBG) (Soltoff et al., 1989) and pyridoxalphosphate-6-azophenyl-2-4-disulfonic acid (PPADS) (Lambrecht et al., 1992). However, they have been shown to additionally inhibit other receptors, pannexin 1 in case of BBG (Qiu and Dahl, 2009) and other P2X receptor family members in case of PPADS (Nicke et al., 1998). In the last few years several new, more specific compounds have been described as P2X7 receptor antagonists – for detailed review see Bartlett et al., 2014 – however, *in vivo* testing and full characterization is still pending for most of them.

This is why there was also great effort to create animal models to study the knockout of the P2X7 receptor not least in order to be able to investigate its function in an *in vivo* environment. Namely three different *P2rx7* knockout mouse lines have been described so far (Solle et al., 2001; Chessell et al., 2005; Basso et al., 2009). However, just like most inhibitors, these knockout mouse models have recently been shown not to be free of flaws. It was shown that due to the design of the knockout some splice variants can escape inactivation (Nicke et al., 2009; Taylor et al., 2009; Masin et al., 2012). Due to these limitations as well as inconsistencies in regard to the findings based on these knockout mice, two new *P2rx7* knockout lines were previously created in our lab (Walser, 2012).

As a first, important step of this work we proved the full absence of all protein coding splice variants of the murine *P2rx7* gene in our new knockout lines. These true null alleles for *P2rx7* are a major advantage compared to previously published knockout mouse lines. The functional validation of the receptor knockout in the conventional *P2rx7* knockout mouse line was already successfully addressed previously. Sandra Walser could show that primary macrophages obtained from these knockout mice were no longer capable to release cytokines in response to LPS stimulation and subsequent stimulation with the receptor agonist BzATP. Furthermore, P2X7 receptor mediated calcium influx into the cell was significantly impaired in cells of those mice (Walser, 2012).

To functionally validate the conditional knockout mice we conducted the very same experiments. Both cytokine secretion as well as calcium influx into the cell upon stimulation of the receptor was ablated in cells obtained from these *P2rx7* knockout mice compared to wild-type littermates. Additionally, we also investigated the pore forming capacity by measuring the ability of primary cells to take up the dye Yo-Pro-1-iodine upon prolonged stimulation of the P2X7R. In this readout we also observed an impaired capacity of knockout compared to wild-type cells, further demonstrating the complete loss of P2X7R function. We included this readout as an additional proof for our knockout line. Additionally it is a well-established readout in the comparison of P2X receptor affinities to different agonists and antagonists as well as in the comparison of the homologs of the receptor from different species like mouse, rat and human (Hibell et al., 2001; Anderson and Nedergaard, 2006; Donnelly-Roberts et al., 2009; Hempel et al., 2013). For stably transfected 1321N1 cells with either the mouse or the human P2X7R, it was shown that receptor activation levels upon stimulation with the same concentration of BzATP are 10-100 times lower for the mouse compared to the human receptor (Donnelly-Roberts et al., 2009). Another study comparing rat and human P2X7R showed that only few amino acids are

responsible for the altered receptor activation levels upon stimulation with ATP (Bradley et al., 2011). Unfortunately, all previous studies investigating inter-species differences of the P2X7 receptor were conducted on heterologous expressing cells. Therefore, we wanted to use this readout to compare the mouse and the human P2X7 receptor, endogenously expressed in primary cells obtained from wild-type mice and our humanized *P2RX7* mice, respectively. To get comparable Yo-Pro-1 uptake levels by the murine receptor we had to stimulate the receptor with ~10 times higher concentrations of BzATP than the cells expressing the human receptor. Similarly we observed that the modulator TFP (trifluoperazine - 3µM) had a potentiating effect on Yo-Pro-1-uptake capacity upon stimulation exclusively on the murine but not on the human receptor. As for the concentration dependency towards the agonist, differences in regard to sensitivity towards different positive and negative modulator have been conducted and described before, for cells transfected with murine and human P2X7 receptors (Nörenberg et al., 2011, 2012; Fischer et al., 2014). Here were could for the first time show differences between murine and human P2X7 receptors in a directly comparable *in vivo* situation. As such our humanized *P2RX7* mice open totally new possibilities for testing new P2X7R modulators under physiological conditions that might be relevant for applications in human subjects.

There are major discrepancies in the phenotypes of previously described *P2rx7* knockout mouse line. Whereas constitutive knockouts are viable and fertile and do not show gross phenotypic alterations, behavioral changes have been described. However, studies based on the above mentioned *P2rx7* knockout lines established by Solle et al. (2001), Chessell et al. (2005) and Basso et al. (2009) are inconsistent in regard to their findings as well as in regard to how the experiments were conducted. The only common finding is a more active stress coping behavior of the knockout mice, i.e. decreased immobility in the FST and TST, compared to the wild-type mice. However, as mentioned, the conditions of the experimental setups were highly inhomogeneous. Furthermore, not all of the tests were conducted on the same sex or with actual littermates as controls. Behavioral experiments conducted by Sandra Walser (Walser, 2012) with our new conventional *P2rx7* knockout mice could not support any of the findings on the so far published knockout lines. Both, male and female knockout mice and wild-type littermates were tested. For male mice no behavioral alterations were identified. For females, if at all, only slightly increased anxiety (as indicated by the OF paradigm) as well as a decreased active stress coping behavior (i.e. increased immobility) of the knockout mice in the FST was detected. This phenotype is in contrast to the previous findings conducted on other *P2rx7*

knockout mouse lines. However, as mentioned before these previous findings bear certain caveats.

To gain more insight we repeated this basal behavioral screening of *P2rx7* knockout mice with our second, conditional knockout mouse line. These mice are humanized for the *P2RX7* gene and at the same time vulnerable to Cre recombinase-mediated inactivation of the gene by insertion of *loxP* sites. By using a Cre-deleter line it is possible to create constitutive *P2rx7* knockouts based on the humanized allele.

However, again none of the conducted paradigms (OF, EPM, DaLi, FST) showed any difference between *P2rx7* knockout and wild-type mice. Further, we included humanized mice expressing the human P2X7R in this test. Again, we could not observe any behavioral alteration in these mice under basal conditions.

Given the fact that our two new knockout lines are, in contrast to previously described knockout mice, indeed null alleles for all known *P2rx7* splice variants, we suggest that under basal conditions the absence of the P2X7 receptor in the mouse does not become manifested in behavioral alterations. At least not in the classical readouts we assessed. Moreover, we do not see phenotypic alterations in our mice expressing the human P2X7 receptor per se or in comparison to knockout mice. It was proposed before that the human receptor is more active than the murine version (Donnelly-Roberts et al., 2009). Our results on pore formation capacity upon stimulation with different levels of the agonist BzATP supported this assumption. If, based on these finding, one assumes that the human receptor can be regarded as a sort of gain-of-function version of the murine receptor, we can further propose that under basal conditions neither the knockout nor an increased *P2rx7* function has direct effects on basal emotion.

Still, the manifestation of mental disorders is highly unlikely to be caused solely by a single risk gene. It is rather a combination of genetic variations and environmental factors that ultimately leads to the manifestation of a certain pathology. Stress in particular has been described over and over again as one of the most important of these environmental factors (Holsboer, 2001; de Kloet et al., 2005; Slavich and Irwin, 2014). Due to that, we exposed our conventional *P2rx7* knockout mice to the well-established chronic social defeat stress (CSDS) paradigm (Nestler and Hyman, 2010; Berton et al., 2012; Hartmann et al., 2012a) to assess whether the knockout of the P2X7 receptor plays a role in in the mice' stress response. The success of the conducted stress protocol was estimated by established readouts (Wagner et al., 2012; Hartmann et al., 2012a; Wang et al., 2013) like thymus atrophy and adrenal gland enlargement as well as a general

decrease in the fur quality of the stressed mice compared to unstressed littermates. We could observe all these physiological and endocrinological changes in our stressed group. Further we could observe a stress effect in all conducted tests except in the FST paradigm which per se is a severe aversive stressor for mice (Kloet and Molendijk, 2016), suggesting that this acute stressor could mask the chronic stress effect. Unfortunately, we could as well not observe a significant stress induced increase in anxiety for the wild-type control group, as investigated by the OF and DaLi paradigms. However, the rather low percentage of time spent in the inner zone of the OF and in the lit compartment of the DaLi of the basal, unstressed wild-type mice make a further decrease hardly possible. Therefore, one has to assume that a floor effect (Weiss et al., 2010) prevents the expression of a stress effect in the wild-type group. In the OF paradigm we could detect a significant decrease in inner zone time as well as inner zone entries for the knockout mice indicating higher vulnerability to stress. However, this effect was not present in the DaLi paradigm - another readout for anxiety-related behavior. Further, as indicated before, basal levels of wild-type and knockout mice differ dramatically in this OF experiment. This is something we did not observe in any previous phenotypic screenings of our knockout mice and thus makes a reliable statement on the outcome of this paradigm rather difficult.

One of the most used and best described readouts for stress susceptibility is the social avoidance paradigm (Haller and Bakos, 2002; Berton and Nestler, 2006b; Golden et al., 2011; Sandi and Haller, 2015). It has been shown that chronic stress leads to social avoidance and social fear towards fellow species (Berton et al., 2006a). In our test we observed that whereas the interaction time with an empty control cage was unaltered, the interaction time with an unfamiliar mouse was as described and expected, heavily reduced for our stressed wild-type controls compared to their unstressed littermates. In contrast, stressed *P2rx7* knockout mice did not show this significant decrease in interaction time with the unfamiliar mouse but spent a similar amount of time exploring it comparable to unstressed wild-type or knockout mice. The same effect is seen if the actual time spent with the unfamiliar mouse in percent of the duration of the experiment, is evaluated. This remarkable finding suggests that *P2rx7* knockout mice might be more resilient towards stress induced effects on social behavior. Yet, further experiments e.g. with the second conditional *P2rx7* knockout mouse line seem to be necessary to confirm this finding. Moreover, the conditional mice would allow for more detailed investigation of the origin of this effect. By breeding with tissue- or cell type-specific Cre recombinase driver mice it would be possible to induce the loss of *P2rx7* only in a certain brain region or certain population of cells. This could help to better understand the underlying

mechanisms conveying resistance towards chronic stress and to more specific therapeutics for stress-related disorders.

9.2. P2X7 receptor expression in the brain

In order to investigate the effect of a cell type-specific knockout in the brain in more detail, precise knowledge of where exactly, and to a certain degree also to which extent *P2rx7* is expressed in the brain, is crucial. However, in this regard there are highly controversial opinions in the field of P2X receptors. This becomes very clear in the latest review of Sperlágh and Illes (2014). In particular neuronal expression of the P2X7 receptor is still up for debate. One of the most critic paper on neuronal expression is from the Surprenant lab that claimed to not "find evidence for P2X7 receptor protein in hippocampal neurons or their input-output projections" (Sim et al., 2004). To finally answer this question of *P2rx7* expression in the mouse brain we conducted a detailed expression analysis based on *in situ* hybridization experiments as well as on quantitative real-time PCR. We chose to investigate *P2rx7* mRNA expression rather than protein since the unspecificity of available P2X7R antibodies in the brain precludes a direct analysis of protein distribution and levels. As described before, the currently available antibodies for mouse P2X7R are a powerful, useful tool for all kinds of peripheral tissue. However, in the brain a reliable immunological detection largely failed so far (Sim et al., 2004; Sánchez-Nogueiro et al., 2005). The P2X7R signal is masked by an "unspecific" signal that is present to the same extent also in knockout mice which makes it impossible to give a statement regarding P2X7R expression in the brain relying on antibody-based detection. This phenomenon was first seen for the available *P2rx7* knockout lines from Glaxo-Smith-Kline and Pfizer (Sim et al., 2004). Later identification of formerly unknown splice variants that escape inactivation in these two "knockout" lines suggested that the signal originates from these splice variants that are still abundant in these mice (Sperlágh and Illes, 2014). Nonetheless, Western blot analyses with our new knockout mice – which do not express any splice variant anymore (compare Figure 11 & Figure 14) – showed the same unspecific band exclusively in brain tissue (data not shown). It therefore seems more likely that in brain tissue – maybe neuronal cells, as proposed by Sim et al., 2004 – other proteins of a very similar size (~75kDa) are expressed that can be recognized by the antibodies. Our findings support this assumption confirming the circumstance that immunohistochemical analyses on brain sections seem impracticable. Therefore, we focused on

mRNA expression instead of protein. To conduct our analysis we used our humanized *P2RX7* mice.

In a first step we compared relative expression levels of the seven P2X receptor family members amongst each other. We investigated both cortical and hippocampal tissue samples as well as primary cultures enriched for either neurons, astrocytes or microglia or not enriched primary cultures referred to as "mixed culture" which we used for several functional experiments.

We could detect expression of all family members in both, cortex and hippocampus. *P2RX7* levels were comparable between both brain regions, while murine *P2rx7* was, as expected, not detectable any more. In the primary cultures we could as well detect expression of all family members except for *P2rx1*, which we detected at a very low level in the mixed culture. The fact that we could not detect it in any of the "pure" cultures favors the assumption that it is probably just right below the detection level. Another exception is the primary microglial culture. Here we could only detect *P2rx4*, *P2rx6* and *P2rx7*. In all cases *P2rx4* outreaches the other family members regarding expression levels. The difference of *P2rx4* to *P2rx7* expression is the least in neurons with around 2 fold higher expression of *P2rx4*. In astrocytes and microglia the difference increases to about 18 fold. Given these results it appears logic that the expression difference in the tissue samples which presents a mixture of those cell-types, lies somewhere in between, with about 2.5 fold in the cortex and 4.5 fold in the hippocampus.

This is an important finding since of all P2X family members, *P2rx4* is the most closely related to *P2rx7* (North, 2002). Moreover, *P2rx4* is up to 10 times more sensitive to the ligands ATP and BzATP than *P2rx7* (Khakh and North, 2012) and both share similar expression and function in the periphery (Guo et al., 2007). It was further proposed that *P2rx4* and *P2rx7* can form functional heteromers (Guo et al., 2007), yet, this assumption has not finally been proven. However, towards a functional analysis of the *P2rx7* receptor *in vivo* these findings regarding the expression of other family members should always be critically kept in mind. Most important though, is the finding that *in vitro* we were able to show *P2rx7* expression for all of the three main cell types of the brain: microglia, astrocytes as well as for neurons. Albeit, it has to be noted that cultivated cells will never fully resemble the *in vivo* situation. In fact it might even be, that the *in vitro* conditions have an inductive effect on *P2rx7* expression. This is why we additionally wanted to investigate *P2rx7* expression directly in the mouse brain.

For this next step we took advantage of the vulnerability of our humanized *P2rx7* allele to Cre recombinase-mediated inactivation. By breeding the humanized mice with Cre driver mice,

P2rx7 expression can be ablated in a tissue- or cell type-specific manner. To investigate *P2rx7* expression on histological brain sections we chose ISH analysis to compare these tissue-specific knockout mice to wild-type littermates. By comparison of the ISH signal one can infer the mRNA expression pattern of *P2rx7*. In this analysis we focused on brain sections covering the dorsal hippocampus regions. This region includes the most prominent expression pattern of *P2rx7*, namely in the CA3 (compare http://mouse.brain-map.org). Based on specific Cre lines for cerebellum, astrocytes, macroglia (astrocytes, oligodendrocytes and radial glia (Eglitis and Mezey, 1997; Borjabad et al., 2010)) and glutamatergic neurons of the forebrain we could address some critical points of debate regarding *P2rx7* expression. We did observe *P2rx7* expression in the cerebellum. The question which precise types of cells express *P2rx7* in the cerebellum we were not able to answer with the used Cre lines. Previous studies claimed astro- and Bergmann-glia to express *P2rx7* in the cerebellum (Carrasquero et al., 2010; Habbas et al., 2011). The question if and to which extent astrocytes express the receptor cannot be fully clarified by ISH analysis. The results suggest that there is a quite homogenous, yet, low astrocytes-derived expression throughout the brain. This is in line with the findings of the qRT-PCR analysis discussed below. An interesting finding was revealed by the knockout of *P2rx7* in cells positive for *Nes-Cre* recombinase. We see a severe signal reduction almost down to a complete knockout, mediated by the Cre-deleter driven by the *Rosa26* regulatory elements. The prominent signal in the CA3 of the hippocampus also fully disappears in the *Nes-Cre* positive mice. Due to the localization of the signal a neuronal origin seemed likely. We could verify this assumption with a Cre line specific for glutamatergic neurons of the forebrain, based on the *Neurod6* regulatory elements. Floxed *hP2RX7* mice positive for *Nex-Cre* do lack the typical CA3 signal as seen in the *Nes-Cre* animals but, they still express low levels of *P2rx7* throughout the brain. This tells us that the signal in the CA3 of the hippocampus origins from *P2RX7* expression in glutamatergic neurons. Comparing them to Cre-deleter positive mice even in the *Nes-Cre* mice a faint ubiquitous signal is visible. This can only be explained by the remaining microglial expression of *P2rx7* which is not covered by *Nes-Cre*. Microglial expression is one of the best described expressions of *P2rx7* in the brain (Friedle et al., 2011; Arnoux et al., 2013).

However, the amount of microglia in the brain in relation to the total amount of cells is rather low. Hence we did not expect to be able to visualize this appropriately in an ISH analysis. Therefore, we decided to additionally conduct quantitative real-time PCR analyses. This technique further enables a better assessment of the actual expression levels of *P2rx7* in the

brain. We isolated RNA from cortex, hippocampus and cerebellum for these analyses. We used mice heterozygous in regard to the humanized *P2RX7* allele. This enabled us to normalize the expression of the human *P2RX7* mRNA to the endogenous *P2rx7* expression levels. Moreover, we included several additional new Cre recombinases in these analyses additionally to the ones we used for the ISH analysis.

In general, the findings of the qRT-PCR based expression analysis fully support the previous findings in the *in situ* hybridization studies. We were no longer able to detect any expression of *hP2RX7* in mice recombined with Cre-deleter. Additionally, we saw a dramatic decrease in expression in the *En1-Cre* positive mice only in the cerebellum, underlining the ISH findings. As expected by the recombination pattern of the *En1-Cre* line (Kimmel et al., 2000), we did not see alteration in the cortex or hippocampus. Trying to further pin down the origin of cerebellar *P2rx7* expression we bred our mice with *Alpha 6-Cre* driver mice. This Cre line (Aller et al., 2003) recombines exclusively in cerebellar granule neurons by using regulatory elements of the $GABA_A$ receptor α6 subunit gene (Lüddens et al., 1990; Wisden et al., 1992). However, we did not observe a reduction in *P2RX7* expression mediated by that Cre recombinase indicating that the cerebellar *P2rx7* expression is not originating from granule cells. *P2rx7* expression in the cerebellum could still be – at least partially - of neuronal origin. Other types of neurons (unipolar brush cells, Purkinje cells or Golgi cells) are not covered by the *Alpha 6*-Cre recombinase. At least for astrocytes, glial *P2rx7* expression has been reported before for the cerebellum (Carrasquero et al., 2010), in other brain regions also for other glial cell types (Cotrina and Nedergaard, 2009). Our results with three different Cre lines covering astrocytes (*Glast*), oligodendrocytes (*CNP*) and microglia (*Cx3cr1*), unmistakably confirm the expression of *P2RX7* in the three main glial cell types in the cerebellum, hippocampus and cortex. Following the results from Figure 23 we observed the strongest reduction in expression in oligodendrocytes followed by astrocytes and microglia. However, these numbers have to be evaluated with caution. They show the actual reduction in *P2RX7* expression compared to the endogenous murine *P2rx7* expression in a certain cell population determined by the specificity of the Cre recombinase. What is not considered in this depiction is the contribution of a certain cell type to the total *P2RX7* expression in regard to the numeral proportion of this cell type in relation to all cells. Unfortunately, there are very few studies regarding the cellular composition or the actual extent to which a certain cell type contributes to the total amount of cells of the brain. We know that the ratio of neurons to glia is highly variable throughout the brain and whereas estimations predicted that in the cerebral cortex glia cells outnumber neurons by the factor four, in the

cerebellum it seems to be exactly the other way around (Azevedo et al., 2009). Our results do not indicate this dramatic difference in cellular composition, though.

Assuming that the relative composition of glial cells in human and mouse brain are comparable, one can try to give a more precise statement on glial *P2RX7* expression based on a study of Pelvig et al. (2008). They claim that about 75% of all glial cells are oligodendrocytes followed by about 17% of astrocytes and 5-7% of microglia (Pelvig et al., 2008). Taken these findings into account glial *P2rx7* expression is probably highest in microglia followed by astrocytes and oligodendrocytes. All these findings account for cortex and hippocampus to the same extend as for cerebellum. The high expression relative to the cell number of *P2rx7* in microglia is not surprising. Immune function is among the best described characteristics of this receptor and has been subject of many studies (for review see Wiley et al., 2011). The expression levels of microglia fit nicely to the reduction observed after recombination with *Nes-Cre* recombinase. These two should more or less cover all types of cells and therefore add up to ~100%. *Nes-Cre* also recombines in cells of the neuronal lineage. For more detailed analysis of this cell type we chose the glutamatergic neuron and GABAergic neuron specific Cre drivers *Nex-Cre* and *Dlx5/6-Cre*, respectively. In the cortex the reduction in *P2rx7* expression after inactivation in *Nex* or *Dlx* positive cells was comparable with the cerebellum, where no or only very week recombination should occur. Therefore, the proof for neuronal expression in the cortex based on these results, is difficult. It is also well possible, that under basal conditions cortical neurons, other than hippocampal, do not express *P2rx7*. For the hippocampus the situation is clear. Here we observed in the analyses with *Nex-Cre*, *Dlx-Cre* and a combination of both, a reduction of *P2rx7* expression after recombination with the respective Cre recombinase. These results fit perfectly to the ISH results and can be seen as a final proof for the long discussed neuronal expression of the P2X7 receptor in the brain.

Summing up, we could show by different readouts that *P2rx7* is expressed in the cortex, hippocampus and cerebellum in the mouse brain. Additionally, we could prove the expression in major cell types of the brain like microglia, oligodendrocytes and astrocytes. Also the long discussed question whether or not *P2rx7* is expressed in neurons of the brain is answered by this study. At least for the hippocampus we attribute the strong expression pattern in the CA3 to glutamatergic neurons. This was seen in ISH analysis and was confirmed by qRT-PCR.

9.3. *P2RX7* and neurodegeneration

As discussed in the previous chapter, the P2X7 receptor is unmistakably expressed in the brain and beyond that, in this work we could show its expression in all major cell types of the adult brain. As a result of this, studies claiming an involvement of the P2X7 receptor in neurodegenerative diseases (for review see Burnstock, 2015) become even more relevant and the possible connections deserve further investigation. Among these neurodegenerative diseases potentially influenced by the activity of the P2X7 receptor are e.g. retina and macular degeneration (Reichenbach and Bringmann, 2015; Hu et al., 2015), amyotrophic lateral sclerosis (Apolloni et al., 2014) and Parkinson's disease (Marcellino et al., 2010). The biggest number of studies though, is found on the potential involvement of the P2X7 receptor in Alzheimer's disease (Parvathenani et al., 2003; McLarnon et al., 2006; Delarasse et al., 2011; Diaz-Hernandez et al., 2012; Darmellah et al., 2012; Ni et al., 2013; Chen et al., 2014b; Miras-Portugal et al., 2015).

In contrast to previous studies investigating the effect of P2X7R in transgenic AD mouse models by downregulation or pharmacological inhibition of the receptor (Diaz-Hernandez et al., 2012; Chen et al., 2014a; Miras-Portugal et al., 2015), we investigated the actual knockout by combining a transgenic mouse model for Alzheimer's disease and our *P2rx7* knockout mice. We studied the *P2rx7* knockout in the previously described AD mouse model (Knobloch et al., 2007; Lerche, 2012) overexpressing human amyloid precursor protein carrying the Swedish and Arctic mutations with regards to cognition as well as APP processing and Aβ deposition.

In a first behavioral screening we investigated basal emotion of the four genotypes of interest. We could observe a slight increase in locomotion of APP transgenic compared to wild-type mice. This finding has already been described in the original publication of the transgenic ArcAβ mice (Knobloch et al., 2007). However, in combination with the knockout of *P2rx7* APP transgenic mice did no longer show hyperlocomotion. Additionally, we saw a slightly reduced locomotion of *P2rx7* knockout mice compared to wild-type mice. This is in contrast to previous findings on this mouse line (Walser, 2012) or other *P2rx7* knockout lines (compare 8.2.4 or Basso et al., 2009; Boucher et al., 2011; Csölle et al., 2012). A possible explanation can be found in the fact that due to the applied breeding scheme, the behavioral screening could not be conducted on direct littermates. In addition, the test mice were significantly older than in previous studies, namely between 11 to 16 months of age. We chose aged mice because we were mainly interested in cognitive behavior. It is of note that *P2rx7* knockout studies were never conducted in mice of

that age before. Therefore, it is possible that the lack of P2X7 receptors indeed favors a hypolocomotive phenotype in aged mice, an effect that was just never observed before. At the same time we did not note differences in cognitive performance in the Y-Maze, object recognition in the Y-Maze (OR-Y-Maze) or in the spatial object recognition (SOR) paradigm. Particularly the transgenic mice did not show decreased performance compared to wild-type mice. The original publication describing this AD mouse model did not investigate mice as old as the mice in this study, however, in their oldest mice (9 months) they could observe cognitive deficits of the transgenic mice compared to wild-type in the Y-Maze test. OR-Y-Maze and SOR were not conducted in the original study (Knobloch et al., 2007).

All three cognition paradigms (Y-Maze, OR in the Y-Maze and SOR) are paradigms investigating memory formation over few hours only. Therefore, we also conducted the fear conditioning paradigm that assesses learning and association over two and three days, respectively (Davis et al., 1999; Marsch et al., 2007). Whereas on day 2 of the fear conditioning paradigm only a slight reduction in freezing behavior of the transgenic compared to wild-type mice was observed, on day 3 the APP transgenic mice showed a significant reduction in freezing behavior which can be considered as a deficit in memory formation. Surprisingly transgenic mice lacking *P2rx7* did not show this memory impairment. The exposure of the mice to the conditioned tone on day 2 of the paradigm is more basolateral amygdala dependent learning, while day 3 with the contextual memory depends more on the memory formation in the hippocampus (Maren, 2005). This indicates a possible beneficial effect of the knockout of *P2rx7* in ArcAβ transgenic mice on mid to long term memory formation. In particular hippocampus dependent memory formation, a brain region with in particular high neuronal *P2rx7* expression and strongly affected in ArcAβ mice, seems to be influenced by the knockout of the P2X7 receptor.

To confirm these initial findings we additionally assessed the water cross maze paradigm (WCM). This hippocampus dependent learning paradigm investigates memory formation over two weeks (Kleinknecht et al., 2012). After the first seven days the so called “learning” trial, we observed a significant learning impairment of both transgenic groups compared to the two groups without the APP transgene. In the original ArcAβ publication Knobloch et al. conducted the Morris water maze (MWM) paradigm with similar findings showing significantly impaired memory formation in the APP transgenic mice compared to wild-type mice from the age of 6 months on (Knobloch et al., 2007). In the water cross maze we assessed a second week of “re-learning” with a switched platform, investigating flexibility in memory but it can also be used as readout for prolonged learning. As such we observed that whereas regular ArcAβ transgenic mice still failed

to reach accuracy above chance levels, APP transgenic mice without P2X7R performed significantly better and were on the same level as wild-type mice or pure *P2rx7* knockout mice. This suggests that the lack of P2X7R signaling can rescue cognitive deficits mediated by the transgenic overexpression of human amyloid precursor protein as in the used ArcAβ AD mouse model. A similar unpublished finding was presented by the group of Cecille Delarasse on the "Purines" meeting in 2014. They as well claimed to see beneficial effects on cognitive performance in transgenic AD model mice in combination with the knockout of *P2rx7* as studied in the Morris water maze paradigm (Delarasse, 2014).

Pure *P2rx7* knockout mice did not show a significant difference in performance compared to wild-type mice at the end of the paradigm. However, these mice reached the criteria of accuracy already on day 4 whereas wild-type animals remained slightly below the 83% level even on the last day of the experiment. This might be an indication that the absence of P2X7 receptor mediated signaling might even have a slight beneficial effect on maintaining memory formation in aged mice, even in the absence of APP overexpression. This is an assumption that gets supported by unpublished results from a Korean group that described better performance of *P2rx7* knockout mice compared to age matched control mice in the abstract book of 2013th SFN meeting (Cho et al., 2013). In this study they as well used the MWM to study cognitive performance. Whereas they could not see an effect of *P2rx7* knockout in young mice, they saw the mentioned beneficial effect of *P2rx7* knockout on memory formation in aged mice (11-14 months).

The molecular bases for the protective effect of the loss of P2X7 receptor function on cognition in aged mice and AD model mice are unclear. The neurotoxic peptide amyloid β is one of the hallmark features of Alzheimer's disease. AD patients are characterized by an excess of this protein in the brain. Therefore, the processing of the amyloid precursor protein (APP) is a long studied field in the struggle to find possible new therapeutic starting points. Ever since its proposed association with the AD pathology a possible role of the P2X7 receptor in APP processing was suggested. Still, if or in which direction it might affect APP processing remains highly discussed. While one study claimed that the knockdown or knockout of P2X7R leads to a downregulation or ablation of α-secretase activity (Delarasse et al., 2011), others claim the opposite, namely increased α-secretase activity upon downregulation of the receptor (Diaz-Hernandez et al., 2012; Miras-Portugal et al., 2015). The processing of APP by α-secretase has a neuroprotective effect because it prevents the formation of the neurotoxic Aβ molecule. As

previous studies are very contradictive we investigated our mice in regard to a possible effect of P2X7R on APP processing, both in the transgenic APP overexpression mice as well as on endogenous APP. Surprisingly, analyzing brains of those mice that showed the beneficial effect of the knockout of *P2rx7* in our behavioral screenings, we did not observe any effect of the *P2rx7* knockout on APP processing or the activity of the known secretases in the ArcAβ transgenic AD mouse model. In particular, we could not observe an increase in α-secretase or a decrease in β- and γ-secretase activity in the APP transgenic *P2rx7* knockout mice compared to the pure transgenic ArcAβ mice. Both alterations would potentially lead to a decreased production of the neurotoxic Aβ peptide and could, therefore, explain the beneficial effect of the *P2rx7* knockout on cognition and memory formation. As mentioned above, other groups already claimed to demonstrate the link between Alzheimer's disease and the P2X7 receptor by showing that the receptor affects APP processing. However, these studies do not reach the same conclusion but are rather contradictory. While a publication of Delarasse et al. claims an absence of α-secretase mediated APP products in *P2rx7* knockout mice (Delarasse et al., 2011) several studies from the University of Madrid propose increased α-secretase activity upon downregulation of the P2X7 receptor (Diaz-Hernandez et al., 2012; Miras-Portugal et al., 2015).

Unfortunately, Delarasse et al. could only show the facilitating effect of P2X7R on α-secretase activity in cell culture but not in brain tissue. It is well known that even primary cultures can have different characteristics compared to cells *in vivo* in the brain. Moreover, they did not investigate endogenous APP processing but upon activation of the P2X7 receptor with probably quite unphysiological levels of the agonist BzATP. This strong activation with up to 1mM of the agonist can lead to the activation of other P2 receptors as well, including P2Y receptors. In particular *in vitro* this high concentration can result in completely different downstream effects and, therefore, alter possible effects on APP processing. These artificial conditions make it difficult to draw a final conclusion. Furthermore, in the above mentioned so far unpublished presentation of a new study, Delarasse put her previous findings in perspective and proposed that in particular in later stages the active P2X7 receptor seems to rather facilitate the process of Alzheimer's disease pathology and, therefore, does probably not enhance α-secretase activity (Delarasse, 2014).

An enhancing effect of the *P2rx7* knockdown on α-secretase activity was also proposed by studies of Diaz-Hernandez and Miras-Portugal. In their studies they propose that the inhibition of P2X7 receptor affects α-secretase mediated APP processing via the glycogen synthase kinase 3β (GSK-3β). They postulate that the pharmacological inhibition of P2X7R (via BBG) leads to

increased phosphorylation of GSK-3β both in a cell culture as well as in an AD animal model (Diaz-Hernandez et al., 2012). Phosphorylation of GSK-3 in particular at certain serine residues has been shown to negatively affect the activity of the enzyme (Jope and Johnson, 2004). In their studies they further show that phosphorylation of GSK-3β correlates with an increase of CTF-α, a α-secretase mediated product of APP processing (Diaz-Hernandez et al., 2012). Unfortunately, their study is based on pharmacological inhibition of the P2X7R by BBG, only. BBG has been shown to be a potent inhibitor of P2X7R (Jiang et al., 2000), however, it is a widely used dye to stain proteins in analytical biochemistry. As such it binds to basic amino acid residues, which leads to an unspecific staining of proteins. This unspecific binding to basically all proteins requires high precaution in estimating its effect in particular by *in vivo* application. Unspecific effects on other proteins, both of positive and negative kind cannot be fully ruled out. Another point that has to be discussed is the fact that previous publications of the group of Miras-Portugal showed that not the inhibition of the P2X7 receptor but its stimulation leads to an increased phosphorylation of GSK-3 (Ortega et al., 2009, 2010). Unfortunately these contrary findings have not been discussed in the Diaz-Hernandez et al. paper (Diaz-Hernandez et al., 2012).

As mentioned earlier, we also studied the effect of the P2X7 receptor on the processing of endogenous APP, both in mice expressing the murine, but also in mice expressing the human P2X7 receptor. Murine and human receptor could have different effects on APP processing, e.g. mediated by their different sensitivity towards the natural ligand ATP (as discussed above). Therefore, it might be important to investigate the effects of the human receptor on APP secretase activity in an *in vivo* situation. Again we did not observe an effect in any of the two *P2rx7* knockout lines compared to wild-type mice. Surprisingly though we saw a reduction of sAPPα and Aη levels in those mice expressing the human P2X7 receptor. Aη is the product of a just recently discovered new secretase in the family of APP secretases named η-secretase (Willem et al., 2015). Still little is known so far regarding the function or effects of η-secretase mediated APP processing. The original publication, though, suggests a rather negative effect on neuronal activity as studied by long term potentiation measurements in the hippocampus (Willem et al., 2015). If this should be the case our findings would indicate a slight protective effect of the human *P2rx7* receptor compared to the murine counterpart in this regard. At the same time we found reduced amounts of sAPPα in those humanized mice. sAPPα is a product of α-secretase mediated APP processing. This undoubtedly has an effect on the formation of the neurotoxic Aβ molecule and would rather facilitate the symptoms of AD pathology. Due to the

low levels of endogenous Aβ a direct effect on these could not be studied in those mice. Further studies based on the combination of the transgenic ArcAβ mice with the humanized *P2RX7* mice will have to be conducted to substantiate these initial findings.

Since we did not find alterations in APP processing in the transgenic ArcAβ mice with and without P2X7 receptor we studied brain sections of these mice regarding alterations in amyloid β plaque load. Depositions of amyloid β peptide, so called Aβ plaques are one of the key pathologic features of Alzheimer' disease brains (Alzheimer, 1907; O'Brien and Wong, 2011; Haass et al., 2012). This is why we expected to see alterations in the amount of Aβ deposits in transgenic ArcAβ mice with vs without P2X7 receptor. Indeed we saw significant changes between the two genotypes in both the amount as well as the size of Aβ plaques. Conversely, we did not observe significantly less but more and even bigger Aβ deposits in the APP transgenic *P2rx7* knockout mice. This is in contrast to the common hypothesis that during progression of Alzheimer's disease with symptomatic exacerbation, the amount of amyloid plaques in the brain is increasing (Roth et al., 1967; O'Brien and Wong, 2011; Selkoe et al., 2012). However, it was shown that the extent of neuronal death, synaptic loss and cognitive impairment does only poorly correlate with the amount of Aβ plaques in a particular brain region (Terry et al., 1999; Sakono and Zako, 2010). In the last years more and more studies indicate that the toxicity of Aβ is not so much mediated by Aβ deposits but it is rather the soluble low molecular weight Aβ oligomers in the brain that have this fatal effect on neuronal vitality and synaptic function (Lambert et al., 1998; Walsh et al., 2002; Hoshi et al., 2003; Haass and Selkoe, 2007; Ono et al., 2009; Shankar and Walsh, 2009). Based on the studies we conducted so far, we cannot provide an explanation for the increased amount of amyloid plaques and the cognitive improvements in ArcAβ *P2rx7* knockout mice compared to pure ArcAβ mice, which we observed in the behavioral screenings. It can be speculated that the knockout of *P2rx7* does, in a so far unknown manner, influence the oligomerization of Aβ and the formation of Aβ fibrils, namely towards longer Aβ oligomers that tend to form plaques. Based on our findings that APP processing in these mice is not altered and, therefore, total Aβ levels do not differ, a cognitive improvement in *P2rx7* KO mice could be explained by more Aβ stored in plaque deposits leading to less free, soluble Aβ oligomers with highly toxic properties.

In this line it could also be speculated that P2X7R which, as we and others showed (Friedle et al., 2011; Arnoux et al., 2013), is highly expressed in microglia affects the phagocytic properties of this cell type. It is reported that *in vitro* the P2X7 receptor is upregulated in microglia treated

with Aβ peptide just as *in vivo* in an Alzheimer's disease mouse model. This suggests a role of P2X7R in microglial inflammatory responses in AD brains (Parvathenani et al., 2003; McLarnon et al., 2006). As such it was described that the downregulation of P2X7R in microglial primary cultures leads to a significant increase of Aβ phagocytosis (Ni et al., 2013). In the same study it was demonstrated that this increased phagocytosis depends on decreased IL-1β release and inhibition of the Cox-2 pathway in those microglial cells, both hallmarks of an inflammatory response. A study that supports the assumption of microglial involvement in the *P2rx7* knockout effect in our transgenic AD model can be found by Parvathenani et al. (2003). In this study they claim that the activation of the P2X7 receptor in microglia leads to neuronal cell death by production of reactive oxygen intermediates (Parvathenani et al., 2003).

Another, completely different explanation for the cognitive improvement and the altered plaque formation properties observed in the transgenic mice lacking P2X7R expression could be seen in a possible effect of the P2X7 receptor on the balance of $A\beta_{40}/A\beta_{42}$. Recent studies showed that the additional 2 residues in $A\beta_{42}$ change the properties of the C-terminal end of the peptide and thereby affect the aggregation capacity. These additional two amino acids strongly facilitate the formation of aggregates in $A\beta_{42}$ compared to the other Aβ isoform (Burdick et al., 1992; Fawzi et al., 2011; Conicella and Fawzi, 2014). Nevertheless, both isoforms share similar neurotoxicity. If the knockout of *P2rx7* should somehow shift the balance of $A\beta_{40}/A\beta_{42}$ towards $A\beta_{42}$ this would result in increased Aβ plaque deposition due to the altered biochemical properties. This phenomenon we indeed observed in our studies. At the same time the levels of soluble, highly neurotoxic Aβ oligomers should decrease which could explain the cognitive phenotypic findings. So far these theories are pure speculations. Further studies e.g. ELISA based investigations of the actual $A\beta_{40}/A\beta_{42}$ ratios in these mice need to be done to give a final statement regarding this hypothesis.

10. Conclusion

The aim of this thesis was to gain more insights into the function and possible involvement of the P2X7 receptor in mental disorders, mainly major depression and the neurodegenerative Alzheimer's disease. To model the function of the P2X7R in an *in vivo* situation two *P2rx7* knockout mouse lines were previously established, a constitutive knockout mouse line and a line in which parts of the murine gene were replaced by the human *P2RX7* transcript resulting in the expression of human *P2RX7* under the control of the murine *P2rx7* regulatory elements. Additionally, the human transcript in these mice is flanked by *loxP* sites making it vulnerable to Cre recombinase-mediated inactivation ultimately leading to P2X7R deficient mice.

After validating the new knockout mouse lines regarding expressional and functional absence of the P2X7 receptor we conducted behavioral screenings comparing wild-type mice and such lacking P2X7R. We found that under basal conditions the lack of the P2X7R does not affect basal emotionality in the mouse. However, *P2rx7* knockout mice showed less susceptibility towards chronic stress induced alterations in social behavior. This strengthens the assumption that the P2X7 receptor is an interesting target for future development of therapeutic strategies to treat mood disorders. For this a more detailed knowledge of which cells mediate the potentially protective effect would be of interest. By utilizing the humanized animals in combination with different cell type-specific Cre drivers, this question should be addressed in the future.

Additionally, we took in this study advantage of the humanized *P2RX7* mice to study *P2rx7* expression in the mouse brain by tissue- and cell type-specific ablation of *P2RX7* expression. We found that P2X7R is expressed throughout the brain and in all major cell types. We thereby could answer the long ongoing discussion of neuronal P2X7R expression by unequivocally showing P2X7R expression in glutamatergic neurons of the hippocampal CA3.

Even though we did not observe any differences in basal emotionality of mice endogenously expressing the murine or the human P2X7 receptor, we did observe differences in the functionality of the two receptor homologs expressed in cells obtained from those animals. The human receptor showed higher activation levels than its murine counterpart upon the same levels of receptor agonist. Further murine and human receptors differed in the response towards certain pharmacological modulators. These results showed that the humanized *P2RX7* mouse model can function as a powerful tool in the development of compounds not only for mood disorders but many other diseases the P2X7 receptor has been associated with.

One of these diseases is Alzheimer's disease, a pathology that gets more and more important in our society that keeps on advancing in age. In a mouse model of AD combined with our *P2rx7* knockout mice we could show that the knockout of the P2X7 receptor can have a protective effect of cognitive function in a progressed stage of the pathology. While the processing of the amyloid precursor protein was not affected by the loss of P2X7R, we found increased numbers of amyloid β plaques in AD mice lacking P2X7R expression compared to those with regular expression. The causes for these differences need to be examined in the future, yet, the preliminary results could hint towards an involvement of the P2X7 receptor in the aggregation of Aβ in a so far unknown manner shifting the balance towards the more toxic soluble isoform.

The involvement of the P2X7 receptor in both, the neurodegenerative Alzheimer's disease as well as in mood disorders needs further investigation and studies to be conducted. Nonetheless, this work provides strong indications and first evidence for its involvement in both pathologies as well as important additional information regarding the function and expression of the P2X7 receptor in the brain.

11. List of references

Adam, D. (2013). On the spectrum. *Nature* 496, 6–8. doi:10.1038/496416a.

Adinolfi, E., Callegari, M. G., Ferrari, D., Bolognesi, C., Minelli, M., Wieckowski, M. R., Pinton, P., Rizzuto, R., and Di Virgilio, F. (2005). Basal activation of the P2X7 ATP receptor elevates mitochondrial calcium and potential, increases cellular ATP levels, and promotes serum-independent growth. *Mol. Biol. Cell* 16, 3260–3272. doi:10.1091/mbc.E04-11-1025.

Adinolfi, E., Raffaghello, L., Giuliani, A. L., Cavazzini, L., Capece, M., Chiozzi, P., Bianchi, G., Kroemer, G., Pistoia, V., and Di Virgilio, F. (2012). Expression of P2X7 receptor increases in vivo tumor growth. *Am. Assoc. Cancer Res.* 72, 2957–2969. doi:10.1158/0008-5472.CAN-11-1947.

Adolfsson, O., Pihlgren, M., Toni, N., Varisco, Y., Buccarello, a. L., Antoniello, K., Lohmann, S., Piorkowska, K., Gafner, V., Atwal, J. K., et al. (2012). An Effector-Reduced Anti- -Amyloid (A) Antibody with Unique A Binding Properties Promotes Neuroprotection and Glial Engulfment of A . *J. Neurosci.* 32, 9677–9689. doi:10.1523/JNEUROSCI.4742-11.2012.

Adriouch, S., Bannas, P., Schwarz, N., Fliegert, R., Guse, A. H., Seman, M., Haag, F., and Koch-Nolte, F. (2008). ADP-ribosylation at R125 gates the P2X7 ion channel by presenting a covalent ligand to its nucleotide binding site. *FASEB J.* 22, 861–869. doi:10.1096/fj.07-9294com.

Aga, M., Johnson, C. J., Hart, A. P., Guadarrama, A. G., Suresh, M., Svaren, J., Bertics, P. J., and Darien, B. J. (2002). Modulation of monocyte signaling and pore formation in response to agonists of the nucleotide receptor P2X(7). *J. Leukoc. Biol.* 72, 222–232.

Aller, M. I., Jones, a., Merlo, D., Paterlini, M., Meyer, a. H., Amtmann, U., Brickley, S., Jolin, H. E., McKenzie, a. N. J., Monyer, H., et al. (2003). Cerebellar granule cell Cre recombinase expression. *Genesis* 36, 97–103. doi:10.1002/gene.10204.

Alves, L. A., da Silva, J. H. M., Ferreira, D. N. M., Fidalgo-Neto, A. A., Teixeira, P. C. N., de Souza, C. A. M., Caffarena, E. R., and de Freitas, M. S. (2014). Structural and molecular modeling features of P2X receptors. *Int. J. Mol. Sci.* 15, 4531–49. doi:10.3390/ijms15034531.

Alzheimer's Association (2014). 2014 Alzheimer's Disease Facts and Figures Includes a Special Report on Women and Alzheimer's Disease. doi:10.1016/j.jalz.2014.02.001.

Alzheimer, A. (1907). Uber eine eigenartige Erkrankung der Hirnrinde. *Allg Zeits Psychi- atry Psych. Med* 64, 146–8.

American Psychiatric Association (2013). *Diagnostic and Statistical Manual of Mental Disorders*. doi:10.1176/appi.books.9780890425596.744053.

Anderson, C. M., and Nedergaard, M. (2006). Emerging challenges of assigning P2X7 receptor function and immunoreactivity in neurons. *Trends Neurosci.* 29, 257–262. doi:10.1016/j.tins.2006.03.003.

Angst, J., Ajdacic-Gross, V., and Rössler, W. (2015). Classification of mood disorders. *Psychiatr. Pol.* 49, 663–671.

Antonio, L. S., Stewart, a. P., Xu, X. J., Varanda, W. a., Murrell-Lagnado, R. D., and Edwardson, J. M. (2011). P2X4 receptors interact with both P2X2 and P2X7 receptors in the form of homotrimers. *Br. J. Pharmacol.* 163, 1069–1077. doi:10.1111/j.1476-5381.2011.01303.x.

Apolloni, S., Amadio, S., Parisi, C., Matteucci, A., Potenza, R. L., Armida, M., Popoli, P., D'Ambrosi, N., and Volonté, C. (2014). Spinal cord pathology is ameliorated by P2X7 antagonism in SOD1-G93A mouse model of amyotrophic lateral sclerosis. *Dis. Model. Mech.*, 1101–1109. doi:10.1242/dmm.017038.

Aprile-Garcia, F., Metzger, M. W., Paez-Pereda, M., Stadler, H., Acuña, M., Liberman, A. C., Senin, S. A., Gerez, J., Hoijman, E., Refojo, D., et al. (2016). Co-expression of Wild-type P2X7R with Gln460Arg Variant Alters Receptor Function. *PLoS One*.

Arnoux, I., Hoshiko, M., Mandavy, L., Avignone, E., Yamamoto, N., and Audinat, E. (2013). Adaptive phenotype of microglial cells during the normal postnatal development of the somatosensory "Barrel" cortex. *Glia*

61, 1582–1594. doi:10.1002/glia.22503.

Ashe, K. H., and Zahs, K. R. (2010). Probing the biology of Alzheimer's disease in mice. *Neuron* 66, 631–645. doi:10.1016/j.neuron.2010.04.031.

Atkinson, L., Batten, T. F. C., Moores, T. S., Varoqui, H., Erickson, J. D., and Deuchars, J. (2004). Differential co-localisation of the P2X7 receptor subunit with vesicular glutamate transporters VGLUT1 and VGLUT2 in rat CNS. *Neuroscience* 123, 761–768. doi:10.1016/j.neuroscience.2003.08.065.

Azevedo, F. a C., Carvalho, L. R. B., Grinberg, L. T., Farfel, J. M., Ferretti, R. E. L., Leite, R. E. P., Filho, W. J., Lent, R., and Herculano-Houzel, S. (2009). Equal numbers of neuronal and nonneuronal cells make the human brain an isometrically scaled-up primate brain. *J. Comp. Neurol.* 513, 532–541. doi:10.1002/cne.21974.

Balsevich, G., Namendorf, C., Gerlach, T., Uhr, M., and Schmidt, M. V. (2015). The bio-distribution of the antidepressant clomipramine is modulated by chronic stress in mice: effects on behavior. *Front. Behav. Neurosci.* 8, 1–7. doi:10.3389/fnbeh.2014.00445.

Barden, N., Harvey, M., Gagné, B., Shink, E., Tremblay, M., Raymond, C., Labbé, M., Villeneuve, A., Rochette, D., Bordeleau, L., et al. (2006a). Analysis of single nucleotide polymorphisms in genes in the chromosome 12Q24.31 region points to P2RX7 as a susceptibility gene to bipolar affective disorder. *Am. J. Med. Genet. B. Neuropsychiatr. Genet.* 141B, 374–82. doi:10.1002/ajmg.b.30303.

Barden, N., Harvey, M., Gagné, B., Shink, E., Tremblay, M., Raymond, C., Labbé, M., Villeneuve, A., Rochette, D., Bordeleau, L., et al. (2006b). Analysis of single nucleotide polymorphisms in genes in the chromosome 12Q24.31 region points to P2RX7 as a susceptibility gene to bipolar affective disorder. *Am. J. Med. Genet. B. Neuropsychiatr. Genet.* 141B, 374–382. doi:10.1002/ajmg.b.30303.

Bartlett, R., Stokes, L., and Sluyter, R. (2014). The P2X7 Receptor Channel: Recent Developments and the Use of P2X7 Antagonists in Models of Disease. *Pharmacol. Rev.* 66, 638–675. doi:10.1124/pr.113.008003.

Basso, A. M., Bratcher, N. a, Harris, R. R., Jarvis, M. F., Decker, M. W., and Rueter, L. E. (2009). Behavioral profile of P2X7 receptor knockout mice in animal models of depression and anxiety: relevance for neuropsychiatric disorders. *Behav. Brain Res.* 198, 83–90. doi:10.1016/j.bbr.2008.10.018.

Bayer, T. A., Cappai, R., Masters, C. L., Beyreuther, K., and Multhaup, G. (1999). It all sticks together--the APP-related family of proteins and Alzheimer's disease. *Mol. Psychiatry* 4, 524–8. doi:10.1038/sj.mp.4000552.

Berk, C., Paul, G., and Sabbagh, M. (2014). Investigational drugs in Alzheimer's disease: current progress. *Expert Opin. Investig. Drugs* 23, 837–46. doi:10.1517/13543784.2014.905542.

Berlau, D. J., Corrada, M. M., Head, E., and Kawas, C. H. (2009). APOE epsilon2 is associated with intact cognition but increased Alzheimer pathology in the oldest old. *Neurology* 72, 829–34. doi:10.1212/01.wnl.0000343853.00346.a4.

Berton, O., Hahn, C.-G., and Thase, M. E. (2012). Are We Getting Closer to Valid Translational Models for Major Depression? *Science (80-.).* 338, 75–79. doi:10.1126/science.1222940.

Berton, O., McClung, C. a, Dileone, R. J., Krishnan, V., Renthal, W., Russo, S. J., Graham, D., Tsankova, N. M., Bolanos, C. a, Rios, M., et al. (2006a). Essential role of BDNF in the mesolimbic dopamine pathway in social defeat stress. *Science (80-.).* 311, 864–868. doi:10.1126/science.1120972.

Berton, O., McClung, C. A., Dileone, R. J., Krishnan, V., Renthal, W., Russo, S. J., Graham, D., Tsankova, N. M., Bolanos, C. A., Rios, M., et al. (2006b). Essential role of BDNF in the mesolimbic dopamine pathway in social defeat stress. *Science* 311, 864–868. doi:10.1126/science.1120972.

Berton, O., and Nestler, E. J. (2006a). New approaches to antidepressant drug discovery: beyond monoamines. *Nat. Rev. Neurosci.* 7, 137–51. doi:10.1038/nrn1846.

Berton, O., and Nestler, E. J. (2006b). New approaches to antidepressant drug discovery: beyond monoamines. *Nat. Rev. Neurosci.* 7, 137–151. doi:10.1038/nrn1846.

Bertram, L., and Tanzi, R. E. (2009). Genome-wide association studies in Alzheimer's disease. *Hum. Mol. Genet.* 18, 137–145. doi:10.1093/hmg/ddp406.

Bhattacharya, A., A. Neff, R., and D. Wickenden, A. (2011). The Physiology, Pharmacology and Future of P2X7 as

An Analgesic Drug Target: Hype or Promise? *Curr. Pharm. Biotechnol.* 12, 1698–1706. doi:10.2174/138920111798357429.

Bhattacharya, A., Vavra, V., Svobodova, I., Bendova, Z., Vereb, G., and Zemkova, H. (2013). Potentiation of inhibitory synaptic transmission by extracellular ATP in rat suprachiasmatic nuclei. *J. Neurosci.* 33, 8035–44. doi:10.1523/JNEUROSCI.4682-12.2013.

Bignante, E. A., Heredia, F., Morfini, G., and Lorenzo, A. (2013). Amyloid β precursor protein as a molecular target for amyloid β-induced neuronal degeneration in Alzheimer's disease. *Neurobiol. Aging* 34, 2525–37. doi:10.1016/j.neurobiolaging.2013.04.021.

Bird, T. D. (1993). Early-Onset Familial Alzheimer Disease. *GeneReviews™* upd. 2012, 1–22. Available at: http://search.ebscohost.com/login.aspx?direct=true&db=cmedm&AN=20301414&site=ehost-live.

Borjabad, A., Brooks, A. I., and Volsky, D. J. (2010). Gene expression profiles of HIV-1-infected glia and brain: toward better understanding of the role of astrocytes in HIV-1-associated neurocognitive disorders. *J. Neuroimmune Pharmacol.* 5, 44–62. doi:10.1007/s11481-009-9167-1.

Boucher, a a, Arnold, J. C., Hunt, G. E., Spiro, a, Spencer, J., Brown, C., McGregor, I. S., Bennett, M. R., and Kassiou, M. (2011). Resilience and reduced c-Fos expression in P2X7 receptor knockout mice exposed to repeated forced swim test. *Neuroscience* 189, 170–7. doi:10.1016/j.neuroscience.2011.05.049.

Bradley, H. J., Baldwin, J. M., Goli, G. R., Johnson, B., Zou, J., Sivaprasadarao, a., Baldwin, S. a., and Jiang, L.-H. (2011). Residues 155 and 348 Contribute to the Determination of P2X7 Receptor Function via Distinct Mechanisms Revealed by Single-nucleotide Polymorphisms. *J. Biol. Chem.* 286, 8176–8187. doi:10.1074/jbc.M110.211284.

Bradshaw, E. M., Chibnik, L. B., Keenan, B. T., Ottoboni, L., Raj, T., Tang, A., Rosenkrantz, L. L., Imboywa, S., Lee, M., Von Korff, A., et al. (2013). CD33 Alzheimer's disease locus: altered monocyte function and amyloid biology. *Nat. Neurosci.* 16, 848–50. doi:10.1038/nn.3435.

Brown, G. W., Bifulco, a, and Harris, T. O. (1987). Life events, vulnerability and onset of depression: some refinements. *Br. J. Psychiatry* 150, 30–42. doi:10.1192/bjp.150.1.30.

Burdick, D., Soreghan, B., Kwon, M., Kosmoski, J., Knauer, M., Henschen, a, Yates, J., Cotman, C., and Glabe, C. (1992). Assembly and aggregation properties of synthetic Alzheimer's A4/beta amyloid peptide analogs. *J. Biol. Chem.* 267, 546–554. doi:1730616.

Burnstock, G. (2015). An introduction to the roles of purinergic signalling in neurodegeneration, neuroprotection and neuroregeneration. *Neuropharmacology*, 1–14. doi:10.1016/j.neuropharm.2015.05.031.

Burnstock, G. (2007). Purine and pyrimidine receptors. *Cell. Mol. Life Sci.* 64, 1471–1483. doi:10.1007/s00018-007-6497-0.

Bussière, T., Bard, F., Barbour, R., Grajeda, H., Guido, T., Khan, K., Schenk, D., Games, D., Seubert, P., and Buttini, M. (2004). Morphological characterization of Thioflavin-S-positive amyloid plaques in transgenic Alzheimer mice and effect of passive Abeta immunotherapy on their clearance. *Am. J. Pathol.* 165, 987–995. doi:10.1016/S0002-9440(10)63360-3.

Cai, N., Bigdeli, T. B., Kretzschmar, W., Li, Y., Liang, J., Song, L., Hu, J., Li, Q., Jin, W., Hu, Z., et al. (2015). Sparse whole-genome sequencing identifies two loci for major depressive disorder. *Nature* 12415800. doi:10.1038/nature14659.

Carrasquero, L. M. G., Delicado, E. G., Sánchez-Ruiloba, L., Iglesias, T., and Miras-Portugal, M. T. (2010). Mechanisms of protein kinase D activation in response to P2Y2 and P2X7 receptors in primary astrocytes. *Glia* 58, 984–995. doi:10.1002/glia.20980.

Catania, C., Sotiropoulos, I., Silva, R., Onofri, C., Breen, K. C., Sousa, N., and Almeida, O. F. X. (2009). The amyloidogenic potential and behavioral correlates of stress. *Mol. Psychiatry* 14, 95–105. doi:10.1038/sj.mp.4002101.

Chartier-Harlin, M. C., Crawford, F., Houlden, H., Warren, a, Hughes, D., Fidani, L., Goate, a, Rossor, M., Roques, P., and Hardy, J. (1991). Early-onset Alzheimer's disease caused by mutations at codon 717 of the

beta-amyloid precursor protein gene. *Nature* 353, 844–846. doi:10.1038/353844a0.

Chen, X., Hu, J., Jiang, L., Xu, S., Zheng, B., Wang, C., Zhang, J., Wei, X., Chang, L., and Wang, Q. (2014a). Brilliant Blue G improves cognition in an animal model of Alzheimer's disease and inhibits amyloid-β-induced loss of filopodia and dendrite spines in hippocampal neurons. *Neuroscience* 279, 94–101. doi:10.1016/j.neuroscience.2014.08.036.

Chen, X., Hu, J., Jiang, L., Xu, S., Zheng, B., Wang, C., Zhang, J., Wei, X., Chang, L., and Wang, Q. (2014b). Brilliant Blue G improves cognition in an animal model of Alzheimer's disease and inhibits amyloid-β-induced loss of filopodia and dendrite spines in hippocampal neurons. *Neuroscience* 279, 94–101. doi:10.1016/j.neuroscience.2014.08.036.

Chessell, I. P., Hatcher, J. P., Bountra, C., Michel, A. D., Hughes, J. P., Green, P., Egerton, J., Murfin, M., Richardson, J., Peck, W. L., et al. (2005). Disruption of the P2X7 purinoceptor gene abolishes chronic inflammatory and neuropathic pain. *Pain* 114, 386–96. doi:10.1016/j.pain.2005.01.002.

Chessell, I. P., Simon, J., Hibell, a D., Michel, a D., Barnard, E. a, and Humphrey, P. P. (1998). Cloning and functional characterisation of the mouse P2X7 receptor. *FEBS Lett.* 439, 26–30. doi:10.1016/S0014-5793(98)01332-5.

Cho, J.-H., Choi, I.-S., and Jang, I.-S. (2010). P2X7 receptors enhance glutamate release in hippocampal hilar neurons. *Neuroreport* 21, 865–70. doi:10.1097/WNR.0b013e32833d9142.

Cho, W., Lee, S. R., Park, J. C., J.R., L., and Han, J. S. (2013). Protective effects of P2X7 receptor deletion on aging-related cognitive status. *Abstr. from SFN Meet.* Poster, 579.17/LLL16. 2013.

Ciechanowski, P., Katon, W., and Russo, J. (2009). Depression and diabetes: impact of depressive symptoms on adherence,function and cost. *Diabetes Care* 8, 203–207. doi:10.1016/j.mppsy.2009.03.009.

Citron, M., Oltersdorf, T., Haass, C., McConlogue, L., Hung, a Y., Seubert, P., Vigo-Pelfrey, C., Lieberburg, I., and Selkoe, D. J. (1992). Mutation of the beta-amyloid precursor protein in familial Alzheimer's disease increases beta-protein production. *Nature* 360, 672–674. doi:10.1038/360672a0.

Clark, A. K., Staniland, A. A., Marchand, F., Kaan, T. K. Y., McMahon, S. B., and Malcangio, M. (2010). P2X7-dependent release of interleukin-1beta and nociception in the spinal cord following lipopolysaccharide. *J. Neurosci.* 30, 573–82. doi:10.1523/JNEUROSCI.3295-09.2010.

Cole, G. M., Teter, B., and Frautschy, S. A. (2007). Neuroprotective effects of curcumin. *Adv. Exp. Med. Biol.* 595, 197–212. doi:10.1007/978-0-387-46401-5_8.

Conejero-Goldberg, C., Gomar, J. J., Bobes-Bascaran, T., Hyde, T. M., Kleinman, J. E., Herman, M. M., Chen, S., Davies, P., and Goldberg, T. E. (2014). APOE2 enhances neuroprotection against Alzheimer's disease through multiple molecular mechanisms. *Mol. Psychiatry* 19, 1–8. doi:10.1038/mp.2013.194.

Conicella, A. E., and Fawzi, N. L. (2014). The C-terminal threonine of A??43 nucleates toxic aggregation via structural and dynamical changes in monomers and protofibrils. *Biochemistry* 53, 3095–3105. doi:10.1021/bi500131a.

Corder, E. H., Saunders, a M., Strittmatter, W. J., Schmechel, D. E., Gaskell, P. C., Small, G. W., Roses, a D., Haines, J. L., and Pericak-Vance, M. a (1993). Gene dose of apolipoprotein E type 4 allele and the risk of Alzheimer's disease in late onset families. *Science* 261, 921–923. doi:10.1126/science.8346443.

Coric, V., van Dyck, C. H., Salloway, S., Andreasen, N., Brody, M., Richter, R. W., Soininen, H., Thein, S., Shiovitz, T., Pilcher, G., et al. (2012). Safety and tolerability of the gamma-secretase inhibitor avagacestat in a phase 2 study of mild to moderate Alzheimer disease. *Arch. Neurol.* 69, 1430–1440. doi:10.1001/archneurol.2012.2194.

Cotrina, M. L., and Nedergaard, M. (2009). Physiological and pathological functions of P2X7 receptor in the spinal cord. *Purinergic Signal.* 5, 223–32. doi:10.1007/s11302-009-9138-2.

Craft, S., Peskind, E., Schwartz, M. W., Schellenberg, G. D., Raskind, M., and Porte, D. (1998). Cerebrospinal fluid and plasma insulin levels in Alzheimer's disease: relationship to severity of dementia and apolipoprotein E genotype. *Neurology* 50, 164–168. doi:10.1212/WNL.50.1.164.

Craigie, E., Birch, R. E., Unwin, R. J., and Wildman, S. S. (2013). The relationship between P2X4 and P2X7: A

physiologically important interaction? *Front. Physiol.* 4 AUG, 1–6. doi:10.3389/fphys.2013.00216.

Csölle, C., Andó, R. D., Kittel, A., Gölöncsér, F., Baranyi, M., Soproni, K., Zelena, D., Haller, J., Németh, T., Mócsai, A., et al. (2012). The absence of P2X7 receptors (P2rx7) on non-haematopoietic cells leads to selective alteration in mood-related behaviour with dysregulated gene expression and stress reactivity in mice. *Int. J. Neuropsychopharmacol.*, 1–21. doi:10.1017/S1461145711001933.

Cunnilingus, F., Suzuki, T., Hide, I., Ido, K., Kohsaka, S., Inoue, K., and Nakata, Y. (2004). Production and release of neuroprotective tumor necrosis factor by P2X7 receptor-activated microglia. *J. Neurosci.* 24, 1–7. doi:10.1523/JNEUROSCI.3792-03.2004.

Darmellah, A., Rayah, A., Auger, R., Cuif, M.-H., Prigent, M., Arpin, M., Alcover, A., Delarasse, C., and Kanellopoulos, J. M. (2012). Ezrin/radixin/moesin are required for the purinergic P2X7 receptor (P2X7R)-dependent processing of the amyloid precursor protein. *J. Biol. Chem.* 287, 34583–95. doi:10.1074/jbc.M112.400010.

Davis, J. a, Paylor, R., McDonald, M. P., Libbey, M., Ligler, a, Bryant, K., and Crawley, J. N. (1999). Behavioral effects of ivermectin in mice. *Lab. Anim. Sci.* 49, 288–296.

Delarasse, C. (2014). Role of the purinergic receptor P2X7 in Alzheimer's disease. *Abstr. from Purines 2014* 10, 657–854. doi:10.1007/s11302-014-9430-7.

Delarasse, C., Auger, R., Gonnord, P., Fontaine, B., and Kanellopoulos, J. M. (2011). The purinergic receptor P2X7 triggers alpha-secretase-dependent processing of the amyloid precursor protein. *J. Biol. Chem.* 286, 2596–606. doi:10.1074/jbc.M110.200618.

Denlinger, L. C., Fisette, P. L., Sommer, J. a, Watters, J. J., Prabhu, U., Dubyak, G. R., Proctor, R. a, and Bertics, P. J. (2001). Cutting edge: the nucleotide receptor P2X7 contains multiple protein- and lipid-interaction motifs including a potential binding site for bacterial lipopolysaccharide. *J. Immunol.* 167, 1871–1876. doi:10.4049/jimmunol.167.4.1871.

Deuchars, S. A., Atkinson, L., Brooke, R. E., Musa, H., Milligan, C. J., Batten, T. F., Buckley, N. J., Parson, S. H., and Deuchars, J. (2001). Neuronal P2X7 receptors are targeted to presynaptic terminals in the central and peripheral nervous systems. *J. Neurosci.* 21, 7143–7152. doi:21/18/7143 [pii].

Diaz-Hernandez, J. I., Gomez-Villafuertes, R., León-Otegui, M., Hontecillas-Prieto, L., del Puerto, A., Trejo, J. L., Lucas, J. J., Garrido, J. J., Gualix, J., Miras-Portugal, M. T., et al. (2012). In vivo P2X7 inhibition reduces amyloid plaques in Alzheimer's disease through GSK3β and secretases. *Neurobiol. Aging* 33, 1816–1828. doi:10.1016/j.neurobiolaging.2011.09.040.

Donnelly-Roberts, D. L., Namovic, M. T., Han, P., and Jarvis, M. F. (2009). Mammalian P2X7 receptor pharmacology: Comparison of recombinant mouse, rat and human P2X7 receptors. *Br. J. Pharmacol.* 157, 1203–1214. doi:10.1111/j.1476-5381.2009.00233.x.

Dotti, C. G., Sullivan, C. A., and Banker, G. A. (1988). The establishment of polarity by hippocampal neurons in culture. *J. Neurosci.* 8, 1454–1468.

Dowlati, Y., Herrmann, N., Swardfager, W., Liu, H., Sham, L., Reim, E. K., and Lanct??t, K. L. (2010). A Meta-Analysis of Cytokines in Major Depression. *Biol. Psychiatry* 67, 446–457. doi:10.1016/j.biopsych.2009.09.033.

Duan, S., Anderson, C. M., Keung, E. C., Chen, Y., Chen, Y., and Swanson, R. a (2003). P2X7 receptor-mediated release of excitatory amino acids from astrocytes. *J. Neurosci.* 23, 1320–1328.

Duan, S., and Neary, J. T. (2006). P2X(7) receptors: properties and relevance to CNS function. *Glia* 54, 738–46. doi:10.1002/glia.20397.

Duthey, B. (2013). Background Paper 6.11 Alzheimer Disease and other Dementias, Update on 2004. *A Public Heal. Approach to Innov.*, 1 – 77.

Eaton, W. W., Martins, S. S., Nestadt, G., Bienvenu, O. J., Clarke, D., and Alexandre, P. (2008). The burden of mental disorders. *Epidemiol. Rev.* 30, 1–14. doi:10.1093/epirev/mxn011.

Eglitis, M. a, and Mezey, E. (1997). Hematopoietic cells differentiate into both microglia and macroglia in the brains of adult mice. *Proc. Natl. Acad. Sci. U. S. A.* 94, 4080–4085. doi:10.1073/pnas.94.8.4080.

Epstein, I., Szpindel, I., and Katzman, M. A. (2014). Pharmacological approaches to manage persistent symptoms of major depressive disorder: rationale and therapeutic strategies. *Psychiatry Res.* 220, S15–S33. doi:10.1016/S0165-1781(14)70003-4.

Erdmann, G., Schütz, G., and Berger, S. (2007). Inducible gene inactivation in neurons of the adult mouse forebrain. *BMC Neurosci.* 8, 63. doi:10.1186/1471-2202-8-63.

Esch, F. S., Keim, P. S., Beattie, E. C., Blacher, R. W., Culwell, a R., Oltersdorf, T., McClure, D., and Ward, P. J. (1990). Cleavage of amyloid beta peptide during constitutive processing of its precursor. *Science* 248, 1122–1124. doi:10.1126/science.2111583.

Faux, N. G., Ritchie, C. W., Gunn, A., Rembach, A., Tsatsanis, A., Bedo, J., Harrison, J., Lannfelt, L., Blennow, K., Zetterberg, H., et al. (2010). PBT2 rapidly improves cognition in alzheimer's disease: Additional phase II analyses. *J. Alzheimer's Dis.* 20, 509–516. doi:10.3233/JAD-2010-1390.

Fawzi, N. L., Ying, J., Ghirlando, R., Torchia, D. a., and Clore, G. M. (2011). Atomic-resolution dynamics on the surface of amyloid-β protofibrils probed by solution NMR. *Nature* 480, 268–272. doi:10.1038/nature10577.

Feil, R., Wagner, J., Metzger, D., and Chambon, P. (1997). Regulation of Cre recombinase activity by mutated estrogen receptor ligand-binding domains. *Biochem. Biophys. Res. Commun.* 237, 752–757. doi:10.1006/bbrc.1997.7124.

Felger, J. C., and Lotrich, F. E. (2013). Inflammatory cytokines in depression: Neurobiological mechanisms and therapeutic implications. *Neuroscience* 246, 199–229. doi:10.1016/j.neuroscience.2013.04.060.

De Felice, F. G., Velasco, P. T., Lambert, M. P., Viola, K., Fernandez, S. J., Ferreira, S. T., and Klein, W. L. (2007). Aβ oligomers induce neuronal oxidative stress through an N-methyl-D-aspartate receptor-dependent mechanism that is blocked by the Alzheimer drug memantine. *J. Biol. Chem.* 282, 11590–11601. doi:10.1074/jbc.M607483200.

Fernando, S. L., Saunders, B. M., Sluyter, R., Skarratt, K. K., Goldberg, H., Marks, G. B., Wiley, J. S., and Britton, W. J. (2007). A polymorphism in the P2X7 gene increases susceptibility to extrapulmonary tuberculosis. *Am. J. Respir. Crit. Care Med.* 175, 360–366. doi:10.1164/rccm.200607-970OC.

Ferrari, D., Pizzirani, C., Adinolfi, E., Lemoli, R. M., Curti, A., Idzko, M., Panther, E., and Di Virgilio, F. (2006). The P2X7 receptor: a key player in IL-1 processing and release. *J. Immunol.* 176, 3877–3883. doi:10.4049/jimmunol.176.7.3877.

Fischer, W., Urban, N., Immig, K., Franke, H., and Schaefer, M. (2014). Natural compounds with P2X7 receptor-modulating properties. *Purinergic Signal.* 10, 313–26. doi:10.1007/s11302-013-9392-1.

Francis, R., McGrath, G., Zhang, J., Ruddy, D. a, Sym, M., Apfeld, J., Nicoll, M., Maxwell, M., Hai, B., Ellis, M. C., et al. (2002). aph-1 and pen-2 are required for Notch pathway signaling, gamma-secretase cleavage of betaAPP, and presenilin protein accumulation. *Dev. Cell* 3, 85–97. doi:S1534580702001892 [pii].

Friedle, S. a, Brautigam, V. M., Nikodemova, M., Wright, M. L., and Watters, J. J. (2011). The P2X7-Egr pathway regulates nucleotide-dependent inflammatory gene expression in microglia. *Glia* 59, 1–13. doi:10.1002/glia.21071.

Fu, W., Ruangkittisakul, a., MacTavish, D., Baker, G. B., Ballanyi, K., and Jhamandas, J. H. (2013). Activity and metabolism-related ca2+ and mitochondrial dynamics in co-cultured human fetal cortical neurons and astrocytes. *Neuroscience* 250, 520–535. doi:10.1016/j.neuroscience.2013.07.029.

Gartland, A., Skarratt, K. K., Hocking, L. J., Parsons, C., Stokes, L., Jørgensen, N. R., Fraser, W. D., Reid, D. M., Gallagher, J. a, and Wiley, J. S. (2012). Polymorphisms in the P2X7 receptor gene are associated with low lumbar spine bone mineral density and accelerated bone loss in post-menopausal women. *Eur. J. Hum. Genet.* 20, 559–64. doi:10.1038/ejhg.2011.245.

Gaynes, B. N., Warden, D., Trivedi, M. H., Wisniewski, S. R., Fava, M., and Rush, A. J. (2009). What did STAR*D teach us? Results from a large-scale, practical, clinical trial for patients with depression. *Psychiatr. Serv.* 60, 1439–45. doi:10.1176/ps.2009.60.11.1439.

Gendron, F.-P., Neary, J. T., Theiss, P. M., Sun, G. Y., Gonzalez, F. a, and Weisman, G. a (2003). Mechanisms of

P2X7 receptor-mediated ERK1/2 phosphorylation in human astrocytoma cells. *Am. J. Physiol. Cell Physiol.* 284, C571–81. doi:10.1152/ajpcell.00286.2002.

Gerhart-Hines, Z., Rodgers, J. T., Bare, O., Lerin, C., Kim, S.-H., Mostoslavsky, R., Alt, F. W., Wu, Z., and Puigserver, P. (2007). Metabolic control of muscle mitochondrial function and fatty acid oxidation through SIRT1/PGC-1alpha. *EMBO J.* 26, 1913–1923. doi:10.1038/sj.emboj.7601633.

Gervais, F. G., Xu, D., Robertson, G. S., Vaillancourt, J. P., Zhu, Y., Huang, J., LeBlanc, a, Smith, D., Rigby, M., Shearman, M. S., et al. (1999). Involvement of caspases in proteolytic cleavage of Alzheimer's amyloid-beta precursor protein and amyloidogenic A beta peptide formation. *Cell* 97, 395–406. doi:10.1016/S0092-8674(00)80748-5.

Ghiringhelli, F., Apetoh, L., Tesniere, A., Aymeric, L., Ma, Y., Ortiz, C., Vermaelen, K., Panaretakis, T., Mignot, G., Ullrich, E., et al. (2009). Activation of the NLRP3 inflammasome in dendritic cells induces IL-1beta-dependent adaptive immunity against tumors. *Nat. Med.* 15, 1170–1178. doi:10.1038/nm.2028.

Gidlöf, O., Smith, J. G., Melander, O., Lovkvist, H., Hedblad, B., Engstrom, G., Nilsson, P., Carlson, J., Berglund, G., Olsson, S., et al. (2012). A common missense variant in the ATP receptor P2X7 is associated with reduced risk of cardiovascular events. *PLoS One* 7, e37491. doi:10.1371/journal.pone.0037491.

Giusti, S. a, Vercelli, C. a, Vogl, A. M., Kolarz, A. W., Pino, N. S., Deussing, J. M., and Refojo, D. (2014). Behavioral phenotyping of Nestin-Cre mice: implications for genetic mouse models of psychiatric disorders. *J. Psychiatr. Res.* 55, 87–95. doi:10.1016/j.jpsychires.2014.04.002.

Goate, a, Chartier-Harlin, M. C., Mullan, M., Brown, J., Crawford, F., Fidani, L., Giuffra, L., Haynes, a, Irving, N., and James, L. (1991). Segregation of a missense mutation in the amyloid precursor protein gene with familial Alzheimer's disease. *Nature* 349, 704–706. doi:10.1038/349704a0.

Goate, A. (2006). Segregation of a missense mutation in the amyloid beta-protein precursor gene with familial Alzheimer's disease. *J. Alzheimers. Dis.* 9, 341–347. Available at: /Users/Maria/Dropbox/Posgrado/pappers/Library/pdf0/1410.pdf.

Goebbels, S., Bormuth, I., Bode, U., Hermanson, O., Schwab, M. H., and Nave, K. A. (2006). Genetic targeting of principal neurons in neocortex and hippocampus of NEX-Cre mice. *Genesis* 44, 611–621. doi:10.1002/dvg.20256.

Golden, S. a, Covington, H. E., Berton, O., and Russo, S. J. (2011). A standardized protocol for repeated social defeat stress in mice. *Nat. Protoc.* 6, 1183–1191. doi:10.1038/nprot.2011.361.

Götz, J., and Ittner, L. M. (2008). Animal models of Alzheimer's disease and frontotemporal dementia. *Nat. Rev. Neurosci.* 9, 532–544. doi:10.1038/nrn2420.

Greenberg, P. E., Kessler, R. C., Birnbaum, H. G., Leong, S. a., Lowe, S. W., Berglund, P. a., and Corey-Lisle, P. K. (2003). The economic burden of depression in the United States: How did it change between 1990 and 2000? *J. Clin. Psychiatry* 64, 1465–1475. doi:10.4088/JCP.v64n1211.

Greenfield, J. P., Tsai, J., Gouras, G. K., Hai, B., Thinakaran, G., Checler, F., Sisodia, S. S., Greengard, P., and Xu, H. (1999). Endoplasmic reticulum and trans-Golgi network generate distinct populations of Alzheimer beta-amyloid peptides. *Proc. Natl. Acad. Sci. U. S. A.* 96, 742–747. doi:10.1073/pnas.96.2.742.

Griffin, W. S., Stanley, L. C., Ling, C., White, L., MacLeod, V., Perrot, L. J., White, C. L., and Araoz, C. (1989). Brain interleukin 1 and S-100 immunoreactivity are elevated in Down syndrome and Alzheimer disease. *Proc. Natl. Acad. Sci. U. S. A.* 86, 7611–5. doi:10.1073/pnas.86.19.7611.

Guerreiro, R., Wojtas, A., Bras, J., Carrasquillo, M., Rogaeva, E., Majounie, E., Cruchaga, C., Sassi, C., Kauwe, J. S. K., Younkin, S., et al. (2013). TREM2 variants in Alzheimer's disease. *N. Engl. J. Med.* 368, 117–27. doi:10.1056/NEJMoa1211851.

Guo, C., Masin, M., Qureshi, O. S., and Murrell-Lagnado, R. D. (2007). Evidence for functional P2X4/P2X7 heteromeric receptors. *Mol. Pharmacol.* 72, 1447–56. doi:10.1124/mol.107.035980.

Haass, C. (2004). Take five--BACE and the gamma-secretase quartet conduct Alzheimer's amyloid beta-peptide generation. *EMBO J.* 23, 483–488. doi:10.1038/sj.emboj.7600061.

Haass, C., Kaether, C., Thinakaran, G., and Sisodia, S. (2012). Trafficking and proteolytic processing of APP. *Cold*

Spring Harb. Perspect. Med. 2, 1–26. doi:10.1101/cshperspect.a006270.

Haass, C., and Selkoe, D. J. (2007). Soluble protein oligomers in neurodegeneration: lessons from the Alzheimer's amyloid β-peptide. *Nat. Rev. Mol. Cell Biol.* 8, 101–112. doi:10.1038/nrm2101.

Habbas, S., Ango, F., Daniel, H., and Galante, M. (2011). Purinergic signaling in the cerebellum: Bergmann glial cells express functional ionotropic P2X7 receptors. *Glia* 59, 1800–12. doi:10.1002/glia.21224.

Haller, J., and Bakos, N. (2002). Stress-induced social avoidance: A new model of stress-induced anxiety? *Physiol. Behav.* 77, 327–332. doi:10.1016/S0031-9384(02)00860-0.

Hartmann, J., Wagner, K. V., Dedic, N., Marinescu, D., Scharf, S. H., Wang, X. D., Deussing, J. M., Hausch, F., Rein, T., Schmidt, U., et al. (2012a). Fkbp52 heterozygosity alters behavioral, endocrine and neurogenetic parameters under basal and chronic stress conditions in mice. *Psychoneuroendocrinology* 37, 2009–2021. doi:10.1016/j.psyneuen.2012.04.017.

Hartmann, J., Wagner, K. V., Gaali, S., Kirschner, a., Kozany, C., Ruhter, G., Dedic, N., Hausl, a. S., Hoeijmakers, L., Westerholz, S., et al. (2015). Pharmacological Inhibition of the Psychiatric Risk Factor FKBP51 Has Anxiolytic Properties. *J. Neurosci.* 35, 9007–9016. doi:10.1523/JNEUROSCI.4024-14.2015.

Hartmann, J., Wagner, K. V., Liebl, C., Scharf, S. H., Wang, X. D., Wolf, M., Hausch, F., Rein, T., Schmidt, U., Touma, C., et al. (2012b). The involvement of FK506-binding protein 51 (FKBP5) in the behavioral and neuroendocrine effects of chronic social defeat stress. in *Neuropharmacology*, 332–339. doi:10.1016/j.neuropharm.2011.07.041.

Hattori, M., and Gouaux, E. (2012). Molecular mechanism of ATP binding and ion channel activation in P2X receptors. *Nature* 485, 207–212. doi:10.1038/nature11010.

Hejjas, K., Szekely, A., Domotor, E., Halmai, Z., Balogh, G., Schilling, B., Sarosi, A., Faludi, G., Sasvari-Szekely, M., and Nemoda, Z. (2009). Association between depression and the Gln460Arg polymorphism of P2RX7 gene: A dimensional approach. *Am. J. Med. Genet. Part B Neuropsychiatr. Genet.* 150, 295–299. doi:10.1002/ajmg.b.30799.

Hempel, C., Nörenberg, W., Sobottka, H., Urban, N., Nicke, A., Fischer, W., and Schaefer, M. (2013). The phenothiazine-class antipsychotic drugs prochlorperazine and trifluoperazine are potent allosteric modulators of the human P2X7 receptor. *Neuropharmacology* 75, 365–79. doi:10.1016/j.neuropharm.2013.07.027.

Hibell, A. D., Thompson, K. M., Simon, J., Xing, M., Humphrey, P. P., and Michel, A. D. (2001). Species- and agonist-dependent differences in the deactivation-kinetics of P2X7 receptors. *Naunyn. Schmiedebergs. Arch. Pharmacol.* 363, 639–48. doi:10.1007/s002100100412.

Hickman, S. E., Kingery, N. D., Ohsumi, T. K., Borowsky, M. L., Wang, L., Means, T. K., and El Khoury, J. (2013). The microglial sensome revealed by direct RNA sequencing. *Nat. Neurosci.* 16, 1896–905. doi:10.1038/nn.3554.

Hide, I., Tanaka, M., Inoue, a, Nakajima, K., Kohsaka, S., Inoue, K., and Nakata, Y. (2000). Extracellular ATP triggers tumor necrosis factor-alpha release from rat microglia. *J. Neurochem.* 75, 965–972.

Holsboer, F. (2001). Stress, hypercortisolism and corticosteroid receptors in depression: implications for therapy. *J. Affect. Disord.* 62, 77–91. doi:10.1016/S0165-0327(00)00352-9.

Holton, F. A., and Holton, P. (1954). The capillary dilator substances in dry powders of spinal roots; a possible role of adenosine triphosphate in chemical transmission from nerve endings. *J. Physiol.* 126, 124–140. Available at: http://www.ncbi.nlm.nih.gov/pmc/articles/PMC1365647/.

Hoshi, M., Sato, M., Matsumoto, S., Noguchi, A., Yasutake, K., Yoshida, N., and Sato, K. (2003). Spherical aggregates of beta-amyloid (amylospheroid) show high neurotoxicity and activate tau protein kinase I/glycogen synthase kinase-3beta. *Proc. Natl. Acad. Sci. U. S. A.* 100, 6370–6375. doi:10.1073/pnas.1237107100.

Howren, M. B., Lamkin, D. M., and Suls, J. (2009). Associations of depression with C-reactive protein, IL-1, and IL-6: a meta-analysis. *Psychosom. Med.* 71, 171–186. doi:10.1097/PSY.0b013e3181907c1b.

Hu, S. J., Calippe, B., Lavalette, S., Roubeix, C., Montassar, F., Housset, M., Levy, O., Delarasse, C., Paques, M.,

Sahel, J. -a., et al. (2015). Upregulation of P2RX7 in Cx3cr1-Deficient Mononuclear Phagocytes Leads to Increased Interleukin-1 Secretion and Photoreceptor Neurodegeneration. *J. Neurosci.* 35, 6987–6996. doi:10.1523/JNEUROSCI.3955-14.2015.

Hyman, S. (2014). Mental health: Depression needs large human-genetics studies. *Nature* 515, 189–191. doi:10.1038/515189a.

Iwatsubo, T., Saido, T. C., Mann, D. M., Lee, V. M., and Trojanowski, J. Q. (1996). Full-length amyloid-beta (1-42(43)) and amino-terminally modified and truncated amyloid-beta 42(43) deposit in diffuse plaques. *Am. J. Pathol.* 149, 1823–1830. doi:10.3168/jds.2011-4476.

Jacobson, K. a (2010). P2X and P2Y Receptors. *Tocris Biosci. Sci. Rev. Ser.* 33, 1–15.

Jiang, L. H., Mackenzie, a B., North, R. a, and Surprenant, a (2000). Brilliant blue G selectively blocks ATP-gated rat P2X(7) receptors. *Mol. Pharmacol.* 58, 82–88. doi:10.1124/mol.58.1.82.

Jonsson, T., Stefansson, H., Steinberg, S., Jonsdottir, I., Jonsson, P. V, Snaedal, J., Bjornsson, S., Huttenlocher, J., Levey, A. I., Lah, J. J., et al. (2013). Variant of TREM2 associated with the risk of Alzheimer's disease. *N. Engl. J. Med.* 368, 107–116. doi:10.1056/NEJMoa1211103.

Jope, R. S., and Johnson, G. V. W. (2004). The glamour and gloom of glycogen synthase kinase-3. *Trends Biochem. Sci.* 29, 95–102. doi:10.1016/j.tibs.2003.12.004.

Kamprath, K., and Wotjak, C. T. (2004). Nonassociative learning processes determine expression and extinction of conditioned fear in mice. *Learn. Mem.* 11, 770–786. doi:10.1101/lm.86104.

Kang, J., and Müller-Hill, B. (1990). Differential splicing of Alzheimer's disease amyloid A4 precursor RNA in rat tissues: PreA4(695) mRNA is predominantly produced in rat and human brain. *Biochem. Biophys. Res. Commun.* 166, 1192–1200. doi:10.1016/0006-291X(90)90992-V.

Kawano, A., Tsukimoto, M., Noguchi, T., Hotta, N., Harada, H., Takenouchi, T., Kitani, H., and Kojima, S. (2012). Involvement of P2X4 receptor in P2X7 receptor-dependent cell death of mouse macrophages. *Biochem. Biophys. Res. Commun.* 419, 374–380. doi:10.1016/j.bbrc.2012.01.156.

Kawate, T., Michel, J. C., Birdsong, W. T., and Gouaux, E. (2009). Crystal structure of the ATP-gated P2X(4) ion channel in the closed state. *Nature* 460, 592–598. doi:10.1038/nature08198.

Keck, M. E. (2006). Corticotropin-releasing factor, vasopressin and receptor systems in depression and anxiety. *Amino Acids* 31, 241–50. doi:10.1007/s00726-006-0333-y.

Kessler, R. C., McGonagle, K. A., Nelson, C. B., Hughes, M., Swartz, M., and Blazer, D. G. (1994). Sex and depression in the national comorbidity survey. II: Cohort effects. *J. Affect. Disord.* 30, 15–26. doi:10.1016/0165-0327(94)90147-3.

Kessler, R., and Chiu, W. (2005). Prevalence, Severity, and Comorbidity of Twelve-month DSM-IV Disorders in the National Comorbidity Survey Replication (NCS- R). *Arch. Gen. …* 62, 617–627. doi:10.1001/archpsyc.62.6.617.Prevalence.

Khakh, B. S., and North, R. A. (2012). Neuromodulation by Extracellular ATP and P2X Receptors in the CNS. *Neuron* 76, 51–69. doi:10.1016/j.neuron.2012.09.024.

Kido, Y., Kawahara, C., Terai, Y., Ohishi, A., Kobayashi, S., Hayakawa, M., Kamatsuka, Y., Nishida, K., and Nagasawa, K. (2013). Regulation of activity of P2X7 receptor by its splice variants in cultured mouse astrocytes. *Glia*, 1–12. doi:10.1002/glia.22615.

Kimmel, R. a., Turnbull, D. H., Blanquet, V., Wurst, W., Loomis, C. a., and Joyner, A. L. (2000). Two lineage boundaries coordinate vertebrate apical ectodermal ridge formation. *Genes Dev.* 14, 1377–1389. doi:10.1101/gad.14.11.1377.

Kleinknecht, K. R., Bedenk, B. T., Kaltwasser, S. F., Grünecker, B., Yen, Y.-C., Czisch, M., and Wotjak, C. T. (2012). Hippocampus-dependent place learning enables spatial flexibility in C57BL6/N mice. *Front. Behav. Neurosci.* 6, 87. doi:10.3389/fnbeh.2012.00087.

de Kloet, E. R., Joëls, M., and Holsboer, F. (2005). Stress and the brain: from adaptation to disease. *Nat. Rev. Neurosci.* 6, 463–475. doi:10.1038/nrn1683.

Kloet, E. R. De, and Molendijk, M. L. (2016). Coping with the Forced Swim Stressor : Towards Understanding an Adaptive Mechanism. 2016.

Knobloch, M., Konietzko, U., Krebs, D. C., and Nitsch, R. M. (2007). Intracellular Abeta and cognitive deficits precede beta-amyloid deposition in transgenic arcAbeta mice. *Neurobiol. Aging* 28, 1297–306. doi:10.1016/j.neurobiolaging.2006.06.019.

Knowles, J. R. (1980). Enzyme-catalyzed phosphoryl transfer reactions. *Annu. Rev. Biochem.* 49, 877–919. doi:10.1146/annurev.bi.49.070180.004305.

Krishnadas, R., and Cavanagh, J. (2012). Depression: an inflammatory illness? *J Neurol Neurosurg Psychiatry* 83, 495–502. doi:10.1136/jnnp-2011-301779.

Kühn, R., and Torres, R. M. (2002). Cre / loxP Recombination System and Gene Targeting. *Methods Mol. Biol.* 180, 175–204. doi:10.1385/1-59259-178-7:175.

LaFerla, F. M., and Green, K. N. (2012). Animal models of Alzheimer disease. *Cold Spring Harb Perspect Med* 2, 1–13. doi:10.1101/cshperspect.a006320.

LaFerla, F. M., Green, K. N., and Oddo, S. (2007). Intracellular amyloid-beta in Alzheimer's disease. *Nat. Rev. Neurosci.* 8, 499–509. doi:10.1038/nrn2168.

Lambert, M. P., Barlow, A. K., Chromy, B. A., Edwards, C., Freed, R., Liosatos, M., Morgan, T. E., Rozovsky, I., Trommer, B., Viola, K. L., et al. (1998). Diffusible, nonfibrillar ligands derived from Abeta1-42 are potent central nervous system neurotoxins. *Proc. Natl. Acad. Sci. U. S. A.* 95, 6448–53. doi:10.1073/pnas.95.11.6448.

Lambrecht, G., Friebe, T., Grimm, U., Windscheif, U., Bungardt, E., Hildebrandt, C., Bäumert, H. G., Spatz-Kümbel, G., and Mutschler, E. (1992). PPADS, a novel functionally selective antagonist of P2 purinoceptor-mediated responses. *Eur. J. Pharmacol.* 217, 217–219. doi:10.1016/0014-2999(92)90877-7.

Lanquillon, M. D., Krieg, J. C., Bening-Abu-Shach, U., and Vadder, M. . (2000). Cytokine Production and Treatment Response in Major Depressive Disorder. *Neuropharmacology* 6, 370–379. doi:10.1016/S0893-133X(99)00134-7.

Lappe-Siefke, C., Goebbels, S., Gravel, M., Nicksch, E., Lee, J., Braun, P. E., Griffiths, I. R., and Nave, K.-A. (2003). Disruption of Cnp1 uncouples oligodendroglial functions in axonal support and myelination. *Nat. Genet.* 33, 366–74. doi:10.1038/ng1095.

Laudisio, A., Marzetti, E., Cocchi, A., Bernabei, R., and Zuccalà, G. (2008). Association of depressive symptoms with bone mineral density in older men: a population-based study. *Int. J. Geriatr. Psychiatry* 23, 1119–1126. Available at: http://search.ebscohost.com/login.aspx?direct=true&AuthType=ip,shib&db=jlh&AN=2010086363&site=ehost-live&scope=site.

Lemoine, D., Jiang, R., Taly, A., Chataigneau, T., Specht, A., and Grutter, T. (2012). Ligand-Gated Ion Channels: New Insights into Neurological Disorders and Ligand Recognition. *Chem. Rev.* 112, 6285–6318. doi:10.1021/cr3000829.

Lenertz, L. Y., Gavala, M. L., Zhu, Y., and Bertics, P. J. (2011). Transcriptional control mechanisms associated with the nucleotide receptor P2X7, a critical regulator of immunologic, osteogenic, and neurologic functions. *Immunol. Res.* 50, 22–38. doi:10.1007/s12026-011-8203-4.

Lerche, K. (2012). Lehrstuhl für Entwicklungsgenetik Dissecting the role of CRH and CRH-R1 in Alzheimer ´ s disease.

Levinson, D. F. (2006). The Genetics of Depression: A Review. *Biol. Psychiatry* 60, 84–92. doi:10.1016/j.biopsych.2005.08.024.

Livak, K. J., and Schmittgen, T. D. (2001). Analysis of relative gene expression data using real-time quantitative PCR and the 2(-Delta Delta C(T)) Method. *Methods* 25, 402–8. doi:10.1006/meth.2001.1262.

Lopez, A. D., and Murray, C. C. . J. . (1998). The global burden of disease , 1990 – 2020. *Nat. Med.* 4, 1241–1243. doi:10.1038/3218.

Lucae, S., Salyakina, D., Barden, N., Harvey, M., Gagné, B., Labbé, M., Binder, E. B., Uhr, M., Paez-Pereda, M., Sillaber, I., et al. (2006). P2RX7, a gene coding for a purinergic ligand-gated ion channel, is associated with major depressive disorder. *Hum. Mol. Genet.* 15, 2438–2445. doi:10.1093/hmg/ddl166.

Lüddens, H., Pritchett, D. B., Köhler, M., Killisch, I., Keinänen, K., Monyer, H., Sprengel, R., and Seeburg, P. H. (1990). Cerebellar GABAA receptor selective for a behavioural alcohol antagonist. *Nature* 346, 648–51. doi:10.1038/346648a0.

Maes, M., Yirmyia, R., Noraberg, J., Brene, S., Hibbeln, J., Perini, G., Kubera, M., Bob, P., Lerer, B., and Maj, M. (2009). The inflammatory & neurodegenerative (I&ND) hypothesis of depression: leads for future research and new drug developments in depression. *Metab. Brain Dis.* 24, 27–53. doi:10.1007/s11011-008-9118-1.

Magdesian, M. H., Carvalho, M. M. V. F., Mendes, F. a., Saraiva, L. M., Juliano, M. a., Juliano, L., Garcia-Abreu, J., and Ferreira, S. T. (2008). Amyloid-β binds to the extracellular cysteine-rich domain of frizzled and inhibits Wnt/β-catenin signaling. *J. Biol. Chem.* 283, 9359–9368. doi:10.1074/jbc.M707108200.

Major Depressive Disorder Working Group of the Psychiatric GWAS Consortium (2012). A mega-analysis of genome-wide association studies for major depressive disorder. *Mol. Psychiatry* 18, 497–511. doi:10.1038/mp.2012.21.

Manolio, T. A., Collins, F. S., Cox, N. J., Goldstein, D. B., Hindorff, L. A., Hunter, D. J., McCarthy, M. I., Ramos, E. M., Cardon, L. R., Chakravarti, A., et al. (2009). Finding the missing heritability of complex diseases. *Nature* 461, 747–753. doi:10.1038/nature08494.

Marcellino, D., Suárez-Boomgaard, D., Sánchez-Reina, M. D., Aguirre, J. a, Yoshitake, T., Yoshitake, S., Hagman, B., Kehr, J., Agnati, L. F., Fuxe, K., et al. (2010). On the role of P2X(7) receptors in dopamine nerve cell degeneration in a rat model of Parkinson's disease: studies with the P2X(7) receptor antagonist A-438079. *J. Neural Transm.* 117, 681–687. doi:10.1007/s00702-010-0400-0.

Marcoli, M., Cervetto, C., Paluzzi, P., Guarnieri, S., Alloisio, S., Thellung, S., Nobile, M., and Maura, G. (2008). P2X7 pre-synaptic receptors in adult rat cerebrocortical nerve terminals: a role in ATP-induced glutamate release. *J. Neurochem.* 105, 2330–42. doi:10.1111/j.1471-4159.2008.05322.x.

Maren, S. (2005). P AVLOVIAN C ONDITIONING : A Functional Perspective. 179–206. doi:10.1146/annurev.psych.55.090902.141409.

Marsch, R., Foeller, E., Rammes, G., Bunck, M., Kössl, M., Holsboer, F., Zieglgänsberger, W., Landgraf, R., Lutz, B., and Wotjak, C. T. (2007). Reduced anxiety, conditioned fear, and hippocampal long-term potentiation in transient receptor potential vanilloid type 1 receptor-deficient mice. *J. Neurosci.* 27, 832–839. doi:10.1523/JNEUROSCI.3303-06.2007.

Masin, M., Young, C., Lim, K., Barnes, S. J., Xu, X. J., Marschall, V., Brutkowski, W., Mooney, E. R., Gorecki, D. C., and Murrell-Lagnado, R. (2012). Expression, assembly and function of novel C-terminal truncated variants of the mouse P2X7 receptor: re-evaluation of P2X7 knockouts. *Br. J. Pharmacol.* 165, 978–93. doi:10.1111/j.1476-5381.2011.01624.x.

McGeer, P. L., and McGeer, E. G. (2007). NSAIDs and Alzheimer disease: Epidemiological, animal model and clinical studies. *Neurobiol. Aging* 28, 639–647. doi:10.1016/j.neurobiolaging.2006.03.013.

McGowan, E., Pickford, F., Kim, J., Onstead, L., Eriksen, J., Yu, C., Skipper, L., Murphy, M. P., Beard, J., Das, P., et al. (2005). Aβ42 is essential for parenchymal and vascular amyloid deposition in mice. *Neuron* 47, 191–199. doi:10.1016/j.neuron.2005.06.030.

McIntyre, R. S., Soczynska, J. K., Konarski, J. Z., and Kennedy, S. H. (2006). The effect of antidepressants on glucose homeostasis and insulin sensitivity: synthesis and mechanisms. *Expert Opin Drug Saf* 5, 157–168. doi:10.1517/14740338.5.1.157.

McKhann, G. M., Knopman, D. S., Chertkow, H., Hyman, B. T., Jack, C. R., Kawas, C. H., Klunk, W. E., Koroshetz, W. J., Manly, J. J., Mayeux, R., et al. (2011). The diagnosis of dementia due to Alzheimer's disease: Recommendations from the National Institute on Aging-Alzheimer's Association workgroups on diagnostic guidelines for Alzheimer's disease. *Alzheimer's Dement.* 7, 263–269. doi:10.1016/j.jalz.2011.03.005.

McLarnon, J. G., Ryu, J. K., Walker, D. G., and Choi, H. B. (2006). Upregulated expression of purinergic P2X(7) receptor in Alzheimer disease and amyloid-beta peptide-treated microglia and in peptide-injected rat hippocampus. *J. Neuropathol. Exp. Neurol.* 65, 1090–1097. doi:10.1097/01.jnen.0000240470.97295.d3.

McQuillin, A., Bass, N. J., Choudhury, K., Puri, V., Kosmin, M., Lawrence, J., Curtis, D., and Gurling, H. M. D. (2009). Case-control studies show that a non-conservative amino-acid change from a glutamine to arginine in the P2RX7 purinergic receptor protein is associated with both bipolar- and unipolar-affective disorders. *Mol. Psychiatry* 14, 614–620. doi:10.1038/mp.2008.6.

Meng, Y., Lee, J. H., Cheng, R., St George-Hyslop, P., Mayeux, R., and Farrer, L. A. (2007). Association between SORL1 and Alzheimer's disease in a genome-wide study. *Neuroreport* 18, 1761–4. doi:10.1097/WNR.0b013e3282f13e7a.

Miller, A. H., Maletic, V., and Raison, C. L. (2009). Inflammation and Its Discontents: The Role of Cytokines in the Pathophysiology of Major Depression. *Biol. Psychiatry* 65, 732–741. doi:10.1016/j.biopsych.2008.11.029.

Miras-Portugal, M. T., Diaz-Hernandez, J. I., Gomez-Villafuertes, R., Diaz-Hernandez, M., Artalejo, A. R., and Gualix, J. (2015). Role of P2X7 and P2Y2 receptors on α-secretase-dependent APP processing: Control of amyloid plaques formation "in vivo" by P2X7 receptor. *Comput. Struct. Biotechnol. J.* 13, 176–181. doi:10.1016/j.csbj.2015.02.005.

Møller, T. C., Wirth, V. F., Roberts, N. I., Bender, J., Bach, A., Jacky, B. P. S., Strømgaard, K., Deussing, J. M., Schwartz, T. W., and Martinez, K. L. (2013). PDZ domain-mediated interactions of G protein-coupled receptors with postsynaptic density protein 95: quantitative characterization of interactions. *PLoS One* 8, e63352. doi:10.1371/journal.pone.0063352.

Monory, K., Massa, F., Egertová, M., Eder, M., Blaudzun, H., Westenbroek, R., Kelsch, W., Jacob, W., Marsch, R., Ekker, M., et al. (2006). The Endocannabinoid System Controls Key Epileptogenic Circuits in the Hippocampus. *Neuron* 51, 455–466. doi:10.1016/j.neuron.2006.07.006.

Mori, T., Tanaka, K., Buffo, A., Wurst, W., Kühn, R., and Gotz, M. (2006). Inducible gene deletion in astroglia and radial glia - A valuable tool for functional and lineage analysis. *Glia* 54, 21–34. doi:10.1002/glia.

Mormino, E. C., Betensky, R. a., Hedden, T., Schultz, A. P., Ward, A., Huijbers, W., Rentz, D. M., Johnson, K. a., and Sperling, R. a. (2014). Amyloid and APOE ε4 interact to influence short-term decline in preclinical Alzheimer disease. *Neurology* 82, 1760–1767. doi:10.1212/WNL.0000000000000431.

Le Mouellic, H., Lallemand, Y., and Brulet, P. (1990). Targeted replacement of the homeobox gene Hox-3.1 by the Escherichia coli lacZ in mouse chimeric embryos. *Proc. Natl. Sci. USA* 87, 4712–4716. doi:10.1073/pnas.87.12.4712.

Mullan, M., Crawford, F., Axelman, K., Houlden, H., Lilius, L., Winblad, B., and Lannfelt, L. (1992). A pathogenic mutation for probable Alzheimer's disease in the APP gene at the N-terminus of beta-amyloid. *Nat. Genet.* 1, 345–347. doi:10.1038/ng0892-345.

Murray, C. J. L., and Lopez, A. D. (2013). Measuring the global burden of disease. *N. Engl. J. Med.* 369, 448–457. doi:10.1056/NEJMra1201534.

Naj, A. C., Jun, G., Beecham, G. W., Wang, L.-S., Vardarajan, B. N., Buros, J., Gallins, P. J., Buxbaum, J. D., Jarvik, G. P., Crane, P. K., et al. (2011). Common variants at MS4A4/MS4A6E, CD2AP, CD33 and EPHA1 are associated with late-onset Alzheimer's disease. *Nat. Genet.* 43, 436–441. doi:10.1038/ng.801.

Nature editorial (2014). The burden of depression. *Nature* 515, 163–163. doi:10.1038/515163a.

Nemeroff, C. (1988). The Role of Corticotropin-Releasing Factor in the Pathogenesis of Major Depression. *Pharmacopsychiatry* 21, 76–82. doi:10.1055/s-2007-1014652.

Nestler, E. J., and Hyman, S. E. (2010). Animal models of neuropsychiatric disorders. *Nat. Neurosci.* 13, 1161–1169. doi:10.1038/nn.2647.

Ni, J., Wang, P., Zhang, J., Chen, W., and Gu, L. (2013). Silencing of the P2X(7) receptor enhances amyloid-β phagocytosis by microglia. *Biochem. Biophys. Res. Commun.* 434, 363–9. doi:10.1016/j.bbrc.2013.03.079.

Nicke, A., Bäumert, H. G., Rettinger, J., Eichele, A., Lambrecht, G., Mutschler, E., and Schmalzing, G. (1998). P2X1 and P2X3 receptors form stable trimers: A novel structural motif of ligand-gated ion channels.

EMBO J. 17, 3016–3028. doi:10.1093/emboj/17.11.3016.

Nicke, A., Kuan, Y. H., Masin, M., Rettinger, J., Marquez-Klaka, B., Bender, O., Górecki, D. C., Murrell-Lagnado, R. D., and Soto, F. (2009). A functional P2X7 splice variant with an alternative transmembrane domain 1 escapes gene inactivation in P2X7 knock-out mice. *J. Biol. Chem.* 284, 25813–25822. doi:10.1074/jbc.M109.033134.

NIH, and National Institute on Aging (2015). Alzheimer ' s Disease Genetics. *Fact sheet* No. 15-642, 1–8.

Nilsberth, C., Westlind-Danielsson, a, Eckman, C. B., Condron, M. M., Axelman, K., Forsell, C., Stenh, C., Luthman, J., Teplow, D. B., Younkin, S. G., et al. (2001). The "Arctic" APP mutation (E693G) causes Alzheimer's disease by enhanced Abeta protofibril formation. *Nat. Neurosci.* 4, 887–893. doi:10.1038/nn0901-887.

Nishino, S., Ueno, R., Ohishi, K., Sakai, T., and Hayaishi, O. (1989). Salivary prostaglandin concentrations: Possible state indicators for major depression. *Am. J. Psychiatry* 146, 365–368.

Nordberg, A. (2015). Dementia in 2014: Towards early diagnosis in Alzheimer disease. *Nat. Rev. Neurol.* 11, 69–70. doi:10.1038/nrneurol.2014.257.

Nörenberg, W., Hempel, C., Urban, N., Sobottka, H., Illes, P., and Schaefer, M. (2011). Clemastine potentiates the human P2X7 receptor by sensitizing it to lower ATP concentrations. *J. Biol. Chem.* 286, 11067–81. doi:10.1074/jbc.M110.198879.

Nörenberg, W., Schunk, J., Fischer, W., Sobottka, H., Riedel, T., Oliveira, J. F., Franke, H., and Illes, P. (2010). Electrophysiological classification of P2X7 receptors in rat cultured neocortical astroglia. *Br. J. Pharmacol.* 160, 1941–52. doi:10.1111/j.1476-5381.2010.00736.x.

Nörenberg, W., Sobottka, H., Hempel, C., Plötz, T., Fischer, W., Schmalzing, G., and Schaefer, M. (2012). Positive allosteric modulation by ivermectin of human but not murine P2X7 receptors. *Br. J. Pharmacol.* 167, 48–66. doi:10.1111/j.1476-5381.2012.01987.x.

North, R. A. (2002). Molecular physiology of P2X receptors. *Physiol. Rev.* 82, 1013–1067. doi:10.1152/physrev.00015.2002.

North, R. A., and Jarvis, M. F. (2013). P2X receptors as drug targets. *Mol. Pharmacol.* 83, 759–69. doi:10.1124/mol.112.083758.

O'Brien, R. J., and Wong, P. C. (2011). Amyloid precursor protein processing and Alzheimer's disease. *Annu. Rev. Neurosci.* 34, 185–204. doi:10.1146/annurev-neuro-061010-113613.

Oliveira, J. F., Riedel, T., Leichsenring, A., Heine, C., Franke, H., Krügel, U., Nörenberg, W., and Illes, P. (2011). Rodent cortical astroglia express in situ functional P2X7 receptors sensing pathologically high ATP concentrations. *Cereb. Cortex* 21, 806–20. doi:10.1093/cercor/bhq154.

Ono, K., Condron, M. M., and Teplow, D. B. (2009). Structure-neurotoxicity relationships of amyloid beta-protein oligomers. *Proc. Natl. Acad. Sci. U. S. A.* 106, 14745–50. doi:10.1073/pnas.0905127106.

Ortega, F., Pérez-Sen, R., Delicado, E. G., and Miras-Portugal, M. T. (2009). P2X7 nucleotide receptor is coupled to GSK-3 inhibition and neuroprotection in cerebellar granule neurons. *Neurotox. Res.* 15, 193–204. doi:10.1007/s12640-009-9020-6.

Ortega, F., Pérez-Sen, R., Morente, V., Delicado, E. G., and Miras-Portugal, M. T. (2010). P2X7, NMDA and BDNF receptors converge on GSK3 phosphorylation and cooperate to promote survival in cerebellar granule neurons. *Cell. Mol. Life Sci.* 67, 1723–33. doi:10.1007/s00018-010-0278-x.

Orvis, G. D., Hartzell, A. L., Smith, J. B., Barraza, L. H., Wilson, S. L., Szulc, K. U., Turnbull, D. H., and Joyner, A. L. (2012). The engrailed homeobox genes are required in multiple cell lineages to coordinate sequential formation of fissures and growth of the cerebellum. *Dev. Biol.* 367, 25–39. doi:10.1016/j.ydbio.2012.04.018.

Otto, C., Fuchs, I., Kauselmann, G., Kern, H., Zevnik, B., Andreasen, P., Schwarz, G., Altmann, H., Klewer, M., Schoor, M., et al. (2009). GPR30 does not mediate estrogenic responses in reproductive organs in mice. *Biol. Reprod.* 80, 34–41. doi:10.1095/biolreprod.108.071175.

Panenka, W., Jijon, H., Herx, L. M., Armstrong, J. N., Feighan, D., Wei, T., Yong, V. W., Ransohoff, R. M., and MacVicar, B. a (2001). P2X7-like receptor activation in astrocytes increases chemokine monocyte chemoattractant protein-1 expression via mitogen-activated protein kinase. *J. Neurosci.* 21, 7135–7142. doi:21/18/7135 [pii].

Parvathenani, L. K., Tertyshnikova, S., Greco, C. R., Roberts, S. B., Robertson, B., and Posmantur, R. (2003). P2X7 mediates superoxide production in primary microglia and is up-regulated in a transgenic mouse model of Alzheimer's disease. *J. Biol. Chem.* 278, 13309–17. doi:10.1074/jbc.M209478200.

Pelvig, D. P., Pakkenberg, H., Stark, a. K., and Pakkenberg, B. (2008). Neocortical glial cell numbers in human brains. *Neurobiol. Aging* 29, 1754–1762. doi:10.1016/j.neurobiolaging.2007.04.013.

Perlmutter, L. S., Barron, E., and Chui, H. C. (1990). Morphologic association between microglia and senile plaque amyloid in Alzheimer's disease. *Neurosci. Lett.* 119, 32–36. doi:10.1016/0304-3940(90)90748-X.

Petit-Demouliere, B., Chenu, F., Bourin, M., and Chenu, B. P. F. (2005). Forced swimming test in mice: a review of antidepressant activity. *Psychopharmacology (Berl).* 177, 245–55. doi:10.1007/s00213-004-2048-7.

Pfaffl, M. (2004). Quantification strategies in real-time PCR Michael W . Pfaffl. *A-Z Quant. PCR*, 87–112. doi:http://dx.doi.org/10.1007/s10551-011-0963-1.

Porsolt, R. D., Bertin, A., and Jalfre, M. (1977). Behavioral despair in mice: a primary screening test for antidepressants. *Arch. Int. Pharmacodyn. Ther.* 229, 327–336. doi:10.1196/annals.1317.038.

Potter, P. E. (2010). With Alzheimer Disease. 110, 27–36.

Prokop, S., Miller, K. R., and Heppner, F. L. (2013). Microglia actions in Alzheimer's disease. *Acta Neuropathol.* 126, 461–477. doi:10.1007/s00401-013-1182-x.

Qiu, F., and Dahl, G. (2009). A permeant regulating its permeation pore: inhibition of pannexin 1 channels by ATP. *Am. J. Physiol. Cell Physiol.* 296, C250–C255. doi:10.1152/ajpcell.00433.2008.

Raison, C. L., and Miller, A. H. (2012). NIH Public Access. 13, 467–475. doi:10.1007/s11920-011-0232-0.Is.

Refojo, D., Schweizer, M., Kuehne, C., Ehrenberg, S., Thoeringer, C., Vogl, A. M., Dedic, N., Schumacher, M., von Wolff, G., Avrabos, C., et al. (2011). Glutamatergic and dopaminergic neurons mediate anxiogenic and anxiolytic effects of CRHR1. *Science* 333, 1903–7. doi:10.1126/science.1202107.

Reichel, J. M., Nissel, S., Rogel-Salazar, G., Mederer, A., KÃ¤fer, K., Bedenk, B. T., Martens, H., Anders, R., Grosche, J., Michalski, D., et al. (2015). Distinct behavioral consequences of short-term and prolonged GABAergic depletion in prefrontal cortex and dorsal hippocampus. *Front. Behav. Neurosci.* 8, 452. doi:10.3389/fnbeh.2014.00452.

Reichenbach, A., and Bringmann, A. (2015). Purinergic signaling in retinal degeneration and regeneration. *Neuropharmacology*, 1–18. doi:10.1016/j.neuropharm.2015.05.005.

Rohan de Silva, H. a, Jen, a, Wickenden, C., Jen, L. S., Wilkinson, S. L., and Patel, a J. (1997). Cell-specific expression of beta-amyloid precursor protein isoform mRNAs and proteins in neurons and astrocytes. *Brain Res. Mol. Brain Res.* 47, 147–156.

Rosenblat, J. D., Kakar, R., and McIntyre, R. S. (2015). The Cognitive Effects of Antidepressants in Major Depressive Disorder: A Systematic Review and Meta-Analysis of Randomized Clinical Trials. *Int. J. Neuropsychopharmacol.*, pyv082. doi:10.1093/ijnp/pyv082.

Rossi, A., Kontarakis, Z., Gerri, C., Nolte, H., Hölper, S., Krüger, M., and Stainier, D. Y. R. (2015). Genetic compensation induced by deleterious mutations but not gene knockdowns. *Nature*. doi:10.1038/nature14580.

Roth, M., Tomlinson, B. E., and Blessed, G. (1967). The relationship between quantitative measures of dementia and of degenerative changes in the cerebral grey matter of elderly subjects. *Proc. R. Soc. Med.* 60, 254–260. doi:10.1192/bjp.114.512.797.

Sakono, M., and Zako, T. (2010). Amyloid oligomers: formation and toxicity of Aβ oligomers. *FEBS J.* 277, 1348–1358. doi:10.1111/j.1742-4658.2010.07568.x.

Sakono, M., Zako, T., Ueda, H., Yohda, M., and Maeda, M. (2008). Formation of highly toxic soluble amyloid beta oligomers by the molecular chaperone prefoldin. *FEBS J.* 275, 5982–93. doi:10.1111/j.1742-4658.2008.06727.x.

Sanacora, G., Treccani, G., and Popoli, M. (2012). Towards a glutamate hypothesis of depression: an emerging frontier of neuropsychopharmacology for mood disorders. *Neuropharmacology* 62, 63–77. doi:10.1016/j.neuropharm.2011.07.036.

Sananbenesi, F., and Fischer, A. (2015). Remodeling the susceptibility to stress-induced depression. *Nat. Med.* 21, 1125–1126. doi:10.1038/nm.3970.

Sánchez-Nogueiro, J., Marín-García, P., and Miras-Portugal, M. T. (2005). Characterization of a functional P2X(7)-like receptor in cerebellar granule neurons from P2X(7) knockout mice. *FEBS Lett.* 579, 3783–8. doi:10.1016/j.febslet.2005.05.073.

Sandi, C., and Haller, J. (2015). Stress and the social brain: behavioural effects and neurobiological mechanisms. *Nat. Rev. Neurosci.* 16, 290–304. doi:10.1038/nrn3918.

Sando, S. B., Melquist, S., Cannon, A., Hutton, M. L., Sletvold, O., Saltvedt, I., White, L. R., Lydersen, S., and Aasly, J. O. (2008). APOE epsilon 4 lowers age at onset and is a high risk factor for Alzheimer's disease; a case control study from central Norway. *BMC Neurol.* 8, 9. doi:10.1186/1471-2377-8-9.

Saura, J., Tusell, J. M., and Serratosa, J. (2003). High-Yield Isolation of Murine Microglia by Mild Trypsinization. *Glia* 44, 183–189. doi:10.1002/glia.10274.

Schroder, K., and Tschopp, J. (2010). Review The Inflammasomes Supplement. *Cell* 140, S1. doi:10.1016/j.cell.2010.01.040.

Schwarz, N., Drouot, L., Nicke, A., Fliegert, R., Boyer, O., Guse, A. H., Haag, F., Adriouch, S., and Koch-Nolte, F. (2012). Alternative Splicing of the N-Terminal Cytosolic and Transmembrane Domains of P2X7 Controls Gating of the Ion Channel by ADP-Ribosylation. *PLoS One* 7, e41269. doi:10.1371/journal.pone.0041269.

Seeman, P., and Seeman, N. (2011). Alzheimer's disease: ??-amyloid plaque formation in human brain. *Synapse* 65, 1289–1297. doi:10.1002/syn.20957.

Selkoe, D., Mandelkow, E., and Holtzman, D. (2012). Deciphering Alzheimer disease. *Cold Spring Harb. Perspect. Med.* 2, a011460. doi:10.1101/cshperspect.a011460.

Seman, M., Adriouch, S., Scheuplein, F., Krebs, C., Freese, D., Glowacki, G., Deterre, P., Haag, F., and Koch-Nolte, F. (2003). NAD-induced T cell death: ADP-ribosylation of cell surface proteins by ART2 activates the cytolytic P2X7 purinoceptor. *Immunity* 19, 571–582. doi:10.1016/S1074-7613(03)00266-8.

Shankar, G. M., and Walsh, D. M. (2009). Alzheimer's disease: synaptic dysfunction and Abeta. *Mol. Neurodegener.* 4, 48. doi:10.1186/1750-1326-4-48.

Shigemoto-Mogami, Y., Koizumi, S., Tsuda, M., Ohsawa, K., Kohsaka, S., and Inoue, K. (2001). Mechanisms underlying extracellular ATP-evoked interleukin-6 release in mouse microglial cell line, MG-5. *J. Neurochem.* 78, 1339–1349. doi:10.1046/j.1471-4159.2001.00514.x.

Sim, J. a, Young, M. T., Sung, H.-Y., North, R. A., and Surprenant, A. (2004). Reanalysis of P2X7 receptor expression in rodent brain. *J. Neurosci.* 24, 6307–6314. doi:10.1523/JNEUROSCI.1469-04.2004.

Sinha, S., Anderson, J. P., Barbour, R., Basi, G. S., Caccavello, R., Davis, D., Doan, M., Dovey, H. F., Frigon, N., Hong, J., et al. (1999). Purification and cloning of amyloid precursor protein b-secretase from human brain. *Nature* 402, 537–540.

Sisodia, S. S. (1992). Beta-amyloid precursor protein cleavage by a membrane-bound protease. *Proc. Natl. Acad. Sci. U. S. A.* 89, 6075–9. doi:10.1073/pnas.89.13.6075.

Slavich, G. M., and Irwin, M. R. (2014). From stress to inflammation and major depressive disorder: a social signal transduction theory of depression. *Psychol. Bull.* 140, 774–815. doi:10.1037/a0035302.

Sleegers, K., Lambert, J.-C., Bertram, L., Cruts, M., Amouyel, P., and Van Broeckhoven, C. (2010). The pursuit of susceptibility genes for Alzheimer's disease: progress and prospects. *Trends Genet.* 26, 84–93. doi:10.1016/j.tig.2009.12.004.

Solle, M., Labasi, J., Perregaux, D. G., Stam, E., Petrushova, N., Koller, B. H., Griffiths, R. J., and Gabel, C. a (2001). Altered cytokine production in mice lacking P2X(7) receptors. *J. Biol. Chem.* 276, 125–32. doi:10.1074/jbc.M006781200.

Soltoff, S. P., McMillian, M. K., and Talamo, B. R. (1989). Coomassie Brilliant Blue G is a more potent antagonist of P2 purinergic responses than Reactive Blue 2 (Cibacron Blue 3GA) in rat parotid acinar cells. *Biochem. Biophys. Res. Commun.* 165, 1279–85. doi:10.1016/0006-291X(89)92741-1.

Sorge, R. E., Trang, T., Dorfman, R., Smith, S. B., Beggs, S., Ritchie, J., Austin, J.-S., Zaykin, D. V, Meulen, H. Vander, Costigan, M., et al. (2012). Genetically determined P2X7 receptor pore formation regulates variability in chronic pain sensitivity. *Nat. Med.* 18, 595–599. doi:10.1038/nm.2710.

Soriano, S., Lu, D. C., Chandra, S., Pietrzik, C. U., and Koo, E. H. (2001). The Amyloidogenic Pathway of Amyloid Precursor Protein (APP) Is Independent of Its Cleavage by Caspases. *J. Biol. Chem.* 276, 29045–29050. doi:10.1074/jbc.M102456200.

Soronen, P., Mantere, O., Melartin, T., Suominen, K., Vuorilehto, M., Rytsälä, H., Arvilommi, P., Holma, I., Holma, M., Jylhä, P., et al. (2011). P2RX7 gene is associated consistently with mood disorders and predicts clinical outcome in three clinical cohorts. *Am. J. Med. Genet. B. Neuropsychiatr. Genet.* 156B, 435–47. doi:10.1002/ajmg.b.31179.

Sotiropoulos, I., Cerqueira, J. J., Catania, C., Takashima, A., Sousa, N., and Almeida, O. F. X. (2008). Stress and glucocorticoid footprints in the brain-The path from depression to Alzheimer's disease. *Neurosci. Biobehav. Rev.* 32, 1161–1173. doi:10.1016/j.neubiorev.2008.05.007.

Sperlágh, B., and Illes, P. (2014). P2X7 receptor: an emerging target in central nervous system diseases. *Trends Pharmacol. Sci.* 35, 537–47. doi:10.1016/j.tips.2014.08.002.

Sperlágh, B., Köfalvi, A., Deuchars, J., Atkinson, L., Milligan, C. J., Buckley, N. J., and Vizi, E. S. (2002). Involvement of P2X7 receptors in the regulation of neurotransmitter release in the rat hippocampus. *J. Neurochem.* 81, 1196–1211. doi:10.1046/j.1471-4159.2002.00920.x.

Stefano, L., Rossler, O. G., Griesemer, D., Hoth, M., and Thiel, G. (2007). P2X(7) receptor stimulation upregulates Egr-1 biosynthesis involving a cytosolic Ca(2+) rise, transactivation of the EGF receptor and phosphorylation of ERK and Elk-1. *J Cell Physiol* 213, 36–44. doi:10.1002/jcp.21085.

Sun, A., Nguyen, X. V, and Bing, G. (2002). Comparative analysis of an improved thioflavin-s stain, Gallyas silver stain, and immunohistochemistry for neurofibrillary tangle demonstration on the same sections. *J. Histochem. Cytochem.* 50, 463–472. doi:10.1177/002215540205000403.

Surprenant, A., Rassendren, F., Kawashima, E., North, R. A., and Buell, G. (1996). The cytolytic P2Z receptor for extracellular ATP identified as a P2X receptor (P2X7). *Science* 272, 735–738. doi:10.1126/science.272.5262.735.

Suzuki, N., Cheung, T. T., Cai, X. D., Odaka, a, Otvos, L., Eckman, C., Golde, T. E., and Younkin, S. G. (1994). An increased percentage of long amyloid beta protein secreted by familial amyloid beta protein precursor (beta APP717) mutants. *Science* 264, 1336–1340. doi:10.1126/science.8191290.

Swartz, T. H., Dubyak, G. R., and Chen, B. K. (2015). Purinergic Receptors: Key Mediators of HIV-1 Infection and Inflammation. *Front. Immunol.* 6, 1–9. doi:10.3389/fimmu.2015.00585.

Tai, L. M., Ghura, S., Koster, K. P., Liakaite, V., Maienschein-Cline, M., Kanabar, P., Collins, N., Ben-Aissa, M., Lei, A. Z., Bahroos, N., et al. (2015). *APOE* -modulated Aβ-induced neuroinflammation in Alzheimer's disease: current landscape, novel data, and future perspective. *J. Neurochem.* 133, 465–488. doi:10.1111/jnc.13072.

Taylor, S. R. J., Gonzalez-Begne, M., Sojka, D. K., Richardson, J. C., Sheardown, S. A., Harrison, S. M., Pusey, C. D., Tam, F. W. K., and Elliott, J. I. (2009). Lymphocytes from P2X7-deficient mice exhibit enhanced P2X7 responses. *J. Leukoc. Biol.* 85, 978–986. doi:10.1189/jlb.0408251.

Terry, R., Maslia, E., and Hansen, L. (1999). *The neuropa- thology of Alzheimer disease and the structural basis of its cogninitve alterations*. Philadelphia: Lipponcott Williams and Wilikins.

Thambisetty, M., An, Y., Nalls, M., Sojkova, J., Swaminathan, S., Zhou, Y., Singleton, A. B., Wong, D. F., Ferrucci,

L., Saykin, A. J., et al. (2013). Effect of complement CR1 on brain amyloid burden during aging and its modification by APOE genotype. *Biol. Psychiatry* 73, 422–428. doi:10.1016/j.biopsych.2012.08.015.

Trivedi, M. H., Rush, a. J., Wisniewski, S. R., Nierenberg, A. a., Warden, D., Ritz, L., Norquist, G., Howland, R. H., Lebowitz, B., McGrath, P. J., et al. (2006). Evaluation of Outcomes With Citalopram for Depression Using Measurement-Based Care in STAR*D: Implications for Clinical Practice. *Am. J. Psychiatry* 163, 28–40. doi:10.1176/appi.ajp.163.1.28.

Tronche, F., Kellendonk, C., Kretz, O., Gass, P., Anlag, K., Orban, P. C., Bock, R., Klein, R., and Schütz, G. (1999). Disruption of the glucocorticoid receptor gene in the nervous system results in reduced anxiety. *Nat. Genet.* 23, 99–103. doi:10.1038/12703.

Ursu, D., Ebert, P., Langron, E., Ruble, C., Munsie, L., Zou, W., Fijal, B., Qian, Y.-W., McNearney, T. a, Mogg, A., et al. (2014). Gain and loss of function of P2X7 receptors: mechanisms, pharmacology and relevance to diabetic neuropathic pain. *Mol. Pain* 10, 37. doi:10.1186/1744-8069-10-37.

Vassar, R., Bennett, B. D., Babu-Khan, S., Kahn, S., Mendiaz, E. a, Denis, P., Teplow, D. B., Ross, S., Amarante, P., Loeloff, R., et al. (1999). Beta-secretase cleavage of Alzheimer's amyloid precursor protein by the transmembrane aspartic protease BACE. *Science* 286, 735–741. doi:10.1126/science.286.5440.735.

Vellas, B., Sol, O., Snyder, P. J., Ousset, P. J., Haddad, R., Maurin, M., Lemarié, J. C., Désiré, L., and Pando, M. P. (2011). EHT0202 in Alzheimer's disease: A 3-month, randomized, placebo-controlled, double-bind study. *Curr. Alzheimer Res.* 8, 203.

Verghese, P. B., Castellano, J. M., and Holtzman, D. M. (2011). Apolipoprotein E in Alzheimer's disease and other neurological disorders. *Lancet Neurol.* 10, 241–52. doi:10.1016/S1474-4422(10)70325-2.

Di Virgilio, F., Ceruti, S., Bramanti, P., and Abbracchio, M. P. (2009). Purinergic signalling in inflammation of the central nervous system. *Trends Neurosci.* 32, 79–87. doi:10.1016/j.tins.2008.11.003.

Virginio, C., Church, D., North, R. A., and Surprenant, A. (1997). Effects of divalent cations, protons and calmidazolium at the rat P2X7 receptor. *Neuropharmacology* 36, 1285–1294. doi:10.1016/S0028-3908(97)00141-X.

Vogl, A. M., Brockmann, M. M., Giusti, S. a, Maccarrone, G., Vercelli, C. a, Bauder, C. a, Richter, J. S., Roselli, F., Hafner, A.-S., Dedic, N., et al. (2015). Neddylation inhibition impairs spine development, destabilizes synapses and deteriorates cognition. *Nat. Neurosci.* 18, 239–51. doi:10.1038/nn.3912.

Volonté, C., Apolloni, S., Skaper, S. D., and Burnstock, G. (2012). P2X7 Receptors : Channels , Pores and More. *CNS Neurol. Disord. - Drug Targets* 11, 705–721. doi:10.2174/187152712803581137.

Wagner, K. V, Marinescu, D., Hartmann, J., Wang, X.-D., Labermaier, C., Scharf, S. H., Liebl, C., Uhr, M., Holsboer, F., Müller, M. B., et al. (2012). Differences in FKBP51 Regulation Following Chronic Social Defeat Stress Correlate with Individual Stress Sensitivity: Influence of Paroxetine Treatment. *Neuropsychopharmacology*. doi:10.1038/npp.2012.150.

Walser, S. M. (2012). Lehrstuhl für Entwicklungsgenetik Validation of P2RX7 and TMEM132D as susceptibility genes for depression using genetic mouse models. 1–145.

Walsh, D. M., Klyubin, I., Fadeeva, J. V, Cullen, W. K., Anwyl, R., Wolfe, M. S., Rowan, M. J., and Selkoe, D. J. (2002). Naturally secreted oligomers of amyloid beta protein potently inhibit hippocampal long-term potentiation in vivo. *Nature* 416, 535–539. doi:10.1038/416535a.

Wang, P. S., Lane, M., Olfson, M., Pincus, H. A., Wells, K. B., and Kessler, R. C. (2005). Twelve-month use of mental health services in the United States: results from the National Comorbidity Survey Replication. *Arch. Gen. Psychiatry* 62, 629–40. doi:10.1001/archpsyc.62.6.629.

Wang, X.-D., Su, Y.-A., Wagner, K. V, Avrabos, C., Scharf, S. H., Hartmann, J., Wolf, M., Liebl, C., Kühne, C., Wurst, W., et al. (2013). Nectin-3 links CRHR1 signaling to stress-induced memory deficits and spine loss. *Nat. Neurosci.* 16, 706–13. doi:10.1038/nn.3395.

Watters, J. J., Sommer, J. a., Pfeiffer, Z. a., Prabhu, U., Guerra, A. N., and Bertics, P. J. (2002). A differential role for the mitogen-activated protein kinases in lipopolysaccharide signaling. The MEK/ERK pathway is not essential for nitric oxide and interleukin 1?? production. *J. Biol. Chem.* 277, 9077–9087.

doi:10.1074/jbc.M104385200.

Weisgraber, K. H., Rall, S. C., and Mahley, R. W. (1981). Human E apoprotein heterogeneity. Cysteine-arginine interchanges in the amino acid sequence of the apo-E isoforms. *J. Biol. Chem.* 256, 9077–9083. Available at: http://www.ncbi.nlm.nih.gov/pubmed/7263700.

Weiss, L. G., Saklofske, D. H., Coalson, D. L., and Raiford, S. E. (2010). "Theoretical, Empirical and Clinical Foundations of the WAIS-IV Index Scores," in *WAIS-IV Clinical Use and Interpretation*, 61–94. doi:10.1016/B978-0-12-375035-8.10003-5.

WHO (2012). Depression-Fact Sheet. *october*. Available at: http://www.who.int/mediacentre/factsheets/fs369/en/.

WHO (2015a). Mental disorders. Available at: http://www.who.int/mediacentre/factsheets/fs396/en/#.Vi4OFPL2hAk.mendeley [Accessed October 26, 2015].

WHO (2015b). WHO | Dementia. Available at: http://www.who.int/mediacentre/factsheets/fs362/en/#.Vi4ZJlHFtdE.mendeley [Accessed October 26, 2015].

Whooley, M. a, Kip, K. E., Cauley, J. a, Ensrud, K. E., Nevitt, M. C., and Browner, W. S. (1999). Depression, falls, and risk of fracture in older women. Study of Osteoporotic Fractures Research Group. *Arch. Intern. Med.* 159, 484–490. doi:10.1001/archinte.159.5.484.

Whooley, M. A., de Jonge, P., Vittinghoff, E., Otte, C., Moos, R., Carney, R. M., Ali, S., Dowray, S., Na, B., Feldman, M. D., et al. (2008). Depressive symptoms, health behaviors, and risk of cardiovascular events in patients with coronary heart disease. *JAMA* 300, 2379–88. doi:10.1001/jama.2008.711.

Wiley, J. S., Sluyter, R., Gu, B. J., Stokes, L., and Fuller, S. J. (2011). The human P2X7 receptor and its role in innate immunity. *Tissue Antigens* 78, 321–332. doi:10.1111/j.1399-0039.2011.01780.x.

Willem, M., Tahirovic, S., Busche, M. A., Ovsepian, S. V., Chafai, M., Kootar, S., Hornburg, D., Evans, L. D. B., Moore, S., Daria, A., et al. (2015). η-Secretase processing of APP inhibits neuronal activity in the hippocampus. *Nature*. doi:10.1038/nature14864.

Wisden, W., Laurie, D. J., Monyer, H., and Seeburg, P. H. (1992). The distribution of 13 GABAA receptor subunit mRNAs in the rat brain. I. Telencephalon, diencephalon, mesencephalon. *J. Neurosci.* 12, 1040–1062.

Wiste, H. J., Weigand, S. D., Rocca, W. a, Knopman, D. S., Mielke, M. M., Lowe, V. J., Senjem, M. L., Preboske, G. M., Pankratz, V. S., Vemuri, P., et al. (2014). Age-specific population frequencies of cerebral β-amyloidosis and neurodegeneration among people with normal cognitive function aged 50–89 years: a cross-sectional study. *Lancet Neurol.* 13, 997–1005. doi:10.1016/S1474-4422(14)70194-2.

Wolfe, M. S., Xia, W., Ostaszewski, B. L., Diehl, T. S., Kimberly, W. T., and Selkoe, D. J. (1999). Two transmembrane aspartates in presenilin-1 required for presenilin endoproteolysis and gamma-secretase activity. *Nature* 398, 513–517. doi:10.1038/19077.

Wu, L., Rosa-Neto, P., Hsiung, G.-Y. R., Sadovnick, a D., Masellis, M., Black, S. E., Jia, J., and Gauthier, S. (2012). Early-onset familial Alzheimer's disease (EOFAD). *Can. J. Neurol. Sci.* 39, 436–45. doi:W4438L6488727555 [pii].

Yamamoto, N., Matsubara, E., Maeda, S., Minagawa, H., Takashima, A., Maruyama, W., Michikawa, M., and Yanagisawa, K. (2007). A ganglioside-induced toxic soluble Aβ assembly: Its enhanced formation from Aβ bearing the arctic mutation. *J. Biol. Chem.* 282, 2646–2655. doi:10.1074/jbc.M606202200.

Yan, R., Bienkowski, M. J., Shuck, M. E., Miao, H., Tory, M. C., Pauley, a M., Brashier, J. R., Stratman, N. C., Mathews, W. R., Buhl, a E., et al. (1999). Membrane-anchored aspartyl protease with Alzheimer's disease beta-secretase activity. *Nature* 402, 533–537. doi:10.1038/990107.

Yang, A. J., Chandswangbhuvana, D., Margol, L., and Glabe, C. G. (1998). Loss of endosomal/lysosomal membrane impermeability is an early event in amyloid Abeta1-42 pathogenesis. *J. Neurosci. Res.* 52, 691–698. doi:10.1002/(SICI)1097-4547(19980615)52:6<691::AID-JNR8>3.0.CO;2-3.

Yegutkin, G. G. (2008). Nucleotide- and nucleoside-converting ectoenzymes: Important modulators of

purinergic signalling cascade. *Biochim. Biophys. Acta - Mol. Cell Res.* 1783, 673–694. doi:10.1016/j.bbamcr.2008.01.024.

Yiangou, Y., Facer, P., Durrenberger, P., Chessell, I. P., Naylor, A., Bountra, C., Banati, R. R., and Anand, P. (2006). COX-2, CB2 and P2X7-immunoreactivities are increased in activated microglial cells/macrophages of multiple sclerosis and amyotrophic lateral sclerosis spinal cord. *BMC Neurol.* 6, 12. doi:10.1186/1471-2377-6-12.

Yona, S., Kim, K.-W., Wolf, Y., Milder, A., Varol, D., Breke, M., Strauss-Ayali, D., Viukov, S., Guilliams, M., Misharin, A., et al. (2013). Fate mapping reveals origins and dynamics of monocytes and tissue macrophages under homeostasis. *Immunity* 38, 79–91. doi:10.1016/j.immuni.2012.12.001.Fate.

Young, C. N., Sinadinos, A., Lefebvre, A., Chan, P., Arkle, S., Vaudry, D., and Gorecki, D. C. (2015). A novel mechanism of autophagic cell death in dystrophic muscle regulated by P2RX7 receptor large-pore formation and HSP90. *Autophagy* 11, 113–130. doi:10.4161/15548627.2014.994402.

Young, M. T., Pelegrin, P., and Surprenant, A. (2007). Amino acid residues in the P2X7 receptor that mediate differential sensitivity to ATP and BzATP. *Mol. Pharmacol.* 71, 92–100. doi:10.1124/mol.106.030163.

Yu, G., Nishimura, M., Arawaka, S., Levitan, D., Zhang, L., Tandon, a, Song, Y. Q., Rogaeva, E., Chen, F., Kawarai, T., et al. (2000). Nicastrin modulates presenilin-mediated notch/glp-1 signal transduction and betaAPP processing. *Nature* 407, 48–54. doi:10.1038/35024009.

Zhang, Y., Thompson, R., Zhang, H., and Xu, H. (2011). APP processing in Alzheimer's disease. *Mol. Brain* 4, 3. doi:10.1186/1756-6606-4-3.

Zheng, H., and Koo, E. H. (2006). The amyloid precursor protein: beyond amyloid. *Mol. Neurodegener.* 1, 5. doi:10.1186/1750-1326-1-5.

12. List of abbreviations

A	adenine
AA	amino acids
AICD	intracytoplasmatic domain of APP
ACTH	adrenocorticotropic hormone
ADP	adenosine diphosphate
ALS	amyotrophic lateral sclerosis
APP	amyloid precursor protein
Arg	Arginine
ATP	adenosine triphosphate
BBG	brilliant blue G
BSA	bovine serum albumin
BzATP	3'-O-(4-benzoyl)benzoyl adenosine 5'-triphosphate
CA	cornu ammonis area
CaMKII	calcium/calmodulin-dependent protein kinase II
cDNA	complementary DNA
CNS	central nervous system
cpm	counts per minute
CRH	corticotropin-releasing hormone
CRISPR	Clustered Regularly Interspaced Short Palindromic Repeats
CSDS	chronic social defeat stress
C-terminus	carboxyl terminus
CTF	carboxyl terminal fragment
Ctx	cortex
Cys	cysteine
Da	Dalton
DAPI	4`,6-diamidino-2-phenylindole
DEA	diethylamide
DEPC	diethyl pyrocarbonate
DH5α	*E. coli* strain DH5α
DIG	Digoxigenin
DMEM	Dulbecco's Modified Eagle's Medium

DMSO	dimethylsulfoxide
DNA	desoxyribonucleic acid
dNTP	desoxyribonucleotide triphosphate
DTT	dithiothreitol
E.coli	*Escherichia coli*
EDTA	ethylenediaminetetraacetic acid
eFAD	early-onset familial Alzheimer's disease
e.g.	exempli gratia, for example
ELISA	enzyme linked immunosorbent assay
ER	endoplasmatic reticulum
ERK	extracellular signal-regulated kinase
ES	embryonic stem
EtOH	ethanol
FAD	familial Alzheimer's disease
FCS	fetal calf serum
Frt	flippase recognition target
FST	forced swim test
GABA	gamma aminobutyric acid
GFAP	Glial fibrillary acidic protein
GSK	Glaxo Smith Kline
GSK-3	glycogen synthase kinase 3
HBSS	Hanks´s balanced salt solution
HCl	hydrochloric acid
HEK293	Human embryonic kidney cell line
HEPES	4-(2-Hydroxyethyl)piperazine-1-ethanesulfonic acid
Hip	hippocampus
HPA	hypothalamic-pituitary-adrenal
HPRT	hypoxanthine-phosphoribosyl-transferase
HRP	horseradish peroxidase
hybmix	hybridization-mix
IB	immunoblot
IL-1β	interleukin -1β
IRES	internal ribosome entry site

ISH	*in situ* hybridization
Kb	kilobase pairs
KO	knockout
LacZ	β-galactosidase gene
LB	lysogeny broth
LOAD	late-onset Alzheimer's disease
loxP	locus of crossover in P1
LPS	lipopolysaccharide
LRT	long terminal repeat
LTD	long-term depression
LTP	Long-term potentiation
MOLT	mature oligodendrocytes transmembrane protein
MRI	magnetic resonance imaging
mRNA	messenger ribonucleic acid
MWM	Morris water maze
NAD	Nicotinamide adenine dinucleotide
NBT/BCIP	nitroblue tetrazolium /5-bromo-4-chloro-3-indolyl-phosphate
NCD	neurocognitive disorder
Neo	neomycin
NGS	normal goat serum
NMDA	*N*-methyl-D-aspartic acid
o.n.	overnight
OD	optical density
OPE	osteopontin enhancer elements
P	postnatal day
P2rx7	Purinergic receptor P2X, ligand gated ion channel, 7 (murine gene)
P2RX7	Purinergic receptor P2X, ligand gated ion channel, 7 (human gene)
P2X7R	Purinergic receptor P2X, ligand gated ion channel, 7 (protein)
pA	polyadenylation sequence
PAM	protospacer adjacent motif
PBS	phosphate buffered saline
PBS-T	phosphate buffered saline – TritonX100
PCR	polymerase chain reaction

PD	panic disorder
PFA	paraformaldehyde
Pen/Strep	penicillin/streptomycin
PET	positron emission tomography
PPADS	pyridoxalphosphate-6-azophenyl-2',4'-disulfonic acid
PVC	polyvinyl chloride
PVDF	polyvinylidene difluoride
qPCR	quantitative real time PCR
RIPA	radioimmunoprecipitation assay
RNA	ribonucleic acid
RPL-19	ribosomal protein L19
RT	room temperature
RT	reverse transcriptase
SA	splice acceptor
sgRNA	single guide ribonucleic acid
SNP	single nucleotide polymorphism
SSC	standard saline citrate
TAE	Tris acetate EDTA
TBS	Tris buffered saline
TBS-T	Tris buffered saline with Tween
TEA	triethanolamine
TFP	trifluoperazine
TMEM132	transmembrane protein 132
TNF-α	tumor necrosis factor α
Tris	tris(hydroxylmethyl)-aminomethan
WB	Western blot
WCM	Water cross maze
WT	wild-type
x	symbol for crosses between mouse lines

13. Addendum

13.1. TMEM132D is a neuronally expressed transmembrane protein affecting stress-coping behavior

Metzger M.W. [1], Walser S.M.[1], Dedic N.[1], Ortiz O. [2], Wurst W.[2], Deussing J.M.[1]

[1] Max Planck Institute of Psychiatry, 80804 Munich, Germany
[2] Helmholtz Zentrum München, German Research Center for Environmental Health, Institute of Developmental Genetics, Neuherberg, Germany

Abstract

Recent studies identified SNPs in *TMEM132D* to be associated with symptoms of anxiety in subjects suffering from panic disorder, unipolar depression or attention-deficit/hyperactivity disorder. Even though these data suggest *TMEM132D* as an interesting candidate gene, the function of *TMEM132D* is completely unknown rendering validation rather difficult. Therefore, we used *in vitro* and *in vivo* approaches to investigate the function of TMEM132D in the brain. We revealed that TMEM132D is a transmembrane protein which co-localizes with actin filaments. Besides a detailed expression analysis of the *Tmem132* family in the mouse brain we generated a *Tmem132d* reporter knockout mouse line based on a gene trap approach. Taking advantage of the LacZ reporter incorporated in this mouse line, we found that TMEM132D is expressed in glutamatergic and GABAergic neurons of the neocortex and hippocampus. Moreover, *Tmem132d* knockout mice showed enhanced active stress coping behavior in the forced swim test. To assess possible compensatory mechanism by the closest *Tmem132* family members, we additionally generated *Tmem132b/Tmem132d* and *Tmem132c/Tmem132d* double knockout mice as well as a *Tmem132b/Tmem132c/Tmem132d* triple knockout mouse line via CRISPR/Cas9-mediated mutagenesis.

Introduction

Neuropsychiatric diseases are one of the main contributors to the global disease burden. However, the progress of developing novel and more effective medications is still limited and validation of susceptibility genes identified by recent genome-wide association studies (GWAS), appears difficult. A recent association study analyzing panic disorder (PD) identified single nucleotide polymorphisms (SNPs) in the gene of the transmembrane protein 132D (*TMEM132D)*. TMEM132D was described as a protein exclusively expressed in mature oligodendrocytes (Nomoto et al., 2003). It is therefore also termed mature oligodendrocyte transmembrane protein (MOLT). TMEM132D belongs to the TMEM132 family that comprises five members from A to E.

In a study including three independent Caucasian samples, Erhard and colleagues found SNPs in the *TMEM132D* gene, located on chromosome 12, to be associated with PD. For the highest associated SNP (rs7309727) a significant case-control association with PD was observed. For rs11060369 a trend towards association was evident. In patients suffering from PD as well as unipolar depression, independent *TMEM132D* SNPs were additionally associated with the severity of anxiety symptoms (Erhardt et al., 2011). Furthermore, enhanced levels of *Tmem132d* mRNA were detected in the anterior cingulate cortex of a mouse model selectively bred for high anxiety-related behavior (Erhardt et al., 2011). The association of *TMEM132D* with PD was replicated by two recent studies strengthening the initial findings (Erhardt et al., 2012; Inoue et al., 2015). The association of certain risk alleles of *TMEM132D* with PD is further supported by recent studies. It has been shown that mRNA expression levels of *TMEM132D* are increased in subjects carrying the *TMEM132D* SNP rs11060369 (Myers et al., 2007; Erhardt et al., 2011). A study by Haaker et al. (2014) showed that homozygous carriers of rs11060369 are characterized by increased anxiety and increased volume of the gray matter of the amygdala, a key component of the fear circuitry. Moreover, rare polymorphisms of *TMEM132D* have been shown to be overrepresented in healthy controls compared to a group of panic disorder patients, as revealed by next generation sequencing. This suggests a protective effect of these rare variants by decreasing the functionality of the corresponding gene (Quast et al., 2012).

The recent association of different SNPs of *TMEM132D* with anxiety symptoms in patients suffering from unipolar depression and most of all panic disorder, suggest *TMEM132D* as a potentially interesting candidate gene. To gain more insight in the function and involvement of

TMEM132D in behaviors related to anxiety and depression, we used a variety of *in vitro* as well as *in vivo* approaches.

Methods

In situ hybridization

Two to three months old mice were sacrificed by an overdose of isoflurane. Brains were carefully removed and immediately shock frozen on dry ice. Frozen brains were cut on a cryostat in 20 µm-thick sections. Sections were processed for *in situ* hybridization as previously described (Deussing et al., 2007). The *Tmem132a* probe comprises nucleotides 3014-3416 of GenBank accession no. NM_133804.2. The *Tmem132b* probe comprises nucleotides 701-1131 of GenBank accession no. NM_001190352.1. The *Tmem132c* probe comprises nucleotides 3499-3954 of GenBank accession no. NM_175432.3. The *Tmem132d* probe comprises nucleotides 3871-4276 of GenBank accession no. NM_172885.2. The *Tmem132e* probe comprises nucleotides 3610-4027 of GenBank accession no. NM_001304439.1. A riboprobe was generated by PCR, labeled and hybridized as previously described (Deussing et al., 2007). The hybridized slides were placed in a film cassette and covered by a photo film (Biomax MR; Kodak, Rochester, NY). Depending on the signal strength the film was exposed for 1-14 days and developed in an automatic developing machine (XP2000, Kodak, Rochester, NY).

RT-PCR analysis

Expression of *Tmem132a-e* in the brain was analyzed by RT-PCR. First-strand cDNA synthesis from 1 µg total RNA was performed with SuperScript™ II reverse transcriptase (Invitrogen, Carlsbad, CA) according to the manufacturer´s protocol using an oligo (dT) primer. The following intron spanning primers were used for gene specific PCRs: *Tmem132a* Exon 6-8: forward 5´-AAC-TGT-CCG-AGT-TCC-TGT-GG-3´, reverse 5´-CGG-ATT-TGT-TCC-AGA-GTG-GT-3´ (amplifying nucleotides 1166-1670 of mouse *Tmem132a* cDNA, GenBank accession no. NM_133804.2). *Tmem132b* Exon 1-3: forward 5´-CAG-CGT-GGT-GGT-CTA-CCC-TA-3´, reverse 5´-TCA-TGG-AGT-CTT-CCA-CAG-GA-3´ (amplifying nucleotides 701-1131 of mouse *Tmem132b* cDNA, GenBank accession no. NM_001190352.1). *Tmem132c* Exon 6-8: forward 5´-GCA-AGA-TGG-ACT-CTG-TGG-TG-3´, reverse 5´-GAG-GTG-GCC-TTG-TTG-TTC-TC-3´ (amplifying nucleotides 1625-2204 of mouse *Tmem132c* cDNA, GenBank accession no. NM_175432.3). *Tmem132d* Exon 6-8: forward 5´-GGC-AAG-GTG-AAC-GTG-GTA-GT-3´, reverse 5´-AGT-GGC-AAA-GAT-GGC-TCT-GT-3´ (amplifying nucleotides 2202-2789 of mouse *Tmem132d* cDNA, GenBank accession no. NM_172885.2). *Tmem132e* Exon 6-8: forward 5´-ATG-AAC-GCC-AGA-GTC-ACC-TT-3´, reverse 5´-ACT-GAC-CTT-CTC-CTC-CGT-CA-3´ (amplifying nucleotides 1414-1923 of mouse *Tmem132e* cDNA, GenBank

accession no. NM_001304439.1). PCR products were analyzed by agarose gel electrophoresis together with a DNA marker (Smart Ladder, Eurogentec, Brussels, BEL).

Animals

All animal experiments were conducted in accordance with the guide for the care and use of laboratory animals of the government of Bavaria, Germany. All animals were housed singly under standard laboratory conditions and were maintained on a 12 h light-dark cycle (lights on between 7:00 a.m. and 7:00 p.m.) with food and water *ad libitum*.

Generation of conditional Tmem132d knockout mice

Conditional knockout mice were generated using a targeted embryonic stem (ES) cell clone (clone ID E302C11; cell line E14TG2a.4 (ES cells 129P2)) received from the German Genetrap Consortium (GGTC) by blastocyst injection. For this clone, a retroviral enhanced conditional gene trap vector, eFlipRosaβgeo, was used, comprising the following components (from 5´ to 3´): a long terminal repeat (LTR) followed by osteopontin enhancer elements (OPE), flanked by heterotypic Flp recombinase target sequences *frt*/*F3*; a splice acceptor (SA) followed by a β-galactosidase/neomycin-phosphotransferase fusion gene (β-Geo) and a polyadenylation sequence (pA). The entire reporter-selection cassette is flanked by heterotypic Cre recombinase target sequences *loxP*/*lox5171* followed again by *frt*/*F3* sites and a long terminal repeat (Figure 4) The insertion of the osteopontin enhancer into a conventional gene trap vector significantly increases the gene trapping efficiency in high-throughput screens and facilitates the recovery of poorly expressed genes (Schnutgen et al., 2008).

Germline transmission of the mutated *Tmem132d* locus was confirmed in the F_1 generation by breeding male chimeras to wild-type C57/BL6 mice. Genotyping was conducted by PCR using the following primer combinations: TD-KO_5´E302C11_for: 5´-ACT-GGT-CAC-ATT-GTA-TCC-ACA-GTC-3´ + TD-KO_5´E302C11_rev: 5´-CCT-ATA-GTG-AGT-CGT-ATT-CTC-CCG-3´ resulting in a 1172 bp product detecting the mutagenic orientation for the reporter/selection cassette. TD-KO_5´E302C11_for + TD-KO_3´E302C11_rev 5´-GAG-GCT-GTA-AGA-CTC-CAC-GTA-AAT-3´ resulted in a 1361 bp product detecting the non-mutagenic inverted orientation of the reporter/selection cassette.

Generation of CRISPR/Cas9 mediated knockout mice

Target sites were selected using http://crispr.mit.edu/ as previously described (Ran et al., 2013). One sgRNA target sequence covering 20 bp upstream of a NGG PAM-sequence for each *Tmem132* family member was selected. The target sequences (underlined) were cloned as complementary sequences with upstream T7 promoter sequence between two BbsI restriction sites into the pbs-U6-T7 plasmid as previously described (Brandl et al., 2015). The sequences were as follows:

Tmem132b: CAC-CTA-ATA-CGA-CTC-ACT-ATA-GGG-CCT-CTT-CTG-CAT-CGG-TGA-CG; *Tmem132c*: CAC-CTA-ATA-CGA-CTC-ACT-ATA-GGG-CGG-TAT-TAA-ACG-TCA-GCT-AT; *Tmem132d*: CAC-CTA-ATA-CGA-CTC-ACT-ATA-GGG-CTA-CAA-ATC-TAG-GCG-ACT-GC. *In vitro* transcriptions was conducted with the MEGAshortscript-Kit (Ambion, Austin, TX) based on templates amplified from the pBS-U6-T7 plasmid (primer T7-tracr1: 5'-GTA-CAA-AAT-ACG-TGA-CGT-AGA-AAG-3'; T7-tracr2: 5'-AAA-AAA-AGC-ACC-GAC-TCG-GTG-3'). Cas9 mRNA production was conducted using the previously described pCAG-Cas9-162A plasmid and the mMESSEGE mMACHINE T7 Ultra-Kit (Ambion, Austin, TX) omitting the polyadenylation step (Brandl et al., 2015). Before injection of the sgRNA and the Cas9 mRNA, RNA concentration and integrity was controlled by using a Bioanalyzer and the RNA 6000 Nano Chips (Agilent, Santa Clara, CA). For the injection mixture including all three sgRNAs and Cas9 mRNA, the RNAs were diluted to a final concentration of 80 ng/µl for Cas9 and to 30 ng/µl for the sgRNAs. RNA mix was finally injected as described before, with the exception that RNA mix was applied to the pronucleus only (Panda et al., 2013). For genotyping the targeted loci were amplified by PCR and subsequently sequenced (Sequiserve, Vaterstetten, GER). Primers for amplification: TB-for: 5'-CCG-TAG-TGG-GAA-GGG-AAG-AA-'3 TB-rev: 5'-AAA-GAT-GGA-GCT-GTC-GAG-GA-'3; TC-for: 5'-AGA-GCC-GAG-ACT-GCA-TTC-TT-'3 TC-rev: 5'-TTG-GGA-TGG-CTC-AGG-TAG-AC-'3; TD-for: 5'-TAC-TGC-CTA-CCT-ACC-TCC-CG-'3 TD-rev: 5'-GGC-AAC-ATC-AAA-TCC-TGG-GG-'3

Behavioral characterization of Tmem132d knockout mice

At an age of seven to eight weeks, mice were separated and habituated to single housing and test room conditions for a period of two weeks; mice of different genders were kept and investigated in two separate rooms. Following the habituation period all animals underwent a series of tests.

All behavioral tests were performed during the light phase, starting at 9 a.m. Scoring was performed by a trained observer, blind to the treatment/genotype, using pre-defined keyboard buttons and automatic video tracking of the ANY-maze software (Stoelting Co., Wood Dale, IL).

Forced Swim Test (FST)

Each mouse was gently placed into a glass beaker (height 24 cm, diameter 12 cm) filled with water (25-26 °C) to a height of 12 cm and the behavior during the 5 min test session was scored directly. At the end of the individual session, mice were removed and transferred to their individual home cage. Duration and frequency of occurrence of the following behaviors were measured: struggling (vigorous attempts at climbing the walls of the beaker); swimming (active swimming around without any upward directed movements); and floating (absence of movement other than necessary to keep balance).

Dark/Light box (DaLi)

The test box consists of black and white PVC and is divided into two compartments, connected by a tunnel (4x7x10 cm). The white compartment (30x20x25 cm) was brightly illuminated by cold light with an intensity of 680-700 lux; light intensity in the dark compartment (15x20x25 cm) was < 5 lux. At the beginning of a 5 min test period each mouse was placed in the center of the dark compartment, facing the tunnel. Mice were filmed from above with two cameras and the following parameters were scored directly from a monitor:

Time spent in each compartment (dark, tunnel, and lit), latency until the first full entry (with four paws) and the number of full entries into the lit compartment. The apparatus was wiped out with water before each trial.

Open Field (OF)

The open field test was used to characterize locomotor activity in a novel environment. The open field was made of grey PVC and consisted of four compartments of the same size (50x50x40 cm), allowing to test four animals in parallel. Light intensity was 15-20 lux. At the beginning of a test, each mouse was placed in the corner of a compartment, facing the middle. During the 15-30 min test period, the animal was recorded by means of a video camera mounted above the apparatus. The distance covered by the animal was analyzed automatically using the ANY-maze software. In this process each compartment was virtually subdivided in an inner (10x10 cm) and an outer

zone. Measured parameters were total distance covered; number, time and latency of inner zone exploration. The compartments were wiped out with water before each trial.

Elevated Plus Maze (EPM)

The elevated plus maze was used to assess anxiety-related behavior The apparatus was made of grey PVC and consisted of a plus-shaped platform with four intersecting arms, elevated 37 cm above the floor. Two opposing open (30x5 cm) and closed arms (30x5x15 cm) were connected by a central zone (5x5 cm). Animals were placed in the center of the apparatus facing the closed arm and were allowed to freely explore the maze for 5 min.

LacZ staining

Mice were sacrificed by an overdose of isoflurane (Baxter, Deerfield, IL) and subsequently intracardially perfused using LacZ-fix solution (for composition see Mombaerts et al., 1996) for 5-7 min, followed by a 1 min washing step with PBS. After preparation, the brain was additionally fixed for 1 h in LacZ-fix and then incubated overnight at 4°C in 20% sucrose/PBS. The next day, the brain was frozen on dry-ice and cut at a cryostat (HM 560 M, Microm, Thermo Fisher Scientific, Waltham, MA) in 50 µm thick sections and collected in cryoprotection solution. The staining was conducted as previously described (Mombaerts et al., 1996) and subsequently mounted on super frost plus slides (Menzel, Thermo Fisher Scientific, Waltham, MA), immersed in xylol and embedded with DPX mounting solution (BDH).

Immunohistochemistry/-cytochemistry

In case of using cell lines, cells were grown on polylysin-coated coverslips (VWR, Radnor, PA) in 24-well plates. In case of using brain tissue, the brain was cut with a cryostat (HM 560 M, Microm, Thermo Fisher Scientific, Waltham, MA) in 50 µm thick sections and collected in cryoprotection solution.

For fixation of cells/brain sections were treated with warmed PFA 4% in 4% sucrose/PBS for 10-30 min at RT. After three 5 min washing steps, cells/sections were permeabilized 3x for 5 min using PBS-Triton X-100 0.1%. Cells/slices were washed for 5 min with PBS and subsequently treated with PBS-Triton X-100 0.1%, 5% BSA for 1 h to block the reaction. Afterwards, cells/sections were washed 2x for 5 min. Incubation with the first antibody, diluted in PBS-Triton 0.01%, 5% BSA, was carried out overnight at 4°C. After a three times washing step with PBS, an Alexa Fluor secondary antibody (Invitrogen, Carlsbad, CA), diluted in PBS-Triton 0.01%, 5% BSA,

was added and incubated for 1 h at RT. Cells/sections were washed three times with PBS and mounted with antifade mounting media (Vector Labs) containing DAPI that was used to stain cellular nuclei. Sections were mounted on super frost plus slides (Menzel, Thermo Fisher Scientific, Waltham, MA) before mounting. The following antibodies were used: mouse anti-NeuN (1:1000, Chemicon, Billerica, MA); rabbit anti-Glu (1:1000, Sigma Aldrich, St. Louis, MO); mouse anti-GAD67 (1:1000, Chemicon, Billerica, MA); chicken anti-β-Gal (1:1000, Abcam, Cambridge, UK); anti-rabbit Alexa 594 (1:1000, I Invitrogen, Carlsbad, CA); anti-mouse Alexa 594 (1:1000, Invitrogen); anti-chicken Alexa 488 (1:1000, Invitrogen, Carlsbad, CA); Rhodamine Phalloidin (1:140; Cytosceleton Inc., Denver, CO).

Statistics

Data and statistical analysis were performed with the computer programs GraphPad Prism 5.0 (La Jolla, CA) and SPSS 16.00 (IBM, Armonk, NY). All results are shown as means ± standard error of the mean (SEM). The effects of genotype and stress on behavior and neuroendocrine data were examined by two-way-multivariate analysis of variance with post-hoc t-test (level of significance, $p < 0.05$).

Results

Expression of *Tmem132* family members

The TMEM132 family comprises five members from A to E. Homology of the family members ranges from 30-60%, comparing amino acid sequences (Figure 1a). As an initial step we investigated the expression of *Tmem132d* and the other *Tmem132* family members in the adult mouse brain. RT-PCR-mediated qualitative expression analyses using RNA from complete mouse brains revealed that all five *Tmem132* members are readily expressed in the adult mouse brain (Figure 1b).

a

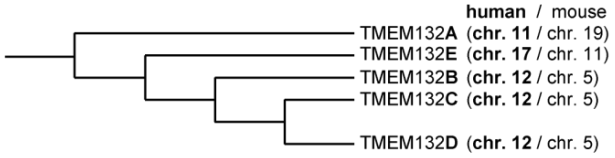

human

	TMEM132A	TMEM132B	TMEM132C	TMEM132D	TMEM132E
TMEM132A	100.00	32.45	34.37	32.83	34.93
TMEM132B	32.45	100.00	52.47	51.35	37.57
TMEM132C	34.37	52.47	100.00	60.48	45.18
TMEM132D	32.83	51.35	60.48	100.00	40.75
TMEM132E	34.93	37.57	45.18	40.75	100.00

mouse

	TMEM132A	TMEM132B	TMEM132C	TMEM132D	TMEM132E
TMEM132A	100.00	33.02	33.17	32.52	34.54
TMEM132B	33.02	100.00	50.24	49.43	36.80
TMEM132C	33.17	50.24	100.00	56.53	42.48
TMEM132D	32.52	49.43	56.53	100.00	39.77
TMEM132E	34.54	36.80	42.48	39.77	100.00

b

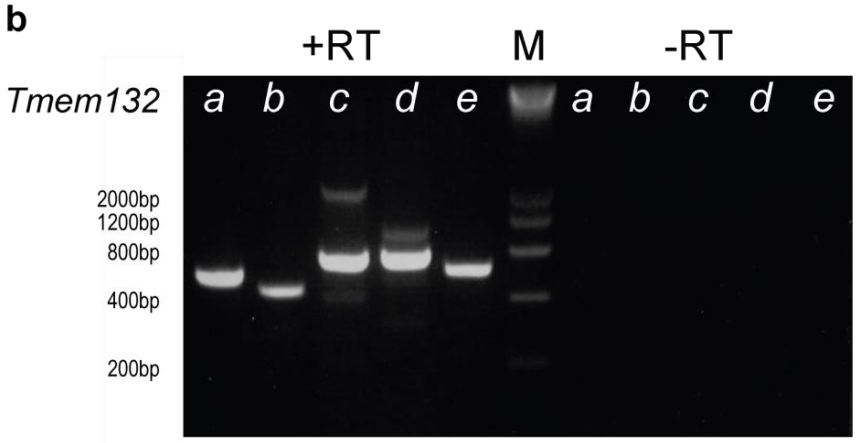

Figure 1: Homology of Tmem132 family members and their expression in the adult mouse brain
a Phylogenetic tree and homology matrix of TMEM132 family members based on their amino acid sequences. **b** RT-PCR based expression analysis revealed the expression of all five *Tmem132* members in the mouse brain. The left lanes show reverse transcriptase (+RT) positive samples, in lanes to the right of the marker (M: 1kb ladder) no reverse transcriptase (–RT) was added.

To reveal the spatial distribution of *Tmem132* family members in the adult brain, the expression was analyzed by *in situ* hybridization (ISH) (Figure 2). Each *Tmem132* family member is specifically expressed with respect to the expression pattern, as well as the intensity in different brain regions. Whereas *Tmem132a* showed highest expression almost ubiquitously throughout the brain, *Tmem132c* and *Tmem132e* showed relative low expression levels mainly in the reticular thalamic nucleus, dentate gyrus and cerebellum. *Tmem132b* expression was mainly detected in forebrain regions, showing a strong overlap with *Tmem132d*. Additional sites of expression are found in the striatum, lateral septum as well as in the CA3 and dentate gyrus of the hippocampal formation. Expression of *Tmem132d* was particularly detected for the following brain regions: glomerular layer of the olfactory bulb, lateral septum, piriform cortex, neocortex (mainly somatosensory cortex), cornu ammonis 1 (CA1) region of the hippocampus, nuclei of the thalamus, dorsomedial hypothalamic nucleus, amygdala, periaqueductal grey, median raphe nucleus, motor nuclei in the hindbrain (Figure 2).

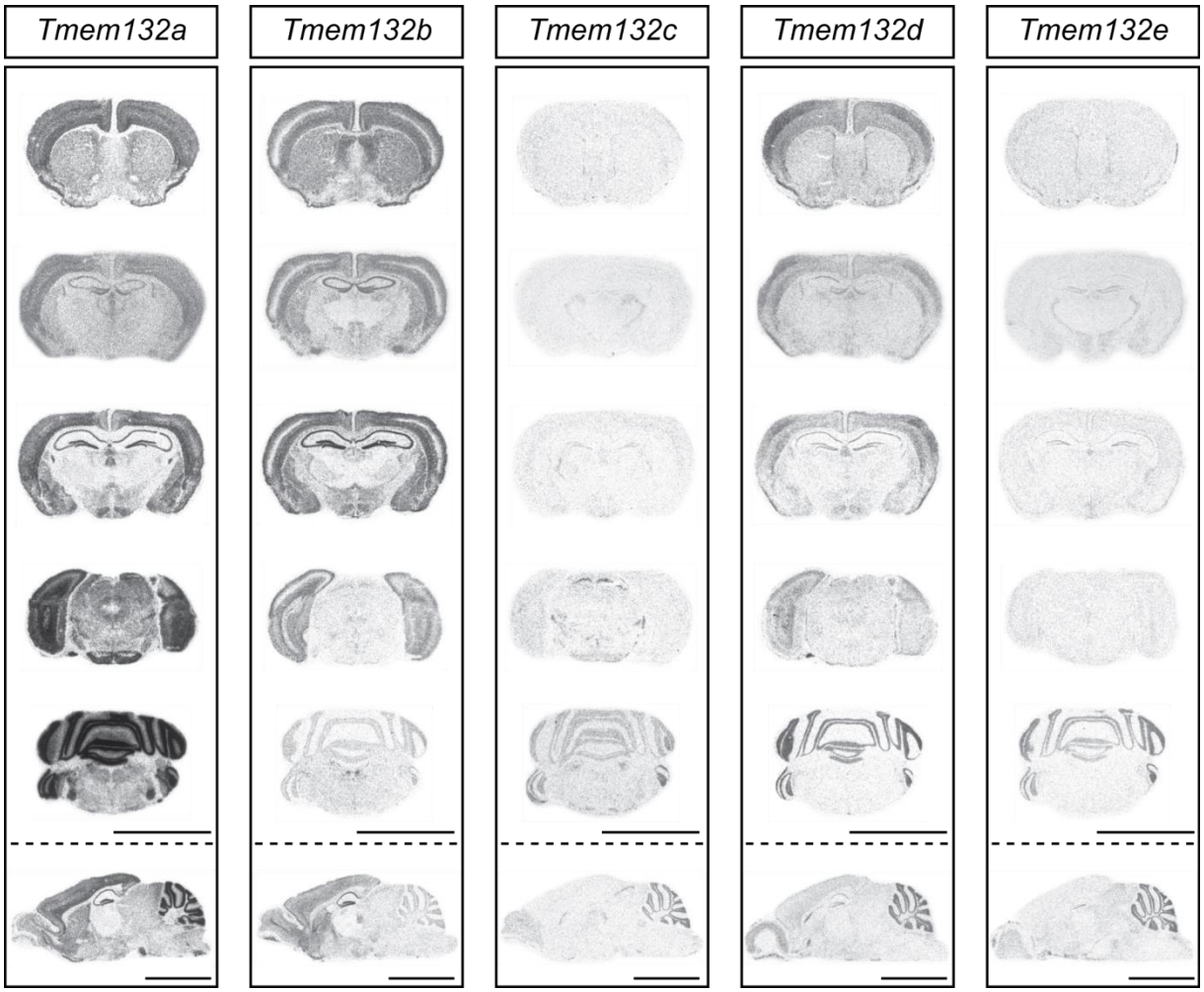

Figure 2: Figure legend see next page

Figure 2: Expression of *Tmem132* family members in the mouse brain
In situ hybridization based expression analysis using riboprobes specific for each of the five *Tmem132* family members. The columns show autoradiographies of the five family members. Each column shows five representative coronal brain sections from rostral (up) to caudal (down); the lowest section in each column (separated by dashed line) shows a representative sagittal section of the brain. Scale bars indicate 500µM.

Subcellular localization of TMEM132D

Little is known about the intracellular distribution of the TMEM132D protein in the cell. *In slico* studies analyzing the amino acid sequence of TMEM132D indicate a transmembrane domain with a long N-terminal domain protruding to the extracellular space. To experimentally determine the intracellular localization of TMEM132D we tagged TMEM132D C-terminally with green fluorescent protein (GFP) and expressed the fusion protein in human embryonic kidney (HEK293) cells. We found that the TMEM132D-GFP fusion protein was exclusively localized to the cell membrane (Figure 3). Moreover, TMEM132D-GFP co-localized with phalloidin stained actin filaments (Barden et al., 1987) in filopodia like structures.

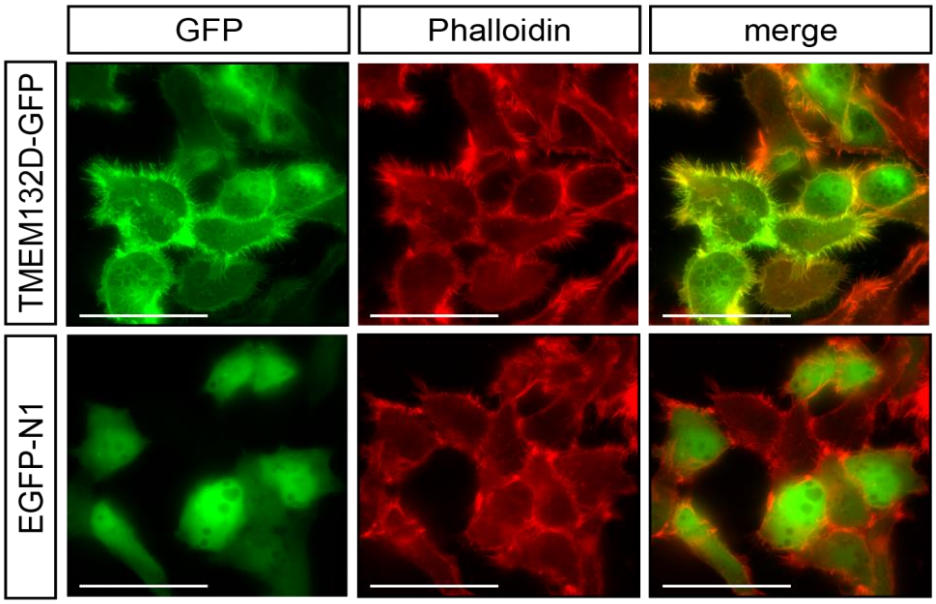

Figure 3: TMEM132D-GFP is localized to the membrane of HEK293 cells
HEK293 cells transfected with a TMEM132D-GFP fusion protein or EGFP-N1 control plasmid, respectively. TMEM132D-GFP is localized to the membrane and shows co-localization with phalloidin. Scale bars indicate 20 µm.

Conditional *Tmem132d* knockout mouse

To analyze the function of *Tmem132d* in an *in vivo* model system, we generated knockout mice. In addition to the knockout of *Tmem132d* these mice carry a LacZ reporter which enables the cell type-specific analysis of *Tmem132d* expression. The integration of the vector into intron 1 of the *Tmem132d* gene results in a splice event from the splice donor of the endogenous exon 1 to the SA of the reporter selection cassette. Subsequently the reporter is expressed and transcription of *Tmem132d* is prematurely terminated by the poly A signal of the integrated cassette. Integration of the vector into intron 1 ensures the disruption of the TMEM132D signal peptide. In this way the β-galactosidase-neomycine (β-Geo) is not secreted but confers resistance to neomycin. In addition, the used gene trap vector comprises recognition sequences for site-specific recombinases (Flp/Cre) that allow the rescue and re-induction of the mutation when activated in succession (Figure 4).

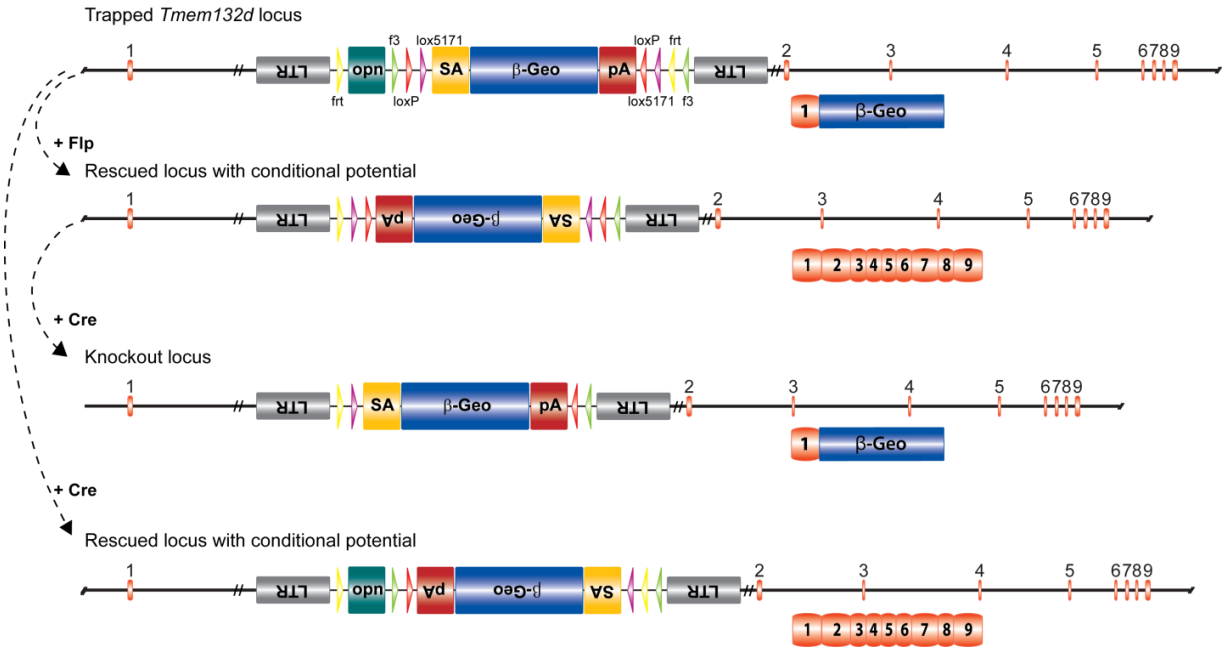

Figure 4: Schematic representation of trapped *Tmem132d* locus

The gene trap vector was integrated into intron 1 of the *Tmem132d* gene. The vector contains a β-Geo reporter selection cassette that is flanked by both Flp and Cre recombinase target sites. By recombination with Flp regular *Tmem132d* expression can be re-introduced. Based on this "flipped" allele the reported knockout can be re-induced by Cre-mediated recombination. Based on the initially trapped locus Cre recombinase can re-introduce *Tmem132d* expression, respectively.

The trapped ES cell clone was used to generate heterozygous knockout mice (*Tmem132d* $^{+/LacZ}$). By crossbreeding of heterozygous *Tmem132d* knockout mice we obtained in the F2 generation homozygous *Tmem132d* knockout mice (*Tmem132d* $^{LacZ/LacZ}$; referred to as *Tmem132d* KO) at Mendelian frequency.

Tmem132d KO mice showed normal development and individuals were indistinguishable from heterozygous or wild-type (WT) littermates. *Tmem132d* KO animals were fertile and reproduced normally. The examination of external and internal organs did not reveal any macroscopic abnormalities in *Tmem132d* KO mice (data not shown).

To confirm the inactivation of the *Tmem132d* gene we conducted an ISH for *Tmem132d* as well as for the *LacZ* reporter on brain sections of homozygous KO mice. Using a specific *Tmem132d* probe covering the 3'UTR we observed a loss of expression in the brains of KO mice. As expected complementary mRNA expression of the *LacZ* reporter gene was detected, resembling the pattern of endogenous *Tmem132d* expression in WT animals. LacZ expression was additionally confirmed by X-Gal staining (Figure 5).

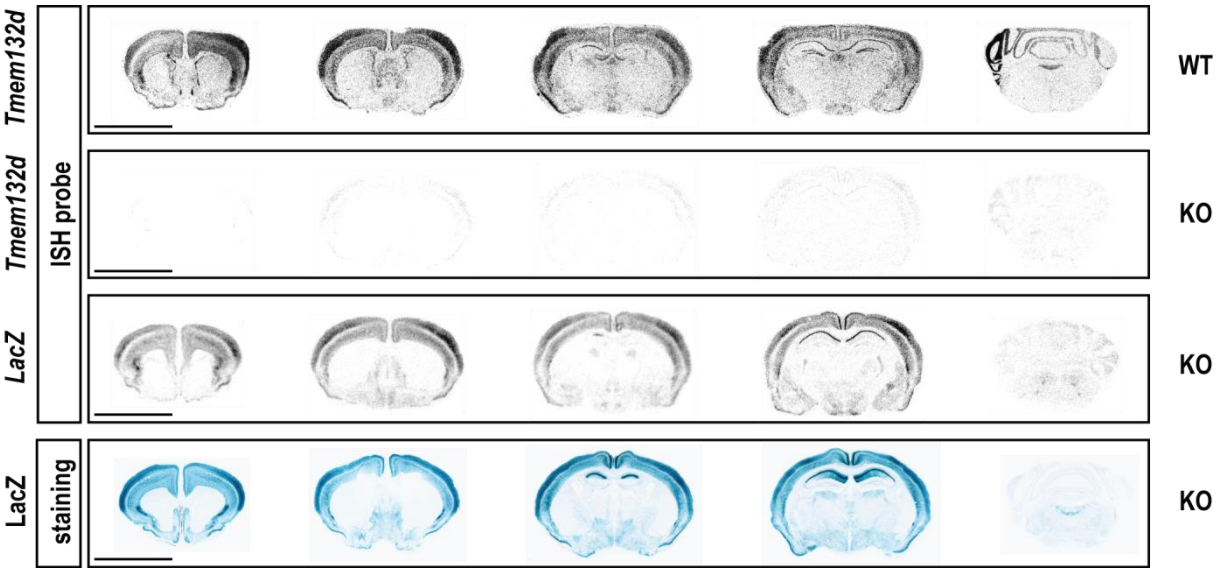

Figure 5: Confirmation of *Tmem132d* knockout by expression analysis

In situ hybridization specific for *Tmem132d* was conducted to confirm absence of *Tmem132d* mRNA expression in brain sections of *Tmem132d* $^{LacZ/LacZ}$ knockout mice (KO) compared to wild-type littermates (WT). Additionally *LacZ* mRNA was detected in KO brain sections by ISH using a *LacZ*-specific riboprobe. LacZ expression in KO mice was also revealed by X-Gal staining. Scale bars indicate 500µM.

To gain more insight in the expression of TMEM132D on cellular level we conducted immunohistochemical-stainings taking advantage of the LacZ reporter allele present in the KO mice. Given the fact, that reliable antibodies for TMEM132D are not available we used an anti-β-Gal antibody to detect the β-Gal reporter protein, resembling endogenous TMEM132D expression. To test whether TMEM132D is expressed in glial cells or neurons we used the neuronal marker NeuN, revealing that TMEM132D is exclusively expressed in neurons. Strong TMEM132D expression was observed in the piriform cortex, the basolateral amygdala as well as in the CA1 of the hippocampus (Figure 6). Additionally we observed co-staining in the somatosensory cortex, the cingulate cortex as well as some thalamic nuclei and motor nuclei of the hindbrain (data not shown).

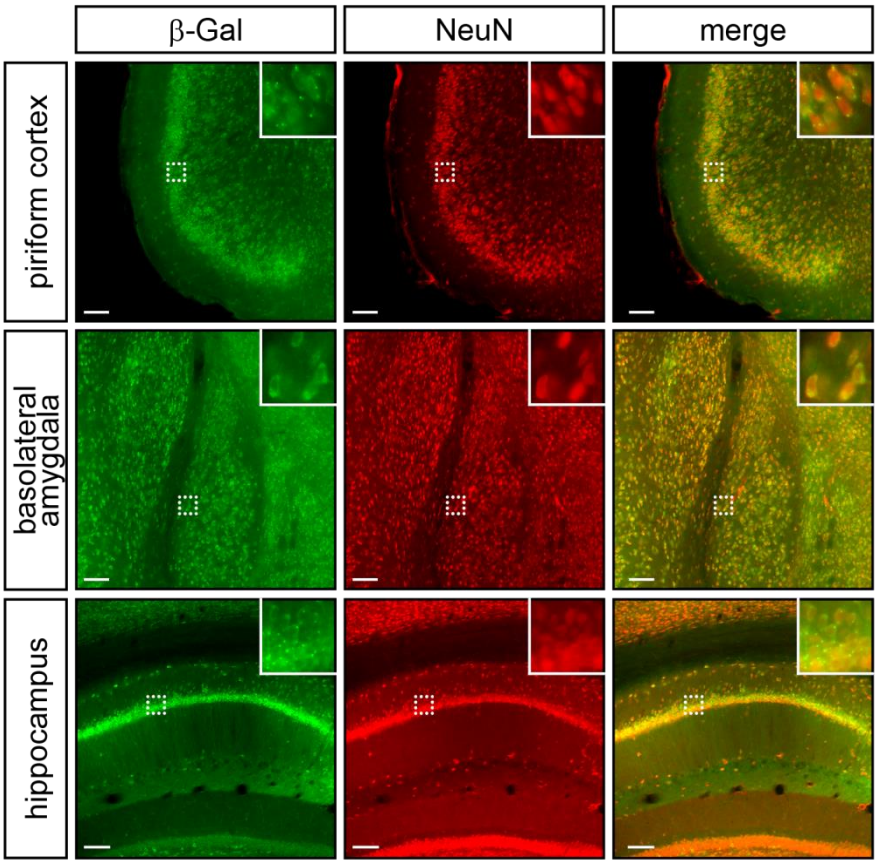

Figure 6: TMEM132D is exclusively expressed in neurons of the mouse brain
Immuno-staining for β-Gal and the neuronal marker NeuN reveals neuronal expression of TMEM132D in the piriform cortex, the basolateral amygdala and the CA1 of the hippocampus. Scale bars indicate 100 µm.

To more specifically determine the neuronal TMEM132D expression, co-stainings for β-Gal and the markers for excitatory glutamatergic (anti-Glu) and for inhibitory GABAergic neurons (anti-GAD67) were analyzed. The immuno-stainings for glutamatergic neurons revealed expression of TMEM132D in glutamatergic cells of the piriform cortex, the basolateral amygdala and the CA1 region of the hippocampus (Figure 7a) as well as in the somatosensory cortex (data not shown). Additionally, we confirmed these findings by re-introduction of *Tmem132d* expression and concomitant termination of LacZ reporter expression specifically in glutamatergic neurons. To this end we bred the *Nex-Cre* driver to *Tmem132d* KO mice. *Nex-Cre* inactivates LacZ expression in forebrain glutamatergic neurons (Figure 7a). Remaining LacZ positive neurons in the hippocampus and cortex are GABAergic TMEM132D expressing neurons.

Co-staining for β-Gal and the GABAergic marker (GAD67) revealed co-expression of *Tmem132d* and Gad67 in GABAergic neurons sparsely located in between the largely excitatory neurons of the piriform cortex (Figure 7b). In other neocortical structures co-localization of β-Gal and GAD67 was not observed (data not shown). In the hippocampus we detected scattered β-Gal/TMEM132D expression co-localizing with GAD67, which is in accordance with the expected distribution of GABAergic neurons in the hippocampal formation. Analogue to glutamatergic neurons we confirmed these stainings by re-introducing *Tmem132d* expression specifically in GABAergic neurons. Therefore, we bred the *Tmem132d* KO mice to the *Dlx5/6-Cre* driver. *Dlx5/6-Cre* inactivates LacZ expression in GABAergic neurons of the forebrain (Figure 7b). Remaining LacZ positive neurons in the cortex and hippocampus reflect *Tmem132d* expression in glutamatergic neurons. The combination of *Nex-Cre* and *Dlx5/6-Cre* fully abolished LacZ expression in the cortex and hippocampus (data not shown), confirming that *Tmem132d* in these structures is exclusively expressed in glutamatergic and GABAergic neurons.

To investigate the effect of *Tmem132d* deficiency on emotional behavior we conducted a behavioral screening comparing *Tmem132d* KO animals and WT littermates. We could not observe any differences between KO and WT animals regarding locomotion or anxiety-related behavior as investigated by the open field (OF), elevated plus maze (EPM) and dark-light box test (DaLi) (Figure 8a,b,c). However, *Tmem132d* KO mice showed increased active stress coping behavior compared to WT littermates as indicated by an increased struggling time and decreased floating time, respectively (Figure 8d). This phenotype was successfully be replicated with an independent batch of animals confirming the findings (data not shown).

These findings provide first evidence that *Tmem132d* might be involved in shaping the animals stress response.

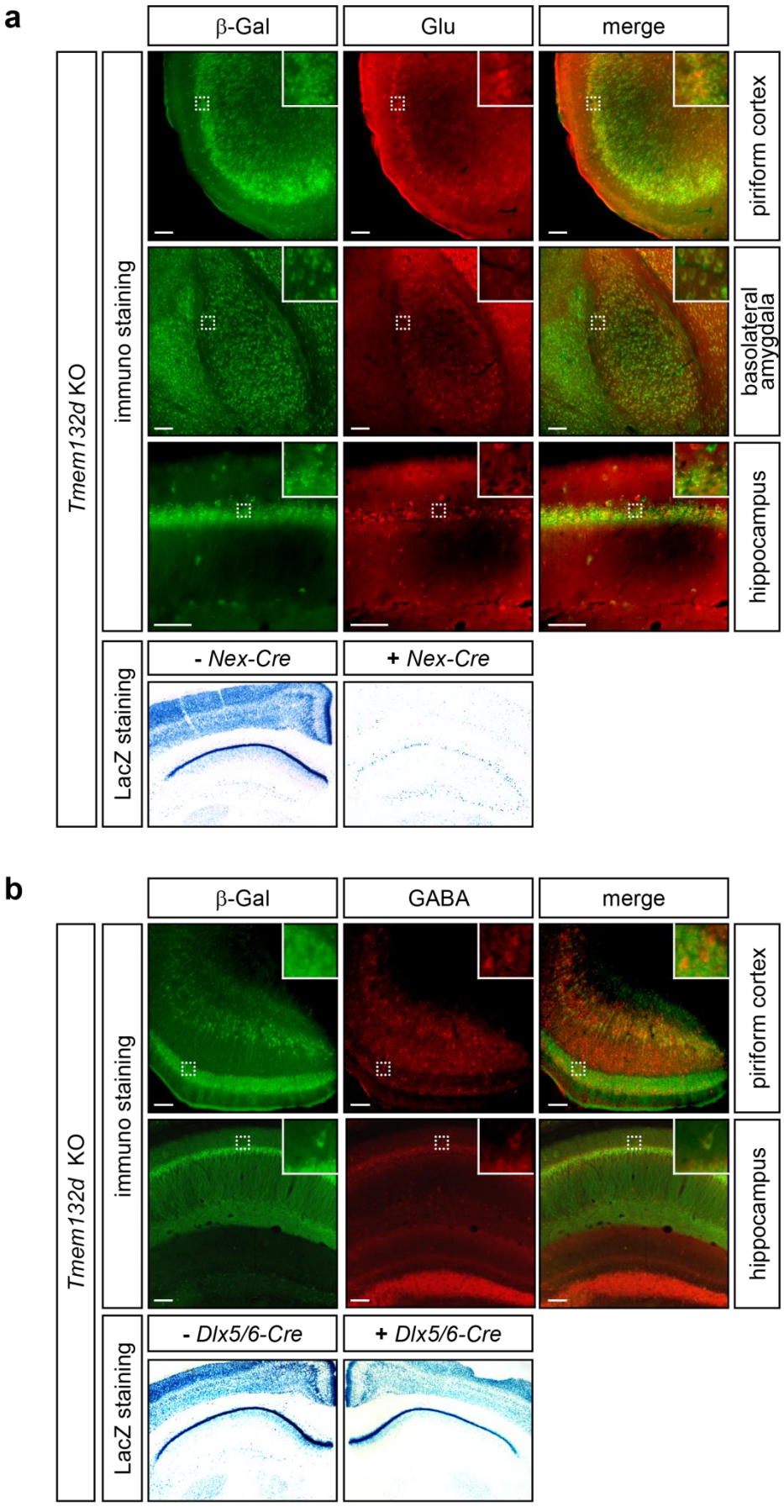

Figure 7: Figure legend see next page

Figure 7: *Tmem132d* is expressed in glutamatergic and GABAergic neurons

(**a**) Immuno-staining for β-Gal resembling TMEM132D expression and glutamate (Glu) reveals TMEM132D localization in glutamatergic neurons of the piriform cortex, the basolateral amygdala and the CA1 of the hippocampus. Hippocampal *Tmem132d* expression in glutamatergic neurons is additionally shown by LacZ staining of *Tmem132d* KO mice bred with the *Nex-Cre* driver. *Nex-Cre* specifically recombines in glutamatergic neurons of the forebrain and thereby re-introduces *Tmem132d* expression switching off reporter gene (*LacZ*) expression. (**b**) Immuno-staining for β-Gal and and GABA shows that TMEM132D is expressed in GABAergic neurons of the cortex and hippocampus. This was confirmed by LacZ staining of *Tmem132d* knockout mice. For re-introduction of *Tmem132d* expression and deletion of reporter gene (*LacZ*) expression specifically in GABAergic neurons of the forebrain, *Tmem132d* KO mice were, bred to *Dlx5/6-Cre* driver mice. Scale bars indicate 100 µm.

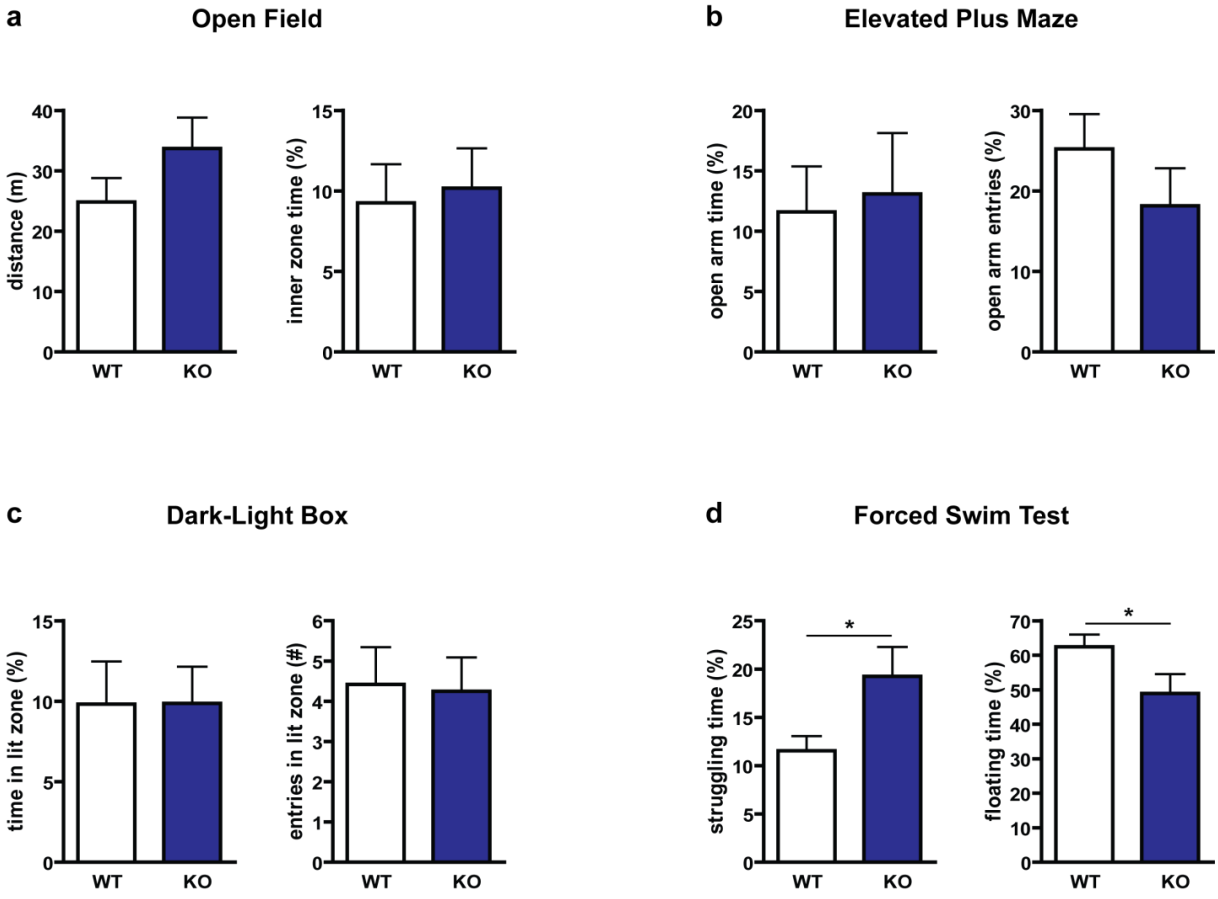

Figure 8: Basal behavioral screen of *Tmem132d* knockout mice

Tmem132d KO mice were subjected to (**a**) the open field test, (**b**) the elevated plus maze and (**c**) the dark-light box test to investigate locomotion and anxiety-related behavior. No differences between KO and WT mice were observed. (**d**) *Tmem132d* KO mice showed increased active stress coping, i.e. increased struggling and decreased floating, compared to WT littermates as investigated by the forced swim test. (Data are expressed as mean values + S.E.M.; *significant; Student's t-test, $p < 0.05$; n=12)

CRISPR/Cas9-mediated generation of triple Tmem132 knockout mice

Three of the five *Tmem132d* family members namely the highly homologous *Tmem132b*, *Tmem132c* and *Tmem132d* are located in a cluster on chromosome 5 (human: chromosome 12) (Figure 9). Moreover, *Tmem132d* and *Tmem132b* show strong overlap in their pattern of expression throughout the murine brain. To rule out possible compensatory mechanisms by the two other family members in the *Tmem132d* KO mice the generation of double and triple knockouts for these family members would be mandatory. The close proximity of the three genes within ~2.7 Mb precludes a regular gene targeting approach and subsequent crossbreeding of targeted alleles (Figure 9). Therefore, we chose the CRISPR/Cas9 system to simultaneously target the three genes. For all three genes specific sgRNAs were designed targeting regions downstream of the translation start site in exon 2 of the respective genes (Figure 10). By simultaneous injection of all three sgRNAs in combination with Cas9 mRNA into the pronucleus of zygotes we prompted mutations caused by the error prone non-homologous-end-joining repair mechanism of the cell. Screening of the founder mice derived from the injected zygotes revealed a chimerism with respect to the introduced mutations. Germline transmission was confirmed by breeding to C57BL/6N wild-type mice. The analysis of this F_1 generation further revealed which of the initial mutation were co-inherited indicating whether they are in cis or trans. We identified single *Tmem132d* mutant mice as well as two double knockouts (*Tmem132b*+*Tmem132d* and *Tmem132c*+*Tmem132d*) and the desired triple knockout (*Tmem132b*+*Tmem132c*+*Tmem132d*) (Table 1). Mutations were initially identified by amplification of the targeted area via PCR and subsequent sequencing of the PCR products. Some mutations could later on be identified by digestion of the PCR products due to disappearing restriction sites (Figure 10).

These new *Tmem132* mutants provide powerful tools to test for compensatory mechanism occurring between the three family members. Comparing the effect of different combinations of double as well as the triple knockout with the single *Tmem132d* knockout in different behavioral paradigms with particular focus on stress coping behavior, will be part of future projects.

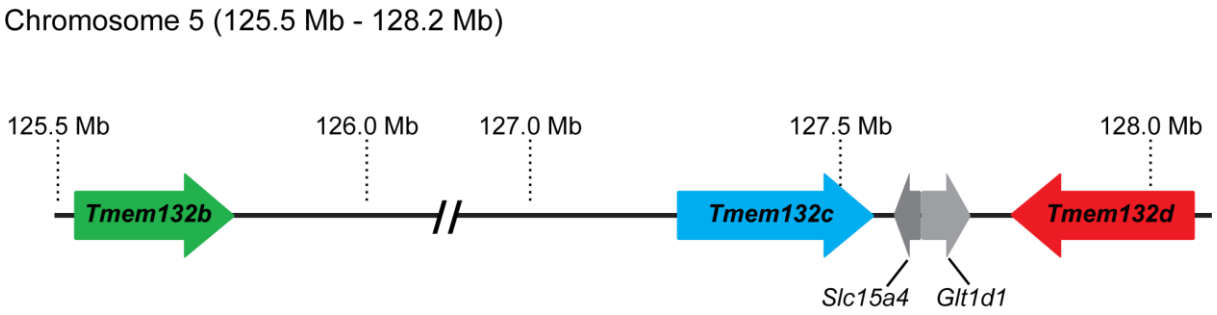

Figure 9: *Tmem132b, c* and *d* are clustered on chromosome 5

Segment of the murine chromosome 5, including the three *Tmem132* family members *b, c* and *d* in close proximity within 2.7 Mb. Between *Tmem132c* and *Tmem132d* two additional genes are located: *solute carrier family 15, member 4* (*Slc15a4*) and *glycosyltransferase 1 domain containing 1* (*Glt1d1*).

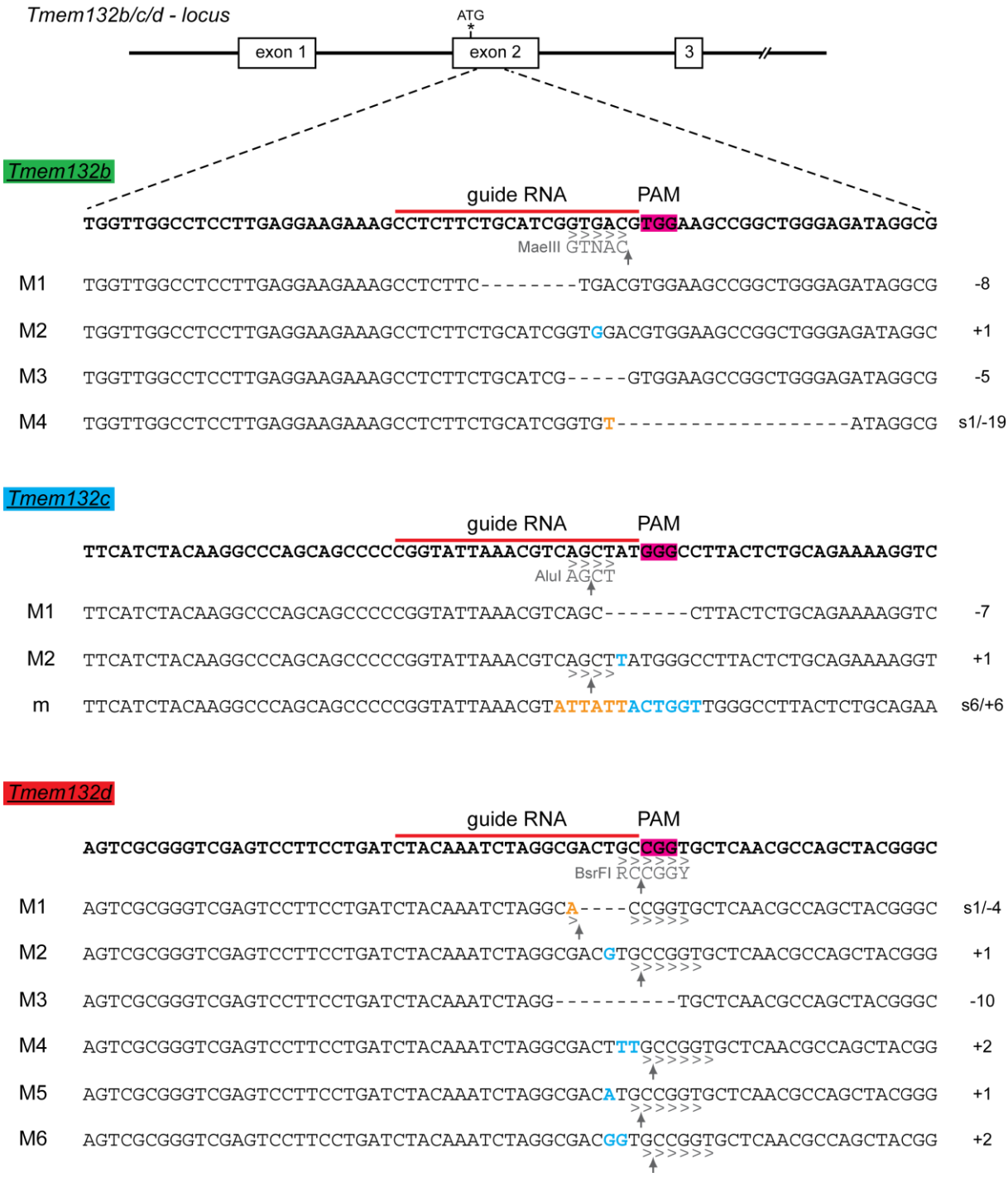

Figure 10: Targeting scheme and resulting mutations of CRISPR/Cas9-mediated knockout approach
Targeted sequences for *Tmem132b*, *Tmem132c* and *Tmem132d* loci are shown. In all cases exon 2 shortly after the translation start site was targeted. The 20nt guide RNA sequence (red) is followed by the PAM (purple) sequence. Restriction sites that disappear in some mutations are marked in gray. (M: mutations leading to a premature stop codon; m: mutations not resulting in a premature stop codon; Deletions are indicated by a dash (-); insertions by blue letters, nucleotide substitutions by orange letters)

gene / type of knockout	*Tmem132b*	*Tmem132c*	*Tmem132d*
single (d)	wildtype	wildtype	M2
double (b+d)	M1	wildtype	M1
double (c+d)	wildtype	M1	M3
triple (b+c+d)	M3	M2	M4

Table 1: CRISPR/Cas9-derived single, double and triple *Tmem132* knockouts
The single *Tmem132d* and the different combinations of double and the triple knockout of *Tmem132b*, *Tmem132c* and *Tmem132d* and their respective mutations are depicted.

Discussion

Polymorphisms in the *TMEM132D* gene have been found to be associated with panic disorder and symptoms of anxiety in depressed patients (Erhardt et al., 2011, 2012; Inoue et al., 2015), making it an interesting new candidate gene to study in the context of anxiety and mood disorders. However, a fact that makes the validation of *TMEM132D* and its polymorphisms very difficult is that all disease associated SNPs are intronic. Moreover, the expression and function of *Tmem132d* in the brain has not been studied so far. To enlighten this we conducted *in vitro* and *in vivo* approaches to elucidate the function of TMEM132D in the brain.

As a first step we investigated the expression of *Tmem132d* and the other four *Tmem132* family members in the mouse brain. Even though some information regarding the expression of *Tmem132a, c, d* and *e* but not for *Tmem132b* in the mouse brain is publicly available (http://www.brain-map.org) the data is not very consistent and only very little additional information regarding the expression of *Tmem132* family members exists. For *Tmem132b* its differential expression in intracranial aneurysm tissue has been demonstrated (Farlow et al., 2015). We demonstrate that all five *Tmem132* family members are expressed in the brain. *In situ* hybridization allowed a more detailed comparison regarding the spatial expression pattern. We observed distinct differences in expression of the individual family members suggesting diverging functions in the adult mouse brain.

To address the question regarding the subcellular localization of the protein, we transfected HEK293 cells with a TMEM132D-GFP fusion construct. We found TMEM132D to be located in the cellular membrane of transfected HEK293 cells. This is in line with the *in silico* studies proposing a single transmembrane domain within the protein. Additionally, we observed a co-localization of TMEM132D with actin filaments as shown by phalloidin staining. The actin cytoskeleton is an important factor in the assembly, maturation and turnover of protrusions like lamellipodia and filopodia as well as adhesion structures (Yamaguchi and Condeelis, 2007; Om Alblazi and Siar, 2015). Both findings support bioinformatics results suggesting an involvement of TMEM132D in cell adhesion and/or migration. A screening for sites and motifs of the TMEM132D protein revealed the potential cell attachment sequence RGD (Arg-Gly-Asp; amino acids 235-237 of murine and 236-238 of human TMEM132D) as well as a sequence (amino acids 472-486 of the murine and 473-487 of human TMEM132D) with high similarity to a thrombospondin type 3 repeat. Thrombospondin is an adhesive glycoprotein with binding capacity for fibrinogen,

fibronectin, laminin and collagen and thereby is able to mediate cell to cell or cell to matrix interactions (Adams, 2001).

As an *in vivo* tool to study the physiological function of the TMEM132D protein and to further investigate the expression of *Tmem132d* in the mouse brain, we generated *Tmem132d* knockout mice. These knockout mice faithfully report *Tmem132d* expression via a LacZ reporter gene based on a gene trap approach. Disruption of *Tmem132d* expression was confirmed by ISH. LacZ reporter expression was confirmed to fully reflect endogenous *Tmem132d* expression, both on the mRNA level by ISH as well as on protein level by X-Gal staining.

We took advantage of the LacZ reporter to conduct a more detailed expression analysis in the brain. Due to the lack of validated TMEM132D antibodies we relied on immune-stainings against the β-Gal reporter. In combination with a staining for the neuronal marker protein NeuN we could indeed show neuronal expression of TMEM132D. This result is in contrast to the initial finding by Nomoto et al. (2003) of TMEM132D being specifically expressed in mature oligodendrocytes which was based on antibody staining. Corresponding to the expression in the ISH we tried to obtain even more precise information by conducting co-stainings with more specific markers for different neurotransmitter systems. Using markers for excitatory and inhibitory neurons revealed that TMEM132D is expressed in glutamatergic neurons, as well as in GABAergic neurons of the cortex and the hippocampus. These findings were confirmed by site specific re-induction of *Tmem132d* expression and combined depletion of reporter LacZ expression in *Tmem132d* knockout animals mediated by cell type-specific Cre drivers. This possibility was enabled by the directional site-specific recombination system (Flp/Cre) of the applied gene trap strategy (Schnütgen et al., 2008). It renders the possibility to rescue and re-induce the gene trap mutation when activated in succession. Cre- or Flp-mediated recombination leads to the inversion of the reporter/selection cassette into a non-mutagenic antisense orientation causing a re-induction of endogenous splicing from exon 1 to exon 2. In case of the Flp-mediated re-introduction of *Tmem132d* expression the loss-of-function mutation can be re-induced by Cre recombinase (Schnütgen et al., 2005). By using specific Cre drivers this construct further enables the tissue or cell-type specific knockout or re-introduction of *Tmem132d* expression.

A first comprehensive behavioral screen of the constitutive *Tmem132d* knockout animals under basal housing conditions did not reveal any differences compared to WT littermates regarding locomotion or anxiety-related behavior. However, we observed in the KO mice an increased

active stress-coping phenotype in the FST suggesting a role of TMEM132D in the regulation of stress- induced behaviors.

A more direct validation of the human association data, i.e. the associated SNPs, in a mouse model is currently difficult. All identified polymorphisms are found in introns of the *TMEM132D* gene which are not conserved between the two species. The knockout of *Tmem132d* may therefore represent a valuable alternative to investigate the impact of TMEM132D on the risk to develop anxiety and mood disorders. However, an important point to be noted is the possibility of compensatory effects mediated by other *Tmem132* family members in these *Tmem132d* knockout animals. In particular the two closest related family members *Tmem132b* and *Tmem132c* have to be considered in this context. All three genes are found in direct proximity to each other on the same chromosome both in human as well as in the mouse. They evolved by gene duplication and therefore are likely able – at least partially – to compensate for each other, even though we did not observe a compensatory change in RNA expression (data not shown). In order to rule this out, we created two double knockouts (*Tmem132b*+*Tmem132d* and *Tmem132c*+*Tmem132d*) and a triple knockout (*Tmem132b*+*Tmem132c*+*Tmem132d*) for all three genes by using a CRISPR/Cas9-mediated gene targeting approach. Only this technique allows the simultaneous targeting (multiplexing) of loci of close proximity, something that is difficult to achieve by conventional gene targeting approaches (Wang et al., 2013; Young et al., 2015). These new knockout lines in combination with the conditional gene trap-based *Tmem132d* knockout line are powerful tools to further study the *in vivo* function and possible involvement of TMEM132D in anxiety and mood disorders in the future.

References

Adams, J. C. (2001). Thrombospondins: multifunctional regulators of cell interactions. *Annu. Rev. Cell Dev. Biol.* 17, 25–51. doi:10.1146/annurev.cellbio.17.1.25.

Barden, J. a, Miki, M., Hambly, B. D., and Dos Remedios, C. G. (1987). Localization of the phalloidin and nucleotide-binding sites on actin. *Eur. J. Biochem.* 162, 583–588. doi:10.1111/j.1432-1033.1987.tb10679.x.

Brandl, C., Ortiz, O., Röttig, B., Wefers, B., Wurst, W., and Kühn, R. (2015). Creation of targeted genomic deletions using TALEN or CRISPR/Cas nuclease pairs in one-cell mouse embryos. *FEBS Open Bio* 5, 26–35. doi:10.1016/j.fob.2014.11.009.

Deussing, J. M., Kühne, C., Pütz, B., Panhuysen, M., Breu, J., Stenzel-Poore, M. P., Holsboer, F., and Wurst, W. (2007). Expression profiling identifies the CRH/CRH-R1 system as a modulator of neurovascular gene activity. *J. Cereb. Blood Flow Metab.* 27, 1476–1495. doi:10.1038/sj.jcbfm.9600451.

Erhardt, a, Czibere, L., Roeske, D., Lucae, S., Unschuld, P. G., Ripke, S., Specht, M., Kohli, M. a, Kloiber, S., Ising, M., et al. (2011). TMEM132D, a new candidate for anxiety phenotypes: evidence from human and mouse studies. *Mol. Psychiatry* 16, 647–63. doi:10.1038/mp.2010.41.

Erhardt, A., Akula, N., Schumacher, J., Czamara, D., Karbalai, N., Muller-Myhsok, B., Mors, O., Borglum, A., Kristensen, A. S., Woldbye, D. P., et al. (2012). Replication and meta-analysis of TMEM132D gene variants in panic disorder. *Transl. Psychiatry* 2, e156. doi:10.1038/tp.2012.85.

Farlow, J. L., Lin, H., Sauerbeck, L., Lai, D., Koller, D. L., Pugh, E., Hetrick, K., Ling, H., Kleinloog, R., Van Der Vlies, P., et al. (2015). Lessons learned from whole exome sequencing in multiplex families affected by a complex genetic disorder, intracranial aneurysm. *PLoS One* 10. doi:10.1371/journal.pone.0121104.

Haaker, J., Lonsdorf, T. B., Raczka, K. a, Mechias, M.-L., Gartmann, N., and Kalisch, R. (2014). Higher anxiety and larger amygdala volumes in carriers of a TMEM132D risk variant for panic disorder. *Transl. Psychiatry* 4, e357. doi:10.1038/tp.2014.1.

Inoue, A., Akiyoshia*, J., Muronagaa, M., Masudaa, K., Aizawaa, S., Hirakawaa, H., Ishitobia, Y., Higumaa, H., Maruyamaa, Y., Ninomiyaa, T., et al. (2015). Association of TMEM132D, COMT, and GABRA6 genotypes with cingulate, frontal cortex and hippocampal emotional processing in panic and major depressive disorder. *Int J Psychiatry Clin Pr.* 19, 192–200.

Mombaerts, P., Wang, F., Dulac, C., Chao, S. K., Nemes, A., Mendelsohn, M., Edmondson, J., and Axel, R. (1996). Visualizing an olfactory sensory map. *Cell* 87, 675–686. doi:10.1016/S0092-8674(00)81387-2.

Myers, A. J., Gibbs, J. R., Webster, J. a, Rohrer, K., Zhao, A., Marlowe, L., Kaleem, M., Leung, D., Bryden, L., Nath, P., et al. (2007). A survey of genetic human cortical gene expression. *Nat. Genet.* 39, 1494–9. doi:10.1038/ng.2007.16.

Nomoto, H., Yonezawa, T., Itoh, K., Ono, K., Yamamoto, K., Oohashi, T., Shiraga, F., Ohtsuki, H., and Ninomiya, Y. (2003). Molecular cloning of a novel transmembrane protein MOLT expressed by mature oligodendrocytes. *J. Biochem.* 134, 231–238. doi:10.1093/jb/mvg135.

Om Alblazi, K. M., and Siar, C. H. (2015). Cellular protrusions - Lamellipodia, filopodia, invadopodia and podosomes - and their roles in progression of orofacial tumours: Current understanding. *Asian Pacific J. Cancer Prev.* 16, 2187–2191. doi:10.7314/APJCP.2015.16.6.2187.

Panda, S. K., Wefers, B., Ortiz, O., Floss, T., Schmid, B., Haass, C., Wurst, W., and Kühn, R. (2013). Highly efficient targeted mutagenesis in mice using TALENs. *Genetics* 195, 703–713. doi:10.1534/genetics.113.156570.

Quast, C., Altmann, A., Weber, P., Arloth, J., Bader, D., Heck, A., Pfister, H., Müller-Myhsok, B., Erhardt, A., and Binder, E. B. (2012). Rare variants in TMEM132D in a case-control sample for panic disorder. *Am. J. Med. Genet. B. Neuropsychiatr. Genet.* 159B, 896–907. doi:10.1002/ajmg.b.32096.

Ran, F. A., Hsu, P. D., Wright, J., Agarwala, V., Scott, D. A., and Zhang, F. (2013). Genome engineering using the CRISPR-Cas9 system. *Nat. Protoc.* 8, 2281–2308. doi:10.1038/nprot.2013.143.

Schnütgen, F., De-Zolt, S., Van Sloun, P., Hollatz, M., Floss, T., Hansen, J., Altschmied, J., Seisenberger, C., Ghyselinck, N. B., Ruiz, P., et al. (2005). Genomewide production of multipurpose alleles for the functional analysis of the mouse genome. *Proc. Natl. Acad. Sci. U. S. A.* 102, 7221–6. doi:10.1073/pnas.0502273102.

Schnütgen, F., Hansen, J., De-Zolt, S., Horn, C., Lutz, M., Floss, T., Wurst, W., Noppinger, P. R., and von Melchner, H. (2008). Enhanced gene trapping in mouse embryonic stem cells. *Nucleic Acids Res.* 36, e133. doi:10.1093/nar/gkn603.

Wang, H., Yang, H., Shivalila, C. S., Dawlaty, M. M., Cheng, A. W., Zhang, F., and Jaenisch, R. (2013). One-step generation of mice carrying mutations in multiple genes by CRISPR/cas-mediated genome engineering. *Cell* 153, 910–918. doi:10.1016/j.cell.2013.04.025.

Yamaguchi, H., and Condeelis, J. (2007). Regulation of the actin cytoskeleton in cancer cell migration and invasion. *Biochim. Biophys. Acta* 1773, 642–52. doi:10.1016/j.bbamcr.2006.07.001.

Young, S. A., Aitken, R. J., and Ikawa, M. (2015). Advantages of using the CRISPR/Cas9 system of genome editing to investigate male reproductive mechanisms using mouse models. *Asian J Androl* 17, 623–627. doi:10.4103/1008-682X.153851.

14. Acknowledgements

My greatest thanks go to both Prof. Dr. Wolfgang Wurst for enabling this work as my thesis supervisor, as well as to Dr. Jan Deussing as my direct supervisor for guiding, directing and supporting me throughout the time of my dissertation.

I would also like to thank the other members of my examination board, Prof. Dr. Aphrodite Kapurniotu and Prof. Dr. Kay Schneitz for their effort, time and support. This also accounts to the additional members of my thesis committee, Dr. Daniela Vogt-Weisenhorn and Dr. Oskar Ortiz. Thank you very much!

Moreover, I am grateful towards Prof. Dr. Dr. Dr. h.c. mult. Florian Holsboer as former director and the current directors of the Max Planck Institute of Psychiatry, Prof. Dr. Elisabeth Binder, Prof. Dr. Alon Chen & Prof. Dr. Dr. Martin Keck for giving me the possibility to work on my thesis in their institute.

In addition I would like to thank my collaborators Prof. Dr. Gerhard Rammes (TU München), Dr. Fernando Aprile-Garcia & Prof. Dr. Eduardo Arzt (Biomedicine Research Institute of Buenos Aires) and Dr. Michael Willem & Prof. Dr. Dr. hc Christian Haass (LMU München).

My heartfelt thanks go to my great colleagues from the MPI for supporting me with work and scientific input but also for making the time very pleasant and special. Special thanks to: Sabrina Bauer, Dr. Julia Bender, Dr. Nina Dedic, Dr. Sebastian Giusti, Dr. Adam Kolaz, Claudia Kühne, Natalia Pino, Dr. Damian Refojo, Julia Richter, Emanuel Roos, Marcel Schieven, Katja Stangl, Sebastian Teschner, Stefanie Unkmeir, Dr. Annette Vogl, Dr. Sandra Walser.

Last but not least I would gratefully thank my parents, my brother, my entire family, my partner, my friends and all the people that accompanied me on this way for having supported me throughout my life and career and without whom I would not be where I am today.

Thank you all!